Northumbria Research Link

Citation: Caverhill, James Ross (2004) Investigation into the use and effects of a Q-switched Nd:YAG laser for the removal of ink from paper. Doctoral thesis, Northumbria University.

This version was downloaded from Northumbria Research Link: http://nrl.northumbria.ac.uk/1608/

Northumbria University has developed Northumbria Research Link (NRL) to enable users to access the University's research output. Copyright © and moral rights for items on NRL are retained by the individual author(s) and/or other copyright owners. Single copies of full items can be reproduced, displayed or performed, and given to third parties in any format or medium for personal research or study, educational, or not-for-profit purposes without prior permission or charge, provided the authors, title and full bibliographic details are given, as well as a hyperlink and/or URL to the original metadata page. The content must not be changed in any way. Full items must not be sold commercially in any format or medium without formal permission of the copyright holder. The full policy is available online: http://nrl.northumbria.ac.uk/policies.html

www.northumbria.ac.uk/nrl

northumbria UNIVERSITY NEWCASTLE

INVESTIGATION INTO THE USE AND EFFECTS OF A Q-SWITCHED Nd:YAG LASER FOR THE REMOVAL OF INK FROM PAPER

JAMES ROSS CAVERHILL

A thesis submitted in partial fulfilment
of the requirements of the
University of Northumbria at Newcastle
for the degree of Doctor of Philosophy

February 2004

ABSTRACT

A Q-switched Nd:YAG laser is used to remove ballpoint pen ink from 'Roma', a 100% cotton rag art paper. The laser was operated at 1064 nm, pulse duration 87 ns, and using a nominal fluence of 41 ± 12 Jcm^{-2}. By shortening the pulse length (63 and 26 ns), using a Glan-Thompson prism the ink removal threshold was reduced to 24 ± 7 and 20 ± 6 Jcm^{-2} respectively.

The physical damage to the paper is observed under SEM and found to be less disruptive to the surface fibres than contemporary mechanical methods of ink removal; scalpel and eraser. The tensile strength of laser treated paper is measured and found to remain unaffected below ink removal threshold fluences, although there is an increased tendency to tear at laser treatment sites. Repeat testing with artificially aged laser treated samples shows a marked decrease in tensile strength in comparison with an aged reference.

Laser treated paper (nominal fluence of 41 ± 12 Jcm^{-2}, pulse length 87 ns) is tested for evidence of thermal degradation, via oxidation and depolymerisation. The tests include the Russell effect test for the presence of peroxides (oxidation), the methylene blue test for the presence of carboxyl groups (oxidation), FTIR spectroscopy to determine the presence of carboxyl, carbonyl, and conjugated groups (oxidation), and GC/MS to test for the presence of sugars (depolymerisation). The tests suggest that there is thermal degradation predominantly via depolymerisation. This is supported by repetition of the tests on laser treated samples prepared in an argon atmosphere.

The laser treated paper is subjected to accelerated ageing in a humid oven to simulate natural ageing, and shows a more marked tendency to discolour than a similarly aged reference. This

is considered to be a reaction between the sizing agent (gelatin) and sugars formed during depolymerisation

The tests are repeated on 'Roma' paper laser treated with shorter laser pulses (nominal fluence 24 ± 7 and 20 ± 6 Jcm^{-2}, pulse durations of 63 and 26 ns), and this is found to have significantly less physical and chemical effect on the paper. Accelerated ageing of short pulse laser treated samples did not result in colour changes with respect to reference samples, indicating a more limited chemical interaction with the paper.

ACKNOWLEDGEMENTS

Dr B W Singer, Director of Studies, Chemistry & Life Science, University of Northumbria

Dr I Latimer, Supervisor, Engineering, University of Northumbria

Bob Best, SEM, Engineering, University of Northumbria

Jason Revell, Photography, photomicroscopy, and Russell effect tests, Fine Art Conservation, University of Northumbria

Gary Askwith, FTIR, Chemistry & Life Science, University of Northumbria

Eileen Rodgers, Tensile testing, Paper Science, UMIST

Dr J Stanley and Phil Tougher, Artificial ageing, Paper Science, UMIST

Dr A Smith, Artificial ageing, The London Institute, Camberwell

CONTENTS

CHAPTER 1:

INTRODUCTION

1.1 Objectives of the research programme

One problem frequently met by paper conservators is the addition of modern writing ink to a paper artefact. Many modern inks tend to preclude the lengthy aqueous treatments favoured by paper conservators, due to their solubility in water. The ink addition may be a museum accession number (Fig.1), framers notes, or deliberate defacement. Whatever the origin, the problem remains the same, the need to remove the ink prior to wet treatments. In some situations solvents can be used to wash out the inks, but generally in practice the ink is removed mechanically with a scalpel and/or erasers. Scalpels and particularly erasers are difficult to accurately control over a confined area, and results can often appear disfiguring.

Clearly there is a need for a more precise and less damaging method of ink removal from artworks on paper. Recently some of the country's larger paper conservation studios have expressed an interest in the use of lasers for cleaning paper artefacts.

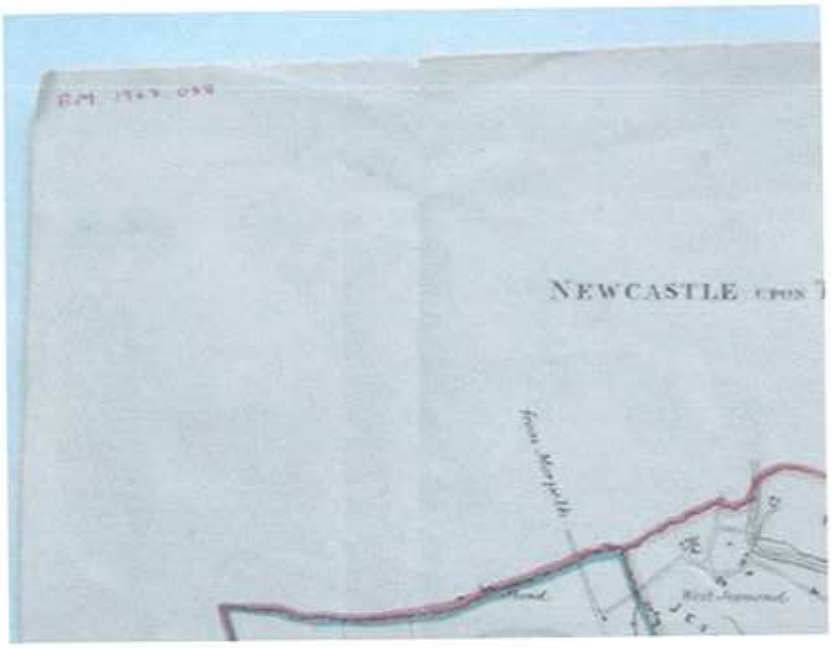

Fig.1 Museum accession number written in red ball-point pen ink, in the top left hand corner of a plan of Newcastle upon Tyne

Laser cleaning is a physical process in which there is strictly limited interaction with the substrate material, and therefore has distinct advantages over traditional cleaning methods which are based on chemical or mechanical action[1]. Conventional treatments mainly involve abrasion techniques or the use of chemical solvents. Watkins[1], has summarised the advantages of lasers;

a) a physical process which ceases shortly after the laser pulse has ended,
b) a selective process which can be tuned for the removal of specific substances, i.e. choice of wavelength for cleaning,
c) a non-contact process,
d) a process that preserves surface relief,
e) versatile – most materials can be removed by correct selection of operating conditions,
f) controllable – a specific thickness of material can be removed,
g) environmentally preferable – no large volumes of waste products.

This research programme is divided into two main parts. Part One aims to investigate the effectiveness of ink removal from paper by laser. The degree of success will be determined by comparison of visible damage with that caused by conventional mechanical ink removal techniques, scalpels and erasers.

Laser treatment of paper artworks could only be considered as an acceptable conservation technique if it were established that the process did not result in significant physical weakening, or chemical degradation of the paper. An investigation into both these areas will form the basis of Part Two.

1.2 Choice of laser for the research programme

In order to choose the type of laser best suited to the treatment of paper, it is necessary to compare the results of previous laser cleaning trials.

Watkins[1] and Larson[2], have reviewed the early use of lasers for cleaning works of art, and suggest that John Asmus was the first person to have the idea of using lasers to clean polluted stonework in the late 60s. Asmus[3-5], observed the effect of the interaction between a focused ruby laser (formerly used for holographic recording) with an encrusted stone statue. It was found that the darker encrustations were selectively removed from the surface, resulting in no apparent damage to the underlying white stone. In 1972 Asmus was persuaded to carry out a demonstration of the removal of black encrusted material from decayed stonework, at the Victoria and Albert Museum. During the 1970s Asmus continued to experiment with lasers on a variety of media, however his findings lacked the rigorous testing that new conservation techniques require to become acceptable[2]. He used a Nd:YAG laser (1064 nm) to clean marble and limestone statues, and found that the darker encrustations were selectively removed from the surface resulting in no apparent damage to the underlying, white stone[6]. He states that the first pulse or two, would be accompanied by an optical flash, and an acoustic report. These flashes and reports ceased when the white surface of the marble emerged from beneath the encrustation. Thus it became apparent that the acoustic report could facilitate process control and that the process was self-limiting. In this respect self limiting means that ablation of material from the surface of an object stops as soon as the dirt layer has been removed, and the clean surface is not damaged by exposure to further laser pulses[7]. From further studies involving stone Asmus concluded that there are two principal cleaning mechanisms[1]. In normal pulse mode the energy impinges on the target slowly (pulse duration approximately 1 μs.- 1 ms), and cleaning occurs as a result of selective vaporisation of the surface material compared to the underlying material, which remains relatively unaffected.

However in Q-switched mode the energy is dumped quickly (pulse duration approximately 5-30 ns.) and a plasma generated shock wave mechanism is responsible for the cleaning effect (see section **1.3 Background on the mechanisms of lasers and laser cleaning**).

By 1986 Asmus had successfully cleaned a wide selection of works of art, with the range of lasers available to him[6]. From his trials with laser cleaning he concluded that carbon dioxide lasers (10.6 μm) were useful for metal cleaning only, Nd:YAG pulsed lasers (1064 nm)were relatively efficient on stone, metal, textiles, skin products, and pottery, and suggested that excimer lasers (ultra-violet) would be useful for cleaning biological material which absorbs in the far ultra-violet.

The successes with Nd:YAG (1064 nm) cleaning of stone artefacts created considerable interest throughout the museum community, and encouraged further stone cleaning programmes[7-17]. Cooper[7], Cooper and Larson[8], and Teppo and Calcagno[9], have studied the effect of a Nd:YAG laser used to clean heavily polluted marble statues. The results show that the laser is more controllable and achieves a more aesthetically pleasing clean than conventional methods. The authors recommend the need for caution when choosing pulse length. Q-switched short pulses are useful for breaking up thick layers of pollution, and are usually preferred over long pulses, which can cause more surface heating.

Laser cleaning using Nd:YAG lasers has been demonstrated on numerous cathedrals in Europe, most notably in France[13,14] and Austria[15]. The results showed that laser cleaning was a more selective process than micro air-abrasive cleaning.

Though stone has proved to be a most suitable surface on which to use a Nd:YAG laser for cleaning purposes, there have been successful cleaning trials with a wide range of artefacts

including, parchment[18], chain mail[19], shells[20], textiles[21], and bronzes[22]. Not all materials and encrustation types are effectively cleaned at the fundamental Nd:YAG wavelength (1064 nm.), leading to the need for alternative laser wavelengths. This need has been met by use of systems for frequency doubling, which halve the fundamental Nd:YAG wavelength (from 1064 nm. to 532 nm; visible light)[23,24], or by the use of a different laser type such as the excimer (ArF;193, KrF;248 or XeCl;308 nm; ultra-violet light)[25-35].

The use of excimer lasers for cleaning artworks is much more recent than that of Nd:YAG lasers. Fotakis[25-28] has had considerable success with an excimer laser (KrF), for the removal of varnish and overpaint from paintings, using a fluence of 10-200 $mJcm^{-2}$. The laser emitted nanosecond pulses (5-20 ns) in the ultra-violet (248 nm). There are three major cleaning issues related to the conservation of paintings:

1. The cleaning of surface layers of varnish or contaminated regions.
2. The cleaning of the support material, usually wood, canvas and paper.
3. The removal of overpaint.

Traditional methods rely on mechanical and/or chemical means, but there is only limited control of the cleaning process. Thus mechanical methods of cleaning may destroy the painting texture, while solvent treatment may affect the pigments and media or cause ageing due to penetration through to the body of the painting.

Fotakis points out that the lasers can be operated selectively to remove firstly, surface dirt and then varnish, leaving the underlying material unaffected thermally or photochemically (see section **1.3 Background on the mechanisms of lasers and laser cleaning**). He states that questions have been raised concerning potential photochemical interferences, for example the extent of free radical formation and oxidation. However he maintains that he has found no

evidence to support these suggestions. He has compared the excimer with the Nd:YAG and suggests that the latter is more useful where gross cleaning is required, as the shock waves produced by the Nd:YAG remove relatively large amounts of material (typical removal of 1-100 μm material for a 5-20 ns pulse). However, if microscopic removal of a surface layer is desired, then excimers are more appropriate (typical removal of 0.5-1 μm material for a 5-20 ns pulse)[25-28].

The cleaning of works of art on paper and parchment by laser has thus far received relatively little attention in the conservation literature. Szczepanowska[23], has investigated the removal of mould stains from paper using green light from a frequency doubled Nd:YAG laser (532 nm). She found the laser very effective for the removal of certain mould stains and in some cases the mycelium. Generally the paper exhibited no visible damage, however with high power outputs, if the pulse repetition rate exceeded 10 Hz, burning of the paper was observed. This is most likely due to thermal degradation[7-9]. The laser was targeted at printing ink and it was found that considerably more, higher energy pulses were required to remove the ink. From the results achieved she concluded that the laser offered a significant advantage for fungal stain removal.

More recently excimer lasers have been used to remove surface dirt from parchment[31-33], and mould stains from paper[34,35]. Kautek[31-33] has used a XeCl laser (308 nm) to remove soot and dirt from parchment using a fluence range of 0.2-1.4 Jcm^{-2} (pulse duration 17 ns), however he warns that care must be taken to set the fluence levels below the ablation and destruction threshold of the parchment whilst keeping above the destruction threshold of any foreign accretions. He suggests that one major drawback for Nd:YAG treatment of parchment is the tendency to disrupt the surface due to the rapid vaporization of water caused by absorption of the laser energy. Water molecules absorb radiation from Nd:YAG laser at 1064 nm more

strongly than in the case of other lasers used for conservation (Nd:YAG 532 nm and excimer 248nm and 308 nm).

Friberg[34,35] used a KrF (248 nm) laser to remove mould and mould stains from paper artworks, using fluences between 0.4–1.5 Jcm^{-2}. Many of the stains were removed as verified by microscopy, however there was unwanted removal of inks, and yellowing to certain papers. Fungi could be removed from certain works with preservation of the underlying image using carefully selected fluences, but constant monitoring of the process was necessary. He acknowledges the work of Szczepanowska[23] using a YAG laser (532 nm), but suggests that the excimer may be more suited due to its ability to remove microscopic layers of a few microns depth. However he also concedes that paper can easily be burned or discolored if laser parameters are not properly chosen, and that there may be chemical alterations to the paper as a result of treatment with high intensity ultra-violet radiation.

The damaging effect of ultra-violet light on paper is well documented and is known to cause discoloration via photo-oxidation[36-40]. Therefore even though Fotakis[25-28] and Friberg[34,35], have successfully removed dirt and mould from paper using excimer lasers, it is likely that the paper would suffer chemical degradation via photo-oxidation.

Visible light can also cause photo-oxidation in paper[41]. Szczepanowska[23] claims the use of a frequency doubled Nd:YAG laser (532 nm), to remove mould from paper caused no visible damage when viewed using SEM. However no testing of chemical or mechanical properties was carried out.

The most appropriate laser for cleaning paper appears to be the infra-red Nd:YAG (1064 nm), but although there has been considerable interest from the paper conservation community, there have also been widely varying accounts of what treatments actually work.
Loton[42], has attempted the removal of various inks, adhesives, and water stains from paper, during demonstrations of his company's Q-switched Nd:YAG laser to museum conservation studios. His results seem encouraging but he has recorded no energy measurements during treatment, or fluence thresholds at which damage to the artefact may take place in varying circumstances. This demonstrates the need for a thorough programme of research to investigate the potential uses, advantages, and drawbacks, of infra-red lasers for paper conservation treatments.

Kolar[43] has studied the effect of short pulsed Nd:YAG (6 ns, 1064 nm) laser treatment on cellulose and found that this did not have a detrimental effect on the appearance, strength, or ageing properties of the test samples, however she did find evidence suggesting cross-linking of the molecules. Based on her results she cautiously advocates the use of the Nd:YAG laser for paper conservation, subject to further testing.

The possibility of cross-linking molecules would be a major concern when considering the use of a laser for paper conservation, however it has not been established whether the problem of cross-linking is witnessed using long laser pulses on paper. Previously Cooper[7], Cooper and Larson[8], and Teppo and Calcagno[9], have described a heating effect associated with longer pulse length, Nd:YAG laser use, but their research has centred primarily on stone cleaning.

The effect of subjecting paper to heat increases, is discussed in section, **1.4 The degradation of cellulose**, and does not involve cross-linking. Therefore it would seem that if very short

laser pulse lengths cause cross-linking, and long pulse lengths could cause thermal degradation, the optimum operating pulse length is likely to lie somewhere in between. For the Nd:YAG laser to be considered an acceptable conservation tool it is essential to know what operating parameters are safe for artworks.

Therefore this research programme used a Q-switched Nd:YAG laser at a wavelength of 1064 nm to investigate ink removal from paper. It was intended that once thresholds for ink removal had been determined, there would be an investigation into the physical and chemical damage caused to paper at these energy thresholds, to establish whether thermal degradation occurred. Later in the research it was intended to explore methods of improving the efficiency of ink removal and reducing any damage that may result during treatment to paper, by manipulation of the pulse length. It was considered that this would give a clearer picture of how appropriate the Nd:YAG is for paper conservation treatments, and how sensitive paper is to the laser.

Once the work by Kolar[43] had been published it was possible to compare the results of long and short pulse lengths from this research programme, with Kolar's work at very short pulse lengths.

1.3 Background on the mechanisms of lasers and laser cleaning

LASER is an acronym for *Light Amplification by Stimulated Emission of Radiation.* Since its invention the laser has become easy to use, and has consequently found wide application for cutting and heat treatment in engineering and surgery. The output radiation from lasers is in the form of a highly collimated beam of electromagnetic radiation at a variety of wavelengths depending on the type of laser[44]. The output beam from a high power laser can be focused by a convex lens, thus concentrating the power into a very small region of a target and so achieve fine control of the heat treated area.

The first device utilising stimulated emission was reported by Gordon, Zeiger and Townes in 1955. This achieved Microwave Amplification by Stimulated Emission of Radiation (hence MASER). The LASER made its appearance with the work of Maiman (1960), who created the ruby laser. Subsequently the industrial laser types known today were established. Chronologically these are the Helium Neon laser (1961), semiconductor (1962), Neodymium YAG (1964), carbon dioxide (1964) and the excimer laser (1976)[45,46].

The schematic diagram of a laser (Fig. 2) shows the gain medium between two mirrors aligned perpendicular to the axis of the gain medium. When the atoms are excited spontaneous emission will produce photons which in turn are amplified by stimulated emission, when there is a population inversion (more atoms in a higher energy level than in a lower one)[47]. The feed back provided by the mirrors means that only one photon is initially required for the light intensity to grow by a very large factor in trips between the reflectors, and the atomic excitation is extracted by the stimulated wave as a collimated narrow coherent beam. In the laser one mirror is highly reflecting while the other is partly reflecting so allowing a fraction of the radiation into the outside world for application. The beam is of high intensity because atoms, which would emit radiation by spontaneous emission in all directions, are being forced to emit light into a narrow beam a few millimetres in diameter.

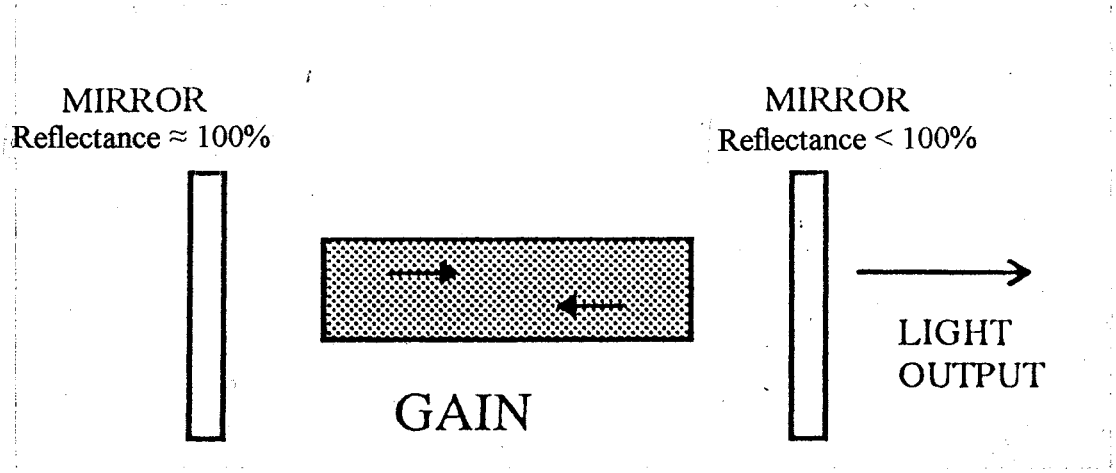

Fig. 2 Schematic diagram of a laser.

The industrial and commercial applications of lasers fall into several basic categories, of which the working and processing of materials, is most relevant to the conservation of artworks.

There are two major industrial laser types, the Nd:YAG; a solid state laser, and carbon dioxide; a gas laser[48]. Recently the excimer laser (gas laser) has emerged as another useful industrial laser. It is complementary to the others, for fine processing of polymers.

The neodymium laser is the most common member of a family known as solid state lasers. Atoms present in impurity level concentrations (ca. 1%) in a crystalline or glass host are excited optically by light from an external source, producing a population inversion in the material. The most common host for neodymium is yttrium aluminium garnet (YAG), which emits infra-red radiation at a wavelength of 1064 nm. The choice of optical pump source (semiconductor laser, pulsed flashlamp, or continuous arc lamp), strongly influences the laser characteristics[44]. Neodymium lasers can generate continuous beams (CW) of a few milliwatts to over a kilowatt, short pulses with peak powers in the gigawatt range, or pulsed beams with

average powers in the kilowatt range. The peak powers depend on both the pulse energy and duration. Neodymium lasers can operate in a variety of pulsed modes, depending on both excitation and control of the energy in the laser cavity;

a) long pulses with duration dependent on the length of the pulse from the excitation source, and the fluorescent lifetime of the medium (200 – 500 μs).

b) Q-switched pulses, lasting from a few nanoseconds to hundreds of nanoseconds.

In Q-switching a shutter in the cavity is kept closed until the population inversion has reached a maximum when it is rapidly opened. The energy stored by the excited atoms can thus be released in one short pulse (Fig. 3)[44,45,49,50].

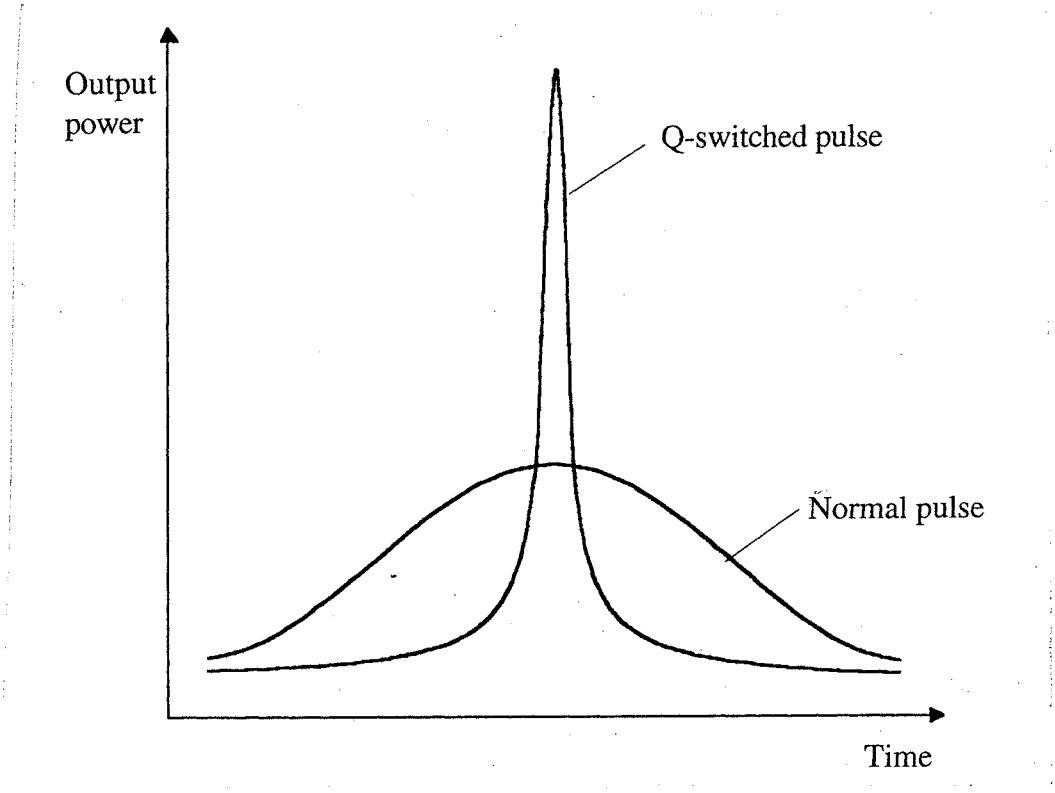

Fig. 3 Schematic representation showing the difference between a Q-switched pulse and a normal pulse[7].

The source of energy for a carbon dioxide laser is an electrical discharge in the gas. The excitation occurs in a low pressure mixture of carbon dioxide, nitrogen and helium, and infra-red radiation is emitted at a wavelength of 10.6 μm. The carbon dioxide laser can produce continuous output powers ranging from under 1 watt to several kilowatts. It can generate pulses from the nanosecond to millisecond regimes

When carbon dioxide or Nd:YAG lasers are focused onto the surface of a material some of the energy is absorbed, and the temperature increases. The temperature rise depends on the material properties, the spot size of the laser, and the pulse energy and duration[49]. The rise in temperature can be used to process several types of materials. Nd:YAG and carbon dioxide lasers are both extensively used for cutting, drilling, and marking or engraving, although the Nd:YAG is considered to be better suited to the heat treatment of metals and ceramics, and the carbon dioxide laser to organic materials like polymers, wood and paper[50,51].

Excimer (which stands for excited dimer) lasers comprise complexes of rare gas halides, XeF (353 nm.), XeCl (308 nm.), KrF (248 nm.) and ArF (193 nm.). All emit powerful pulses lasting nanoseconds or tens of nanoseconds at wavelengths in the ultra-violet region of the spectrum[52]. Typical average output powers range from under a watt to 1 kW. Excimer lasers tend to be lower powered than the infra-red lasers but their shorter wavelength allows them to be focused to smaller spots giving greater precision in the heat treated area. They emit ultra-violet photons with sufficient energy to break bonds in molecules, particularly the C-H bond present in most organic compounds[53]. The energy E, of a photon is dependent on the wavelength of the radiation and is defined as equation (1),

$$E = h\nu = \frac{hc}{\lambda} \qquad (1)$$

where h, is Planck's constant, c the velocity of light, ν the frequency (in Hz), and λ the wavelength.

To break the same material apart with infra-red radiation requires the absorption of many photons to raise the temperature and dissociate some of the molecules[53]. However such high temperatures can often result in combustion, charring, and melting of the surrounding material. One advantage of excimer laser is that their use causes very little heating effect[53], and therefore excimer lasers have become extremely useful for cutting objects and marking.

In order to have an effect on a surface, laser radiation must be absorbed. The effect on a given surface is determined by the beam power, or the rate at which energy is delivered to the surface, and the total energy. A certain proportion of the incident energy is absorbed by the surface and converted to thermal (infra-red), or chemical (ultra-violet) energy. There is a threshold above which the beam power must be raised to bring about a change to the material. Ablation occurs at some point above this threshold[7]. Ablation describes the process of ejection of material from a solid surface as a result of laser irradiation.

Laser ablation can proceed photothermally, where the photon is used to heat the surface, or photochemically, where the photon is used to break chemical bonds within the surface without heating[7]. Photothermal ablation occurs in the infra-red and visible part of the spectrum, while photochemical ablation which occurs with covalently bonded materials, requires ultra-violet photons.

When a laser interacts with a solid target, a variety of events may take place including selective excitation and evaporation, thermal and photochemical ablation, shock wave formation with mechanical disruption of the surface layers, and vaporisation of organic

debris[1,2,6,7,9,25,26]. Each of these interactions can be produced by the appropriate selection of the laser parameters including wavelength, peak power, pulse duration, pulse shape, repetition rate, mode profile and laser spot size[44,54,55,56]. The characteristics of the material to be treated, and the pollutant are also important. These include the absorption coefficient, reflectivity, thermal diffusivity, enthalpy of evaporation and heat capacity[57,58,59]. The nature of pollutant bonding to the substrate will also affect the fluence required for removal. The viability of the cleaning method for a particular medium depends on the relative thermal and optical properties of the polluting layer compared to the medium, and will have to take into account the susceptibility of the substrate medium to physical or chemical damage.

Where gross cleaning effects are desired such as the removal of black encrustations from marble, photothermal ablation by Nd:YAG lasers is most suitable. Normal-mode Nd:YAG lasers (pulse duration approximately 1 μs-1 ms), will remove surface pollutants through superficial evaporation, however the longer pulse durations can cause the heat to diffuse to the substrate, especially with high average power operation[1,2,26].

Cooper[7], has made a detailed study of cleaning by short pulse radiation (5-30 ns), as with Q-switched lasers, and suggests the process occurs via a combination of four main mechanisms. The dominant mechanism and hence selectivity is determined by the incident energy density, the type of dirt and its bonding to the surface.

Rapid thermal expansion

At low fluence levels the main mechanism operating is thought to be rapid thermal expansion, in which strong absorption of the laser energy by the target leads to a rapid rise in the temperature, and subsequent expansion. The resultant force is away from the surface and can be sufficient to eject material from the surface.

Explosive vaporization

At slightly higher fluence levels there is sufficient heat to bring about vaporization. This process occurs extremely quickly and vaporization takes place explosively.

Surface relaxation due to plasma effects

Plasma formation (gaseous mixture of ions and electrons together with neutral evaporated species) occurs when material is ablated from a surface at very high fluences. The irradiation of the target leads to the generation of a plume of vaporized material just above the surface. Further absorption of energy gives rise to intense heating and ionization of the vapour producing an intense spark, or plasma. Rapid expansion of the plasma applies a compression to the irradiated region of the surface. Once the laser pulse has finished the surface relaxes. This compression and relaxation can lead to further ejection of material from the surface (Fig. 4). This is believed to be the shock wave mechanism which Asmus[6], describes.

Acoustic shock-induced surface disruption

At very high fluences particle ablation can be sufficiently rapid to generate an acoustic wave in the air audible as a snapping sound[57]. Propagation of the acoustic shock wave along the surface of a material can generate stresses sufficient to cause disruption of the material in the vicinity of the laser pulse.

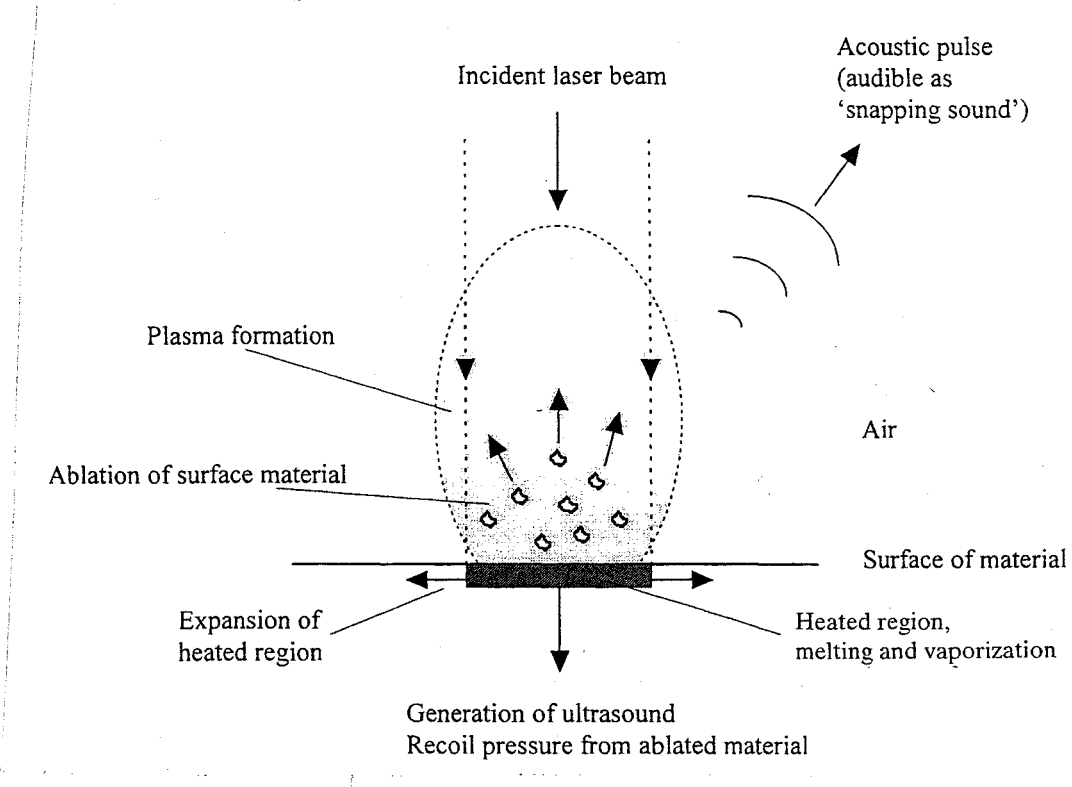

Fig. 4 Schematic representation of the effects of absorption of a high power laser beam[7].

If the removal of microscopic surface layers is desired, photochemical ablation by excimer lasers is more appropriate[25-28]. Photons emitted in the far ultra-violet are sufficiently energetic to break many covalent bonds directly upon absorption without heating. Absorption then initiates a chemical reaction in which the products have a larger volume than the original material. Hence the reaction products are ejected (ablated) from the surface as a result of the sudden volume change[7,25,26,53].

However cleaning artworks with excimer lasers does not afford the operator with the same degree of selectivity as working with Nd:YAG at 1064 nm, because photoablation will continue to take place after the polluting layer has been removed. Controllable removal of microscopic layers can only be achieved if monitoring and analytical techniques are used as part of the process.

1.4 The degradation of cellulose

Until the latter part of the eighteenth century practically all paper of European origin had been made of cotton or linen rags[60]. The principal constituent of these sources is cellulose, a polymeric carbohydrate composed of long linear chains of β-linked anhydroglucopyranose[61] (Fig. 5). The chains in cellulose are composed of as many as 10,000 glucose units, the number of glucose units per chain is known as the degree of polymerization (DP).

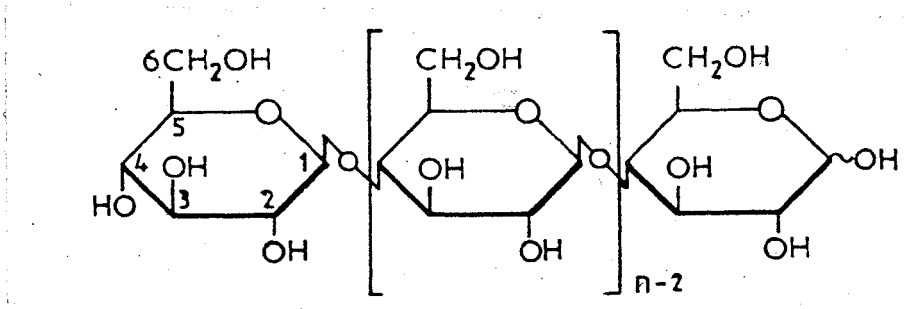

Fig. 5 The structure of cellulose, illustrating the conventional numbering of the carbon atoms.

The shortage of available rags in the late 1700s encouraged papermakers to seek out a more plentiful material with which to make to paper. The early 1800s saw the production of mechanical woodpulp papers, and by the latter part of the century a range of chemical processes had been developed to produce papers with specific properties[60]. The chemical constituents of modern papers comprise cellulose, hemicellulose, lignin, and extracts from wood[36,61]. Hemicellulose is an amorphous polymeric carbohydrate having a slightly branched structure, with a DP of between 200-500 sugar units per molecule. Lignin is a three-dimensional, highly crosslinked, amorphous polymer that is partly aromatic. The monomer is primarily coniferyl alcohol but with a number of similar compounds incorporated (Fig. 6). Most modern papers also contain additions of fillers (e.g. clay and inert white pigments),

sizing agents (e.g. gelatin, starch and rosin), and other materials such as dyes and optical brighteners to improve paper quality[60,62,63].

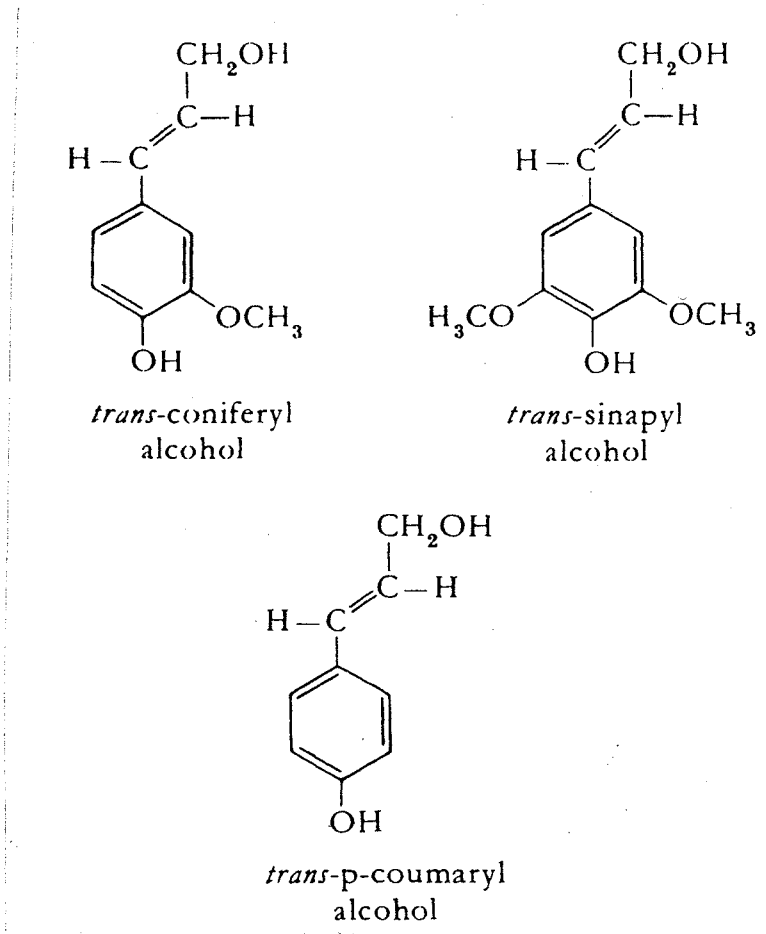

Figure 6 Monomers which polymerize to give lignin

The main factors responsible for the deterioration of paper are, acid-catalysed hydrolysis[64], oxidation[36-41,65-67], photo-oxidation[38-41] and thermal degradation particularly at high temperatures[68,69].

The glycosidic linkage (and hence the degree of polymerization) in cellulose is susceptible to acid catalysed hydrolysis. The mechanism of the reaction comprises three stages: rapid protonation of the glycosidic oxygen atom, slow transfer of the positive charge to C-1 with formation of a carbonium ion and fission of the glycosidic bond, and rapid attack on the

carbonium ion by water to give the free sugar residue and to reform the hydroxonium ion (Fig 7)[64]. Analysis has shown that 99.9% of the glycosidic bonds in cellulose are identical, and that all bonds except those at the chain ends, break at the same rate[70]. However there have been reports of 'weak bonds' that are more prone to hydrolysis than the rest. Nevell[64] cites the presence of a few sugar units other than anhydroglucose as the possible cause of acid sensitivity. Whitmore and Bogaard[71,72], and Ranby[73] suggest that weak links are created due to the oxidation of cellulose resulting in the formation of carbonyl and/or carboxyl groups along the cellulose chains as opposed to the chain ends.

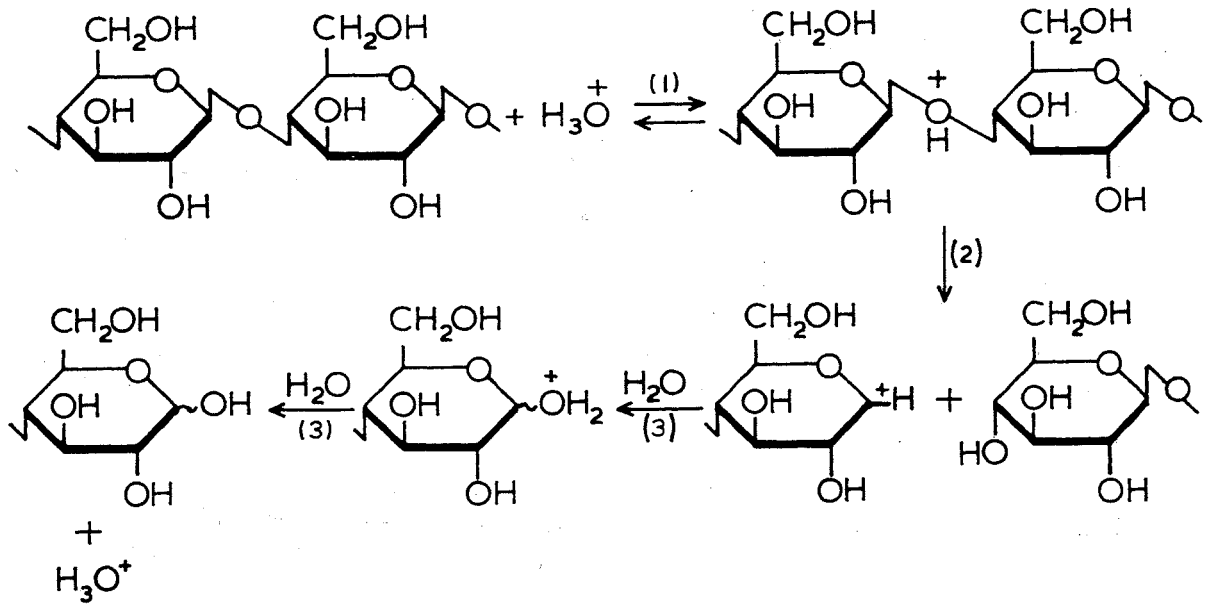

Fig. 7 Mechanism for the hydrolysis of cellulose.

The oxidation of cellulose is complicated for three reasons;

a) the three alcohol groups in each chain unit have different reactivities,

b) different parts of a cellulose fibre have different accessibilities

c) different oxidants behave in different ways

There are numerous ways in which the chain units in cellulose can be oxidized while the glycosidic linkages remain intact, however the type of transformation may depend greatly on the reagent[65]. The hydroxyl groups on cellulose are the most reactive centres, and these are oxidized to aldehyde, ketone, and carboxylic acid groups (Fig. 8). Aldehyde groups may be formed on the C2 and C3 carbon atoms (a), causing a ring scission and C6 (c). These can subsequently be oxidized to carboxylic groups (b) and (d). Ketones may be created on either C2 or C3 (e), or both (f).

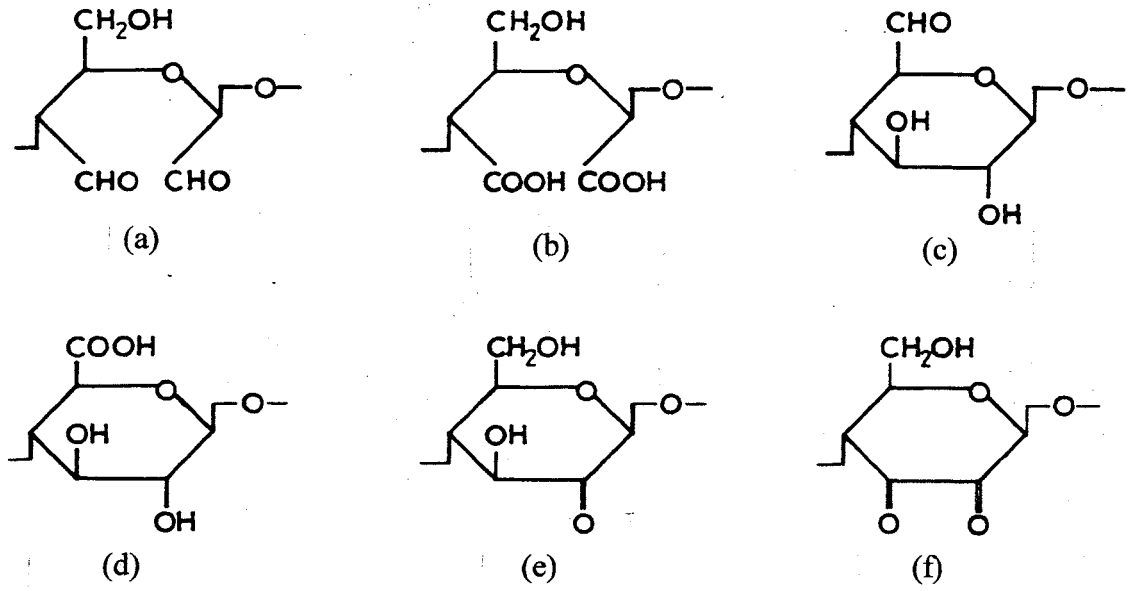

Fig. 8 Oxidized anhydroglucose units.

One of the major factors in the deterioration of paper is the result of interaction of visible and ultra-violet light on cellulose[37-41,66,67].

It is a basic photochemical principle that only light which is absorbed by a molecule, is effective in producing chemical change. The extent to which radiation can be absorbed by matter is dependent on chemical structure. The molecule which absorbs the radiation is

excited, and may consequently undergo chemical change. The amount of energy E, in a photon of radiation is given by equation (1),

$$E = h\nu = \frac{hc}{\lambda}$$

Photons of infra-red light have relatively low energies which are sufficient to cause changes in vibrational and rotational energies in molecules. To break bonds within the molecule, or to excite the electrons in the bonds to higher energy levels, requires higher energies corresponding to the shorter wavelengths of visible and ultra-violet radiation[38]. Visible light has wavelengths between 400 and 700 nm (violet to red), and ultra-violet from normal light sources and sunlight, 280 and 380 nm.

Single valence bonds (sigma bonds) have a large energy gap between the σ orbital and the excited σ^* orbital and only absorb in the far ultra-violet. Consequently compounds containing only sigma bonds show no near ultra-violet or visible spectra. Double bonds comprise two types of bond, sigma bonds and π-bonds. The π-π^* gap is much less than the σ-σ^* gap, and as the π system becomes delocalised, there are more π and π^* orbitals, so that the gap between the highest occupied molecular orbital (HOMO) and lowest unoccupied molecular orbital (LUMO) decreases. Therefore the region of light absorption moves into the near ultra-violet and with highly unsaturated systems, into the visible as the gap between π and π^* orbitals becomes less[38].

Light with wavelengths greater than 310 nm, is not absorbed by many bonds, and therefore cannot induce degradation of cellulose directly, but certain dyes and related compounds such as hemicelluloses, lignin and metal ions, are capable of absorbing light in the near ultra-violet

or visible part of the spectrum, and in their excited state can induce degradation[65]. These processes can be described as photosensitized degradations of cellulose, and follow the general radical –chain mechanism shown in Figure 9. The mechanism can be discussed in terms of initiation reactions during which free radicals are formed, propagation reactions during which free radicals are converted into other radicals, and termination reactions which involve the combination of two radicals with the formation of stable products.

Initiation	RH	+	I	→	R^*	+	HI^*	
Propagation	HI^*	+	O_2	→	I	+	HOO^*	
	R^*	+	O_2	→	ROO^*			
	ROO^*	+	RH	→	ROOH	+	R^*	
	ROO^*	+	H_2O	→	RO^*	+	H_2O_2	
	ROO^*	+	H_2O	→	ROH	+	HOO^*	
	RH	+	HOO^*	→	R^*	+	H_2O_2	
Chain Branching	ROOH			→	RO^*	+	OH^*	
	RO^*	+	RH	→	ROH	+	R^*	
	OH^*	+	RH	→	H_2O	+	R^*	
Termination	R^*	+	R^*					
	ROO^*	+	ROO^*	→	end products			
	R^*	+	ROO^*					

*Fig. 9 Mechanism for the photo-oxidation of cellulose, where I represents an excited sensitiser, R represents cellulose and * represents a radical.*

The initiation step shows the abstraction of hydrogen from cellulose RH, by the excited sensitiser I, to produce a cellulose radical R^*. Oxygen propagates the reaction by reacting with the radical intermediates. The reaction branches as a variety of reactive radical species are formed, but terminate due to the tendency of these species to react with each other.

The pulp and paper industry shows great interest in tendency of cellulose to oxidize as this results in the yellowing of paper[36-38, 66,67]. Yellow/brown degradation products may be obtained from several components of paper, either separately or in combination with each other. Any substance will appear coloured if it absorbs light in the visible region of the spectrum. Organic molecules contain chromophores, which are conjugated and are frequently composed of alternating single and double bonds. As degradation proceeds, more double bonds are formed. Small conjugated systems absorb light in the ultra-violet, but as the system becomes more conjugated, the absorption moves into the visible region and violet light is absorbed, the material in question appearing yellow[66]. The polyene carotenoid pigments, for example, are bight yellow or orange due to their absorption maxima in the blue region (Fig. 10)[38].

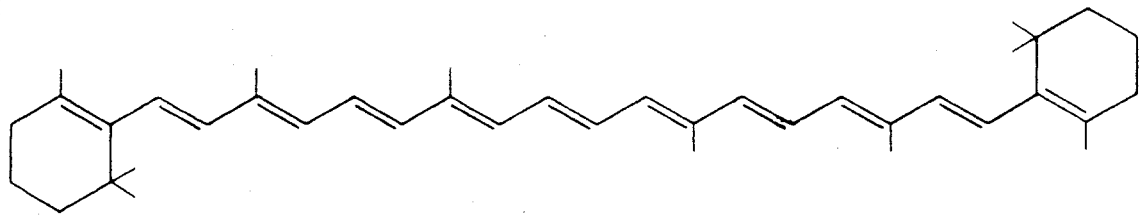

Figure 10 The structure of β-carotene

Papers which contain many aldehyde groups tend to discolour easily, and these groups appear as a result of several degradation processes; alkaline hydrolysis[64], oxidation[65] and pyrolytic chain scission[68,69]. Also the rate of acid hydrolysis[64], is increased by the introduction of aldehyde groups on the cellulose.

Daniels[66], has reviewed the work which has been carried out by the foodstuffs industry, on protein-sugar mixtures which tend to brown rapidly. Degraded paper contains reducing sugars and frequently protein is present as a gelatin size, therefore Daniels suggests this is one possible reason for browning in certain degraded papers.

Thermal degradation of cellulose has attracted considerable attention from Shafizadeh[68,69], who has reviewed the pyrolytic reactions of cellulose as the molecule is heated at increasingly high temperatures. He states that there are basically three reaction pathways, which are shown in Figure. 11.

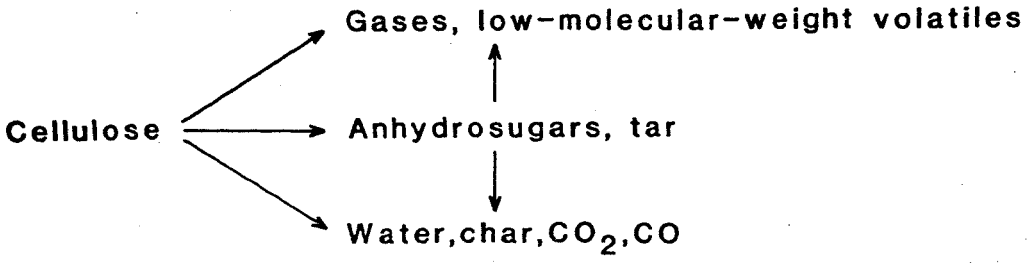

Fig.11 Competing pathways for cellulose pyrolysis

Lower temperatures result in the decomposition of the glycosyl units of cellulose by evolution of water, carbon dioxide and carbon monoxide. Below 300°C the chemical reactions of cellulose include reduction of the degree of polymerization (DP) by bond scission, appearance of free radicals, elimination of water, and the formation of carbonyl, carboxyl and hydroperoxide groups. Indeed it can be difficult to distinguish between thermal degradation and the normal ageing of cellulose, which is accelerated by heating.

Cellulose heated above 300°C undergoes a rapid decomposition until at approximately 390°C the reactions cease, leaving a non-volatile char. The general products obtained from the pyrolysis of cellulose include a tar or heavy oil fraction, which volatilizes out of the heated

zone, a gaseous fraction and residual char. At temperatures in the region of 340°C there is depolymerisation of the molecule by cleavage of glycosyl units to form mainly 1,6-anhydro-β-D-glucopyranose (levoglucosan), (Fig. 12). This reaction is accompanied by decomposition of the original molecule as well as the anhydro sugar products.

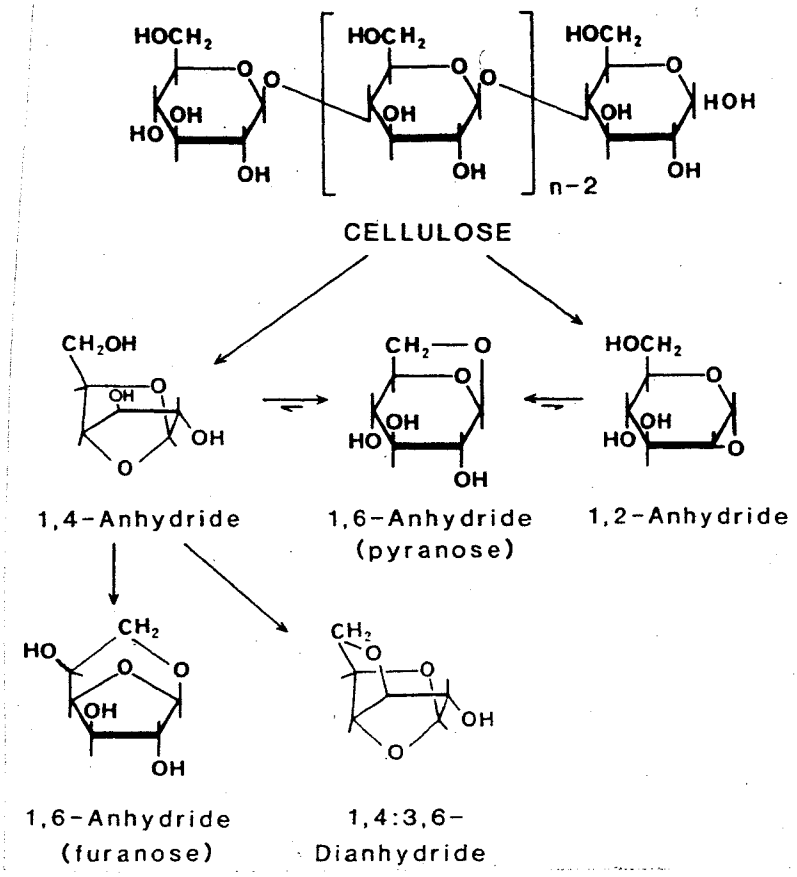

Fig. 12 Pyrolysis of cellulose to anhydro sugars and other compounds by transglycosidation reactions.

Still higher temperatures result in the breakdown of the molecule to lower weight gaseous products, including carbon dioxide, carbon monoxide, water, hydrocarbons and hydrogen (Fig. 13). Studies by Shafizadeh[68,69], have shown that as the temperature of the char is increased, there are increases in the concentration of carbonyl groups, and aromatic carbons.

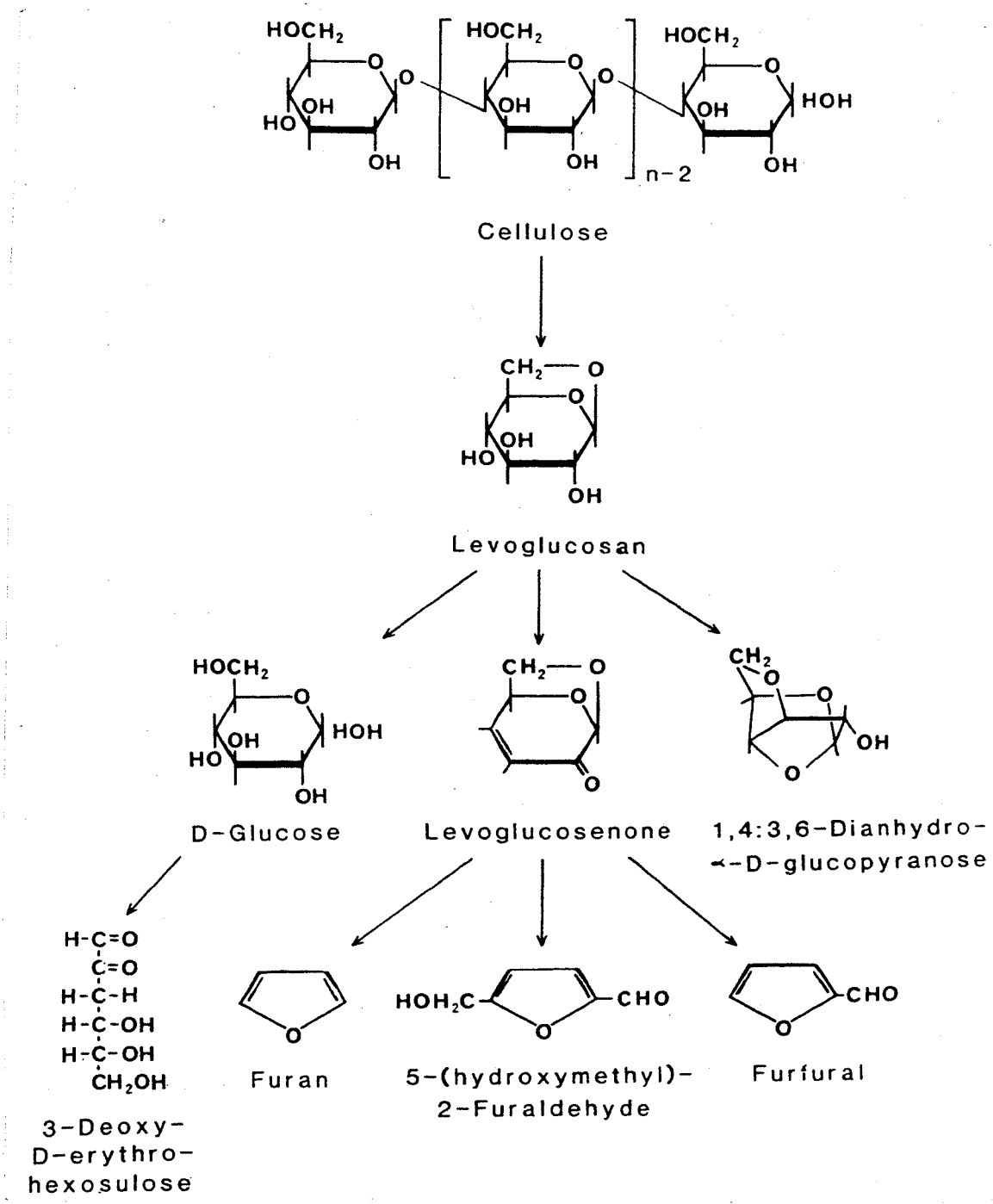

Fig. 13 Dehydration products from cellulose

1.5 Tests for the degradation of cellulose

The degradation of cellulose results primarily in a lowering of the degree of polymerization (DP) by hydrolysis which would eventually give glucose, and also the production of carbonyl groups, carboxyl groups, and the sugars due to oxidation, and thermal decomposition.

The most common manifestation of deterioration is a decrease in average DP of the cellulose evidenced by a loss in tensile strength[74-77]. Determination of the viscosity of a solution of cellulose is the simplest and most commonly used method of estimating the average degree of polymerization of cellulose. This method is based on the fact that in general for long chain molecules solution viscosity increases with chain length[78]. In addition to the average degree of polymerization, chain length uniformity is important. The relative chain length uniformity of different cellulose samples may be determined by fractional solution or precipitation of the derived cellulose nitrates[79]. Size exclusion chromatography (SEC) or gel permeation chromatography (GPC) have become useful methods of determining changes in the molecular weight distribution of paper samples[80-82].

Reductions in DP are also accompanied by a loss of strength. In the pulp and paper industry strength refers to the ability to withstand one or more kinds of applied force[77]. TAPPI (Technical Association of the Pulp and Paper Industry) is considered the authority for setting the standards for paper tests such as tensile strength[83], bursting strength[84], tear resistance and folding endurance[85]. Tensile strength is determined by applying a gradually increasing force to a strip of paper until it breaks[77]. The percentage of elongation of the strip (stretch) before fracture is often measured simultaneously[86]. Tensile testing does not give a quantitative figure for the reduction in DP, but it is fairly sensitive to small changes in DP, and does not introduce additional degradation. It has the advantage of being a very quick and cheap test to perform. The bursting strength is determined by clamping an area of the sheet against a rubber

diaphragm, and applying an increasing force, using hydraulic pressure until the paper bursts. The bursting strength more or less correlates with the tensile strength in the direction in which the paper has the least stretch[77]. The folding endurance of a sheet is the number of double folds that a strip under tension will withstand on a line across its width until fracture[77].

Scanning electron microscopy (SEM) has been used to examine fibres broken in tensile tests[87,88], in order to gain an understanding of the failure mechanism. Results suggest the fracture morphology of the cellulose fibres can yield considerable information on the level of deterioration of the sample.

The oxidation of cellulose results in the formation of carbonyl and carboxyl groups[65]. This even occurs at room temperature in dark conditions due to auto-oxidation[89,90]. Auto-oxidation like photosensitized oxidation (section **1.4 The degradation of cellulose**), seems to proceed by a variety of free radical mechanisms, which generally involve the production of peroxides. Daniels[90-92], has discussed the production of peroxides during the propagation steps of cellulose auto-oxidation (Fig. 9). He has carried out several studies of the peroxides present in oxidising materials, using the Russell effect. The Russell effect is so named because in the course of his experiments, William Russell found that some organic materials were capable of forming a developable image when placed in contact with a photographic film[93-95]. Russell found that hydrogen peroxide was also capable of affecting a photographic plate[96], and suggested that the two results were linked.

Daniels has shown the Russell effect to be a useful method of photographically recording localised increases in the evolution of hydrogen peroxide from paper objects. Unfortunately modern films do not respond to small quantities of peroxides, and need to be specially sensitized using Clifford's method[97]. This involves a sheet of reproduction film being

immersed in dilute aqueous ammonia for a few minutes and then being allowed to dry. This process is called 'ripening' of the emulsion and produces an ultrasensitive film of large grain size.

Although the exact mechanism of image formation using this technique remains unclear, it is assumed that the peroxides cause the silver ions to be reduced to silver metal, as light does during the normal exposure of a film[98].

Eusman[98], has recently used the Russell effect to identify peroxide activity in the tidelines caused by water damage to paper objects. Tidelines are thought be caused by two main mechanisms; firstly the migration of soluble degradation products to the wet/dry boundary, followed by enhanced oxidation at the wet/dry interface, leading to the production of reducing sugars which transform into unsaturated coloured compounds on ageing.

Eusman's Russell images showed the tidelines as dark areas on the film, indicating a higher concentration of peroxides in this region. The Russell effect test provides a fairly simple qualitative test for the presence of peroxides, however if quantitative results are required spectroscopic techniques should be employed. Lomax[99,100], confirmed the presence of peroxides in Eusman's tideline samples by reacting them with iodide ions, to form tri-iodide ions which were measured spectrophotometrically at 362 nm.

Methylene blue (Fig. 14) is frequently used as a quantitative test method for determining the amount of carboxyl groups in cellulose, with dye concentrations measured spectrophotometrically at 625 nm[101,102].

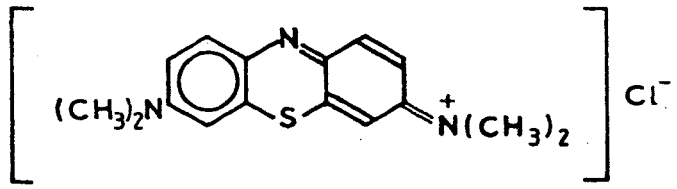

Fig. 14 Structure of methylene blue.

Methylene blue is a basic dye and reacts with acidic groups present on the oxidised cellulose by a cation exchange process[101]. This reaction forms the basis of the standard test for the carboxyl content of cellulose[102].

$$R\text{-}COOH + Mb^{+} \rightarrow R\text{-}COOMb + H^{+} \qquad (2)$$

However, because methylene blue is an easily used and easily visible dye, it has become popular (in fine art conservation research) as a qualitative method for highlighting the presence of carboxyl groups[98,103].

Eusman[98] and Dupont[103], found methylene blue an excellent tool for disclosing the presence of carboxylic acid groups in cellulose tidelines. Strips of paper bearing tidelines were immersed in a methylene blue solution, and increased absorption in the tideline region was observed.

The yellowing of paper is primarily due to the presence of carbonyl groups on the cellulose chains[36,37,67]. The presence of carbonyl groups is usually determined by use of condensation and addition reactions that are characteristic of these groups[65]. Typical examples are the formation of oximes and cyanohydrins (equations 3 and 4 respectively).

$$RCOR^{*} + NH_2OH \leftrightarrow RR^{*}C{=}NOH + H_2O \quad (3)$$

$$RCOR^{*} + NaCN + H_2O \leftrightarrow RR^{*}C(CN)OH + NaOH \quad (4)$$

A different method for measuring the concentration of carbonyl groups in paper consists of reducing them to alcohol groups with sodium borohydride[65,104,105]. Borohydride consumption is estimated from the volume of hydrogen produced by acidifying the solution (equations 5 and 6)

$$4RCOR^{*} + BH_4^{-} + 2H_2O \rightarrow 4RCHOHR^{*} + BO_2^{-} \quad (5)$$

$$BH_4^{-} + H_3O^{+} + H_2O \rightarrow HBO_2 + 4H_2 \quad (6)$$

The tests described have dealt with methods of measuring the results of fairly major chemical change to cellulose. However for more subtle chemical changes, particularly those at the surface of paper, infra-red spectroscopy has become an important technique. Since their introduction in the 1980s Fourier Transform infrared (FTIR) instruments have become widely used for the analysis of chemical change in both paper and cotton textiles[106-114]. The measurement of reflection spectra is thought to be the best method for analysing surfaces[107]. Reflection techniques can be divided into four main categories; specular reflection, diffuse reflection, internal or attenuated total reflection (ATR), and reflection/absorption. Diffuse Reflectance Infrared Fourier Transform (DRIFT) spectroscopy has been widely used for paper analysis since it requires little sample preparation and produces relatively clear spectra of the surface[115,116]. The main absorption peaks for paper have frequently been reported[117-120]. The main peaks of interest are shown in Figure 15. The peaks associated with gelatin are also included as this is frequently found in paper used as a sizing agent[61-63].

Absorbing peak	Wavenumber/ cm^{-1}
Aldehydes	
strong C=O stretching	1740-1720
moderate C-H stretch doublet	2900-2820 and 2775-2700
C=O stretching shifted by conjugation	1705-1680
Ketones	
strong C=O stretching	1725-1705
C=O stretching shifted by conjugation	1685-1665
Acids	
strong C=O stretching	1725-1700
broad complex band due to O-H stretching	3000-2500
carboxylate anion stretching	1610-1550 and 1400-1300
Protein (from gelatin size)	
C=O stretching	1690-1650
N-H stretching	3320-3140
N-H bending, in plane	1680-1580
Carbon skeleton	
C=C stretching shifted by conjugation	1680-1610
C-H stretching	2960-2850
C-H bending	1500-1350
Other sources of peaks	
C-O stretching from carbon dioxide in sample	2350
O-H stretching from water vapour in sample	1640-1630
C-C stretching or 'ring breathing' from aromatics	1600-1450
C-O stretching from alcohols	1450-1300

Fig. 15 Table showing the main infra-red absorption peaks to be expected from a gelatin sized piece of paper.

Paper that has been exposed to high levels of ultra-violet radiation, or extreme acidic conditions for lengthy periods will appear obviously degraded, however for a good quality paper, it may take a considerable time for visible discoloration to occur under normal conditions. Accelerated ageing is an attempt to simulate in a short time the effects of natural ageing over a much longer period[121-133] . It is generally used to test for the permanence of materials or the effects of treatments on the permanence of materials. Accelerated ageing can consist of exposure to changes in any combination of damaging environmental factors including heat, humidity, light, oxygen and pollution. It is assumed that accelerated ageing

simply speeds up the degradation reactions which occur under normal conditions. However the relative rates of these competing reactions are not known and their contributions to the deterioration of cellulose have not been established[134-137]. Striking artificial ageing results can be achieved very quickly using extreme conditions, however these are unlikely to represent natural ageing with much accuracy. There is no accepted set of standard accelerated ageing conditions, therefore workers in this field are obliged to choose techniques and conditions they feel most adequately serve their purpose.

Light ageing[121], can be used to simulate, over a short period, the exposure of an object to long periods of natural light. Ultra-violet light and to certain extent visible light can lead to the photo-oxidation and consequent discoloration of cellulose[37-41]. This is more likely to happen if parts of the cellulose or associated materials are able to absorb ultra-violet light (section **1.4 The degradation of cellulose**). Therefore light ageing is useful in determining the extent of conjugation within the cellulose, and the extent of chromophoric material present[38,66].

Oven ageing cellulose[122-133], tends to accelerate the rate of degradation[121]. If the oven is kept dry and maintained at a high temperature, then oxidation reactions[68,69], will tend to dominate over hydrolytic scissions which are catalysed by acidic aqueous conditions[64,65].

Humid oven ageing[122-128], is generally operated at lower temperatures than dry oven ageing. This allows for both thermal oxidation and hydrolysis reactions to take place, but hydrolysis is the dominating factor. This results in the scission of cellulose chains (section **1.4 The degradation of cellulose**). Colour changes in paper have frequently been observed after humid ageing[122,130,132,133]. Kleinert and Marraccini[132,133], suggest that the colour changes are due to the presence of chromophoric groups formed at random along the cellulose chains.

These unsaturated bonds represent weak links where chain splitting takes place, thus producing small, unsaturated molecules with increased absorption of near ultra-violet light. The presence of sugars in degraded cellulose can be determined using gas chromatography[138]. This technique can be used to separate and analyse the components of complex compounds with a high degree of sensitivity. For gas chromatography (GC) the sample is derivatised to make it volatile then injected into the carrier gas that forms the mobile phase. This carries it onto and through the column, which is a coiled glass tube the insides of which are coated with the stationary phase. Compounds are detected as they emerge from the column, each having a characteristic retention time depending on its polarity and volatility. The temperature of the column is gradually raised in order to ensure that even the less volatile compounds pass through. Compounds can be identified by comparing the retention times with those of reference compounds, held in the computer's data banks, or run through the column. If the GC is connected to a mass spectrometer (MS) then this can provide further means of identification from the mass spectra of the compounds. Dupont[139] has used GC/MS to investigate the compounds present in the discoloration created at the wet/dry interface of water stained paper. This involves a derivatisation stage which Vallance[140], has modified.

1.6 The anticipated outcome of Nd:YAG (1064 nm) laser use on paper

Previous research using Nd:YAG lasers for cleaning purposes, has led to discussion on estimating the temperature rise at the material surface[1,6,7,57]. The estimates assume a fairly absorbent medium and though they vary considerably, all exceed 370° C. The estimates represent the temperature rise at the pulse impact site, the temperature rise to surrounding material would be considerably less. These calculations assume the use of very short duration Q-switched laser pulses, which means that the pulse has finished before significant amounts of heat can be conducted into the material. Where longer pulses are employed, the heating effect of the Nd:YAG laser is likely to be more in evidence[1,2,26].

Shafizadeh[68,69] (**1.4 The degradation of cellulose**), has shown the thermal degradation of cellulose to occur via oxidation and depolymerisation, resulting in the production of carbonyl groups, carboxyl groups and sugars. Engel[141], and has studied the pyrolysis products produced by the use of CO_2 lasers on wood. The predominant products were found to be saturated and unsaturated hydrocarbons, alcohols, carbonyls, carboxylic acids and aromatics.

These previous pieces of research infer the most likely chemical effect of relatively long Nd:YAG (1064 nm) laser pulses (100 ns), on cellulose will be oxidation and/or depolymerisation.

CHAPTER 2:

EXPERIMENTAL

2.1 Strategy of the research programme

The laser used for the research was a Q-switched Nd:YAG operated at its fundamental wavelength of 1064 nm. Characterisation of the laser showed that the pulse duration range was from 25 ns to over 200 ns, depending on the output (see section **2.2 Laser characterisation**).

The aim of this research programme was primarily to investigate the efficiency of the laser as a tool for ink removal from paper, and to assess the physical and chemical effect of laser interaction with paper. The secondary goal was an exploration of methods to improve the efficiency of ink removal and to reduce any damage caused during treatment.

The laser had pulse repetition rate options of single shot, 10Hz, 20Hz and 30Hz. Most of this research was undertaken with a focused laser, and therefore single shot operation was considered impractical due to the spot size. The pulse repetition rate of 10Hz was chosen and used throughout this research programme. It was assumed that if the laser had a tendency to cause heat increases in paper, then allowing as much time as possible for heat dissipation between pulses, was desirable.

Experimental Part One involves an investigation into the effectiveness of ink removal from paper by the laser. The purpose of this section was to establish whether the Nd:YAG laser could be used to remove modern inks from paper, and to determine threshold levels for a) ink removal and, b) visible damage to, paper samples.

It was beyond the scope of this research to test all ink types and all paper types, therefore a small selection of papers and inks were chosen to represent the entire range. The most

commonly occurring modern inks found added to works of art are from ball-point pens, fibre tip pens, and highlighter pens. Therefore a selection of coloured ball-point pens, fibre tip pens and highlighter pens were used for the ink removal studies.

The type of paper on which works of art are painted largely depends on the era from which they were executed. Originally paper was hand made from cotton and linen, but since the early 1800s there has been increasingly widespread use of woodpulp[60]. Modern papermaking manufacturers can produce a wide range of paper products ranging from the poorest quality mechanical woodpulp paper, to chemically processed woodpulp, and cotton papers. Four paper types were chosen to carry out preliminary tests, a hand made cotton paper, a machine made cotton paper, a chemically processed woodpulp paper and mechanical woodpulp paper.

The effectiveness of the Nd:YAG laser for ink removal was also assessed in an argon atmosphere, to determine whether ink removal by laser was dependent on the presence of oxygen.

Experimental Part Two involves an investigation into the physical and chemical damage caused to paper as a result of laser treatment (see sections **2.4 Investigation of physical damage to Nd:YAG treated paper**, and **2.5 Investigation of chemical damage to Nd:YAG treated paper**). The laser parameters chosen for Part Two were dependent on the ink removal threshold fluences established in Part One however, in these sections the paper samples were left un-inked to establish the nature of the interaction between laser and paper. It must be understood that the results do not necessarily mirror the physical and chemical damage caused during ink removal. It is assumed that ink (particularly dark ink), will absorb infra-red radiation and be vaporized without conduction of significant heat into the paper

substrate. The purpose of Experimental Part Two is to establish whether laser treatment of paper can be considered self-limiting in the same way as treatment of marble and stone[1,2,6-9].

It was anticipated that changes to paper caused by laser treatment may not become apparent until some time in the distant future. Accelerated ageing (see section **1.5 Tests for the degradation of cellulose**) tests were carried out on laser treated paper and compared with similarly aged untreated paper[121-133].

2.2 Laser characterisation

2.2.1 Laser operation and safety.

The laser used for the research programme was a Nd:YAG System 2000 from J.K. Lasers Ltd. Rugby, with a pulsed flashlamp as the pump source. The laser was operated according to guidelines given in BS EN 60825:1992 Radiation safety of laser products. A fully interlocked room was employed and the laser was automatically switched off if the door was opened during operation. The room was adequately lit and all operators wore safety glasses with an optical density sufficient to reduce the optical exposure to the eye below the maximum permissible exposure (MPE) level for intra beam viewing as outlined in BS EN 60825:1992.

Many pulsed lasers can produce a train of pulses as shown (Fig. 16) and if these are directed on to a thermal detector an average power will be recorded provided the response time of the detector is much longer than the time between the pulses (pulse period).

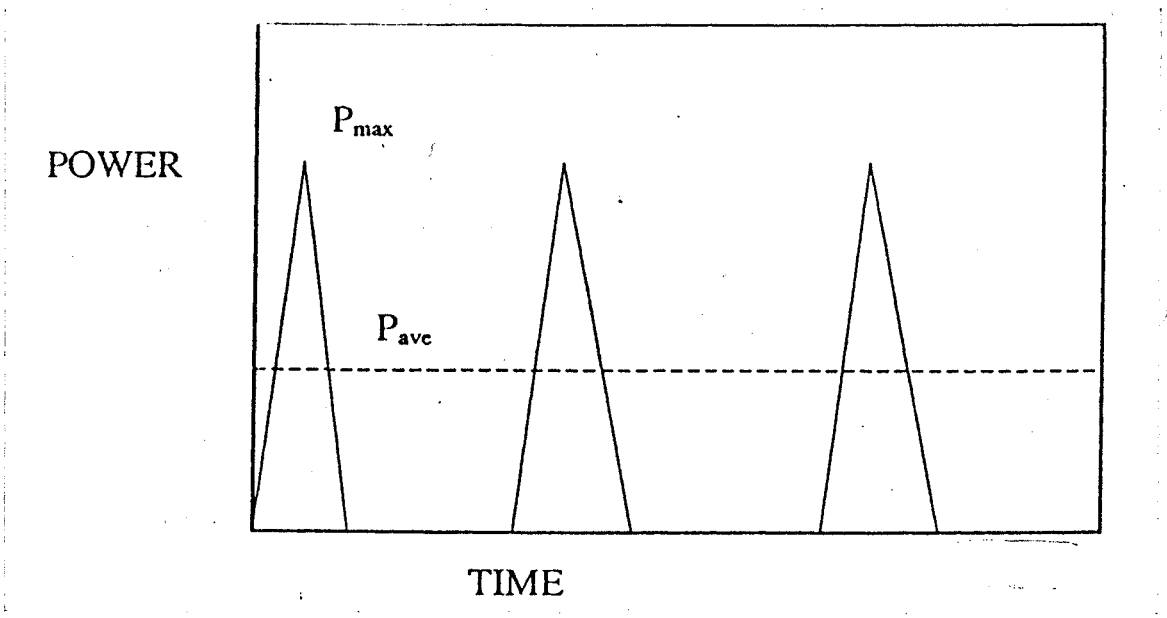

Fig. 16 Schematic diagram of ideal laser pulses.

This is very different to the maximum power (or peak power) in the pulse. Dividing the measured average power by the number of pulses per second will give the average energy per pulse. For heat treatment of any kind it is usually the power (for a CW laser), or energy (for a pulsed laser) delivered per unit area, which is important. Fluence is defined as the energy per unit area in units of Jm^{-2} or Jcm^{-2}. Average fluence can therefore be calculated by dividing the energy per pulse by the spot area, assuming that the energy is evenly distributed across the beam. To determine these parameters it is necessary to know the radius of the beam and, if the beam is not uniform, its radial power or energy distribution.

For the simplest beam, one with a fundamental or TEM_{00} mode the single-peak bell-shaped profile has a mathematical form of a Gaussian function[56,142,143]. This leads to a definition for the beam diameter 2w, as the distance between points where the intensity falls to $1/e^2$ (13.5%) of peak value I_0, (Fig. 17).

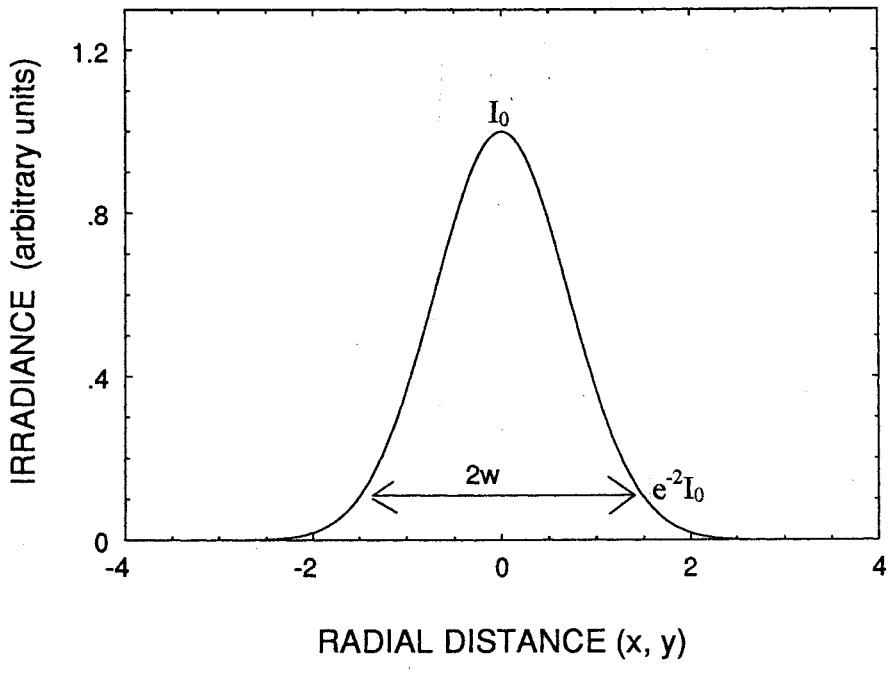

Fig. 17 Intensity distribution profile for a TEM_{00} mode beam.

All TEM_{00} laser beams, when focused by a convex lens converge to a smallest diameter $2w_0$ called the waist, and then diverge as they propagate[143]. This can be expressed by the equation,

$$w_z = w_0[\,1 + (\lambda z/\pi\, w_0{}^2)^2]^{0.5} \qquad (7)$$

where w_z is the radius of a laser beam at a distance, z, from the waist position, w_0 is the radius at the waist, and λ is the wavelength of the light.

Many lasers produce beams that comprise modes of higher order than the TEM_{00} mode, and consequently equation (7) does not accurately describe how these beams propagate. Sasnett[142], has shown that as higher order modes propagate, the square of the beam diameter will increase proportionally as the square of the distance from the waist, and that the proportionality constant is M^2. This means that the radius of a higher order mode beam W_0, is larger than the TEM_{00} mode equivalent w_0 by a factor M, and this remains the case at any distance z from the waist position. Therefore,

$$W_0 = Mw_0 \quad \text{and} \quad W_z = Mw_z \qquad (8)$$

substituting into equation (7) gives,

$$W_z = W_0[\,1 + (M^2\,\lambda\, z/\pi\, W_0{}^2)^2]^{0.5} \qquad (9)$$

2.2.2 Determination of the location and spot size for the Nd:YAG laser at the waist.

There are several methods of experimentally determining the parameters of a Gaussian beam[144-148]. One of the simplest methods makes use of a knife edge to chop the beam at several distances z, from the waist position[144,145]. For a Gaussian beam the diameter $2w_z$ at each point is the distance between the positions where the transmitted power equals 86.5% ($1 - 1/e^2$), and 13.5% ($1/e^2$), peak value[142,143]. For a higher order mode, with a top hat profile, such as the beam used in this research, a more accurate definition of spot diameter $2w_z$ is the distance between positions where the knife edge i) first attenuates, and ii) completely attenuates the beam (see section **2.2.3 Determination of beam profile..**).

The spot radius at the waist and the waist location can be determined by making a plot of equation (9), using the values of w_z and z, recorded during knife edge profiling.

A 10 cm focal length convex lens was placed in the path of the laser beam and the power recorded by a calorimeter (Scientec) positioned approximately 1 m. from the lens. The calorimeter was aligned using a thermal imaging plate. The plate has a thermoluminescent coating, which does not emit light when infra-red radiation hits it, and thus a dark spot is formed on the plate in the presence of IR. This property was used to estimate the beam diameter as approximately 15 mm. at a distance of 1 m. from the lens. The aperture of the calorimeter was approximately 30 mm. in diameter, and therefore all the energy from the beam was assumed to have been collected by the meter.

A knife-edge mounted on a micrometer screw was placed between the lens and the detector, at a distance z_1 (where $z_1 < 10$ cm.) from the lens such that it did not interfere with the passage of the laser beam to the detector (Fig. 18).

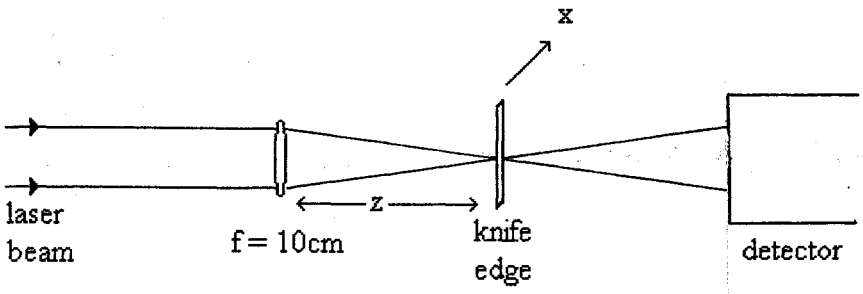

Fig. 18 Arrangement of apparatus for the scanning knife edge experiment, used to determine the spot size (Wz), of the laser beam at a given distance (z), from the lens.

The knife-edge was moved in stages across the beam until all laser light was incident on the knife blade, thus preventing any from reaching the detector. The decrease in power transmitted to the detector was recorded at each stage. The knife-edge was repositioned further from the lens z_2 and moved across the beam as before. This process was repeated several times until the knife-edge had passed beyond the focal length of the lens, Tables 1 - 20. A graph, showing the decrease in transmitted power as the knife passed through the laser beam, was plotted for each position z of the knife-edge from the lens (Fig. 19). In each case the spot radius Wz was calculated for position z, (Table 21), assuming a top hat beam profile (see section **2.2.3**).

The experiment was completed over several days, during which time other researchers made use of the laser, and consequently a different output was achieved for each calculation of z (see Tables 1–20). However a flashlamp voltage of 625 V ± 5 V, was used on each occasion to ensure uniform pulse durations. The beam size was assumed to be independent of energy for the spot radius calculations, Table 21.

The graph of spot radius Wz against knife edge position z, was plotted and shows the spot size at the waist, W_0 to be 125 ± 18 μm, and the position of the waist to be 10.3 ± 0.1 cm. from the lens (Fig. 20). The error on the spot size was determined using equation 1, Appendix 1.

Micrometer reading / $10^{-3} \pm 1x10^{-3}$ cm	Transmitted power / mW ± 1 mW	Micrometer reading / $10^{-3} \pm 1x10^{-3}$ cm	Transmitted power / mW ± 1 mW
1300	46	1220	22
1290	46	1210	17
1280	46	1200	13
1270	45	1190	9
1260	41	1180	6
1250	36	1170	3
1240	31	1160	1
1230	27	1150	0

Table 1. Power transmitted as the knife edge (7cm. from the lens) is moved across the path of the Nd:YAG laser beam.

Micrometer reading / $10^{-3} \pm 1x10^{-3}$ cm	Transmitted power / mW ± 1 mW	Micrometer reading / $10^{-3} \pm 1x10^{-3}$ cm	Transmitted power / mW ± 1 mW
1320	44	1250	16
1310	44	1240	10
1300	44	1230	6
1290	40	1220	3
1280	35	1210	1
1270	28	1200	0
1260	23		

Table 2. Power transmitted as the knife edge (8cm. from the lens) is moved across the path of the Nd:YAG laser beam.

Micrometer reading / $10^{-3} \pm 1x10^{-3}$ cm	Transmitted power / mW ± 1 mW	Micrometer reading / $10^{-3} \pm 1x10^{-3}$ cm	Transmitted power / mW ± 1 mW
1320	43	1280	14
1310	43	1275	10
1305	39	1270	6
1300	34	1265	3
1295	29	1260	1
1290	23	1255	0
1285	19		

Table 3. Power transmitted as the knife edge (9cm. from the lens) is moved across the path of the Nd:YAG laser beam.

Micrometer reading / $10^{-3} \pm 1x10^{-3}$ cm	Transmitted power / mW ± 1 mW	Micrometer reading / $10^{-3} \pm 1x10^{-3}$ cm	Transmitted power / mW ± 1 mW
1330	45	1290	17
1320	45	1285	11
1310	43	1280	7
1305	39	1275	3
1300	32	1270	1
1295	23	1265	0

Table 4. Power transmitted as the knife edge (9.5cm. from the lens) is moved across the path of the Nd:YAG laser beam.

Micrometer reading / $10^{-3} \pm 1x10^{-3}$ cm	Transmitted power / mW ± 1 mW	Micrometer reading / $10^{-3} \pm 1x10^{-3}$ cm	Transmitted power / mW ± 1 mW
1330	45	1290	20
1320	45	1285	13
1310	45	1280	7
1305	44	1275	3
1300	38	1273	1
1295	29	1270	0

Table 5. Power transmitted as the knife edge (9.7cm. from the lens) is moved across the path of the Nd:YAG laser beam.

Micrometer reading / $10^{-3} \pm 1x10^{-3}$ cm	Transmitted power / mW ± 1 mW	Micrometer reading / $10^{-3} \pm 1x10^{-3}$ cm	Transmitted power / mW ± 1 mW
1330	43	1310	15
1325	43	1305	7
1320	34	1300	2
1315	23	1295	0

Table 6. Power transmitted as the knife edge (10cm. from the lens) is moved across the path of the Nd:YAG laser beam.

Micrometer reading / $10^{-3} \pm 1x10^{-3}$ cm	Transmitted power / mW ± 1 mW	Micrometer reading / $10^{-3} \pm 1x10^{-3}$ cm	Transmitted power / mW ± 1 mW
1330	41	1270	16
1290	41	1265	8
1285	41	1260	1
1280	37	1255	0
1275	24		

Table 7. Power transmitted as the knife edge (10.1cm. from the lens) is moved across the path of the Nd:YAG laser beam.

Micrometer reading / $10^{-3} \pm 1x10^{-3}$ cm	Transmitted power / mW ± 1 mW	Micrometer reading / $10^{-3} \pm 1x10^{-3}$ cm	Transmitted power / mW ± 1 mW
1330	40	1275	12
1290	40	1270	4
1288	37	1268	1
1285	30	1265	0
1280	19		

Table 8. Power transmitted as the knife edge (10.2cm. from the lens) is moved across the path of the Nd:YAG laser beam.

Micrometer reading / $10^{-3} \pm 1x10^{-3}$ cm	Transmitted power / mW ± 1 mW	Micrometer reading / $10^{-3} \pm 1x10^{-3}$ cm	Transmitted power / mW ± 1 mW
1330	42	1280	18
1295	42	1275	8
1290	40	1271	1
1285	25	1270	0

Table 9. Power transmitted as the knife edge (10.3cm. from the lens) is moved across the path of the Nd:YAG laser beam.

Micrometer reading / $10^{-3} \pm 1x10^{-3}$ cm	Transmitted power / mW ± 1 mW	Micrometer reading / $10^{-3} \pm 1x10^{-3}$ cm	Transmitted power / mW ± 1 mW
1320	48	1295	26
1310	48	1290	14
1305	46	1285	1
1300	38	1280	0

Table 10. Power transmitted as the knife edge (10.4cm. from the lens) is moved across the path of the Nd:YAG laser beam.

Micrometer reading / $10^{-3} \pm 1x10^{-3}$ cm	Transmitted power / mW ± 1 mW	Micrometer reading / $10^{-3} \pm 1x10^{-3}$ cm	Transmitted power / mW ± 1 mW
1320	48	1300	27
1310	48	1295	14
1308	45	1290	2
1305	39	1285	0

Table 11. Power transmitted as the knife edge (10.5cm. from the lens) is moved across the path of the Nd:YAG laser beam.

Micrometer reading / $10^{-3} \pm 1x10^{-3}$ cm	Transmitted power / mW ± 1 mW	Micrometer reading / $10^{-3} \pm 1x10^{-3}$ cm	Transmitted power / mW ± 1 mW
1320	48	1300	23
1315	48	1295	8
1310	43	1293	3
1305	34	1290	0

Table 12. Power transmitted as the knife edge (10.6cm. from the lens) is moved across the path of the Nd:YAG laser beam.

Micrometer reading / $10^{-3} \pm 1x10^{-3}$ cm	Transmitted power / mW ± 1 mW	Micrometer reading / $10^{-3} \pm 1x10^{-3}$ cm	Transmitted power / mW ± 1 mW
1330	48	1295	16
1320	48	1290	5
1310	46	1287	1
1305	38	1285	0
1300	29		

Table 13. Power transmitted as the knife edge (10.7cm. from the lens) is moved across the path of the Nd:YAG laser beam.

Micrometer reading / $10^{-3} \pm 1x10^{-3}$ cm	Transmitted power / mW ± 1 mW	Micrometer reading / $10^{-3} \pm 1x10^{-3}$ cm	Transmitted power / mW ± 1 mW
1330	48	1305	24
1320	48	1300	12
1315	42	1295	1
1310	34	1290	0

Table 14. Power transmitted as the knife edge (10.8cm. from the lens) is moved across the path of the Nd:YAG laser beam.

Micrometer reading / $10^{-3} \pm 1x10^{-3}$ cm	Transmitted power / mW ± 1 mW	Micrometer reading / $10^{-3} \pm 1x10^{-3}$ cm	Transmitted power / mW ± 1 mW
1370	43	1340	25
1360	43	1335	17
1355	41	1330	8
1350	36	1325	1
1345	30	1320	0

Table 15. Power transmitted as the knife edge (11cm. from the lens) is moved across the path of the Nd:YAG laser beam.

Micrometer reading / $10^{-3} \pm 1x10^{-3}$ cm	Transmitted power / mW ± 1 mW	Micrometer reading / $10^{-3} \pm 1x10^{-3}$ cm	Transmitted power / mW ± 1 mW
1410	41	1370	21
1400	41	1365	18
1395	38	1360	13
1390	35	1355	10
1385	32	1350	6
1380	28	1345	3
1375	25	1340	0

Table 16. Power transmitted as the knife edge (12cm. from the lens) is moved across the path of the Nd:YAG laser beam.

Micrometer reading / $10^{-3} \pm 1x10^{-3}$ cm	Transmitted power / mW ± 1 mW	Micrometer reading / $10^{-3} \pm 1x10^{-3}$ cm	Transmitted power / mW ± 1 mW
1470	40	1400	19
1460	40	1390	13
1450	39	1380	18
1440	37	1370	4
1430	33	1365	2
1420	29	1360	0
1410	24		

Table 17. Power transmitted as the knife edge (13cm. from the lens) is moved across the path of the Nd:YAG laser beam.

Micrometer reading / $10^{-3} \pm 1x10^{-3}$ cm	Transmitted power / mW ± 1 mW	Micrometer reading / $10^{-3} \pm 1x10^{-3}$ cm	Transmitted power / mW ± 1 mW
1510	40	1430	22
1500	40	1420	18
1490	39	1410	14
1480	37	1400	10
1470	35	1390	7
1460	32	1380	4
1450	28	1370	1
1440	25	1365	0

Table 18. Power transmitted as the knife edge (14cm. from the lens) is moved across the path of the Nd:YAG laser beam.

Micrometer reading / $10^{-3} \pm 1x10^{-3}$ cm	Transmitted power / mW ± 1 mW	Micrometer reading / $10^{-3} \pm 1x10^{-3}$ cm	Transmitted power / mW ± 1 mW
1620	39	1480	17
1600	39	1460	13
1580	37	1440	8
1560	34	1420	4
1540	30	1410	1
1520	26	1400	0
1500	22		

Table 19. Power transmitted as the knife edge (16cm. from the lens) is moved across the path of the Nd:YAG laser beam.

Micrometer reading / $10^{-3} \pm 1x10^{-3}$ cm	Transmitted power / mW ± 1 mW	Micrometer reading / $10^{-3} \pm 1x10^{-3}$ cm	Transmitted power / mW ± 1 mW
1800	46	1610	22
1790	46	1570	16
1770	44	1530	9
1730	40	1490	3
1690	35	1470	1
1650	29	1450	0

Table 20. Power transmitted as the knife edge (20cm. from the lens) is moved across the path of the Nd:YAG laser beam.

Position of knife edge (z) from lens (A) / cm ± 0.1 cm	Value of x where knife edge first attenuates laser beam A / $10^{-3} \pm 2.5x\ 10^{-3}$ cm	Value of x where knife edge completely attenuates laser beam B / $10^{-3} \pm 2.5x\ 10^{-3}$ cm	Spot radius W_z (A-B)/2 μm ± 18 μm
7.0	1280	1150	650
8.0	1300	1200	500
9.0	1310	1255	275
9.5	1320	1265	275
9.7	1310	1270	200
10.0	1325	1295	150
10.1	1285	1255	150
10.2	1290	1265	125
10.3	1295	1270	125
10.4	1310	1280	150
10.5	1310	1285	125
10.6	1315	1290	125
10.7	1320	1285	175
10.8	1320	1290	150
11.0	1360	1320	200
12.0	1400	1340	300
13.0	1460	1360	500
14.0	1500	1365	675
16.0	1600	1400	1000
20.0	1790	1450	1700

Table 21. Measurements for the determination of Nd:YAG laser spot radius Wz, incident on a knife edge at a distance (z), from a 10 cm. lens.

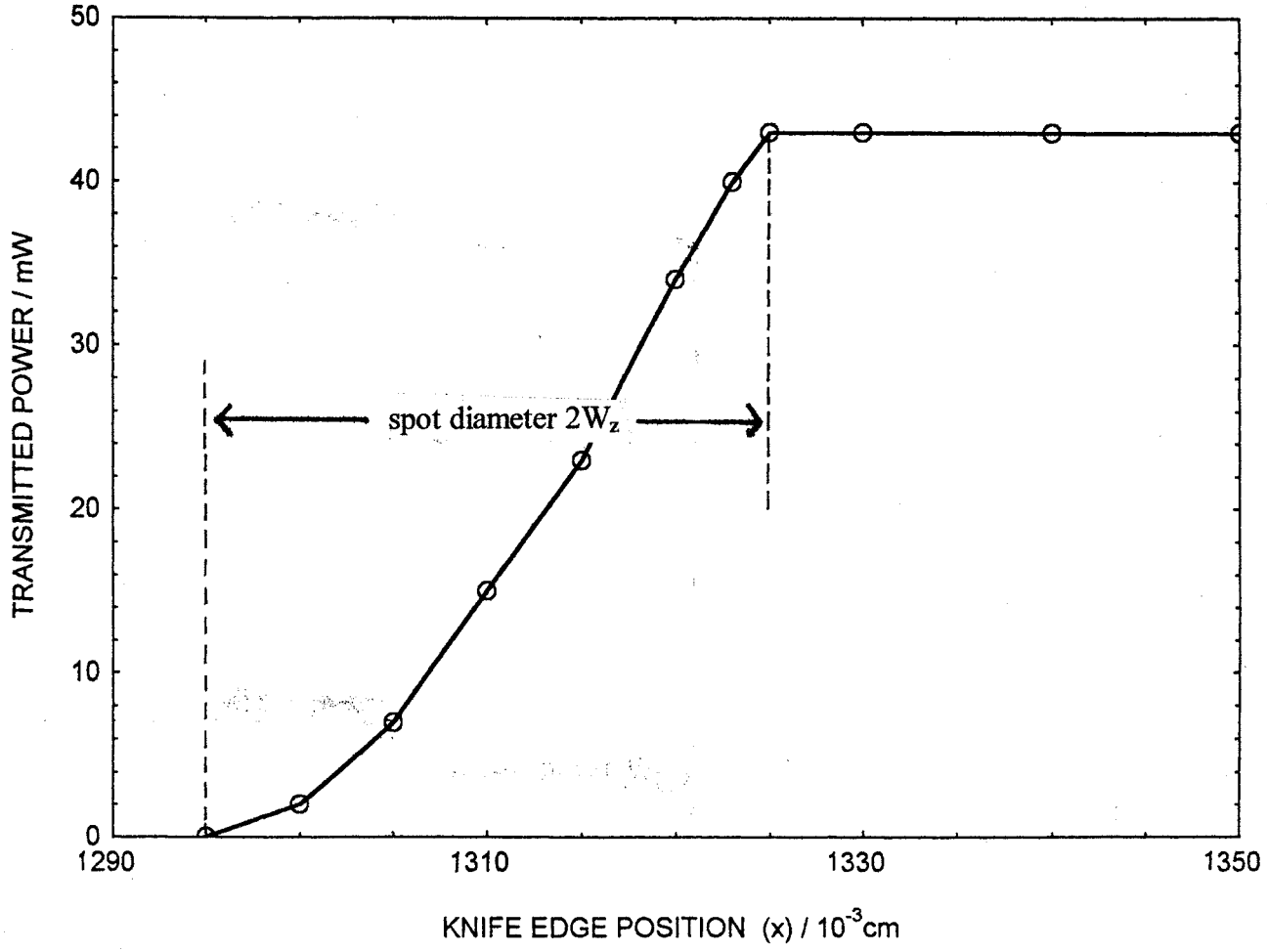

Fig. 19 Graph showing the amount of power transmitted as a knife-edge is moved across the Nd:YAG laser beam, and how the spot diameter is determined

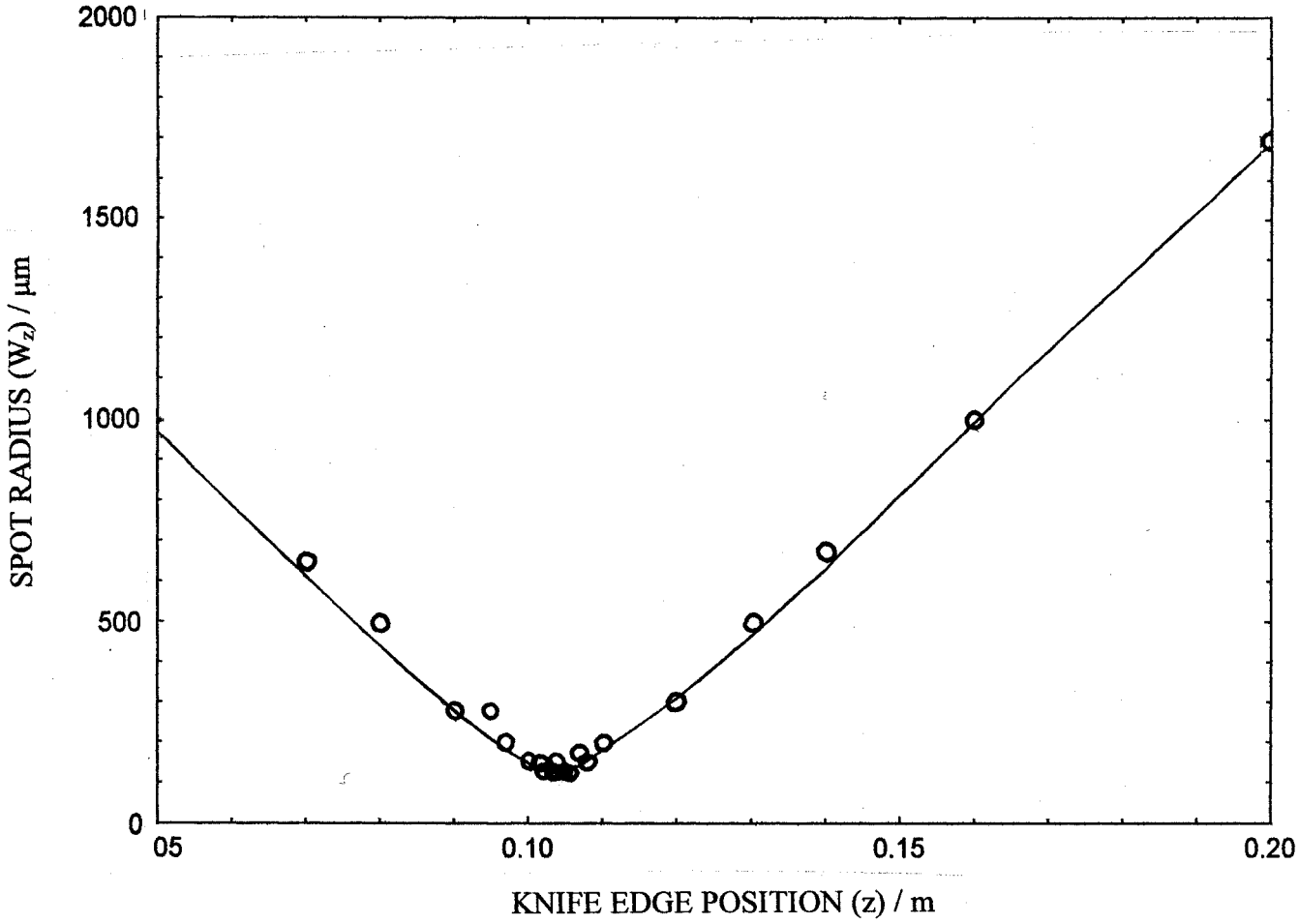

Fig. 20 Graph showing the relationship between spot size of the Nd:YAG beam, and the position of a target (knife-edge) from a 10 cm. lens.

2.2.3 Determination of the beam profile for the Nd:YAG laser.

The intensity distribution across a beam at a point along its propagation axis is readily obtained with a beam profiler[142,143]. This instrument moves a pinhole through the beam and measures the transmitted power to present a plot of the relative intensity versus the distance off the beam axis.

A recent paper by Wazen[149], presented a comparison between Gaussian and top hat shaped, higher order beam distributions for laser cleaning applications. The Gaussian distribution produces a maximum intensity at the centre and decreases when going to the edge, while the top hat laser beam intensity distribution is flat and drops off sharply at the edges, hence the re-definition of the beam diameter as the distance between positions where a knife edge i) first attenuates, and ii) completely attenuates the beam (see section **2.2.2**).

The results show that for efficiency, selectivity of cleaning and homogeneity, the top hat laser beam intensity distribution is preferred. Wazen found that for a given pulse energy, nearly 100% of the energy contributes to cleaning for the top hat beam, in contrast to a 40% contribution from the Gaussian beam.

An aluminium disc with a 1 mm pinhole through the centre was mounted on a micrometer screw and placed in the path of the unfocused Nd:YAG laser (flashlamp voltage 580 V) and the power recorded by a calorimeter (Fig. 21).

The pinhole was positioned so that the centre of the beam was aligned with the pinhole. The pinhole was moved horizontally, and vertically across the laser beam and the power transmitted to the detector recorded at regular increments. The experiment was repeated four times and the average value of each result noted, Tables 22 & 23.

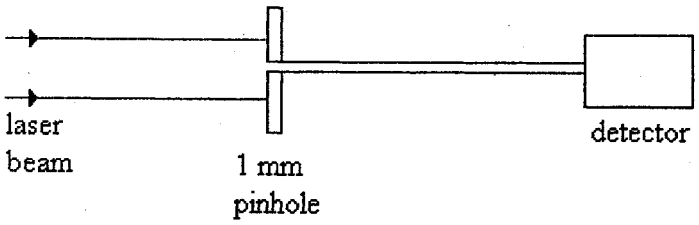

Fig. 21 Arrangement of apparatus for the determination of the beam profile of the Nd:YAG laser.

Graphs of transmitted power against pinhole position (vertical and horizontal) were plotted to show the laser beam profile (Figs. 22 & 23). These show that the energy distribution of the laser at the surface of a target is uniform (within 30 %), and that the diameter of the beam was roughly the same vertically as horizontally. The beam profile results (Figs. 22 & 23) showed that the beam resembled a top hat profile far more closely than a Gaussian profile, and therefore suggested that the spot size calculations (see section **2.2.2**), should be determined as the distance between positions where a knife edge i) first attenuates, and ii) completely attenuates the beam. For fluence calculations the beam was assumed to be circular, the energy distribution uniform, and the beam size independent of energy. The average fluence values calculated throughout the research were therefore calculated by dividing the pulse energy by the spot area. The determination of the spot size (see section **2.2.2),** lead to an uncertainty of ±18 μm. (see **Appendix 1, Calculation of errors**).This value of uncertainty in the spot size produces an uncertainty in the spot area of roughly 30 %, and hence an absolute uncertainty in average fluence of 30 %, although the relative uncertainties are smaller. Throughout this research the values of average fluence used will be referred to as nominal fluence and will have an error of 30 %.

Micrometer reading / mm ± 0.5 mm	Transmitted power / mW ± 0.1 mW
16	0
16.5	0.7
17	2.0
17.5	3.8
18	7.0
18.5	10.5
19	12.0
19.5	12.4
20	12.4
20.5	12.3
21	11.6
21.5	12.0
22	11.3
22.5	5.0
23	1.5
23.5	0.2
24	0

Table 22. Transmitted power against pinhole position, as a 1 mm. pinhole is moved vertically across the unfocused laser beam, passing through the centre.

Micrometer reading / mm ± 0.5 mm	Transmitted power / mW ± 0.1 mW
3	0
3.5	2.0
4	5.9
4.5	8.7
5	9.8
5.5	10.0
6	10.0
6.5	10.5
7	12.0
7.5	12.1
8	11.4
8.5	11.1
9	12.0
9.5	11.0
10	6.5
10.5	2.8
11	1.1
11.5	0

Table 23. Transmitted power against pinhole position, as a 1 mm. pinhole is moved horizontally across the unfocused laser beam, passing through the centre.

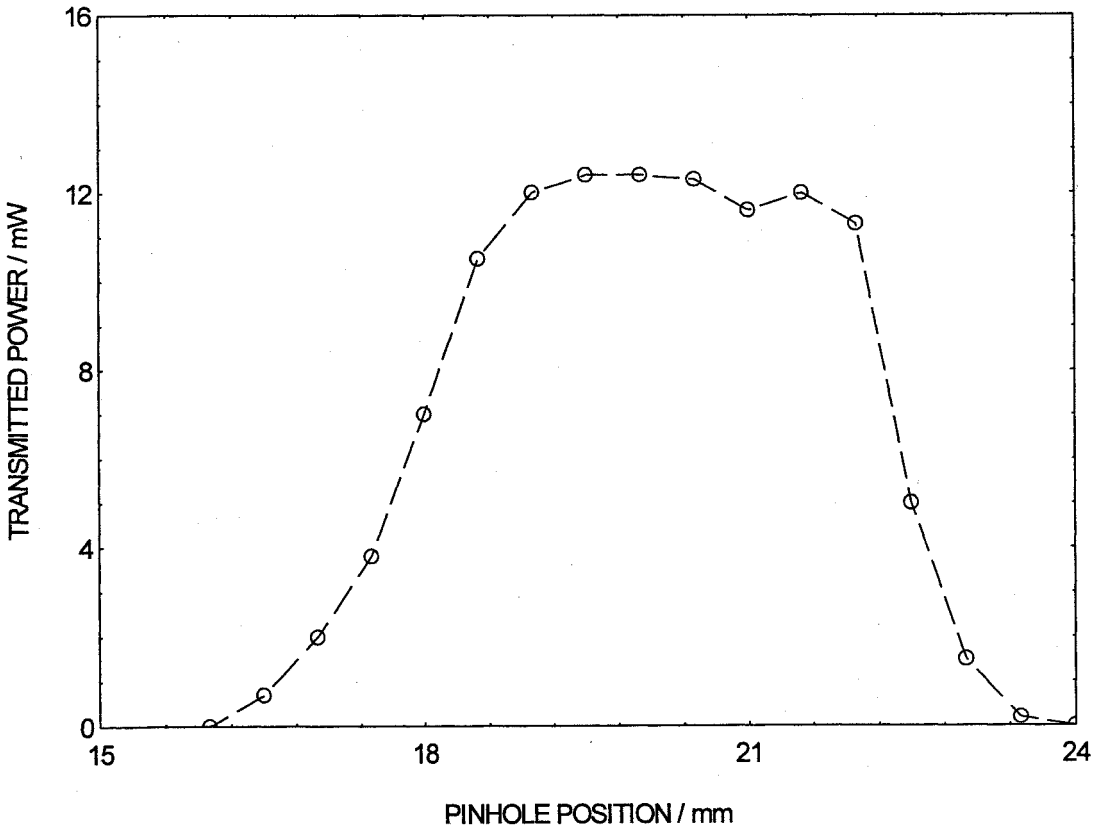

Fig. 22 Profile of the Nd:YAG laser beam measured as the pinhole was moved vertically through its centre.

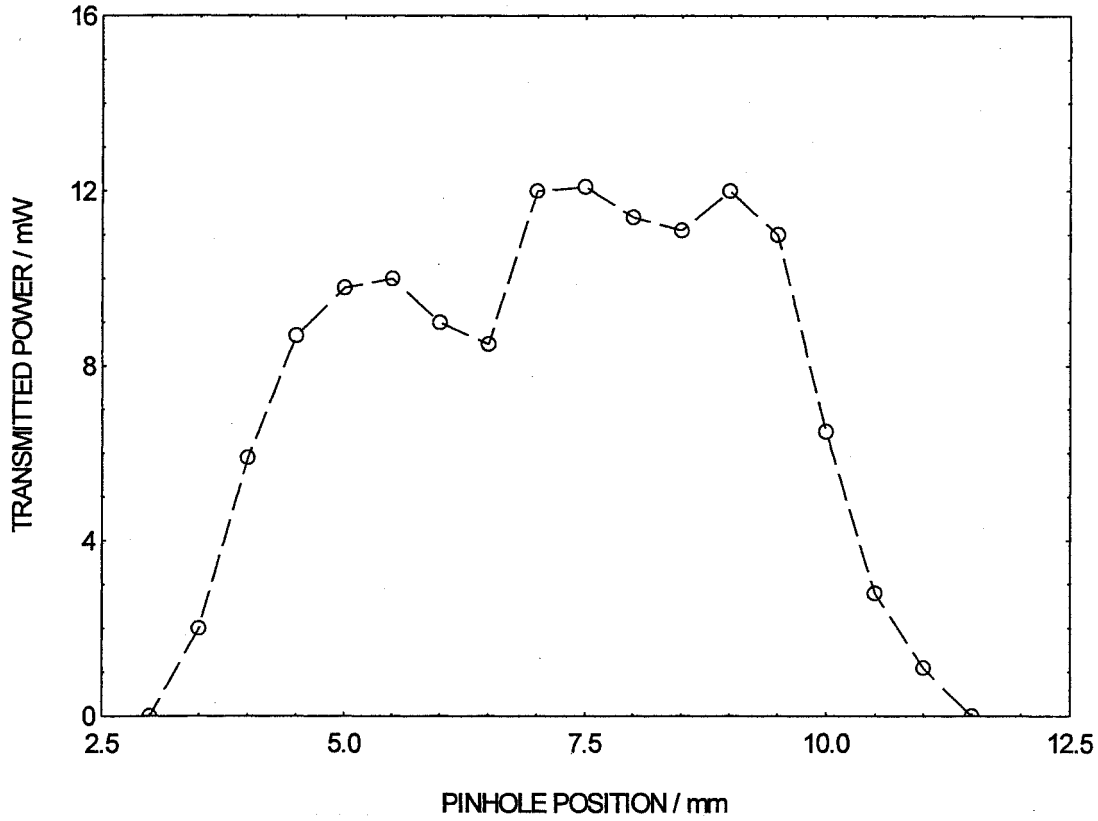

Fig. 23 Profile of the Nd:YAG laser beam measured as the pinhole was moved horizontally through its centre.

2.2.4 Measurement of output, pulse duration, and peak power determination for the Q-switched Nd:YAG laser.

The pulse profile can be observed using a fast oscilloscope. A typical pulse is shown in Figure 24. The shape of the laser pulse is roughly triangular (Fig. 25), and the pulse energy is determined as the area under the pulse. The pulse length is defined as the width of the pulse at half the maximum power (FWHM). The peak power can therefore be determined from measurement of energy, and pulse duration,

$$P_{peak} = \frac{E}{\Delta t} \qquad (10)$$

where P_{peak} is the peak power, E is the pulse energy, and Δt is the pulse duration[56].

The average energy output from the Nd:YAG laser was recorded over a range of flashlamp voltages (525 - 800 V), and the results recorded, (Fig. 26; Table 24). The pulse rise times and durations (FWHM) were determined using a GaAs detector connected to a 500 MHz oscilloscope. These measurements were repeated ten times on individual pulses and the average value recorded, Table 24. The relationship between the pulse rise time and the flashlamp voltage is presented graphically, (Fig. 27). The peak power of laser pulses over the voltage range 570 – 800 V, was determined and recorded, Table 24. The error for each value of peak power was determined using equation 3, Appendix 1.

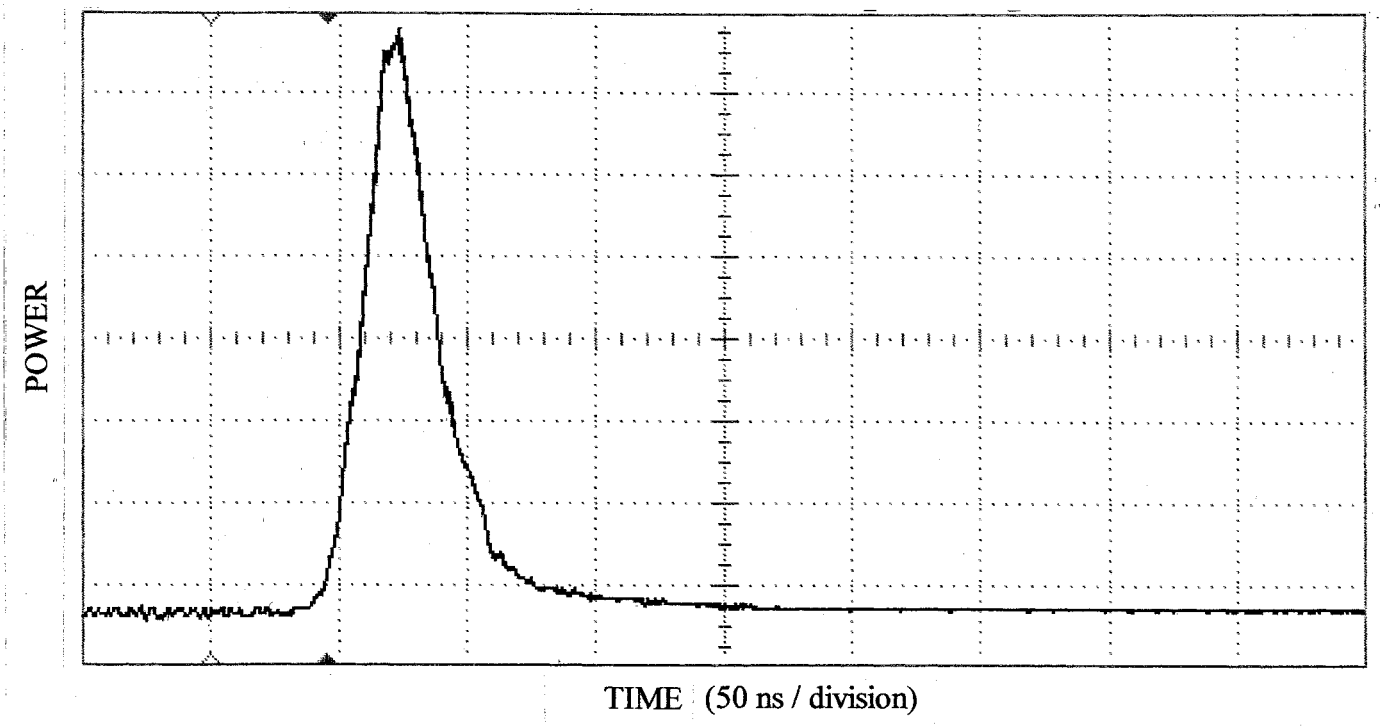

Fig. 24 Typical pulse profile for a Q-switched Nd:YAG laser, recorded by a fast silicon photodiode and displayed on an oscilloscope. The fast rising edge and longer tail is characteristic of a Q-switched pulse.

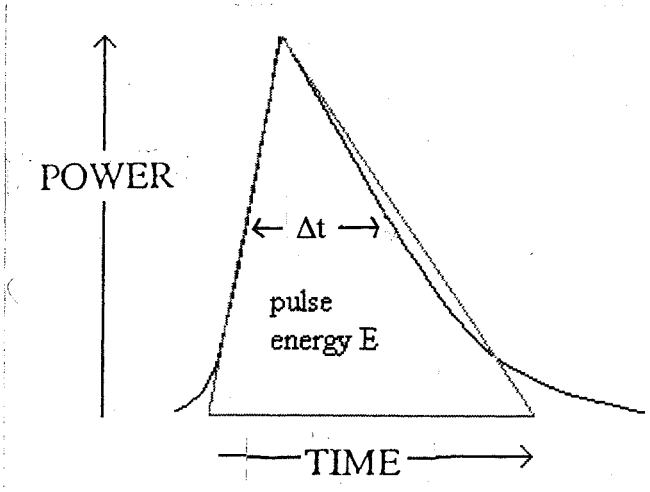

Fig. 25 The variation of laser output with time over a laser pulse, may be approximated by a triangle, and can be used to determine the energy of the pulse.

Voltage / V ± 1V	Energy per pulse / mJ ± 0.5 mJ	Rise time / ns ± 3 ns	Pulse duration (FWHM)/ ns ± 3 ns	Peak power per pulse / MW
525	1.5	-	-	-
550	9	-	-	-
570	17	68	160	0.106 ± 0.004
580	21	59	110	0.19 ± 0.01
590	25	46	75	0.33 ± 0.01
600	30	40	63	0.48 ± 0.02
625	43	29	50	0.86 ± 0.05
650	57	26	42	1.36 ± 0.10
675	71	23	31	2.29 ± 0.22
700	85	21	29	2.93 ± 0.30
725	101	19	27	3.74 ± 0.41
750	120	18	26	4.62 ± 0.53
775	136	17	25	5.44 ± 0.65
800	150	16	25	6.00 ± 0.72

Table 24. The output, peak power, and pulse rise and fall time of the Nd:YAG laser as the flashlamp voltage is increased. Pulse repetition rate was 10 Hz.

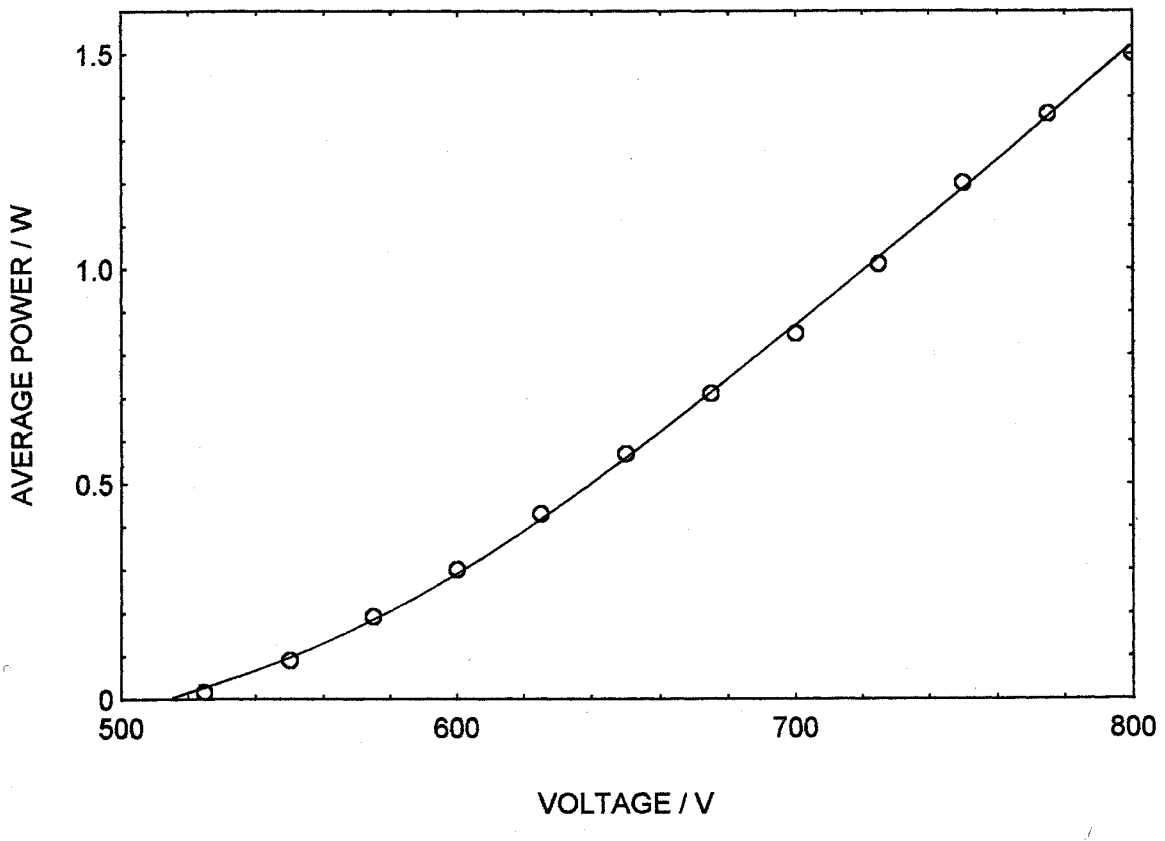

Fig. 26 Graph showing the rise in average output power of the Nd:YAG laser as the flashlamp voltage is increased.

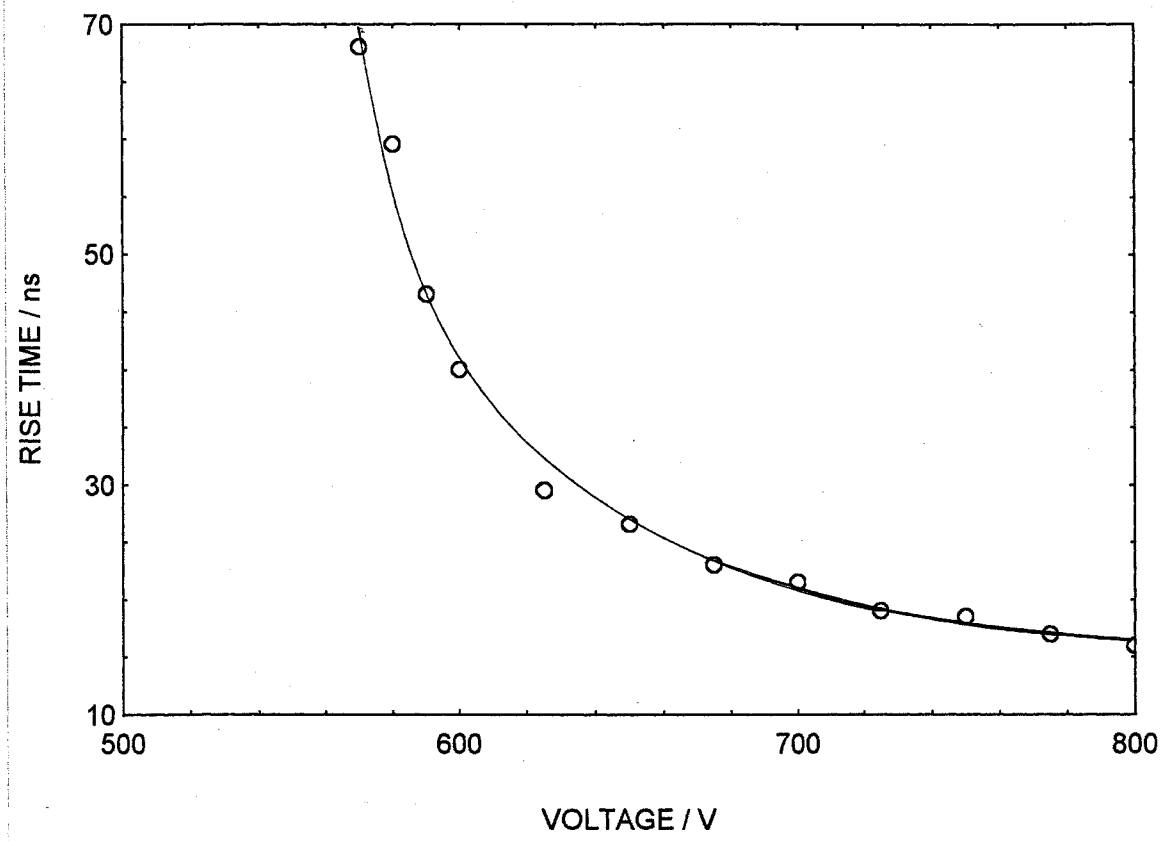

Fig. 27 Graph showing the decrease in rise time for the Nd:YAG laser as the flashlamp voltage is increased.

2.2.5 The use of a Glan –Thompson prism to shorten the pulse length of the Q-switched Nd:YAG laser.

Previous investigations into the use of lasers for cleaning have determined that the longer pulse durations can cause heating of the substrate, especially with high average power operation[1,2,10,26]. Therefore having established the efficiency of operation of the Nd:YAG laser using long pulses (see section **3.1.1 Preliminary tests**), the aim was to shorten the pulses to determine whether efficiency was improved. However, it has been shown previously that shorter pulse lengths are achieved by increasing the flashlamp voltage and hence output power (Figs. 26 & 27, Table 24; section 2.2.4). Simply increasing the output power to achieve shorter pulse lengths is clearly not an option, as the level of damage would become prohibitive. However attenuating the output energy incident on the target can alleviate this problem.

A Glan-Thompson prism can be used to manipulate the energy output as the pulse length is shortened[150,151]. Fig. 28 shows a Glan-Thompson prism, which comprises two right angle prisms, positioned so that light must enter the prism at right angles to the face of the prism. The optic axis of the left hand prism is perpendicular to the plane of the page. Unpolarized light enters the prism. The component with polarization parallel to the optic axis behaves as an extraordinary ray when it enters the prism and is totally reflected. The optic axis OA is shown as a dot to indicate its direction normal to the page, the vertical component of polarization is similarly shown as a series of dots along the ray. The component of polarization in the plane of the page (indicated by slashes) passes through the prism but emerges nearly parallel to the interface between the prisms. The second prism is provided to redirect the refracted ray to its original direction of propagation. The optic axis of the second prism is parallel to the direction of propagation, to ensure that the ray remains an ordinary ray.

The light from the laser is plane polarized. The input light to the prism will have components that are parallel and perpendicular to the optic axis. The apex angle of the prism θ is cut so that it is greater than the critical angle of the extraordinary ray, but less than that of the ordinary ray.

The critical angle θ_c is given by[151],

$$\sin \theta_c = \frac{1}{n} \qquad (11)$$

In the case of quartz, θ must be between 37.1° and 42.3°, which in the case of the prism used during this research was 40.2°

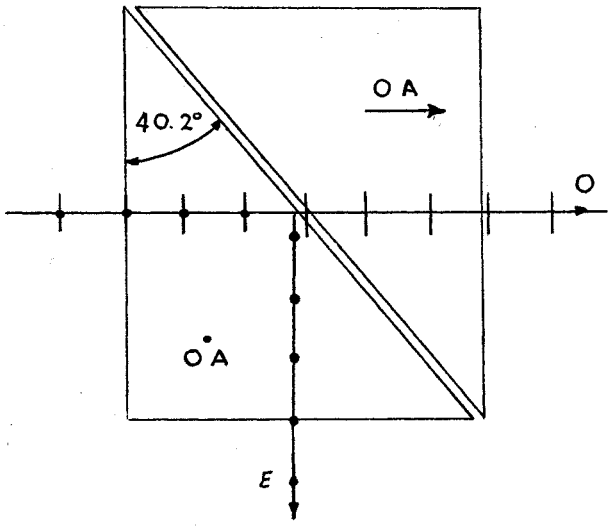

Fig. 28 The Glan-Thompson prism

If I_0, represents the maximum transmitted intensity of radiation, then Malus' law states that when the prism is rotated through an angle θ the intensity of transmission will decrease,

$$I = I_0 \cos^2 \theta \qquad (12)$$

Therefore by rotating the prism through 90° the intensity of power can be manipulated between maximum and minimum values. This was demonstrated by placing the Glan-Thomson prism in the path of the laser beam, and measuring the output with a calorimeter as the prism was rotated, Table 25. The results are presented graphically to show the variation in laser output power as the beam is passed through a Glan-Thompson prism (Fig. 29).

Angle of rotation of prism / ± 1°	Transmitted output power / W ± 0.05 W
0	1.00
13	0.95
25	0.90
38	0.80
49	0.60
59	0.40
72	0.20
78	0.10
84	0.05
92	0.00

Table 25. Output power of the Q-switched Nd:YAG laser, transmitted through a Glan -Thompson prism rotated through 90°.

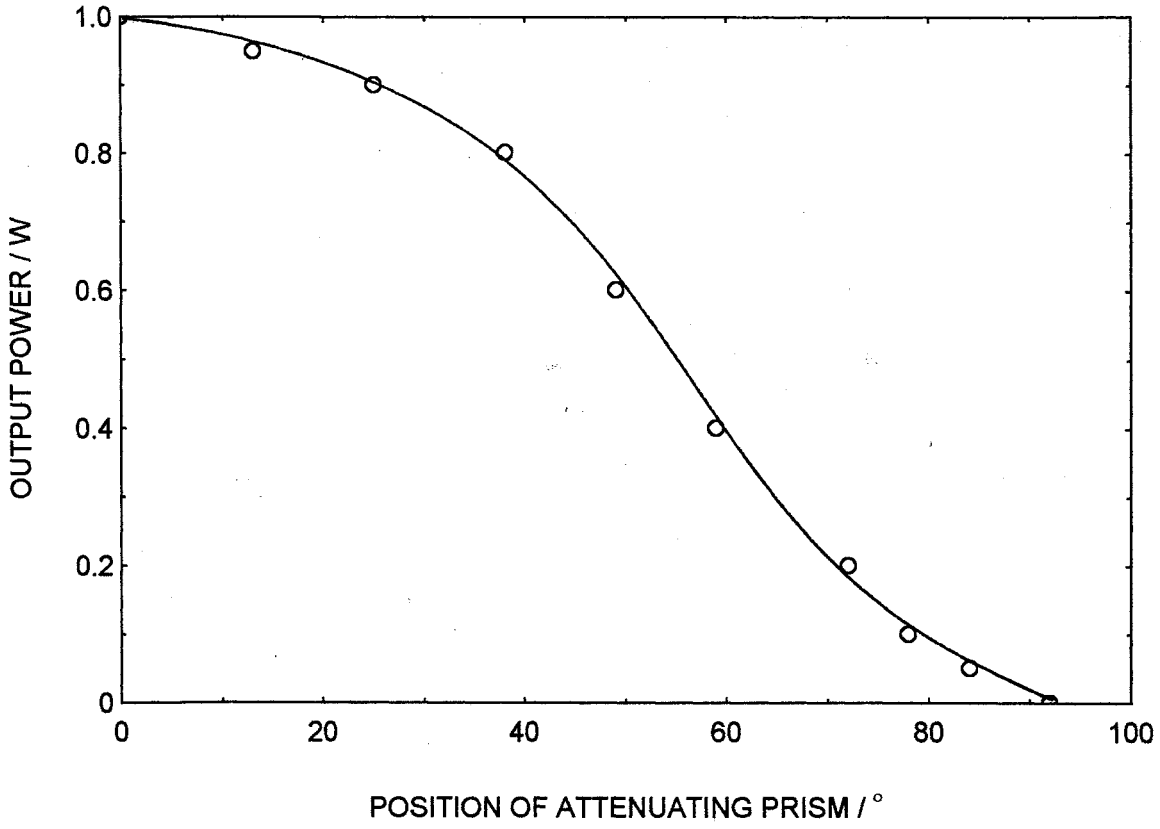

Fig. 29 Graph showing the variation in output of Nd:YAG laser, as a function of the angle, as the beam is passed through a Glan-Thompson prism.

2.2.6 The use of a Nd:YAG laser in an argon atmosphere

It was anticipated that if laser treatment of paper resulted in a significant temperature rise within the substrate then oxidation and/or depolymerisation of the cellulose could occur (see section **1.6**).

Shafizadeh and Bradbury[152], Major[153], and Philipp[154] have compared the pyrolysis of cellulose in both normal atmospheres and nitrogen atmospheres. They conclude that at low temperatures, oxygen plays a dominant role and oxidative degradation progressively proceeds faster than pyrolysis in nitrogen. At higher temperatures (above 300 °C) pyrolysis proceeds rapidly via transglycosylation reactions, leading to anhydro sugars as the principle products. These processes overshadow the effect of oxygen or an oxidative environment. At temperatures above 300°C, the rate of pyrolysis is essentially the same in both air and nitrogen, indicating that thermal degradation is independent of the oxidative reactions.

In order to help determine whether damage was caused primarily by oxidation, or depolymerisation reactions it was planned to carry out laser treatment of paper in an argon atmosphere and compare the damage with that caused under normal atmospheric conditions. A vacuum chamber was designed for use with argon, comprising an aluminium chamber with a fused silica lid (Fig. 30). Paper samples were cut and fixed to the base of the chamber, and the silica lid clamped shut. Argon gas was allowed through under pressure for a few minutes to purge the air from the chamber, and then the valves were closed maintaining an argon environment for the sample throughout the experiment.

The silica disc was placed in front of a calorimeter, in the path of the Q-switched Nd:YAG laser beam. The average power transmitted through the disc over an incident power range 0.02 - 1.4 W, was recorded and expressed as a percentage of the whole.

The percentage of infrared radiation transmitted by the silica disc was found to be 93% ± 1%. This slight loss of transmitted power was taken into account during laser treatment of paper samples.

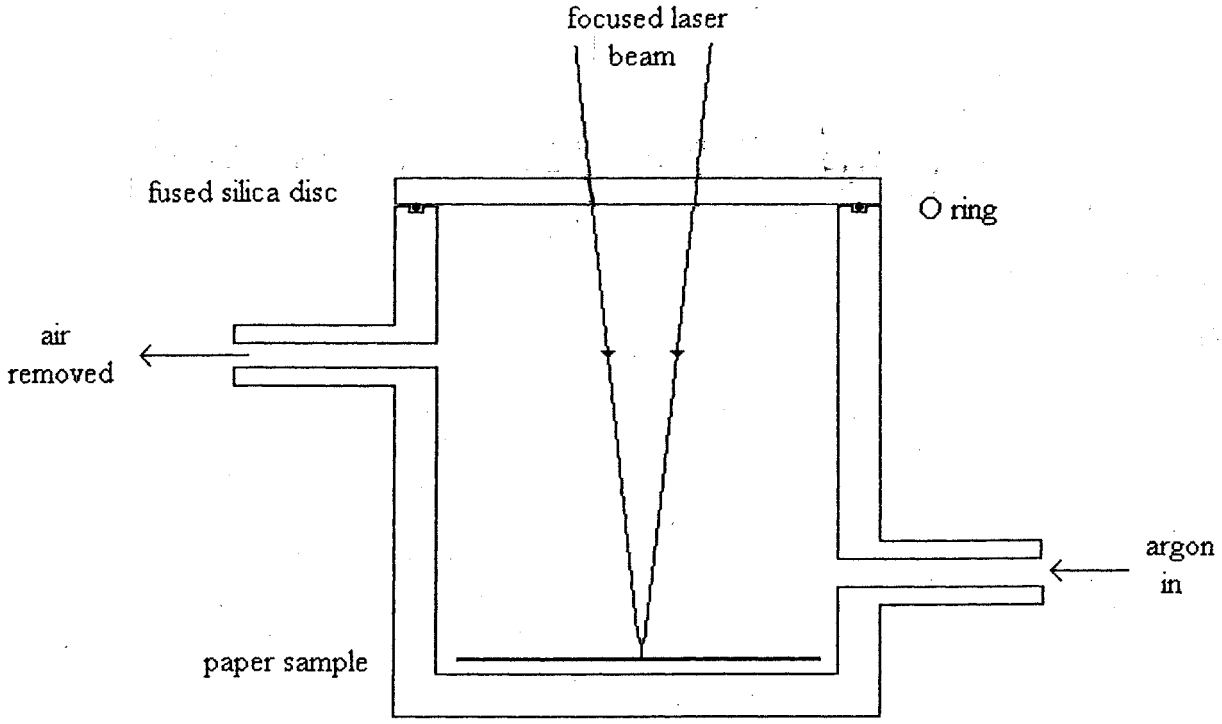

Fig. 30 The design of a vacuum chamber for Nd:YAG laser treatment of paper in an argon atmosphere. (Height 80 mm, external diameter 65 mm, internal diameter 50 mm)

2.3 Effectiveness of ink removal from paper, using a Nd:YAG laser

2.3.1 Preliminary tests.

The inks selected for the preliminary tests were;

i) Bic ball-point - black, blue, red and green.

ii) W.H. Smith fibre-tip - black, blue, red and green.

iii) W.H. Smith highlighter - pink and yellow.

Detailed information concerning the ingredients present in the various inks chosen was withheld by the companies in question, however in general the colorants for ball-point pen and fibre tip pen ink are largely the same but their carrier's are different. Fibre tip pens and highlighters are based on low viscosity dye or pigment preparations in water/glycol mixtures, with small amounts of acrylic resin to prevent feathering on the paper surface[155]. Ball-point pen inks are high viscosity pastes based on pigments and/or dyes in solvents, with 25% resin. The dyes used in these formulations are largely non-volatile basic blue, red, violet and yellow dyes[156].

As a result of the preliminary tests, the research proceeded initially with only black ball-point pen ink, and ultimately with blank paper. It would have been useful to know the make up of the inks chosen for the preliminary tests, but the actual composition was not critical to the investigation since it was anticipated that the colour of ink, and the amount of penetration of the ink into the paper fibres would probably have a greater effect than the individual dyes.

The paper samples selected for the preliminary tests were;

i) 'Roma' 100% cotton paper (hand made, gelatin sized) – Atlantis Fine Art, 146 Brick Lane, London

ii) 100% cotton endleaf archival paper (machine made, gelatin sized) - Atlantis Fine Art, 146 Brick Lane, London

iii) chemical woodpulp cartridge paper (machine made, aquapel (alkyl ketene dimer) sized, calcium carbonate filler) – Conservation By Design, Timecare Works, 5 Singer Way, Kempston, Bedford

iv) mechanical woodpulp paper (machine made unprocessed woodpulp, rosin size)– Finnboard, P.O.B 36, 00131 Helsinki, Finland

The surface of each paper sample was coloured with ink from the writing pens. The paper samples were held in the path of the unfocused Nd:YAG laser. The pulse repetition rate was 10 Hz and the pulse energy used over the entire range 1.5 – 150 mJ (see section **2.2.4**, Table 24). There was no discernible effect to either the ink or the paper samples.

The 10 cm focal length convex lens used for spot size determination (see section **2.2.2**), was placed between the laser and the paper samples, and brought to a focus on the paper surface. In order to compare the effect of the laser on the various inks and papers, it was desirable that the laser be made to follow a path across the samples, which could be reproducible for each sample. Therefore the paper samples were fixed to an X-Y translator with the surface perpendicular to the laser beam, which was itself reflected by a mirror and directed through the 10 cm. lens (Fig. 31).

A computer programme linking the laser with the stage was used to translate the targets across the Nd:YAG laser beam stepwise with an overlap between adjacent laser spots. The pulse rate was 10 Hz and the distance across the target covered at a rate of 400 μms^{-1}. This means that four pulses were received by the paper at the centre of each line of pulses, and two pulses were received by paper at the outside edge of the pulse line. The programme was set to make the laser follow two 10 mm lines 0.7 mm. apart. The paper targets were moved back and forth in the focused beam, increasing the laser beam pulse energy for each pair of lines, and using an initial fluence insufficient to visibly affect the inks or paper. An un-inked sample of each paper was given the same laser treatment for comparison of damage. The energy levels were monitored with a calorimeter (Scientec). The average fluence at each power level was calculated (see section **2.2.1 Laser operation and safety**), and the effect on the inked paper sample recorded visually.

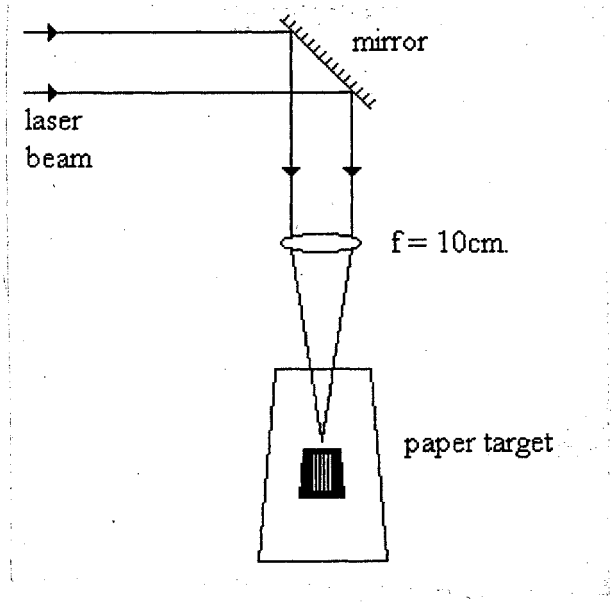

Fig. 31 Arrangement of apparatus for focusing the Q-switched Nd:YAG laser beam onto paper targets during ink removal tests.

2.3.2 Microscopic examination of the damage to the surface of 'Roma' 100% cotton paper, as a result of black ball-point pen ink removal by Nd:YAG laser.

The results of the preliminary ink removal tests (see section **3.1.1 Preliminary tests**) were useful for establishing which inks could be removed from which paper samples. At this stage the examination of ink removal and damage had been assessed visually, and was not therefore totally objective.

The results, however, did suggest that the laser was most effective in the removal of black ball-point pen ink from 'Roma' 100% cotton paper. Therefore a more rigorous assessment of ink removal, and damage thresholds was carried out microscopically using this combination.

1. Ink removal using a pulse length range 87 - >200 ns, normal atmosphere

A row of squares (20 x 20 mm.) were drawn on a piece of the 'Roma' paper, and in each was drawn an 'X' shaped cross, in black ball-point pen ink. The paper was fixed to the mobile stage beneath the laser. The Q-switched laser was focused over the first square, and the pulse energy set to produce a nominal fluence (4 ± 1 Jcm^{-2}) insufficient to visibly affect the paper or ink (see Table 27, section **3.1.1 Preliminary tests**). The laser was made to follow a series of short lines 1 mm. apart, back and forth over the paper target (Fig. 32).

When the first square had been covered in this way, the laser was positioned over the second square, the pulse energy increased and the process repeated. The pulse energy was increased for each square, until a fluence more than sufficient to remove the ink was reached, Table 26. The effect of the laser on the ink was observed and recorded using photomicroscopy (see section **2.4.1 Microscopy and photomicroscopy**). The physical damage to the inked, and un-inked paper

surface was investigated using a Hitachi S-2400 scanning electron microscope SEM (see section **2.4.2 SEM**).

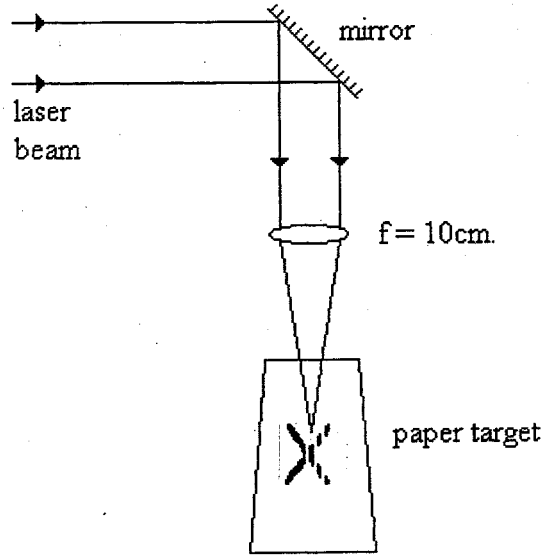

Fig. 32 Arrangement of apparatus for focusing the Q-switched Nd:YAG laser beam onto targets in preparation for microscopic examination of damage to 'Roma' paper.

Input voltage / V	Energy per pulse / mJ ± 0.5 mJ	Fluence / Jcm^{-2}	Pulse duration (FWHM)/ ns ± 3 ns
530	2	4 ± 1	-
535	4	8 ± 2	-
542	6	12 ± 4	-
549	8	16 ± 5	-
556	10	20 ± 6	-
562	12	24 ± 7	-
568	14	29 ± 9	170
573	16	33 ± 10	135
578	18	37 ± 11	112
584	20	41 ± 12	87
587	22	45 ± 14	82
590	24	49 ± 15	75
593	26	52 ± 16	70
597	28	57 ± 17	65
600	30	61 ± 18	62

Table 26. The energy and fluence per pulse, for increasing flashlamp voltage. Pulse repetition rate was 10 Hz. The error in fluence was determined using equation 3, Appendix 1.

The aim of the first set of experiments was to investigate the use of the laser for ink removal using long pulse lengths, and to record the difference in effect as the pulse length was shortened (see section **2.1 Strategy of the research programme**). Therefore, the experiment involving the laser treatment of black ball-point pen ink crosses was repeated using increasingly short pulse durations.

2. Ink removal using an attenuated beam, pulse length of 63 ns, normal atmosphere

The pulse length of the focused laser, at the fluence required to remove ink was 87 ns (see section **3.1.2**). It was felt that such a long pulse length may give rise to a heating effect[7,8,9], therefore efforts were made to shorten the pulse length.

The flashlamp voltage was increased to 600 V, producing a pulse duration of 63 ns (see Table 24; **2.2.4**). The Glan-Thompson prism was used to attenuate the beam to produce a nominal fluence (4 ± 1 Jcm^{-2}) insufficient to visibly affect the paper or ink. As before the laser was made to follow a series of short lines over the paper target (Fig. 33).

When the first square had been covered in this way, the laser was positioned over the second square, and the pulse energy increased by manipulation of the attenuating prism. The pulse energy was increased for each square, until a fluence more than sufficient to remove the ink was reached. The effect of the laser on the ink was observed and recorded using microscopy.

3. Ink removal using an attenuated beam pulse length of 29 ns, normal atmosphere

For these experiments the flashlamp voltage was increased to 700 V, producing a pulse duration of 29 ns (see Table 24; **2.2.4**). As previously described, the Glan-Thompson prism was used to attenuate the beam, to produce a range of fluences between that insufficient to

affect the ink, and that more than sufficient to remove the ink. The effect of the laser on the ink was observed and recorded using microscopy.

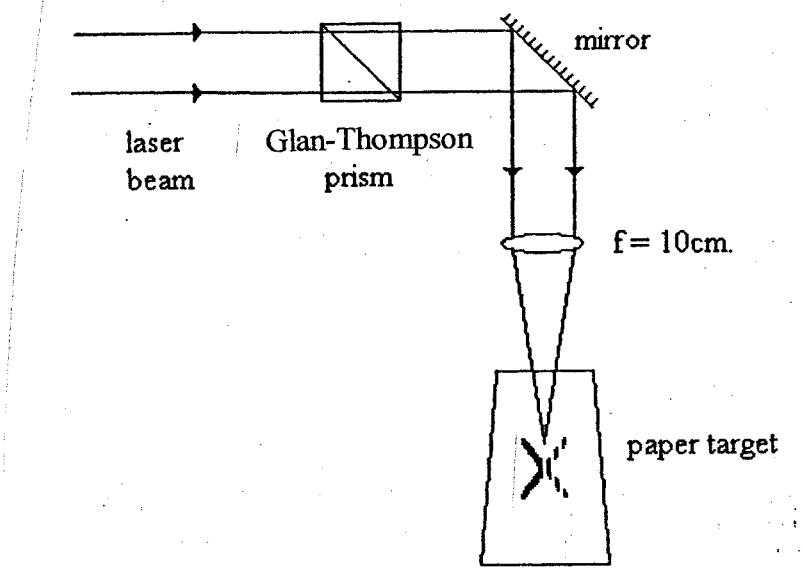

Fig. 33 Arrangement of apparatus for focusing the Q-switched attenuated Nd:YAG laser beam onto targets in preparation for microscopic examination of damage to 'Roma' paper.

4. Ink removal using an attenuated beam pulse length of 26 ns, normal atmosphere

Experiment 3 (above) was repeated using a flashlamp voltage of 750 V, producing a pulse duration of 26 ns

5. Ink removal using a pulse length range 87 - >200 ns, argon atmosphere

Experiment 1, described above (pulse length range 87 - >200 ns, normal atmosphere), was repeated using paper samples in an argon atmosphere, to see if ink removal was dependent on the presence of oxygen. The argon atmosphere was created using the vacuum chamber (see

section **2.2.6**). The laser was not attenuated for these tests, therefore the pulse durations were in the range shown in Table 26. The fluence received by the paper targets was assumed to be 93 % of the calculated value due to absorption of energy by the silica lid of the chamber (see section **2.2.6**). The energy per pulse could have been increased to make up for the loss due to the silica lid, however this would have shortened the pulse duration, which would have produced a greater disparity.

2.3.3 Microscopic comparison of the damage to the surface of 'Roma' paper, as a result of black ball-point pen ink removal by Nd:YAG laser, and contemporary mechanical methods.

The ink removal tests (see section **2.3.2**) showed that the most obvious damage was caused to the 'Roma' paper when using the longer pulse lengths (ca.100 ns) in a normal atmosphere. Therefore as the worst case scenario, this was compared with the damage caused via contemporary mechanical methods.

A line of black ball-point pen ink was drawn across a sheet of 'Roma' paper, which was then cut into four pieces labeled A-D. The first piece A, was fixed to the mobile stage, the Q-switched Nd:YAG laser focused on the ink line, and the ink removed using pulses of 37 ± 11 Jcm^{-2}, pulse duration 112 ns. This fluence having been established as the ink removal threshold (see Table 34, section **3.1.2**).

The ink line from B was removed using a typing eraser followed by a tablet eraser. The ink line from C was removed using a scalpel, and the line from D was removed using a

combination of scalpel and erasers. The resulting damage was visually compared using a Hitachi S-2400 SEM.

2.3.4 Preparation of paper samples for Part Two: Investigation of physical and chemical damage to Nd:YAG treated paper.

'Roma' being a 100% cotton paper offers a reasonably pure sample with which to carry out chemical testing, however it does have a gelatin size. It was assumed that the gelatin could have a major bearing on the outcome of any chemical tests. A size free, cellulose rich paper such as Whatman filter paper is often used as the basis for cellulose testing[71,72,98,99,100,103], however chemical testing of a laser treated, size free, totally pure paper would give little indication of the damage likely to occur to an artwork during laser treatment. It was decided to carry out simultaneous tests on the standard 'Roma' paper, some 'Roma' paper from which the size had been removed, and Whatman No1 filter paper.

The presence of a gelatin size was established using a Ponceau S stain test[38]. A few fibres of damp 'Roma' paper were teased away from the body of the paper on a microscope slide. A drop of distilled water was pipetted onto the fibres and a slide cover placed on top. A drop of Ponceau S stain was pipetted onto the edge of the cover, and using Whatman No.1 filter paper as a wick on the other side of the cover, the stain was drawn past the 'Roma' paper fibres. The stain was allowed to colour the fibres before being flushed through with distilled water. The fibres were washed thoroughly with distilled water and examined under a microscope, which revealed pink stained particles of gelatin.

Enzymes are frequently used by paper conservators to remove starch and animal glue adhesives from works of art[157]. Gelatin size can also be removed from paper by the use of protease enzymes.

Several sheets of the 'Roma' paper were washed for 10 minutes and placed in a bath of warm water. Protease enzymes were added and the bath maintained at a temperature of approximately 40° C for 2 hours. The enzymes in the paper were denatured by a hot wash of approx. 90° C, followed by an immersion in IMS. The sheets of 'Roma' were given a further 2 hour wash in several changes of cold water.

Microscopic examination (see section **2.3.2**) indicated no immediate colour change to the laser treated 'Roma' samples, however under normal environmental conditions it can take a long time for chemical alteration to the cellulose to become manifest. In order to study chemical changes to the cellulose, artificial ageing tests are frequently used (see section **1.5 Tests for the degradation of cellulose**), in an attempt to simulate in a short time the effects of natural ageing over a much longer period[121-133]. It was anticipated that results from accelerated ageing of laser treated 'Roma' paper, would help in directing the investigation of chemical damage to laser treated papers (see section **2.5**).

Small samples of the standard sized 'Roma', size removed 'Roma', and Whatman No 1 filter paper were laser treated as described previously (section **2.3.2**), using a nominal fluence range of 4-41 Jcm^{-2}.The samples were divided into three groups, and sent to Dr J Stanley, and Mr P Tougher, of the Paper Science Department, UMIST for artificial ageing using their standard ageing conditions.

Group one was placed in a light box delivering 800,000 Lux with a uv component of 180 $mWcm^{-2}$, group two was placed in a dry oven maintained continuously at 90°C. Group three was placed in a humid oven maintained continuously at 90°C, and 50% R.H. The light aged samples were exposed for 120 hours. The dry and humid aged samples were aged for one month respectively.

2.4 Investigation of physical damage to Nd:YAG treated paper

2.4.1 Microscopy and photomicroscopy

The effect of the Nd:YAG laser for ink removal from paper (see section **2.3.1** and **2.3.2**) was observed using an Olympus SZ Series binocular microscope. The most interesting results were recorded using photomicroscopy. The Olympus SZ Series microscope has two eyepieces, one with a diopter correction to correct for long or short sightedness, the other eyepiece has no correction. To carry out photomicroscopy, the microscope was brought to a focus on the paper, the non corrected eyepice was removed, and a Pentax K 1000 camera was attached in its place.

2.4.2 Scanning electron microscopy SEM

An Hitachi S-2400 SEM was used to assess the level of physical damage caused to paper by Nd:YAG laser treatment.

In the SEM an electron gun produces a beam of electrons which hit the specimen. The specimen emits secondary electrons. The electron beam is scanned line by line over a small area of the surface of the specimen synchronously with the electron beam in a T.V. tube. The secondary electrons which are generated during this process by every single point of the specimen are picked up by a detector. The output signal of the detector controls the intensity of the beam in the T.V. tube. Thus the amount of light emitted by each point of the T.V. screen is proportional to the number of electrons emitted by the corresponding point of the specimen's surface.

Thus line by line an image of the specimen's surface appears on the T.V. screen. Recording is achieved by photographing the T.V. screen.

To improve the yield of electrons and obtain a reasonable image of the paper samples it was necessary to apply a thin (1 nm) coating of gold. This was performed by Mr Best using a sputter coater.

2.4.3 Reflectance measurements of humid aged, Nd:YAG laser treated 'Roma' paper

Results from artificially ageing laser treated paper (**2.3.4**), suggested that there were no discernible colour changes after light, or dry oven ageing, however there was a significant colour change to humid aged laser treated 'Roma' paper. Further investigations were made.

1. Ageing after laser treatment using a pulse length of 87 ns, normal atmosphere

The ink removal tests (see Table 34, section **3.1.2**) established the nominal threshold fluence for even ink removal as 37 ± 11 Jcm^{-2}, when using the normal un-attenuated beam (pulse duration 112 ns). However it was anticipated that in practice operators wishing to remove ink may use marginally more energy per pulse to effect a thorough clean, with potentially damaging results. Therefore the pulse energy was set to 20 mJ, producing a nominal fluence of 41 ± 12 Jcm^{-2} (pulse duration 87 ns), more than sufficient to remove ink. Small blank samples of the standard sized, and size removed 'Roma' paper were fixed to the mobile stage and treated with the focused Q-switched Nd:YAG laser.

The laser was made to follow a series of straight lines 10 mm. long at a distance of 0.5 mm. apart, thus creating a 10 x10 mm. square of laser treated surface. The samples were split into groups,

which were aged between one day, and one month, in a humid oven maintained continuously at 90°C, and 50% R.H. The change in reflectance (400-700 nm) of the humid aged, Nd:YAG laser treated, paper samples was determined using a Hitachi U3000 spectrophotometer.

The reflectance was recorded using a 5° specular reflectance accessory. This comprised a black box approximately 25 x 20 x 15 cm with two holes in the top. Initially the holes were covered by two round, flat mirrors, and a reference baseline was run. One of the mirrors was removed, replaced by the paper sample, and the spectrum recorded. Thus the reflectance spectrum of the paper was recorded relative to, and as a percentage of the reflectance of the reference mirror.

2. Ageing after laser treatment using an attenuated pulse lengths of 63, and 26 ns

The results from ageing, standard and size removed 'Roma' with a 87 ns pulse length (see section **3.2.1**), showed considerable discoloration to the sized paper, but not the size removed paper. Therefore the tests were repeated for the standard sized paper, using shorter pulse lengths to establish if this would lead to less discoloration on ageing.

The ink removal tests (see Tables 35 & 37, section **3.1.2**), had established nominal thresholds for even ink removal of 20 ± 6 Jcm^{-2} and 16 ± 5 Jcm^{-2}, when using pulse lengths of 63 and 26 ns, however it was assumed that in practice marginally more energy per pulse may be used to effect a thorough clean. Therefore the humid ageing tests were repeated for blank samples of standard sized 'Roma', prepared using short pulse lengths, 63 ns (600V), and 26 ns (750V), which produced nominal fluences more than sufficient to remove ink, 24 ± 7 Jcm^{-2} and 20 ± 6 Jcm^{-2} respectively. The short pulses were achieved using the Glan-Thompson prism. The

change in reflectance (400-700 nm) of the paper samples was determined using the Hitachi U3000 spectrophotometer.

3. Ageing after laser treatment using a pulse length of 87 ns, argon atmosphere

The ink removal tests in an argon atmosphere produced very similar results to those achieved in a normal atmosphere. This suggested that the atmosphere did not have significant bearing on the reaction between the laser energy and the ink. This theory was tested by humid ageing standard sized 'Roma' samples, prepared in an argon atmosphere, using a nominal fluence of 38 ± 11 Jcm^{-2}, more than sufficient to remove ink (see Table 38, section **3.1.2**). The change in reflectance (400-700 nm) of the paper samples was determined using the Hitachi U3000 spectrophotometer.

2.4.4 The effect on the tensile strength and tendency to tear, of Nd:YAG laser treated 'Roma' paper.

The damage to the surface of 'Roma' by laser treatment was found to be less visibly disruptive than contemporary methods of ink removal (see section **2.3.3**), however microscopy did not yield any information about the possible loss in strength of the paper due to the treatment. There are several methods of determining loss of paper strength (see section **1.5 Tests for the degradation of cellulose**), however microscopy suggested that the damage caused during laser treatment was limited to the paper surface. It was assumed that methods which require analysis of cellulose solutions; solution viscosity[78], chain length uniformity[79], and gel permeation chromatography (GPC)[80-82], would not be capable of registering slight changes in DP to the surface of a sheet of paper.

Tensile strength testing[83-87], offers a far more sensitive method of identifying change in DP. The most commonly used strength tests are tensile[83], and burst strength tests[84]. Tensile testing does not give a quantitative figure for the reduction in DP, but it is fairly sensitive to small changes in DP, and does not introduce additional degradation[77]. It has the advantage of being a very quick and cheap test, and is simpler to perform than burst strength testing. Instron tensile testing equipment housed in the Paper Science Department, UMIST was used to assess whether laser treatment caused a lowering of tensile strength.

Blank sheets of 'Roma' paper (approx. 200 x 150 mm.) were fixed to the moving stage and the Q-switched Nd:YAG laser brought to a focus. The samples were positioned so that the laser spot could traverse the centre of the paper, from one side to another, parallel to the longer side (Fig. 34). The computer programme linking the laser with the stage, was used to move the paper targets during laser pulses. Samples were laser treated, both in the direction of, and at right angles to the laid lines. The samples were laser treated over the nominal fluence range 4-61Jcm^{-2} (see Table 26; section **2.3.2**).

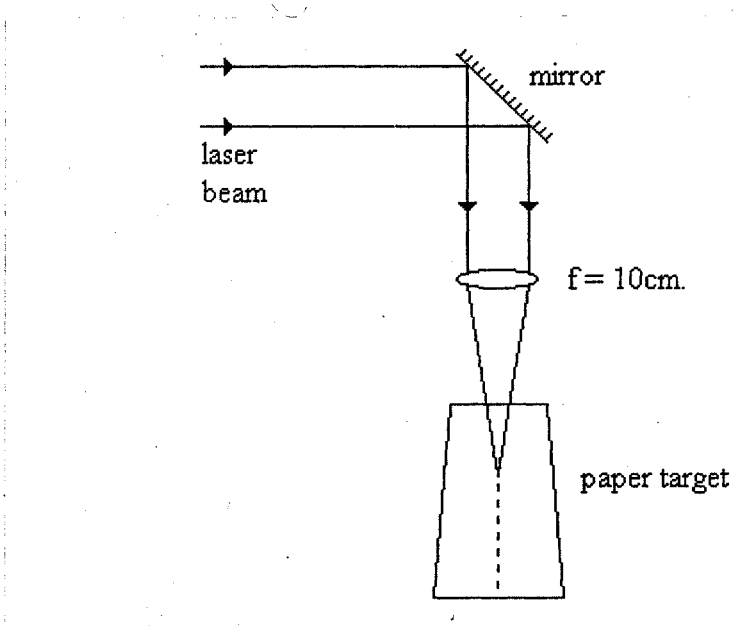

Fig. 34 Arrangement of apparatus for focusing the Q-switched Nd:YAG laser beam onto targets in preparation for the tensile strength testing of 'Roma' paper.

The samples were then cut into strips 15 ± 1 mm. wide and 140 ± 5 mm. long with the laser path spanning the width at the centre of each strip. The strips were weighed and the grammage, gm^{-2} calculated for each sample. Ten strips from each sample were successively clamped in the jaws of an Instron tensile tester, and stretched to breaking point. Any samples which snapped, at the edge, or within the jaws of the equipment were discounted and replaced with new strips. The tensile strength was recorded for each fluence level.

The Instron tensile testing equipment records values of force per unit width required to break a sample (tensile strength), however this assumes an even density of paper sample. 'Roma' 100% cotton paper is a mould made laid paper, produced by hand[60]. The laid lines are indentations to the finished sheet, created during the papermaking process by metal wires in the mould, and consequently the sheets are thinner at the site of the laid lines. A more accurate method of comparing the tensile strength of such test samples is the tensile index, which was determined using equation 13.

$$\text{Tensile index, } Nmg^{-1} = \frac{\text{Tensile strength, } Nm^{-1}}{\text{Grammage, } gm^{-2}} \qquad (13)$$

The number of strips tearing at laser treatment sites was noted for each sample and plotted as a histogram. SEM was used to compare the tears at laser treatment sites with those of untreated 'Roma' paper samples.

Aged samples were also tested for signs of weakening due to laser treatment. Further sheets of 'Roma' paper were prepared for tensile testing over the nominal fluence range 4-41 Jcm^{-2}. The

sheets were sent to the Paper Science Department, UMIST, where they were placed in a humid oven for 29 days at constant temperature 90°C, and relative humidity, RH. 50%. The samples were prepared, snapped in the tensile tester, and the data presented as before. SEM was used to compare the fractures at laser treatment sites with those of humid aged, untreated 'Roma' paper samples.

2.4.5 Surface profiling of Nd:YAG laser treated 'Roma' paper.

The impact depth of the laser pulses was studied using a Rank Taylor Hobson Talysurf profiler. The profiler comprises a sensitive stylus on the end of a long arm, which records the shape of surfaces over which it is pulled. Townsend[158], has used the Talysurf profiler to study the surfaces of varnishes used for paintings. Her primary interest was the depth and width of fissures in the varnish layer, but the Talysurf can also be used to study the surface of paper.

The Q-switched Nd:YAG laser was focused on blank samples of 'Roma' paper mounted to the mobile stage. The laser was made to follow a path of three short lines, 2 mm. apart for each sample. Samples were laser treated both in the direction of, and at right angles to the laid lines, using a pulse energy of 20 mJ, nominal fluence of 41 ± 12 Jcm^{-2}, and pulse duration 87 ns. The nominal fluence of 41 ± 12 Jcm^{-2} was chosen, as it was slightly greater than the ink removal threshold (see section **2.4.3**). The surface profiles of the laser treated regions of the paper samples were recorded using the profiler, which was dragged over the laser lines to see if the laser left an indentation (Fig. 35).

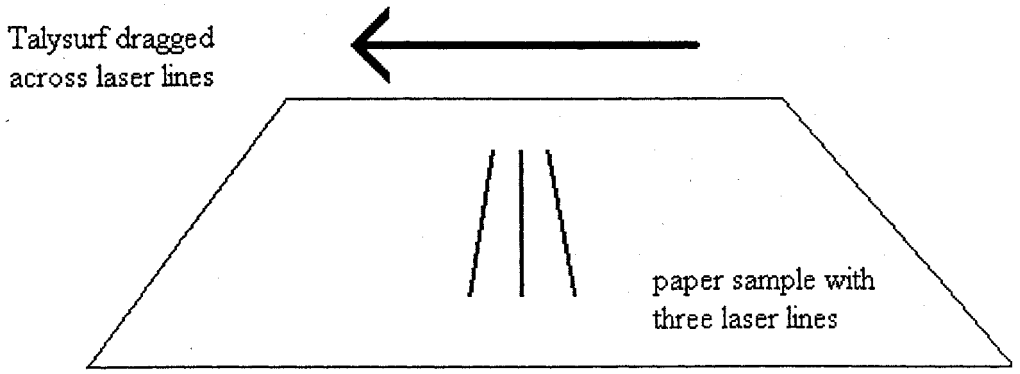

Fig. 35 Talysurf profiling of Q-switched Nd:YAG laser treated 'Roma' paper. Three laser lines were produced on the 'Roma' paper surface, and the Talysurf profiler was dragged across the laser lines to measure the impact on the paper surface.

2.5 Investigation of chemical damage to Nd:YAG treated paper

The microscopic appearance of laser treated 'Roma' paper (see section **2.4.1**), showed no sign of discoloration or charring. This suggested that, though there was surface disruption to the paper, the cellulose was not subject to the type of high temperature (above 300 °C) reaction involving the production of tars and oils as described by Shafizadeh[68,69] (see section **1.4 The degradation of cellulose**). It seemed more likely that the cellulose would have suffered the oxidation reactions which occur at lower temperatures[68,69]. Such oxidation reactions could be identified by the formation of peroxides, carbonyl groups and carboxyl groups.

2.5.1 The use of the Russell effect to investigate whether Nd:YAG laser treatment of 'Roma' paper causes a local increase in abundance of peroxides.

1. Russell effect after laser treatment using a pulse length range of 87 - >200 ns, normal atmosphere

Blank samples of the standard sized, and size removed 'Roma' paper, and Whatman No 1 filter paper were treated with the focused Q-switched Nd:YAG laser, over the nominal fluence range 4-41 Jcm^{-2}. Each level comprised three laser lines 12 mm long and 10 mm apart. To ensure maximum contrast the paper samples were kept in the dark for several weeks before laser treatment to minimise the background peroxide activity due to photo-oxidation. Russell images were created immediately after laser treatment, and then once weekly for three weeks. Film for the Russell effect tests was prepared using Kodak LPF4 film immersed in 0.005 M ammonium hydroxide solution for two minutes, and allowed to dry in a light-tight box. The process was carried out in a darkroom with safelight illumination created using a Kodak OA

red filter. Film was prepared on the day of the test in order to minimise the chances of fogging. The Russell images were created by placing the paper samples face up on a sheet of glass in a large lidded box. The film was placed over the paper samples. To ensure good contact another sheet of glass was placed over the film, and the box closed (Fig. 36). The standard sized samples were left for 24 hours. The size removed samples required 48 hours to create an image due to absence of size. The film was developed using Ilford ID11 stock solution and fixed with Kodak Unifix 1:5. Reference samples of standard sized, and size removed 'Roma' and Whatman No 1 filter paper were scratched using a scalpel, and the Russell effect tests repeated.

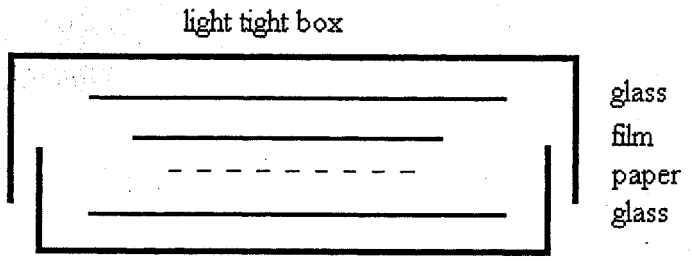

Fig. 36 Arrangement of equipment for the Russell effect tests to show the local increase in abundance of peroxides in Q-switched Nd:YAG laser treated 'Roma' paper.

2. Russell effect after laser treatment using attenuated pulse lengths of 63, and 26 ns

The results from the Russell effect tests using an 87 ns pulse length (see section **3.3.1**, Tables 43 &44), showed that the effect of laser treatment on standard sized paper was considerably more long lived than that of treatment to the sized removed equivalent, suggesting greater peroxide activity. Therefore the tests were repeated for the standard sized paper, using shorter

pulse lengths to establish if this would lead to a reduction in the amount of peroxides produced.

The Russell effect test was repeated on standard sized 'Roma' paper using the Glan-Thompson prism to attenuate the beam to allow for shorter pulses. The flashlamp voltages used were 600, and 750V, thus producing pulse durations of 63, and 26 ns respectively. The nominal fluence range used in each case was that required to completely remove ink 4-24 Jcm^{-2}, and 4-20 Jcm^{-2} respectively (see section **2.3.2**).

3. Russell effect after laser treatment using a pulse length range 87 - >200 ns, argon atmosphere

Experiment 1, described above (pulse length range 87 - >200 ns, normal atmosphere), was repeated using paper samples in an argon atmosphere, to see if the production of peroxides was dependent on the presence of oxygen. The nominal fluence received by the paper targets was assumed to be 93 % of the calculated value due to absorption by the silica lid of the chamber. The energy per pulse could have been increased to make up for the loss of energy due to the silica lid, however this would have shortened the pulse duration which, it was assumed, would produced a greater disparity.

2.5.2 The use of methylene blue to investigate whether Nd:YAG laser treatment of 'Roma' paper causes a local increase in abundance of carboxyl groups.

1. Methylene blue test after laser treatment using a pulse length of 87 ns, normal atmosphere

Blank samples of the standard sized, and size removed 'Roma', and Whatman No 1 filter paper were fixed to the mobile stage and treated with the focused Q-switched Nd:YAG laser, using a pulse energy of 20 mJ, nominal fluence of 41 ± 12 Jcm^{-2}, and pulse duration 87 ns. The fluence of 41 ± 12 Jcm^{-2} was chosen, as it was slightly greater than the ink removal threshold (see section **2.4.3**). The laser was made to follow a series of straight lines 10 mm. long at a distance of 0.5 mm. apart, thus creating a 10 x 10 mm. square of laser treated surface. The samples were placed in a 0.01% methylene blue solution for 10 minutes and washed for 3 hours in several changes of cold water. The samples were dried, and photographed. Samples of the paper were scratched with a scalpel, and treated with methylene blue as before for comparison.

2. Methylene blue test after laser treatment using attenuated pulse lengths of 63, and 26 ns

The methylene blue test was repeated for samples of standard sized 'Roma', prepared using nominal fluences more than sufficient to remove ink, 24 ± 7 Jcm^{-2} and 20 ± 6 Jcm^{-2} respectively (see Tables 35 & 37, section **3.1.2**). The short pulse lengths, 63 ns (600V), and 26 ns (750V), were achieved using the Glan-Thompson prism.

3. Methylene blue test after laser treatment using a pulse length of 87 ns, argon atmosphere

The methylene blue test 1, was repeated for samples of standard sized 'Roma', prepared in an argon atmosphere to determine if the result achieved was dependent on oxygen. Samples were prepared using a nominal fluence of 38 ± 11 Jcm^{-2}, a fluence slightly greater than the ink removal threshold (see Table 38, section **3.1.2**).

2.5.3 The use of Fourier Transform infrared (FTIR) spectroscopy to show the possible oxidation of 'Roma' paper as a result of Nd:YAG laser treatment.

Diffuse Reflectance Infrared Transform (DRIFT) spectroscopy was used to assess the level of oxidation to laser treated 'Roma' paper, because it can record the spectrum at the surface of a sample with little sample preparation. To record a spectrum small discs of paper were taken out of the sample using a hole punch and attached to a flat metal sample mount. Before sample spectra were recorded a scan of the metal mount was run as a baseline.

DRIFT spectroscopy combines reflectance and transmission. The Perkin Elmer Paragon 1000 responds linearly to energy falling on the detector, and the value of transmission (recorded on the ordinate scale) is simply the ratio of the energy in the presence of the sample, to the energy without the sample (Fig. 37). The sample spectrum transmission is recorded as a percentage of the baseline transmission for each wavenumber. Previous studies using FTIR for the investigation of paper materials have concluded that paper is too thick for direct analysis in transmission[115], therefore the recorded value of transmission on the spectrum ordinate using DRIFT spectroscopy, is effectively a measure of the infra-red reflectance of the paper sample at varying wavelengths.

The Perkin Elmer Paragon 1000 has a difference function, which can subtract one spectrum from another. In order to perform the subtraction, the instrument converts the recorded values of transmission, to relative absorption values for both spectra and one spectrum can be subtracted from the other. The instrument then recalculates the resulting absorbance 'difference' spectrum into transmission. Difference spectra are very sensitive to small changes in the shapes and positions of the bands, therefore it is essential that identical instrument conditions are used for spectra involved in any subtraction.

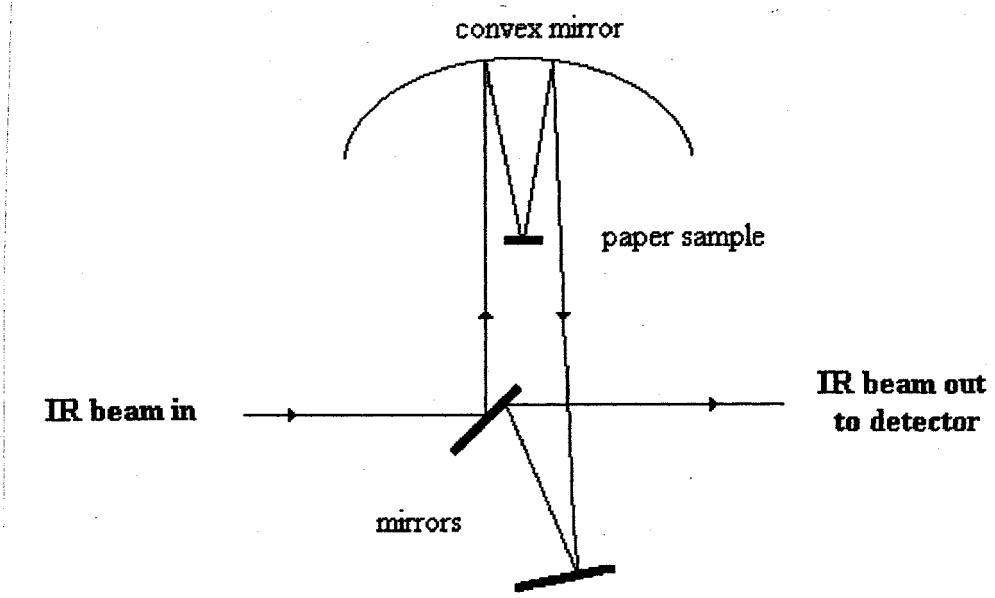

Fig. 37 Arrangement of mirrors for transmission data collection within the Perkin Elmer Paragon 1000

The spectra of standard sized and size removed 'Roma' paper, and Whatman No. 1 filter paper, were recorded for reference in the 3000-1350 cm^{-1} region, using a Perkin Elmer Paragon 1000. Small blank samples of the three papers were laser treated as described previously (section **2.5.2**), using a pulse energy of 20 mJ, nominal fluence of 41 ± 12 Jcm^{-2}, and pulse duration 87 ns. The nominal fluence of 41 ± 12 Jcm^{-2} was chosen, as it was slightly more than sufficient to remove ink (see section **2.4.3**). The DRIFT spectra of the laser treated regions were recorded as before and compared with the reference spectra.

The spectrum of gelatin, the sizing agent for 'Roma', was also recorded for reference in the 3000-1350 cm^{-1} region.

2.5.4 The use of sodium borohydride to assist in the detection of possible oxidation of 'Roma' paper as a result of Nd:YAG laser treatment.

DRIFT spectroscopy (**2.5.3**) did not give particularly clear 'difference' spectra, and it was felt that one possible reason could be the age of the paper samples. The retailer could not give any information about the production date of the paper, and therefore it was possible that the cellulose had already been oxidized prior to the laser treatment experiments. Any such oxidation could mask oxidation caused by the laser treatment. It was decided to reduce some of the paper samples prior to laser treatment to allow oxidation caused by the laser to be detected more readily by FTIR. Sodium borohydride is frequently used by paper conservators to reduce the carbonyl groups present on partially oxidized cellulose, to harmless alcohol groups[104,105].

Blank sheets of standard sized and size removed 'Roma' cotton paper, and Whatman filter paper No. 1, were immersed in a freshly prepared (0.1%) sodium borohydride solution for one hour, washed in several changes of water, and allowed to dry. The DRIFT spectrum for the 3000-1350 cm^{-1} region was recorded for each sample, using a Perkin Elmer Paragon 1000. These were compared with the reference spectra of standard sized and size removed 'Roma' paper, and Whatman filter paper No. 1. Small samples of the freshly reduced papers were laser treated as described previously (see section **2.5.3**), using a pulse energy of 20 mJ, nominal fluence of 41± 12 Jcm^{-2}, and pulse duration 87 ns. The DRIFT spectrum of each laser treated region was recorded as before using the Perkin Elmer Paragon 1000, and compared with the spectrum of the appropriate reduced reference sample. Spectra were recorded immediately after laser treatment, after one week and after five weeks had elapsed.

2.5.5 The use of Gas Chromatography (GC) to identify the presence of sugars caused by humid oven ageing of Nd:YAG laser treated 'Roma' paper.

The microscopic appearance of laser treated 'Roma' (see section **2.4.1**), showed no sign of discoloration or charring. This suggested that though there was surface disruption to the paper the cellulose was not subject to the type of high temperature (above 300 °C) reaction involving the production of tars and oils as described by Shafizadeh[68,69] (see section **1.4 The degradation of cellulose**). Also, the Russell effect tests, the methylene blue tests, and FTIR spectroscopy did not produce strong evidence to suggest that there was oxidation of the cellulose on paper freshly treated with the laser. However, the results of similar tests on samples which had been subjected to humid ageing (particularly the standard sized 'Roma'), showed that there was a significant chemical reaction in the paper perhaps induced by the laser. It was decided to investigate the possible presence of sugars, produced during depolymerisation reactions above 300 °C as described by Shafizadeh[68,69].

The presence of sugars in degraded cellulose can be determined using gas chromatography[139,140]. The preparation for GC/MS analysis requires that the sample extracts undergo hydrolysis and be made volatile via derivatisation.

Methods involving the formation of methylated methyl glycosides, acetals, acetates, trimethylsilyl ethers, and alditol acetate derivatives of monosaccharides have enjoyed popularity in the past. Today, however trimethylsilyl (TMS) derivatives of carbohydrates are among the most widely used, due to their high volatility and ease of preparation[140]. During this procedure the non-volatile -OH groups are converted to volatile non-polar, $-OSi(CH_3)_3$ trimethylsilyl ether groups.

Blank samples of standard sized, and size removed 'Roma' paper were laser treated as described previously (section **2.5.3**), using a pulse energy of 20 mJ, nominal fluence of 41 ± 12 Jcm^{-2}, and pulse duration 87 ns. The samples were placed in a humid oven maintained continuously at 90°C, and 50% R.H., and aged for one month. Small squares (10 mm x 10 mm), were cut from both laser treated, and untreated regions of the samples, and extracted in distilled water for 24 hours at 60 °C, to extract any sugars present. The extracts were desiccated until dry.

2 drops of trifluoroacetic acid were added to each extract sample, and heated at 105 °C for 45 minutes. The samples were cooled to room temperature and 4 drops of pyridine added to each extract. 6 drops of hexamethyldisilazane (HMDS) and 2 drops of trifluoroacetic acid were added to the samples, stirred for 30 seconds and allowed to stand for 24 hours prior to analysis.

Separation and analysis was carried out using GC/MS with selected ion monitoring. A 5890 Series II Gas Chromatograph was used with MS-Chemstation programme control and data processing and G1034B software package (HP). The column was type DB-5, 30 m long, with internal diameter 0.25 mm and a coating of 0.25 microns (Fisher Scientific). The temperature programme was 43 minutes long; the initial temperature was 100 °C, which was held for 2 minutes, then increased at a rate of 6 °C per minute up to 285 °C at which point it was held for 10 minutes. The retention times of the compounds present in the extracts, were compared with those of standard compounds, and their identities were determined by comparison of mass spectra with the mass spectra of references in the computer's search libraries, Databases; sugars 1, sugars 2.1, and nbs 75k.1.

CHAPTER 3:

RESULTS

3.1 Part one: Preliminary tests

3.1.1 Effectiveness of ink removal from paper, using a Q-switched Nd:YAG laser.

The laser operating parameters for the preliminary ink removal tests are shown in Table 26. Results from the preliminary ink removal tests are shown in Tables 27-33. Fluences were increased incrementally over the nominal fluence range 4 – 61 Jcm^{-2}. The results were recorded by eye and consequently it was difficult to discern the difference in effect of individual fluence increments on the paper samples. The results in Tables 27-33 are drawn from observations of experiments repeated on six separate samples. For each Table, column 2 shows a series of fluence ranges over which, the reported effect described in column 3, was observed. Thus for a sample of 'Roma' paper with black ball-point pen ink (Table 27) slight ink removal would be expected between 8 ± 2 and 12 ± 4 Jcm^{-2}, but clearly visible ink removal was unlikely to be observed until at least a nominal fluence of 16 ± 5 Jcm^{-2}.

Ink type	Range of fluences over 6 experiments/ Jcm^{-2} ± 30%	Effect on ink/paper recorded visually
Black ball-point pen ink	4	No visible effect
	8-12	Slight ink removal
	16-53	Clearly visible ink removal
	45-61	Clearly visible damage
Blue ball point pen ink	4	No visible effect
	8-12	Slight ink removal
	16-53	Clearly visible ink removal
	45-61	Clearly visible damage
Red ball-point pen ink	4-24	No visible effect
	29-33	Slight ink removal
	37-45	Clearly visible ink removal
	53-61	Clearly visible damage
Green ball-point pen ink	4-24	Clearly visible ink removal
	29-61	Clearly visible damage
Un-inked standard	4-16	No visible effect
	20-33	Slight damage
	37-61	Clearly visible damage

Table 27. Effect of variation of laser fluence on ball-point pen ink removal, and damage threshold for Roma 100% cotton paper.

Ink type	Range of fluences over 6 experiments/ $Jcm^{-2} \pm 30\%$	Effect on ink/paper recorded visually
Black fibre tip pen ink	4-16	No visible effect
	20-24	Slight ink removal
	29-61	Clearly visible ink removal
Blue fibre tip pen ink	4-24	No visible effect
	29-33	Slight ink removal
	37-61	Clearly visible ink removal
Green fibre tip pen ink	4-24	No visible effect
	29-33	Slight ink removal
	37-61	Clearly visible ink removal
Red fibre tip pen ink	4-12	No visible effect
	16-24	Slight ink removal
	29-33	Clearly visible ink removal
	37-61	Clearly visible damage
Pink highlighter pen ink	4-24	No visible effect
	29-33	Slight ink removal
	37-41	Clearly visible ink removal
	45-61	Clearly visible damage
Yellow highlighter pen ink	4-8	No visible effect
	12-20	Slight charring
	24-61	Charring and damage

Table 28. Effect of variation of laser fluence on fibre tip and highlighter pen ink removal, and damage threshold for Roma 100% cotton paper.

Ink type	Range of fluences over 6 experiments/ $Jcm^{-2} \pm 30\%$	Effect on ink/paper recorded visually
Black ball-point pen ink	4-8	Slight ink removal
	12-24	Clearly visible ink removal
	29-41	Clearly visible damage
	45-61	Excessive damage
Blue ball point pen ink	4-8	Slight ink removal
	12-24	Clearly visible ink removal
	29-41	Clearly visible damage
	45-61	Excessive damage
Red ball-point pen ink	4-12	No visible effect
	16-29	Slight ink removal
	33-45	Clearly visible ink removal
	45-61	Clearly visible damage
Green ball-point pen ink	4-8	Slight ink removal
	12-24	Clearly visible ink removal
	29-41	Clearly visible damage
	45-61	Excessive damage
Un-inked standard	4-12	No visible effect
	16-29	Slight damage
	33-45	Clearly visible damage
	45-61	Excessive damage

Table 29. Effect of variation of laser fluence on ball-point pen ink removal, and damage threshold for Endleaf 100% cotton paper.

Ink type	Range of fluences over 6 experiments/ $Jcm^{-2} \pm 30\%$	Effect on ink/paper recorded visually
Black fibre tip pen ink	4-12	No visible effect
	16-20	Slight ink removal
	24-41	Clearly visible ink removal
	45-61	Clearly visible damage
	57-61	Charring and damage
Blue fibre tip pen ink	4-33	No visible effect
	37-45	Slight ink removal
	57-61	Charring and damage
Green fibre tip pen ink	4-33	No visible effect
	37-45	Slight ink removal
	57-61	Charring and damage
Red fibre tip pen ink	4-33	No visible effect
	37-45	Slight ink removal
	57-61	Charring and damage
Pink highlighter pen ink	4-12	No visible effect
	16-20	Slight ink removal
	24-41	Clearly visible damage
	45-61	Slight charring and damage
	57-61	Charring and damage
Yellow highlighter pen ink	4-12	No visible effect
	16-20	Slight ink removal
	24-41	Clearly visible damage
	45-61	Slight charring and damage
	57-61	Charring and damage

Table 30. Effect of variation of laser fluence on fibre tip and highlighter pen ink removal, and damage threshold for Endleaf 100% cotton paper.

Ink type	Range of fluences over 6 experiments/ $Jcm^{-2} \pm 30\%$	Effect on ink/paper recorded visually
Black ball-point pen ink	4-12	Clearly visible ink removal
	16-24	Clearly visible damage
	29-61	Excessive damage
Blue ball point pen ink	4-12	Clearly visible ink removal
	16-24	Clearly visible damage
	29-61	Excessive damage
Red ball-point pen ink	4-8	No visible damage
	12-16	Slight ink removal
	20-37	Clearly visible damage
	29-61	Excessive damage
Green ball-point pen ink	4-12	Clearly visible ink removal
	16-24	Clearly visible damage
	29-61	Excessive damage
Un-inked standard	4-12	Slight damage
	16-24	Clearly visible damage
	29-61	Excessive damage
	57-61	Charring and damage

Table 31. Effect of variation of laser fluence on ball-point pen ink removal, and damage threshold for mechanical woodpulp paper.

Ink type	Range of fluences over 6 experiments/ $Jcm^{-2} \pm 30\%$	Effect on ink/paper recorded visually
Black fibre tip pen ink	4-8	No visible effect
	12-16	Slight ink removal
	20-29	Slight damage
	33-37	Clearly visible damage
	41-61	Excessive damage
	57-61	Charring and damage
Blue fibre tip pen ink	4-8	No visible effect
	12-16	Slight ink removal
	20-29	Slight damage
	33-37	Clearly visible damage
	41-61	Excessive damage
	57-61	Charring and damage
Green fibre tip pen ink	4-8	No visible effect
	12-16	Slight ink removal
	20-29	Slight damage
	33-37	Clearly visible damage
	41-61	Excessive damage
	57-61	Charring and damage
Pink highlighter pen ink	4-8	Slight damage
	12-24	Clearly visible damage
	29-41	Excessive damage
	45-61	Charring and damage
Yellow highlighter pen ink	4-8	Slight damage
	12-24	Clearly visible damage
	29-41	Excessive damage
	45-61	Charring and damage

Table 32. Effect of variation of laser fluence on fibre tip and highlighter pen ink removal, and damage threshold for mechanical woodpulp paper.

Operation of the laser using single shot mode, and 10 Hz mode were compared. It was observed that any damage which occurred was caused over the first two or three pulses, and subsequent pulses caused no further damage.

Photomicrographs were taken of the effect of laser treatment on, black ball-point pen ink on 'Roma' (4-41 Jcm^{-2}, Fig. 38), yellow highlighter pen ink on mechanical woodpulp paper (4-37 Jcm^{-2}, Fig. 39), and the un-inked standard mechanical woodpulp paper (4-24 Jcm^{-2}, Fig. 40).

Ink type	Range of fluences over 6 experiments/ $Jcm^{-2} \pm 30\%$	Effect on ink/paper recorded visually
Black ball-point pen ink	4-8	No visible effect
	12-24	Clearly visible ink removal
	29-37	Slight damage
	41-61	Charring and damage
Blue ball point pen ink	4-8	No visible effect
	12-24	Clearly visible ink removal
	29-37	Slight damage
	41-61	Charring and damage
Red ball-point pen ink	4-8	No visible effect
	12-24	Clearly visible ink removal
	29-37	Slight damage
	41-61	Charring and damage
Green ball-point pen ink	4-8	No visible effect
	12-24	Clearly visible ink removal
	29-37	Slight damage
	41-61	Charring and damage
Un-inked standard	4-8	No visible effect
	12-37	Slight damage
	29-61	Charring and damage

Table 33. Effect of variation of laser fluence on ball-point pen ink removal, and damage threshold for chemical woodpulp paper.

Microscopic investigation showed that the ball-point pen inks tended to form viscous clots on the surface fibres of the paper, whereas the ink from the fibre tip pens flowed more freely resulting in considerable coverage of the surface fibres, and also some of the underlying fibres.

3.1.2 Microscopic examination of the damage to the surface of 'Roma' paper, as a result of black ball-point pen ink removal by Nd:YAG laser.

1. Ink removal using a pulse length range 87 - >200 ns, normal atmosphere (Table 26)

The results of laser removal of the black ball-point pen ink from the 'Roma' paper are recorded in Table 34. Table 34 represents the results typical of the six experiments carried out.

There was no visible effect on the ink until a nominal fluence of 16 ± 5 Jcm^{-2} was used. At this fluence the ink was partially removed (Fig. 41), however cleaning was uneven. The threshold for a continuous, even, removal of ink was 37 ± 11 Jcm^{-2}, however the paper appeared more thoroughly cleaned at a nominal fluence of 41 ± 12 Jcm^{-2} (Fig.42). Removal of ink at this fluence was accompanied by considerable sparking and cracking, though this was not solely confined to inked areas.

Scanning electron microscopy (SEM) showed that the threshold for damage to the inked paper was 24 ± 7 Jcm^{-2}, but that threshold for damage to un-inked paper was 37 ± 11 Jcm^{-2}. Figures 43-46 show the SEM record of the damage caused to the paper by nominal laser fluences of 29, 37, and 41 Jcm^{-2} respectively.

Input voltage / V	Energy per pulse / mJ ± 0.5 mJ	Fluence / Jcm^{-2}	Effect on ink as determined by optical microscope	Damage caused to inked paper as determined by SEM	Damage caused to un-inked paper as determined by SEM
530	2	4 ± 1	no effect	no effect	no effect
535	4	8 ± 2	no effect	no effect	no effect
542	6	12 ± 4	no effect	no effect	no effect
549	8	16 ± 5	partial removal	no effect	no effect
556	10	20 ± 6	partial removal	no effect	no effect
562	12	24 ± 7	partial removal	slight damage	no effect
568	14	29 ± 9	partial removal	slight damage	no effect
573	16	33 ± 10	partial removal	slight damage	no effect
578	18	37 ± 11	ink removal	damage	damage
584	20	41 ± 12	ink removal	damage	damage

Table 34. Microscopic examination of surface damage on 'Roma' paper, due to Q-switched Nd:YAG laser treatment over a fluence range of 4-41 Jcm^{-2}. (Spot size 125 μm. ±18 μm, pulse repetition rate 10 Hz, pulse duration as for Table 26).

Figures 47 & 48 show the appearance of 'Roma' cotton paper before and after laser treatment using a fluence of 37 ± 11 Jcm^{-2}.

2. Ink removal using an attenuated beam, pulse length of 63 ns, normal atmosphere (Table 24)

The results of laser removal of the black ball-point pen ink from the 'Roma' paper using a pulse length of 63 ns, are recorded in Table 35. Table 35 represents the results typical of the six experiments carried out.

There was no visible effect on the ink until a nominal fluence of 8 ± 2 Jcm^{-2} was used. At this fluence the ink was partially removed, however cleaning was uneven. The threshold for a continuous, even, removal of ink was 20 ± 6 Jcm^{-2} (Fig. 49), however the paper appeared more thoroughly cleaned at a nominal fluence of 24 ± 7 Jcm^{-2}. Removal of ink at this fluence was accompanied by considerable sparking and cracking.

SEM showed that the threshold for damage to the inked paper was 16 ± 5 Jcm^{-2}, but that threshold for damage to un-inked paper was 20 ± 6 Jcm^{-2}. Figures 50 & 51 show the SEM record of the damage caused to the paper by an average laser fluence of 24 ± 7 Jcm^{-2}.

Energy per pulse / mJ ± 0.5 mJ	Fluence / Jcm^{-2}	Effect on ink as determined by optical microscope	Damage caused to inked paper as determined by SEM	Damage caused to un-inked paper as determined by SEM
2	4 ± 1	no effect	no effect	no effect
4	8 ± 2	partial removal	no effect	no effect
6	12 ± 4	partial removal	no effect	no effect
8	16 ± 5	partial removal	slight damage	no effect
10	20 ± 6	ink removal	slight damage	slight damage
12	24 ± 7	ink removal	damage	damage

Table 35. Microscopic examination of surface damage on 'Roma' paper, due to Q-switched Nd:YAG laser treatment, using a flashlamp voltage of 600 V and pulse duration of 63 ns. (Spot size 125 μm. ± 18 μm, pulse repetition rate 10 Hz).

3. Ink removal using an attenuated beam pulse length of 29 ns, normal atmosphere (Table 24)

The results of laser removal of the black ball-point pen ink from the 'Roma' paper using a pulse length of 29 ns, are recorded in Table 36. Table 36 represents the results typical of the six experiments carried out.

There was no visible effect on the ink until a nominal fluence of 8 ± 2 Jcm^{-2} was used. At this fluence the ink was partially removed, however cleaning was uneven. The threshold for a continuous, even, removal of ink was 16 ± 5 Jcm^{-2}, however the paper appeared more thoroughly cleaned at a nominal fluence of 20 ± 6 Jcm^{-2}. Sparking was evident at this fluence but not as noticeable as that witnessed using longer pulses (87 ns).

SEM showed that the threshold for damage to the inked paper was 12 ± 4 Jcm^{-2} , but that threshold for damage to un-inked paper was 16 ± 5 Jcm^{-2}.

Energy per pulse / mJ ± 0.5 mJ	Fluence / Jcm^{-2}	Effect on ink as determined by optical microscope	Damage caused to inked paper as determined by SEM	Damage caused to un-inked paper as determined by SEM
2	4 ± 1	no effect	no effect	no effect
4	8 ± 2	partial removal	no effect	no effect
6	12 ± 4	partial removal	slight damage	no effect
8	16 ± 5	ink removal	slight damage	slight damage
10	20 ± 6	ink removal	damage	damage

Table 36. Microscopic examination of surface damage on 'Roma' paper, due to Q-switched Nd:YAG laser treatment, using a flashlamp voltage of 700 V and pulse duration of 29 ns. (Spot size 125 μm. ± 18 μm, pulse repetition rate 10 Hz).

4. Ink removal using an attenuated beam pulse length of 26 ns, normal atmosphere (Table 24)

The results of laser removal of the black ball-point pen ink from the 'Roma' paper using a pulse length of 26 ns, are recorded in Table 37. Table 37 represents the results typical of the six experiments carried out.

There was no visible effect on the ink until a nominal fluence of 8 ± 2 Jcm^{-2} was used. At this fluence the ink was partially removed, however cleaning was uneven. The threshold for a continuous, even, removal of ink was 16 ± 5 Jcm^{-2} (Fig.52), however the paper appeared more thoroughly cleaned at a nominal fluence of 20 ± 6 Jcm^{-2}. Sparking was evident at this fluence but not as noticeable as that witnessed using longer pulses (87 ns.).

SEM showed that the threshold for damage to the inked paper was 12 ± 4 Jcm^{-2} , but that threshold for damage to un-inked paper was 16 ± 5 Jcm^{-2}. Figures 53 & 54 show the SEM record of the damage caused to the paper by an average laser fluence of 20 ± 6 Jcm^{-2}.

Energy per pulse / mJ ± 0.5 mJ	Fluence / Jcm^{-2}	Effect on ink as determined by optical microscope	Damage caused to inked paper as determined by SEM	Damage caused to un-inked paper as determined by SEM
2	4 ± 1	no effect	no effect	no effect
4	8 ± 2	partial removal	no effect	no effect
6	12 ± 4	partial removal	slight damage	no effect
8	16 ± 5	ink removal	slight damage	slight damage
10	20 ± 6	ink removal	damage	damage

Table 37. Microscopic examination of surface damage on 'Roma' paper, due to Q-switched Nd:YAG laser treatment, using a flashlamp voltage of 750 V and pulse duration of 26 ns. (Spot size 125 μm. ± 18 μm, pulse repetition rate 10 Hz).

Figure 55 shows the appearance of 'Roma' cotton paper after laser treatment using an average fluence of 20 ± 6 Jcm^{-2}.

5. Ink removal using a pulse length range 87 - >200 ns, argon atmosphere (Table 26)

The results of laser removal of the black ball-point pen ink from the 'Roma' paper are recorded in Table 38. Table 38 represents the results typical of the six experiments carried out.

There was no visible effect on the ink until a nominal fluence of 11± 3 Jcm^{-2} was used. At this fluence the ink was partially removed, however cleaning was uneven. The threshold for a continuous, even, removal of ink was 34 ± 10 Jcm^{-2}, however the paper appeared more thoroughly cleaned at a nominal fluence of 38 ± 11 Jcm^{-2} (Fig.56). Removal of ink at this fluence was accompanied by considerable sparking and cracking.

SEM showed that the threshold for damage to the inked paper was 30 ± 9 Jcm^{-2}, but that the threshold for damage to un-inked paper was 34 ± 10 Jcm^{-2}. Figures 57 - 59 show the SEM record of the damage caused to the paper by an average laser fluence of 38 ± 11Jcm^{-2}.

Input voltage / V	Energy per pulse / mJ ± 0.5 mJ	Fluence / Jcm^{-2}	Effect on ink as determined by optical microscope	Damage caused to inked paper as determined by SEM	Damage caused to un-inked paper as determined by SEM
530	2	4 ± 1	no effect	no effect	no effect
535	4	8 ± 2	no effect	no effect	no effect
542	6	11 ± 3	partial removal	no effect	no effect
549	8	15 ± 5	partial removal	no effect	no effect
556	10	19 ± 6	partial removal	no effect	no effect
562	12	23 ± 7	partial removal	no effect	no effect
568	14	27 ± 8	partial removal	no effect	no effect
573	16	30 ± 9	partial removal	slight damage	no effect
578	18	34 ± 10	ink removal	slight damage	slight damage
584	20	38 ± 11	ink removal	damage	damage

Table 38. Microscopic examination of surface damage on 'Roma' paper, due to Q-switched Nd:YAG laser treatment in an argon environment over a range of fluences. (Spot size 125 μm. ± 18 μm, pulse repetition rate 10 Hz, pulse duration as for Table 26).

3.1.3 Microscopic comparison of the damage to the surface of 'Roma' paper, as a result of black ball-point pen ink removal by Nd:YAG laser, and contemporary mechanical methods.

The damage caused by removal of the black ball-point pen ink line from sample A (laser 37 Jcm^{-2}), B (eraser), C (scalpel), and D (scalpel and eraser) is shown by SEM (Figs. 60-63 respectively).

3.1.4 The effect of accelerated ageing on the appearance of Nd:YAG laser treated paper.

The results of light ageing, and dry oven ageing are equivocal as there was no discernible difference in appearance between the laser treated regions and the un-treated areas.

Humid oven ageing yielded far more interesting results (Fig. 64), where there was considerable local red/brown discoloration to standard sized paper samples, laser treated with a nominal fluence of 41 ± 12 Jcm^{-2}. Even after one day of humid ageing, the site of laser treatment at 41 ± 12 Jcm^{-2} was noticeable. Observation of the paper in cross-section shows that the discoloration is confined to the surface, and is not witnessed in the body of the paper (Fig. 65).

The humid aged, size removed samples gave very different results. There was hardly any noticeable difference in appearance between the laser treated regions and the untreated regions. The laser treated regions of the samples were only marginally darker than their untreated equivalents, even after one month of humid ageing.

There was no visible difference between the laser treated, and untreated filter paper samples.

3.2 Investigation of physical damage to Nd:YAG treated paper

3.2.1 Reflectance measurements of humid aged, Nd:YAG laser treated paper.

1. Ageing after laser treatment using a pulse length of 87 ns, normal atmosphere

Figure 66 shows the change in the reflectance spectrum of humid aged, laser treated standard sized 'Roma' paper. The samples were prepared using a nominal fluence of 41± 12 Jcm^{-2}, with a pulse duration of 87 ns, in a normal atmosphere (see section **2.4.3**). The changes were recorded as humid ageing was increased from one day, to one month. Humid ageing resulted in an overall yellow/brown discoloration to the paper, in comparison with an unaged reference, and considerable local discoloration to the laser treated regions.

There is a decreasing tendency for the paper to reflect light from the blue end of the spectrum (400 nm.). Figure 67 shows the reflectance spectra of laser treated, and untreated, standard sized 'Roma' after one month of humid ageing, and an unaged reference. At 400 nm, there is approximately 15% less visible light reflected by the laser treated sample compared to the untreated background sample.

Figure 68 shows the minimal difference between the reflectance spectra of laser treated, and untreated size removed 'Roma' paper, after one month of humid ageing. The sample was prepared using a nominal fluence of 41 ± 12 Jcm^{-2}, with a pulse duration of 87 ns, in a normal atmosphere (see section **2.4.3**).

At 400 nm, there is approximately 2% less visible light reflected by the laser treated sample compared to the untreated background sample.

2. Ageing after laser treatment using an attenuated pulse lengths of 63, and 26 ns

The paper samples prepared using shorter laser pulse lengths of 63 ns (see section **2.4.3**), did exhibit localized discoloration after humid ageing for one month. Figure 69 shows the relative decrease in reflectance of light across the visible spectrum, with respect to the untreated background sample.

At 400 nm, there is approximately 5% less visible light reflected by the laser treated sample compared to the untreated sample.

A different piece of 'Roma' paper was used to that illustrated in Figures 66, & 67 which explains why the reference spectrum is not the same. 'Roma' is a handmade paper and each sheet may contain a slightly different amount of gelatin, thus producing a difference in the spectra. Gelatin is a stronger absorber of ultra-violet radiation than cellulose and consequently the reference spectra differ mostly at the blue end of the spectrum. The reference for Figures 69 & 70 appears similar to that for Figure 68, this is purely coincidental and presumably due to a thin application of size during manufacture.

The paper samples prepared using shorter laser pulse lengths of 26 ns, nominal fluence 20 $\pm$ 6 Jcm^{-2} (see section **2.4.3**), did exhibit some localized discoloration after humid ageing for one month. Figure 70 shows the relative decrease in reflectance of light across the visible spectrum, with respect to the untreated background sample.

At 400 nm, there is approximately 3% less visible light reflected by the laser treated sample compared to the untreated sample.

3. Ageing after laser treatment using a pulse length of 87 ns, argon atmosphere

Figure 71 shows the reflectance spectra of laser treated, and untreated, standard sized 'Roma' after one month of humid ageing, and an unaged reference. The samples were prepared using a nominal fluence of 38 ± 11 Jcm^{-2}, with a pulse duration of 87 ns, in an argon atmosphere (see section **2.4.3**). A different piece of 'Roma' paper was used to that illustrated in Figures 66,67 & 69, which explains why the reference spectrum is not the same.

At 400 nm, there is approximately 30% less visible light reflected by the laser treated sample compared to the untreated background sample.

Humid ageing resulted in an overall yellow/brown discoloration to the paper, in comparison with an unaged reference, and considerable local discoloration to the laser treated regions (Fig. 72).

3.2.2 The effect on the tensile strength and tendency to tear, of Nd:YAG laser treated 'Roma' paper.

Data from the tensile strength experiments are recorded in Tables 39 & 40. The errors for mean tensile index were calculated using equation 3, Appendix 1.

The tendency to tear at laser treatment sites, with increasing fluence is illustrated by two histograms (Figs. 73 & 74).

SEM was used to observe the broken fibres created at the tear sites during tensile testing. Two samples were compared, a typical break in a standard untreated sample (Fig. 75), and a break at a laser treatment site produced using a nominal fluence of 41 ± 12 Jcm^{-2} (Fig. 76).

Individual broken fibres from the tear sites were compared (Figs. 77 & 78).

Laser fluence / Jcm^{-2}	Mean tensile strength / $kNm^{-1} \pm 0.01\ kNm^{-1}$	Grammage / $gm^{-2} \pm 6\ gm^{-2}$	Mean tensile index / Nmg^{-1}
standard	5.00	153	32.7 ± 1.3
4 ± 1	5.56	166	33.5 ± 1.2
8 ± 2	5.67	170	33.4 ± 1.2
12 ± 4	4.27	136	31.4 ± 1.4
16 ± 5	3.84	116	33.1 ± 1.7
20 ± 6	4.13	124	33.3 ± 1.6
24 ± 7	4.04	119	33.9 ± 1.7
29 ± 9	4.70	143	32.9 ± 1.4
33 ± 10	4.99	152	32.8 ± 1.3
37 ± 11	5.77	171	33.7 ± 1.2
41 ± 12	4.83	152	31.8 ± 1.3
45 ± 14	4.92	157	31.3 ± 1.2
49 ± 15	5.07	162	31.3 ± 1.2
52 ± 16	4.79	157	30.5 ± 1.2
57 ± 17	4.92	167	29.5 ± 1.1
61 ± 18	4.52	157	28.8 ± 1.1

Table 39 Tensile testing of 'Roma' cotton paper, laser treated at right angles to the laid lines. (Spot size 125 μm. ±18 μm, pulse repetition rate 10 Hz, pulse duration as for Table 26).

Laser fluence / Jcm^{-2}	Mean tensile strength / $kNm^{-1} \pm 0.01\ kNm^{-1}$	Grammage / $gm^{-2} \pm 6\ gm^{-2}$	Mean tensile index / Nmg^{-1}
standard	4.97	154	32.3 ± 1.3
4 ± 1	5.18	170	30.5 ± 1.1
8 ± 2	4.90	148	33.1 ± 1.3
12 ± 4	4.86	135	36.0 ± 1.6
16 ± 5	5.16	160	32.2 ± 1.2
20 ± 6	4.76	142	33.5 ± 1.4
24 ± 7	4.80	139	34.5 ± 1.5
29 ± 9	4.34	133	32.6 ± 1.5
33 ± 10	5.27	155	34.0 ± 1.3
37 ± 11	5.27	155	34.0 ± 1.3
41 ± 12	5.10	151	33.8 ± 1.3
45 ± 14	4.14	133	31.1 ± 1.4
49 ± 15	5.94	167	35.6 ± 1.3
52 ± 16	4.63	148	31.3 ± 1.3
57 ± 17	4.30	143	30.1 ± 1.3
61 ± 18	4.82	162	29.8 ± 1.1

Table 40. Tensile testing of 'Roma' cotton paper, laser treated in the direction of the laid lines. (Spot size 125 μm. ±18 μm, pulse repetition rate 10 Hz, pulse duration as for Table 26).

Data from the tensile strength experiments using humid aged 'Roma' samples are recorded in Tables 41 & 42. The errors for mean tensile index were calculated using equation 3, Appendix 1.

Laser fluence / Jcm^{-2}	Mean tensile strength / $kNm^{-1} \pm 0.01\ kNm^{-1}$	Grammage / $gm^{-2} \pm 6\ gm^{-2}$	Mean tensile index / Nmg^{-1}
standard	4.98	162	30.7 ± 1.1
4 ± 1	3.68	119	30.9 ± 1.6
8 ± 2	3.28	110	29.8 ± 1.6
12 ± 4	5.10	162	31.5 ± 1.2
16 ± 5	4.12	133	31.0 ± 1.4
20 ± 6	3.97	124	32.0 ± 1.6
24 ± 7	4.81	157	30.6 ± 1.2
29 ± 9	4.34	152	28.6 ± 1.1
33 ± 10	4.99	167	29.9 ± 1.1
37 ± 11	4.67	152	30.7 ± 1.2
41 ± 12	4.67	157	29.7 ± 1.1

Table 41. Tensile testing of 'Roma' cotton paper, laser treated at right angles to the laid lines, and aged for one month at 90 °C, and 50% RH.
(Spot size 125 μm. ±18 μm, pulse repetition rate 10 Hz, pulse duration as for Table 26).

Laser fluence / Jcm^{-2}	Mean tensile strength / $kNm^{-1} \pm 0.01\ kNm^{-1}$	Grammage / $gm^{-2} \pm 6\ gm^{-2}$	Mean tensile index / Nmg^{-1}
standard	4.78	186	25.7 ± 0.8
4 ± 1	4.46	152	29.3 ± 1.2
8 ± 2	4.08	143	28.5 ± 1.2
12 ± 4	4.36	138	31.6 ± 1.4
16 ± 5	4.85	157	30.9 ± 1.2
20 ± 6	5.04	162	31.1 ± 1.2
24 ± 7	4.32	142	30.4 ± 1.3
29 ± 9	4.91	157	31.3 ± 1.2
33 ± 10	4.23	143	29.6 ± 1.2
37 ± 11	4.50	147	30.6 ± 1.3
41 ± 12	5.29	167	31.7 ± 1.1

Table 42. Tensile testing of 'Roma' cotton paper, laser treated in the direction of the laid lines, and aged for one month at 90 °C, and 50% RH.
(Spot size 125 μm. ±18 μm, pulse repetition rate 10 Hz, pulse duration as for Table 26).

The tendency to tear at laser treatment sites, with increasing fluence is illustrated by two histograms (Figs. 79 & 80).

SEM was used to observe the broken fibres created at the tear sites during tensile testing. Two samples were compared, a typical break in a standard untreated humid aged sample, and a break at a humid aged laser treatment site produced using a nominal fluence of 41 ± 12 Jcm^{-2} (Fig. 81). Individual broken fibres from the tear sites were compared (Figs. 82 & 83).

3.2.3 Surface profiling of Nd:YAG laser treated 'Roma' paper.

Figures 84a and 84b show, a) the Talysurf reference profile of the standard 'Roma' paper, taken at right angles to the laid lines, and b) the profile across the three laser lines running parallel to the laid lines.

Figures 85a and 85b show, a) the Talysurf reference profile of the standard 'Roma' paper, taken in the direction of the laid lines, and b) the profile across the three laser lines running at right angles to the laid lines.

3.3 Investigation of chemical damage to Nd:YAG treated paper

3.3.1 The use of the Russell effect to investigate whether Nd:YAG laser treatment of 'Roma' paper causes a local increase in abundance of peroxides.

1. Russell effect after laser treatment using a pulse length range of 87 - >200 ns, normal atmosphere

The Russell effect test results for standard sized and size removed 'Roma' paper are shown in Tables 43 & 44 respectively. The laser was operated over the nominal fluence range 4 - 41 Jcm^{-2} (see section **2.3.2**, Table 26), in a normal atmosphere (see section **2.5.1**). 'Roma' is a handmade paper and each sheet may contain a different amount of gelatin, therefore the experiment was repeated on separate sheets to determine consistency of results. Each result in Tables 43-45 represents a typical result obtained from four identical tests.

Figure 86 shows the typical Russell effect image taken from standard sized 'Roma', a) immediately after, and b) one week after laser treatment.

Figure 87 shows the typical Russell effect image taken from size removed 'Roma', a) immediately after, and b) one week after laser treatment.

The Russell effect test results from scratched standard sized, and size removed 'Roma' are shown in Table 45.

The Russell effect images of laser treated and scratched Whatman filter paper did not register any significant darkening of the film.

Fluence / Jcm^{-2}	Immediate Russell image	One week old Russell image	Two week old Russell image	Three week old Russell image
41 ± 12	white lines	black lines	black lines	faint black lines
37 ± 11	white lines	black lines	black lines	faint black lines
33 ± 10	white lines	black lines	faint black lines	faint black lines
29± 9	white lines	black lines	faint black lines	no lines
24 ± 7	white lines	no lines	no lines	no lines
20 ± 6	white lines	no lines	no lines	no lines
16 ± 5	white lines	no lines	no lines	no lines
12 ± 4	no lines	no lines	no lines	no lines
8 ± 2	no lines	no lines	no lines	no lines
4 ± 1	no lines	no lines	no lines	no lines

Table 43. The change in appearance over time, of the Russell images of standard sized 'Roma' cotton paper, treated using a Q-switched Nd:YAG laser, over a range of fluence levels. (Spot size 125 μm. ± 18 μm, pulse repetition rate 10 Hz, pulse duration as for Table 26).

Fluence / Jcm^{-2}	Immediate Russell image	One week old Russell image	Two week old Russell image	Three week old Russell image
41 ± 12	black lines	faint black lines	no lines	no lines
37 ± 11	black lines	faint black lines	no lines	no lines
33 ± 10	black lines	faint black lines	no lines	no lines
29± 9	black lines	no lines	no lines	no lines
24 ± 7	black lines	no lines	no lines	no lines
20 ± 6	no lines	no lines	no lines	no lines
16 ± 5	no lines	no lines	no lines	no lines
12 ± 4	no lines	no lines	no lines	no lines
8 ± 2	no lines	no lines	no lines	no lines
4 ± 1	no lines	no lines	no lines	no lines

Table 44. The change in appearance over time, of the Russell images of size removed 'Roma' cotton paper, treated using a Q-switched Nd:YAG laser, over a range of fluence levels. (Spot size 125 μm. ± 18 μm, pulse repetition rate 10 Hz, pulse duration as for Table 26).

Paper type	Immediate Russell image	One week old Russell image	Two week old Russell image	Three week old Russell image
Standard sized	black lines	black lines	faint black lines	faint black lines
Size removed	black lines	faint black lines	faint black lines	no lines

Table 45. The change in appearance over time, of the Russell images of standard sized and size removed 'Roma' cotton paper, scratched with a scalpel blade.

2. Russell effect after laser treatment using attenuated pulse lengths of 63, and 26 ns

The results of attenuated laser treatment of 'Roma', are shown in Tables 46 & 47. The laser was operated over the energy range shown in Table 26, in a normal atmosphere using pulse durations of 63, and 26 ns respectively (see section **2.5.1**). Each result in Tables 46 & 47 represents a typical result obtained from four identical tests.

Fluence / Jcm^{-2}	Immediate Russell image	One week old Russell image	Two week old Russell image	Three week old Russell image
24 ± 7	white lines	faint white lines	faint black lines	no lines
20 ± 6	white lines	faint white lines	no lines	no lines
16 ± 5	white lines	faint white lines	no lines	no lines
12 ± 4	white lines	no lines	no lines	no lines
8 ± 2	white lines	no lines	no lines	no lines
4 ± 1	no lines	no lines	no lines	no lines

Table 46. The change in appearance over time, of the Russell images of standard sized 'Roma' cotton paper, treated using an attenuated Q-switched Nd:YAG laser, using a flashlamp voltage of 600 V and pulse duration of 63 ns. (Spot size 125 μm. ± 18 μm, pulse repetition rate 10 Hz).

Fluence / Jcm^{-2}	Immediate Russell image	One week old Russell image	Two week old Russell image	Three week old Russell image
20 ± 6	white lines	faint white lines	faint black lines	no lines
16 ± 5	white lines	faint white lines	no lines	no lines
12 ± 4	white lines	faint white lines	no lines	no lines
8 ± 2	white lines	no lines	no lines	no lines
4 ± 1	no lines	no lines	no lines	no lines

Table 47. The change in appearance over time, of the Russell images of standard sized 'Roma' cotton paper, treated using an attenuated Q-switched Nd:YAG laser, using a flashlamp voltage of 750 V and pulse duration of 26 ns. (Spot size 125 μm. ± 18 μm, pulse repetition rate 10 Hz).

Figure 88 shows the typical Russell effect image taken from the paper, a) immediately after, and b) two weeks after laser treatment, using a pulse duration of 63 ns.

Figure 89 shows the typical Russell effect image taken from the paper, a) immediately after, and b) two weeks after laser treatment, using a pulse duration of 26 ns.

3. Russell effect after laser treatment using a pulse length range 87 - >200 ns, argon atmosphere

The Russell effect test results for standard sized 'Roma' paper laser treated in an argon atmosphere are shown in Table 48. The laser was operated over the energy range shown in Table 26 (see section **2.5.1**). Each result in Table 48 represents a typical result obtained from four identical tests.

Fluence / $Jcm^{-2} \pm 3\ Jcm^{-2}$	Immediate Russell image	One week old Russell image	Two week old Russell image	Three week old Russell image
38 ± 11	white lines	black lines	black lines	faint black lines
34 ± 10	white lines	black lines	faint black lines	faint black lines
30 ± 9	white lines	no lines	no lines	no lines
27 ± 8	white lines	no lines	no lines	no lines
23 ± 7	white lines	no lines	no lines	no lines
19 ± 6	white lines	no lines	no lines	no lines
15 ± 5	white lines	no lines	no lines	no lines
11 ± 3	no lines	no lines	no lines	no lines
8 ± 2	no lines	no lines	no lines	no lines
4 ± 1	no lines	no lines	no lines	no lines

Table 48. The change in appearance over time, of the Russell images of standard sized 'Roma' cotton paper, treated using a Q-switched Nd:YAG laser, over a range of fluence levels, in an argon atmosphere. (Spot size 125 μm. ± 18 μm, pulse repetition rate 10 Hz, pulse duration as for Table 26).

Figure 90 shows the typical Russell effect image taken from the 'Roma' paper, immediately after laser treatment in an argon atmosphere.

3.3.2 The use of methylene blue to investigate whether Nd:YAG laser treatment of 'Roma' paper causes a local increase in abundance of carboxyl groups.

1. Methylene blue test after laser treatment using a pulse length of 87 ns, normal atmosphere

The absorption of methylene blue by the laser treated, standard sized and size removed 'Roma' paper (nominal fluence 41 ± 12 Jcm^{-2}, see section **2.5.2**), was photographed (Figs. 91 & 92). The photographs show an increased absorption of dye in the laser treated regions, however there was also a slight increase in absorption of dye by the scalpel scratched test sample.

The experiments were repeated four times on separate sheets. The result recorded is typical of the four experiments.

The Whatman filter paper showed a slight increase in absorption of dye in the laser treated regions. The colour change was on a par with that caused by scratching the 'Roma' samples.

2. Methylene blue test after laser treatment using attenuated pulse lengths of 63, and 26 ns

Laser treatment of standard sized 'Roma' using 63 ns pulse lengths (nominal fluence 24 ± 7 Jcm^{-2}), did not cause any visible change in absorption of methylene blue.

Laser treatment of standard sized 'Roma' using 26 ns pulse lengths (nominal fluence 20 ± 6 Jcm^{-2}), appeared to cause a reduction in absorption of methylene blue, giving rise to a light coloured square (Fig. 93).

3. Methylene blue test after laser treatment using a pulse length of 87 ns, argon atmosphere

Laser treatment of standard sized 'Roma' in an argon atmosphere (nominal fluence 38 ± 11 Jcm^{-2}), appeared to cause a reduction in absorption of methylene blue, giving rise to a light coloured square (Fig. 94).

3.3.3 The use of Fourier Transform infrared (FTIR) spectroscopy to show the possible oxidation of 'Roma' paper as a result of Nd:YAG laser treatment.

The DRIFT spectra of the standard sized 'Roma' reference, and the size removed 'Roma' reference were recorded. The experiment was repeated six times on separate sheets. The result recorded is typical of the six experiments.

The spectra from the two samples were extremely similar. This can be seen in Figure 95 where spectra (representative of the reference samples, and recorded using identical conditions), have been arranged in close proximity. The difference between the spectra could only be assessed by subtraction of one spectrum from another.

Figure 96 shows the difference spectrum (see section **2.5.3**), obtained when the spectrum of size removed 'Roma' paper (B), was subtracted from the standard sized equivalent (A). There is a peak at 2350 cm^{-1} due to carbon dioxide in the sample, and a broad band between 1700 – 1450 cm^{-1}, however individual peaks are not resolvable.

Figure 97 shows the spectrum of gelatin, the sizing agent for 'Roma' paper.

Figure 98 shows the difference spectrum obtained when the spectrum of laser treated 'Roma' paper (C) (nominal fluence 41± 12 Jcm^{-2}), was subtracted from standard sized 'Roma' paper

(A). No difference spectrum was achieved when (A) was subtracted from (C), because the instrument could not show transmittances > 100 %. There is a broad band between 1700 – 1450 cm^{-1}, however individual peaks are not resolvable.

Figure 99 shows the difference spectrum obtained when the spectrum of size removed 'Roma' paper (B) (nominal fluence 41 ± 12 Jcm^{-2}), was subtracted from laser treated, size removed 'Roma' paper (D). There are peaks at 2900, and 2350 cm^{-1} due to C–H stretching and carbon dioxide respectively. There is a small broad band between 1700 – 1500 cm^{-1}, and a larger band between 1500 – 1300 cm^{-1}, however individual peaks are not resolvable.

The difference spectrum obtained when the spectrum of Whatman filter paper (E), was subtracted from laser treated, Whatman filter paper (F) (nominal fluence 41 ± 12 Jcm^{-2}), showed no identifiable peaks.

3.3.4 The use of sodium borohydride to assist in the detection of possible oxidation of 'Roma' paper as a result of Nd:YAG laser treatment.

The DRIFT spectra of the reduced standard sized 'Roma' reference, and the reduced size removed 'Roma' reference were recorded six times, however when the reduced paper reference spectra were subtracted from laser treated, reduced paper spectra, no identifiable peaks were obtained.

3.3.5 The use of Gas Chromatography (GC) to identify the presence of sugars caused by humid oven ageing of Nd:YAG laser treated 'Roma' paper.

A reasonable separation of the extract samples was obtained by GC (Figs. 100 & 101). The sugar, and sugar related components of the extract were identified by a match of at least 75%, with the mass spectra of references in the computer's search libraries, Databases; sugars 1, sugars 2.1, and nbs 75k.1.

The most abundant sugar and sugar related compounds identified are recorded in Tables 49 & 50, and their structures illustrated (Fig. 102).

Retention time	Compound	Not laser treated peak size	Laser treated peak size
20.45	α-D-glucopyranose	medium	medium
24.18	Mannonic acid	small	very large
31.64	Maltose	very large	-
31.90	Maltose	very large	small
32.38	Maltose	medium	-

Table 49. Compounds identified from the extraction of Nd:YAG laser treated, and untreated standard sized 'Roma' paper, after humid oven ageing.

Retention time	Compound	Not laser treated peak size	Laser treated peak size
15.37	D-arabinofuranose	medium	medium
17.01	Levoglucosan	medium	medium
18.51	β-D-galactofuranose	-	large
20.45	α-D-glucopyranose	very small	medium
24.19	Mannonic acid	-	small

Table 50. Compounds identified from the extraction of Nd:YAG laser treated, and untreated size removed 'Roma' paper, after humid oven ageing.

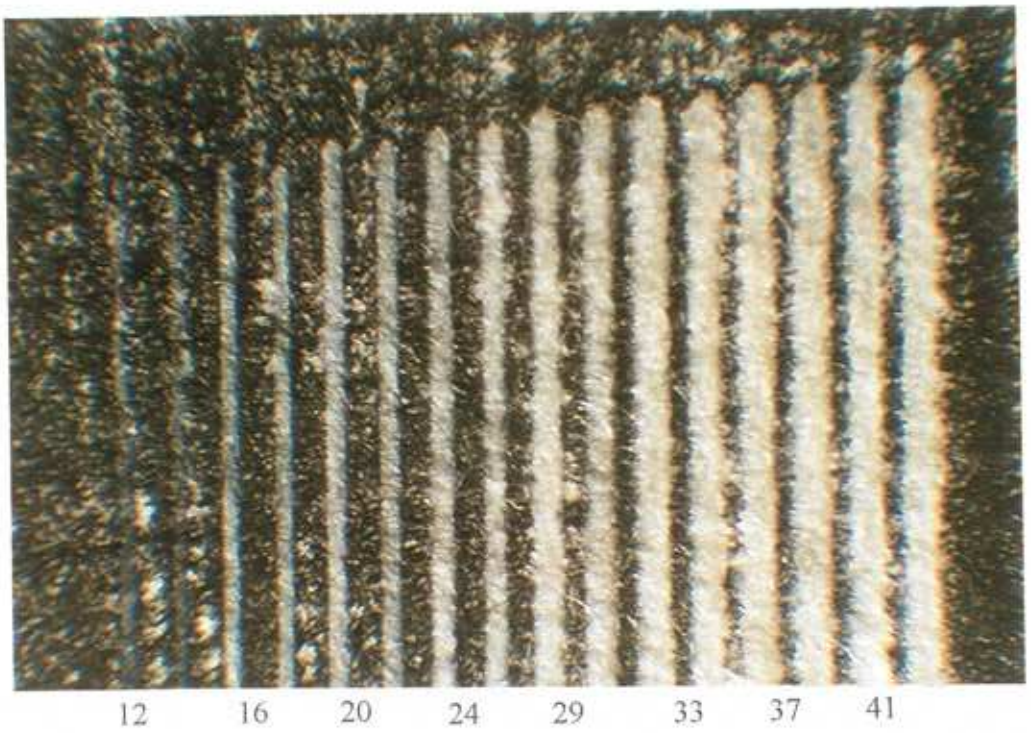

Fig. 38 Photomicrograph (x10) of black ball-point pen ink on 'Roma' paper treated with the Q-switched Nd:YAG laser over a fluence range of 4-41 Jcm^{-2}. One of six experiments. In this experiment slight ink removal was visible at 12 ± 4 Jcm^{-2}. For data on all six experiments see Table 27.

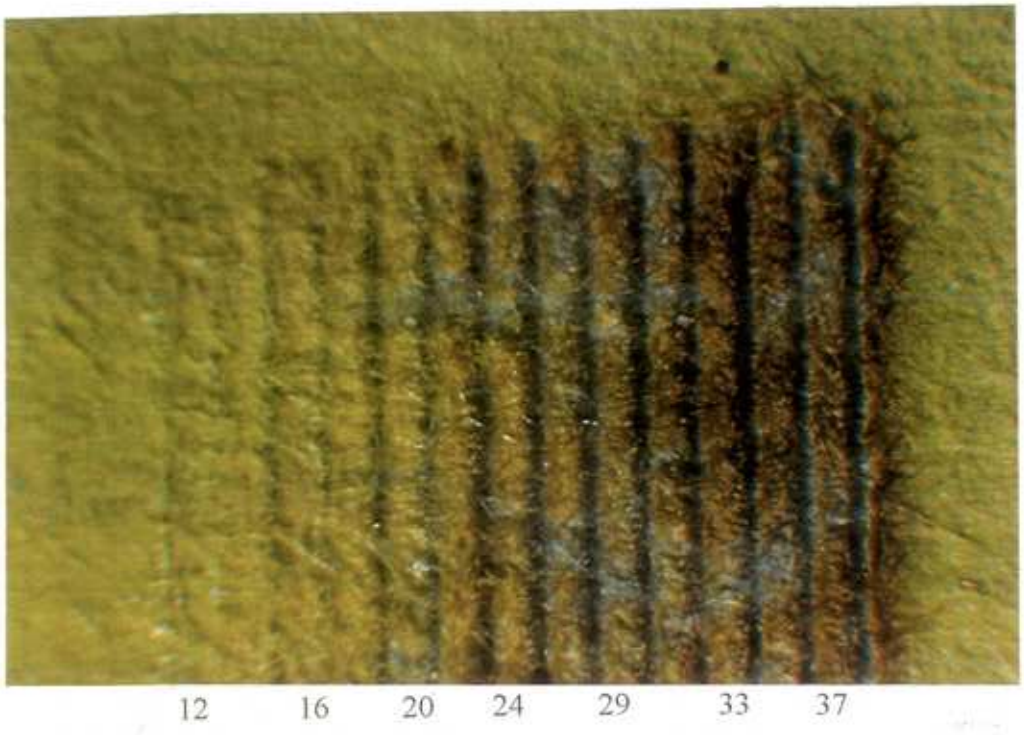

Fig. 39 Photomicrograph (x10) of yellow highlighter pen ink on mechanical woodpulp paper treated with the Q-switched Nd:YAG laser over a fluence range of 4-37 Jcm^{-2}. One of six experiments. In this experiment damage was visible at 12 ± 4 Jcm^{-2}. For data on all six experiments see Table 32.

Fig. 40 Photomicrograph (x10) of un-inked standard mechanical woodpulp paper treated with the Q-switched Nd:YAG laser over a fluence range of 4-33 Jcm^{-2}. One of six experiments. In this experiment damage was visible at 16 ± 5 Jcm^{-2}. For data on all six experiments see Table 31.

Fig. 41 Photomicrograph (x20) of the initial removal of black ball-point pen ink from 'Roma' paper, by Q-switched Nd:YAG laser, using a nominal fluence of 16 ± 5 Jcm^{-2}. For data see Table 34.

Fig. 42 Photomicrograph (x20) of the complete removal of black ball-point pen ink, from 'Roma' paper, by Q-switched Nd:YAG laser, using a nominal fluence of 41 ± 12 Jcm^{-2}. For data see Table 34.

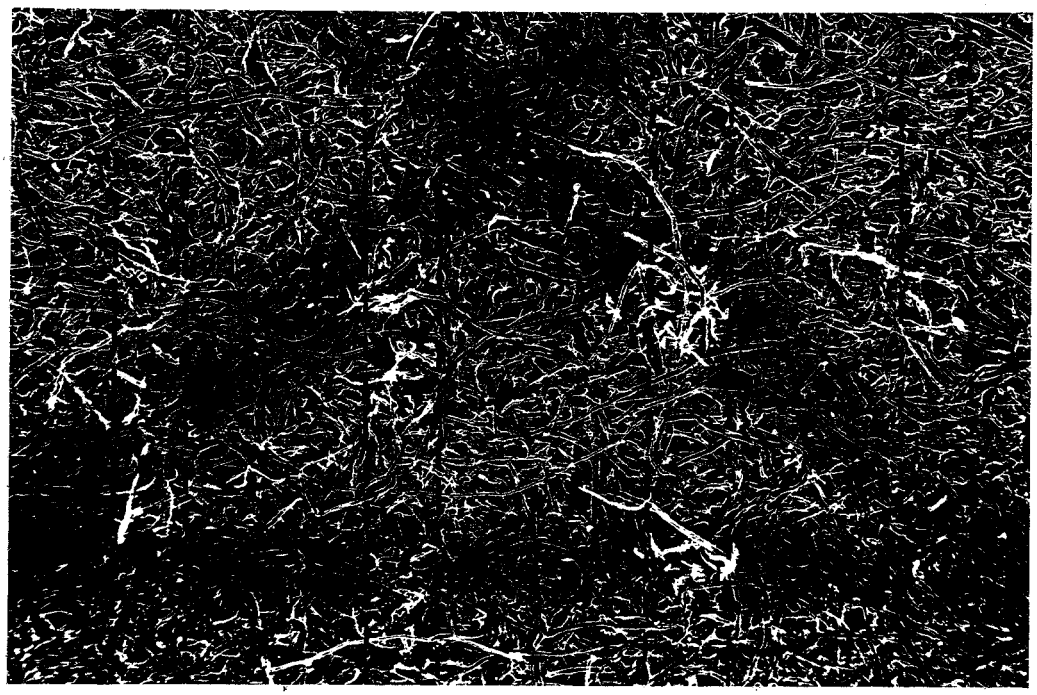

Fig. 43 SEM photograph (x20) of the effect of a nominal laser fluence of 29 ± 9 Jcm^{-2}, on a black ball-point pen ink 'X', on 'Roma' paper. The dotted line indicates the path of the laser. There is damage to the paper where the laser has passed over inked areas.

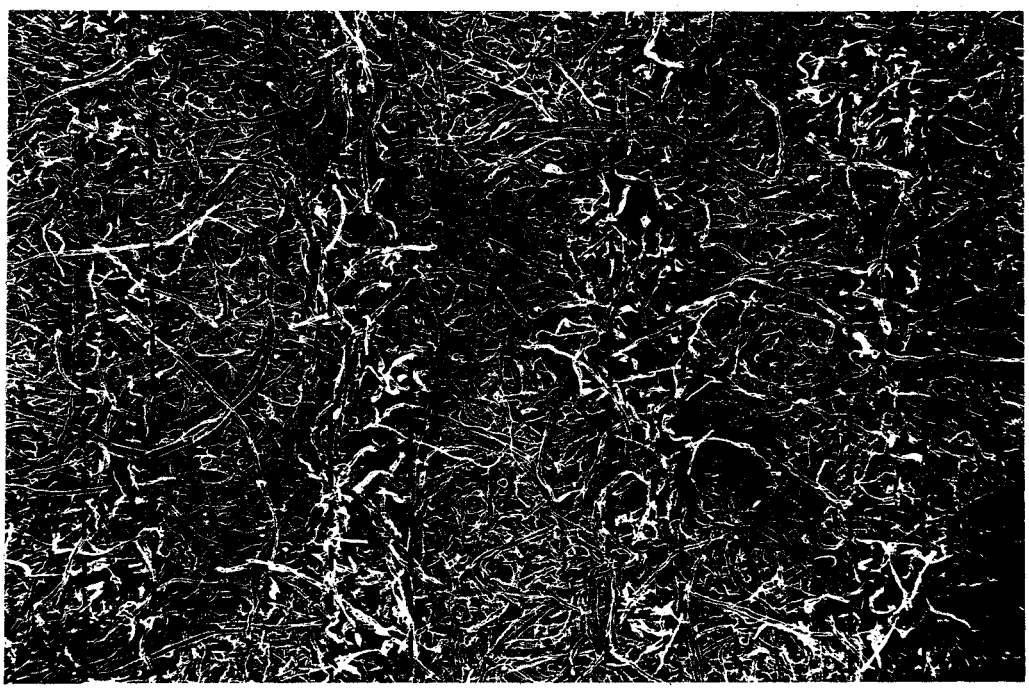

Fig. 44 SEM photograph (x20) of the effect of a nominal laser fluence of 37 ± 11 Jcm^{-2}, on a black ball-point pen ink 'X', on 'Roma' paper. The dotted line indicates the path of the laser. Both the inked and un-inked regions of 'Roma' paper are disrupted by the passage of the laser.

Fig. 45 Side view SEM photograph (x30) of the effect of a nominal laser fluence of 41 ± 12 Jcm^{-2}, on a black ball-point pen ink 'X', on 'Roma' paper. The impact of the laser pulses has blown the fibres at right angles to the body of the paper. For data see Table 34.

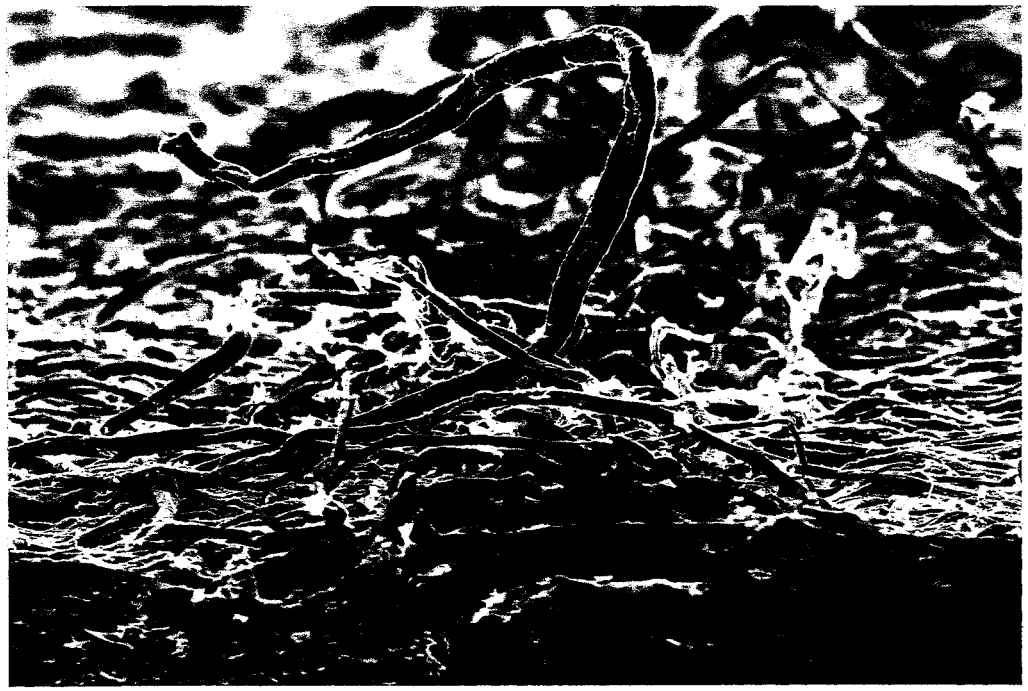

Fig. 46 Side view SEM photograph (x100) of the effect of a nominal laser fluence of 41 ± 12 Jcm^{-2}, on a black ball-point pen ink 'X', on 'Roma' paper. For data see Table 34.

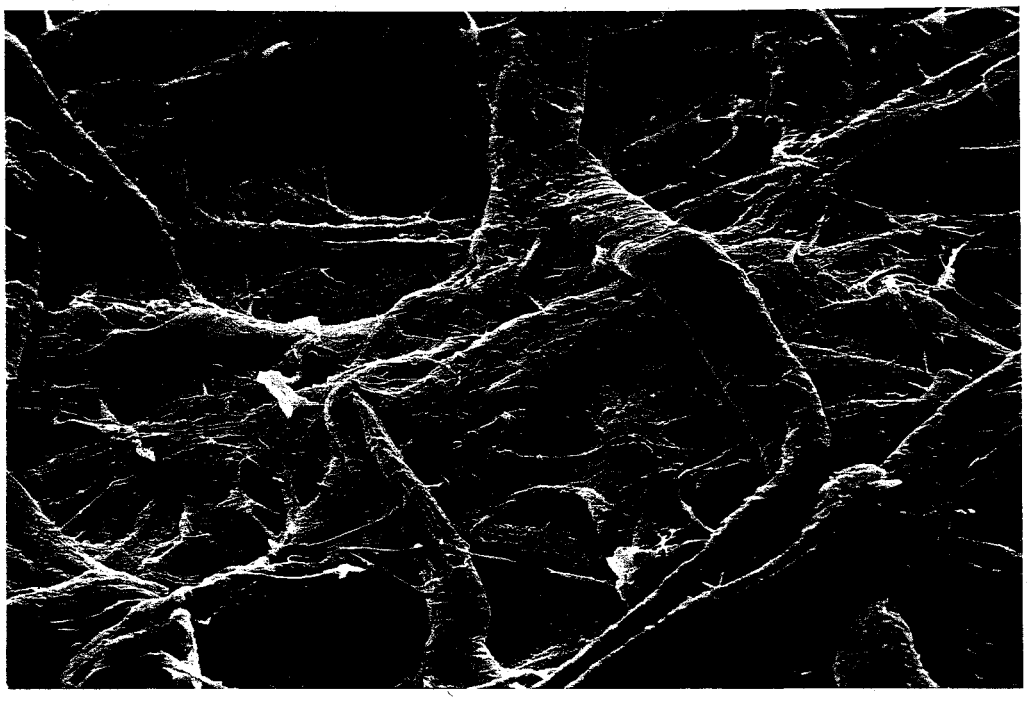

Fig. 47 SEM photograph (x400) of the 'Roma' paper fibres prior to laser treatment. The fibres are thoroughly coated in a gelatin size.

Fig. 48 SEM photograph (x400) of the 'Roma' paper fibres after laser treatment. The gelatin has been removed as a result of laser treatment.

Fig. 49 Photomicrograph (x15) of the complete removal of black ball-point pen ink, from 'Roma' paper, by a Q-switched Nd:YAG laser. The beam was attenuated to maintain pulse duration of 63 ns as the nominal fluence (20 ± 6 Jcm^{-2}), was achieved.

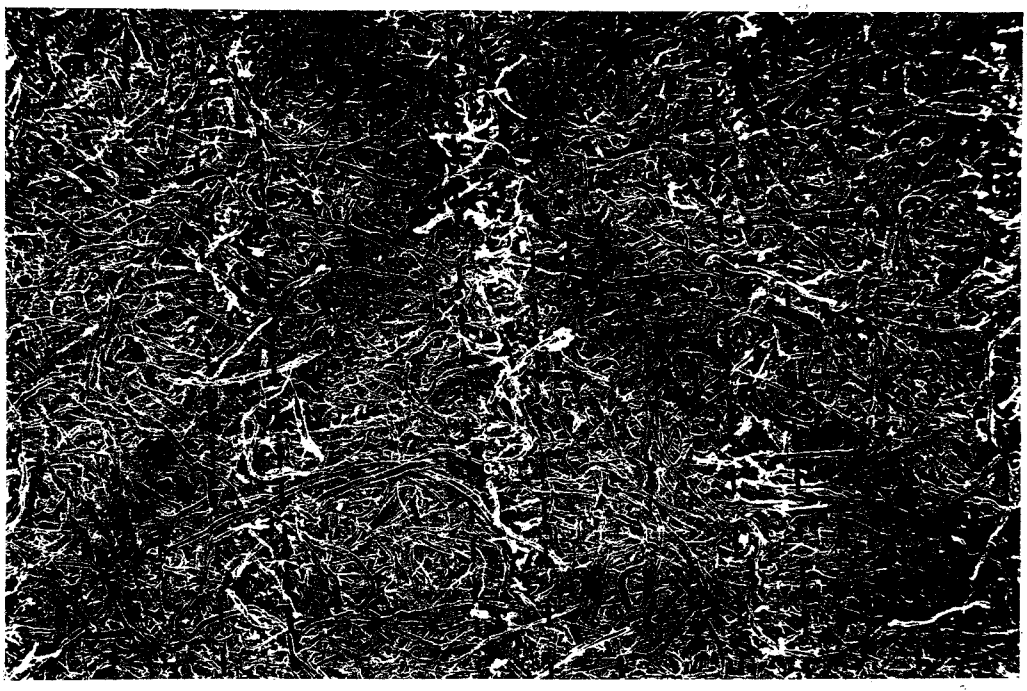

Fig. 50 SEM photograph (x20) of the effect of a nominal laser fluence of 24 ± 7 Jcm^{-2}, on a black ball-point pen ink 'X', on 'Roma' paper. The beam was attenuated to maintain pulse duration of 63 ns, as the fluence was achieved. The dotted line indicates the path of the laser. Both the inked and un-inked regions of 'Roma' paper are disrupted by the passage of the laser.

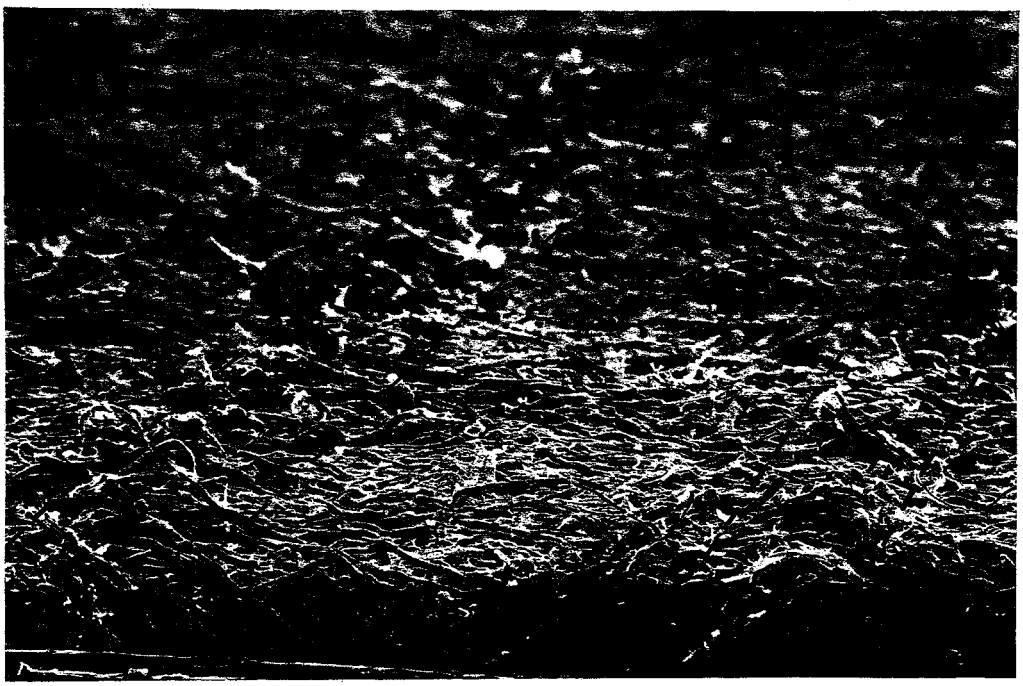

Fig. 51 Side view SEM photograph (x50) of the effect of a nominal laser fluence of 24 ± 7 Jcm^{-2}, on a black ball-point pen ink 'X', on 'Roma' paper. The beam was attenuated to maintain pulse duration of 63 ns, as the fluence was achieved. The impact of the laser pulses has caused some disruption to the fibre lattice.

Fig. 52 Photomicrograph (x15) of the complete removal of black ball-point pen ink, from 'Roma' paper, by a Q-switched Nd:YAG laser. The beam was attenuated to maintain pulse duration of 26 ns as the nominal fluence (16 ± 5 Jcm^{-2}), was achieved.

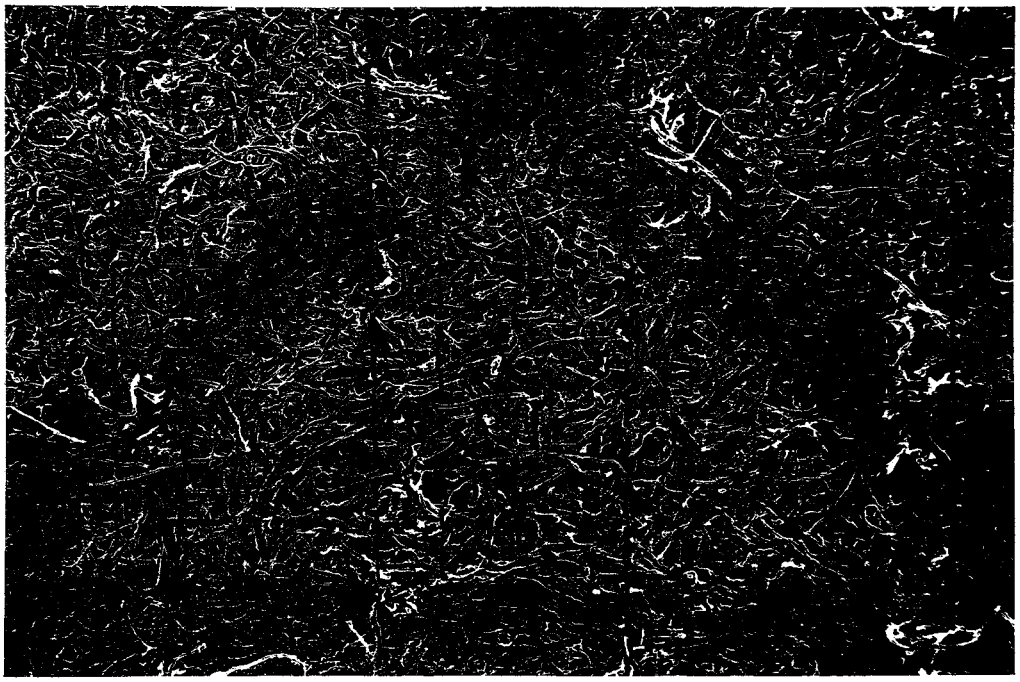

Fig. 53 SEM photograph (x20) of the effect of a nominal laser fluence of 20 ± 6 Jcm^{-2}, on a black ball-point pen ink 'X', on 'Roma' paper. The beam was attenuated to maintain pulse duration of 26 ns, as the fluence, was achieved. The dotted line indicates the path of the laser. Both the inked and un-inked regions of 'Roma' paper are disrupted by the passage of the laser.

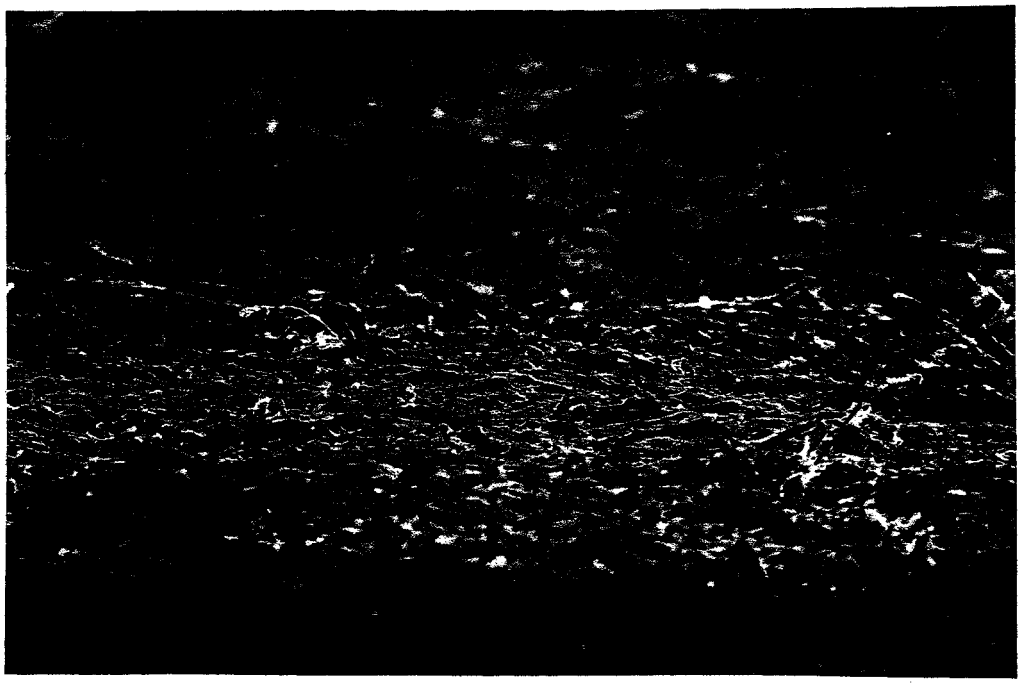

Fig. 54 Side view SEM photograph (x50) of the effect of a nominal laser fluence of 20 ± 6 Jcm^{-2}, on a black ball-point pen ink 'X', on 'Roma' paper. The beam was attenuated to maintain pulse duration of 26 ns, as the fluence was achieved. The impact of the laser pulses has caused slight disruption to the fibre lattice.

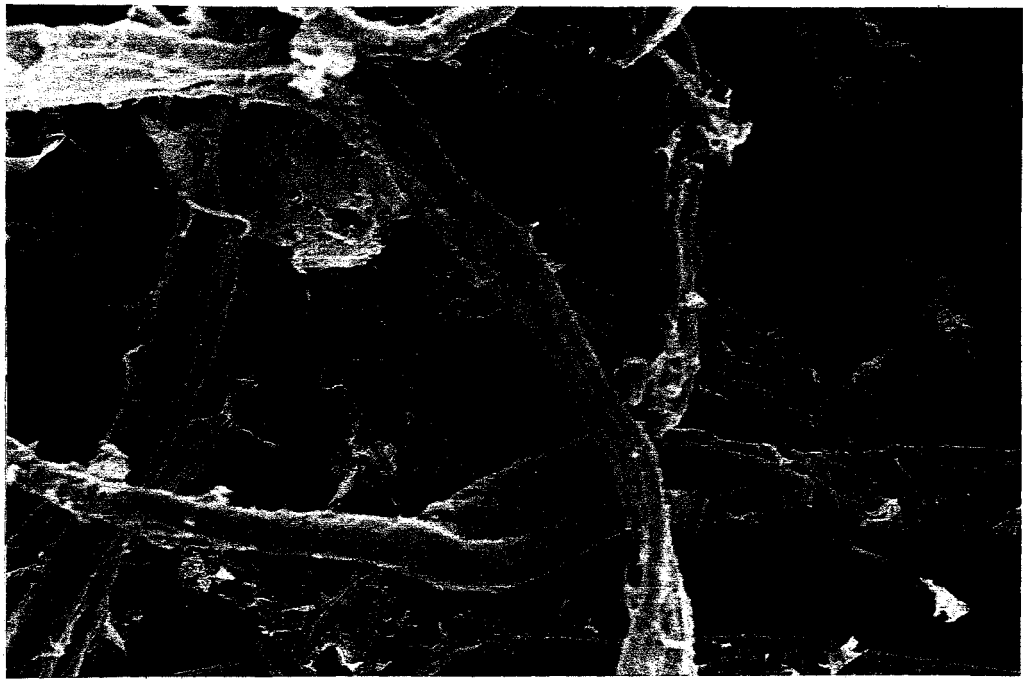

Fig. 55 SEM photograph (x500) of the 'Roma' paper fibres after laser treatment. The beam was attenuated to maintain pulse duration of 26 ns as the nominal fluence (20 ± 6 Jcm^{-2}), was achieved. The gelatin size has been partially removed as a result of laser treatment.

Fig. 56 Photomicrograph (x10) of the complete removal of black ball-point pen ink, from 'Roma' paper in a argon atmosphere, by a Q-switched Nd:YAG laser, using a nominal fluence of 38 ± 11 Jcm^{-2}.

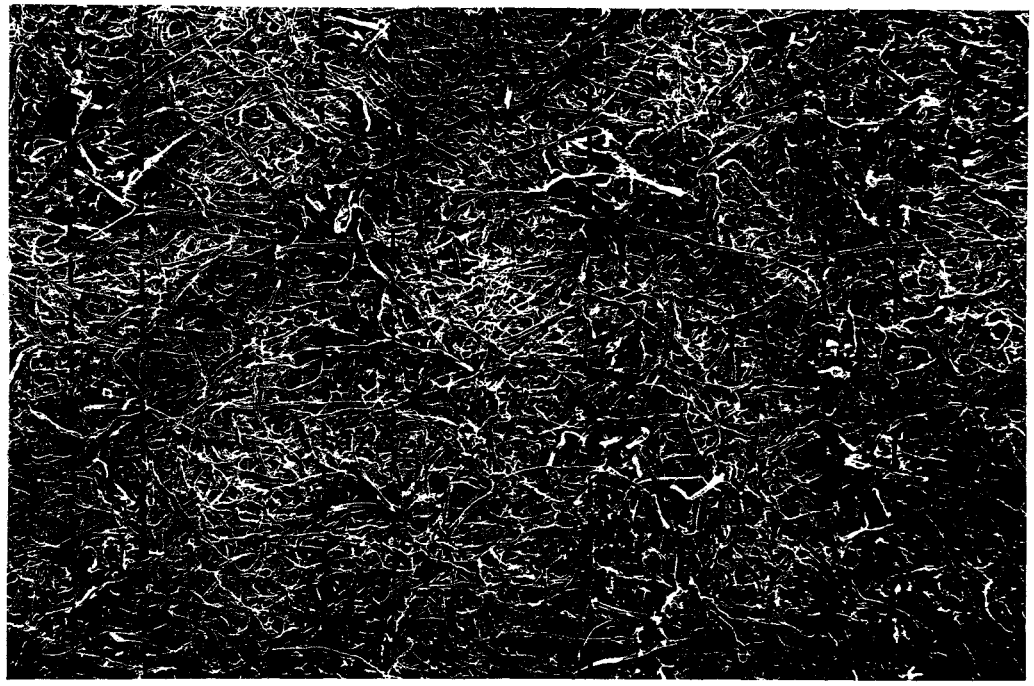

Fig. 57 SEM photograph (x20) of the effect of a nominal laser fluence of 38 ± 11 Jcm^{-2}, on a black ball-point pen ink 'X', on 'Roma' paper in an argon atmosphere. The dotted line indicates the path of the laser. Both the inked and un-inked regions of 'Roma' paper are disrupted by the passage of the laser.

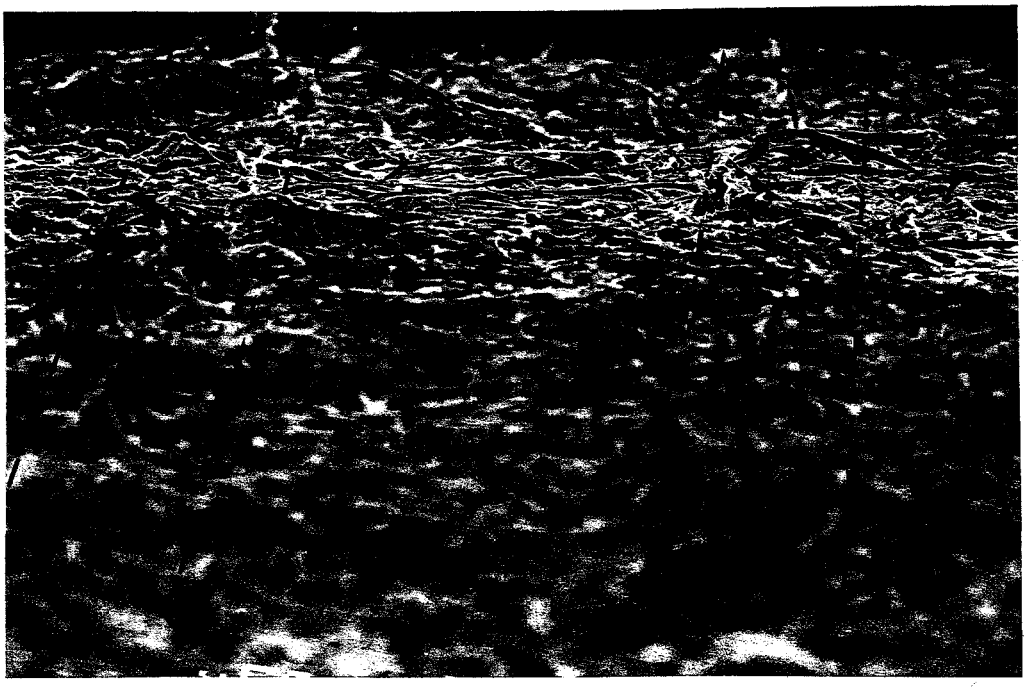

Fig. 58 Side view SEM photograph (x50) of the effect of a nominal laser fluence of 38 ± 11 Jcm^{-2}, on a black ball-point pen ink 'X', on 'Roma' paper in an argon atmosphere. The impact of the laser pulses has caused some disruption to the fibre lattice, but significantly less than that witnessed using the laser in a normal atmosphere (Fig. 45).

Fig. 59 SEM photograph (x500) of the 'Roma' paper fibres after laser treatment in an argon atmosphere. The gelatin size has been partially removed as a result of laser treatment.

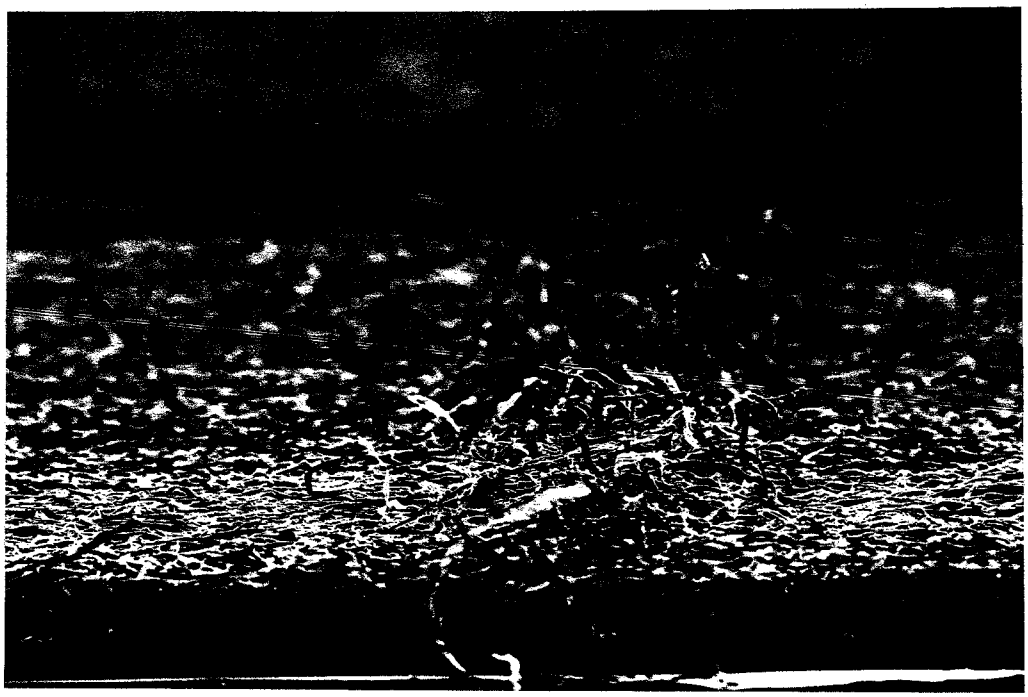

Fig. 60 Side view SEM photograph (x30) of the effect of a nominal laser fluence of 37 ± 11 Jcm^{-2}, used to remove a black ball-point pen ink line, on 'Roma' paper. For data see Table 34.

Fig. 61 Side view SEM photograph (x30) of the effect of an eraser, used to remove a black ball-point pen ink line, on 'Roma' paper.

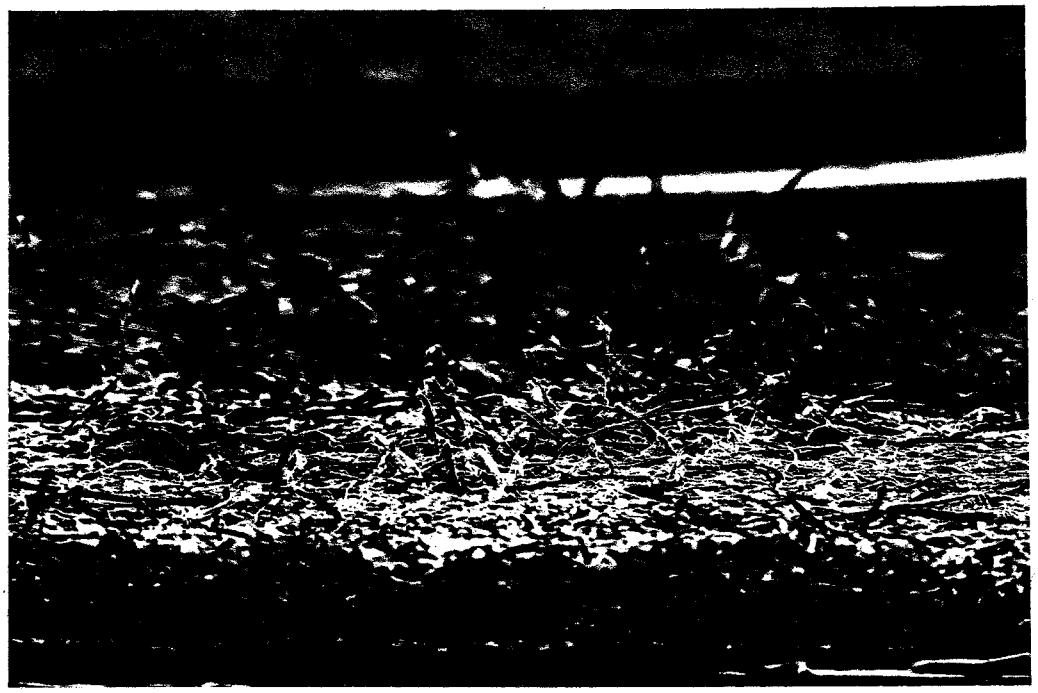

Fig. 62 Side view SEM photograph (x30) of the effect of a scalpel, used to remove a black ball-point pen ink line, on 'Roma' paper.

Fig. 63 Side view SEM photograph (x30) of the effect of a scalpel and an eraser, used to remove a black ball-point pen ink line, on 'Roma' paper.

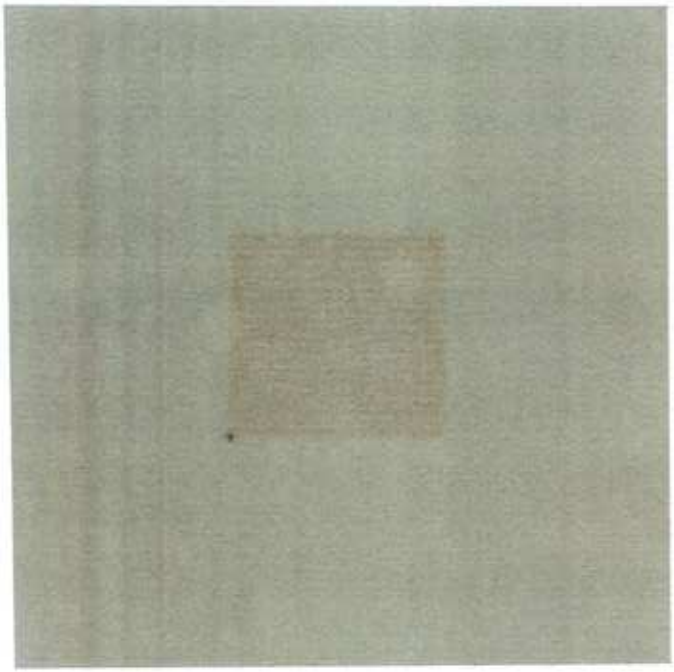

Fig. 64 Photograph of 'Roma' cotton paper, laser treated using a nominal fluence of 41 ± 12 Jcm^{-2} (pulse duration 87 ns), and aged for one month in a humid oven, at 90°C and 50% R.H. The laser treated region is clearly more discoloured than the untreated region.

Fig. 65 Photomicrograph of the cross-section of 'Roma' cotton paper, Nd:YAG laser treated using a nominal fluence of 41 ± 12 Jcm^{-2} (pulse duration 87 ns), and aged for one month in a humid oven, at 90°C and 50% R.H. The cross-section shows that discoloration is confined to the surface fibres only, and does not extend into the body of the paper.

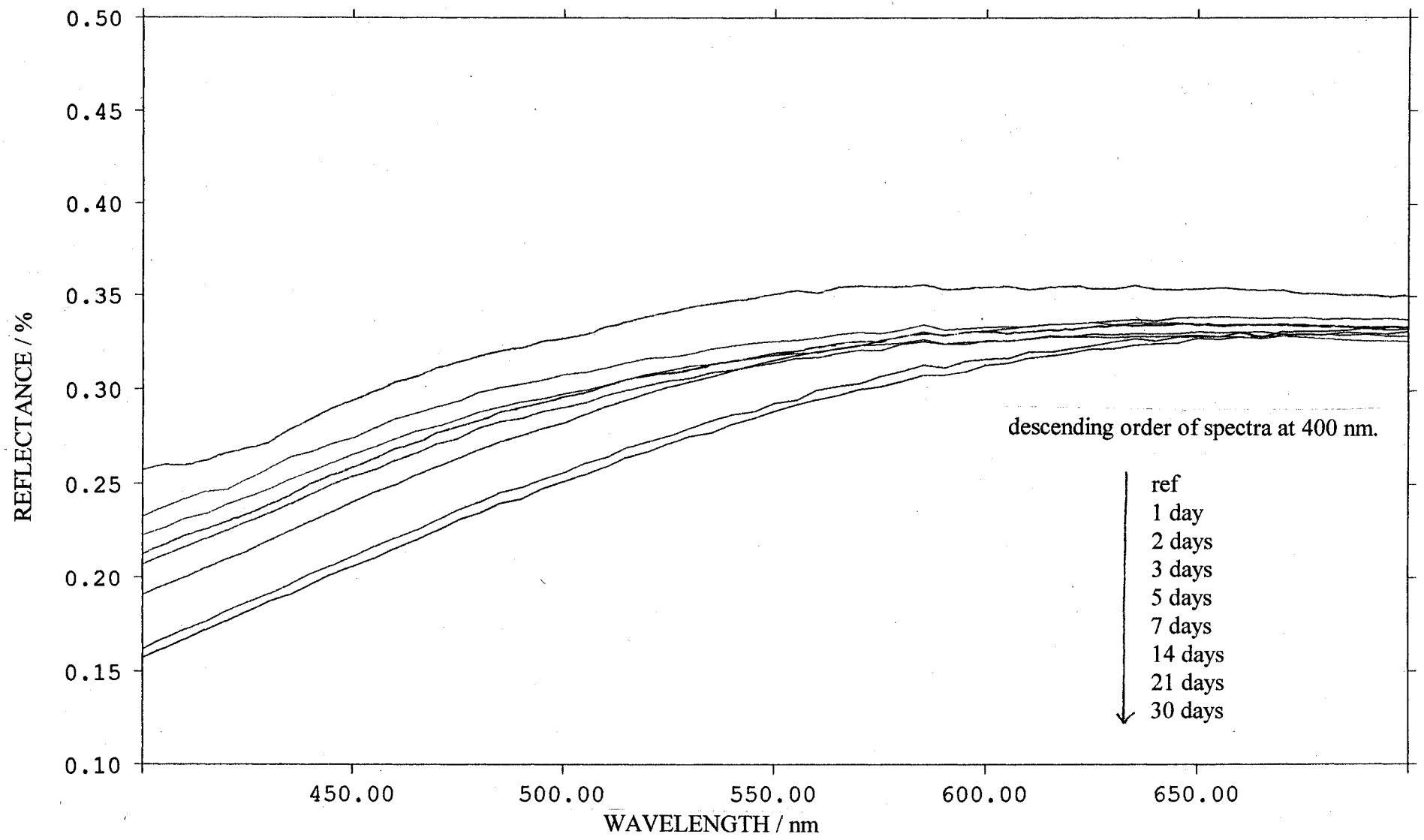

Fig. 66 Visible light reflectance spectra of standard sized 'Roma' cotton paper, Nd:YAG laser treated using a nominal fluence of 41 ± 12 Jcm^{-2}, and aged in a humid oven at 90°C and 50% R.H., for between 1 and 30 days. The spectra show the gradual decrease in reflectance of blue light by the laser treated areas, as the exposure to artificial ageing is lengthened.

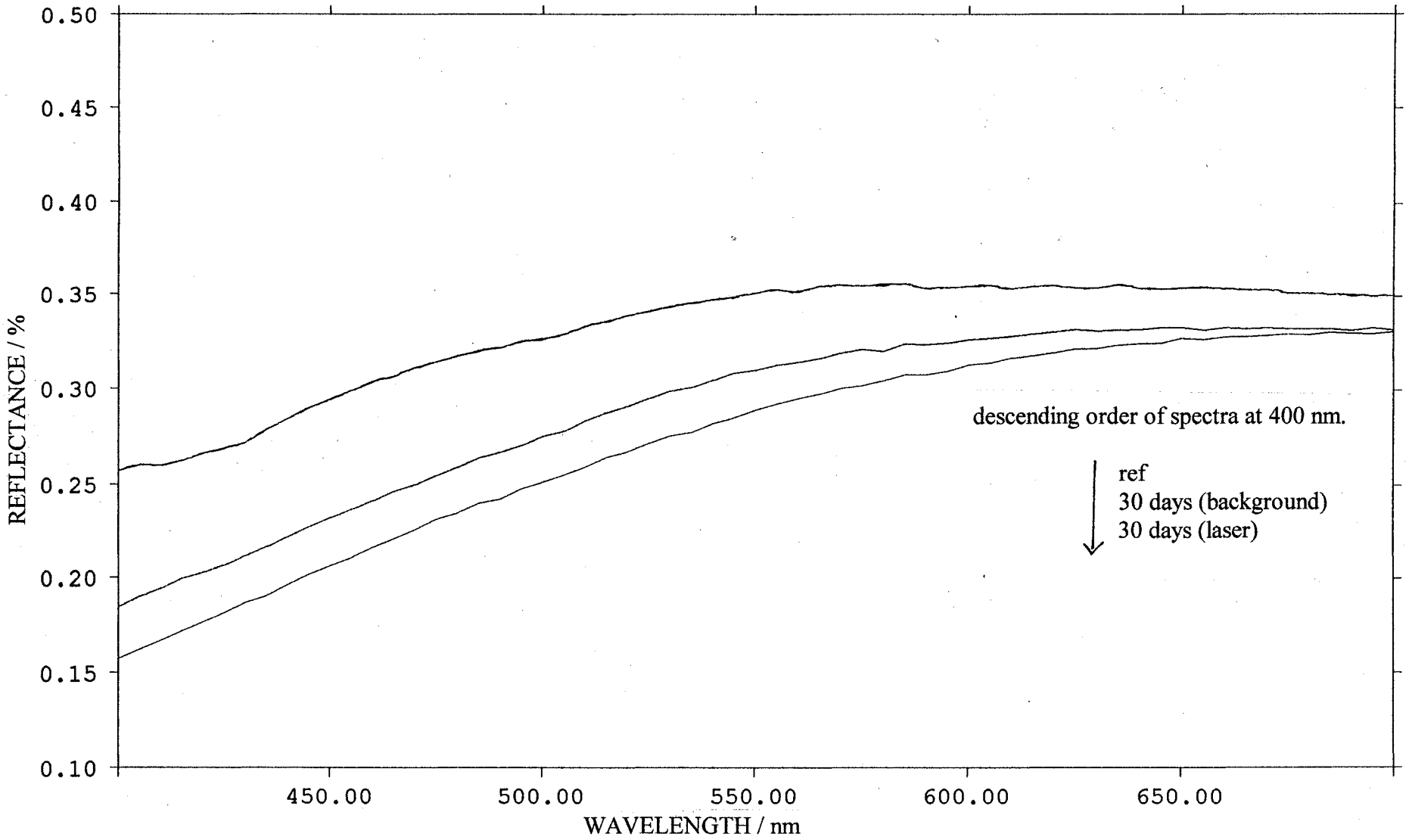

Fig. 67 Visible light reflectance spectra of humid aged standard sized 'Roma' cotton paper, Nd:YAG laser treated using a nominal fluence of 41 ± 12 Jcm^{-2}. Samples were aged in a humid oven at 90 °C and 50% R.H., for one month. There is approximately 15 % less light reflected by the laser treated sample, at 400 nm.

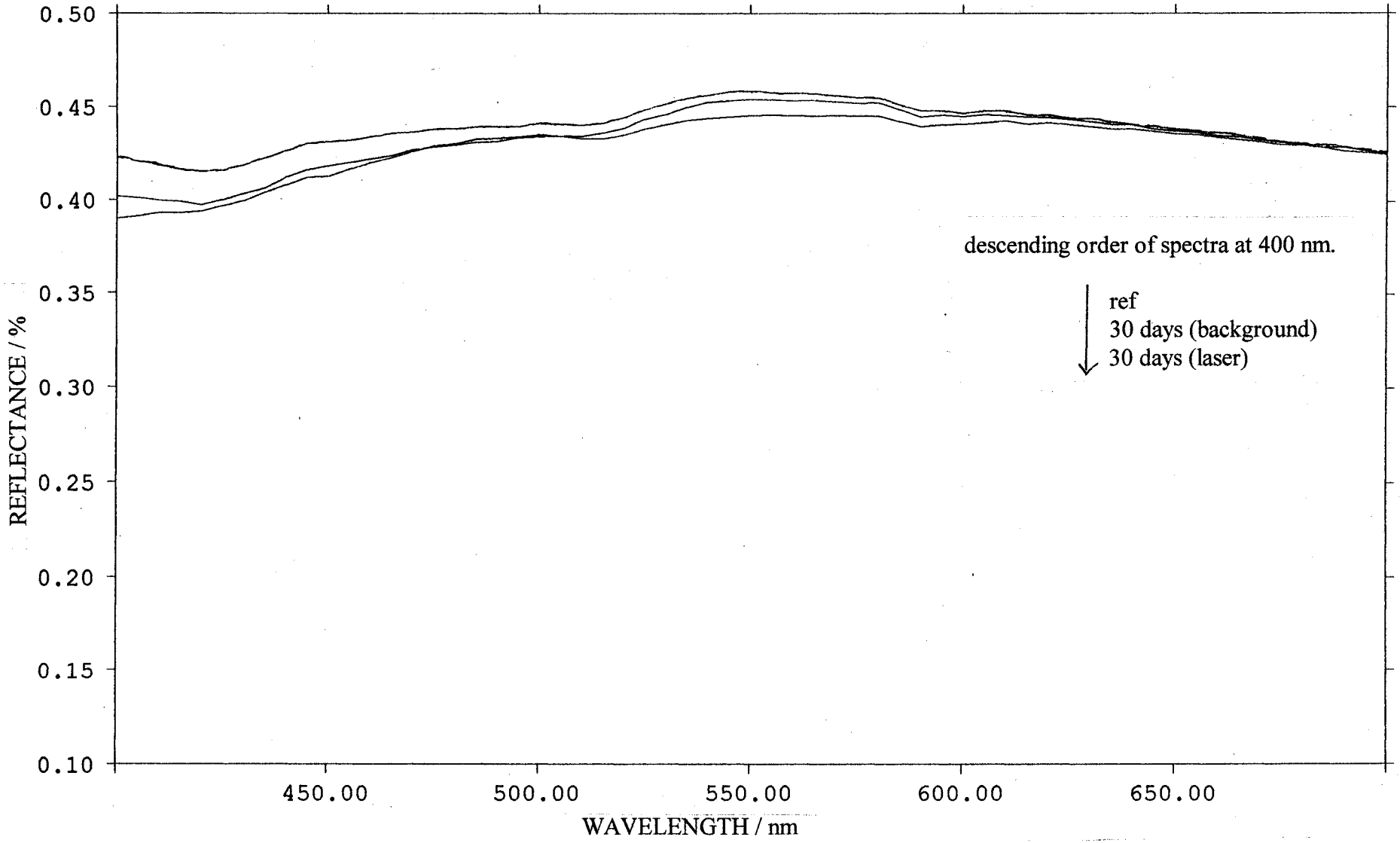

Fig. 68 Visible light reflectance spectra of humid aged size removed 'Roma' cotton paper, Nd:YAG laser treated using a nominal fluence of 41 ± 12 Jcm^{-2}. Samples were aged in a humid oven at 90 °C and 50% R.H., for one month. There is approximately 2 % less light reflected by the laser treated sample, at 400 nm.

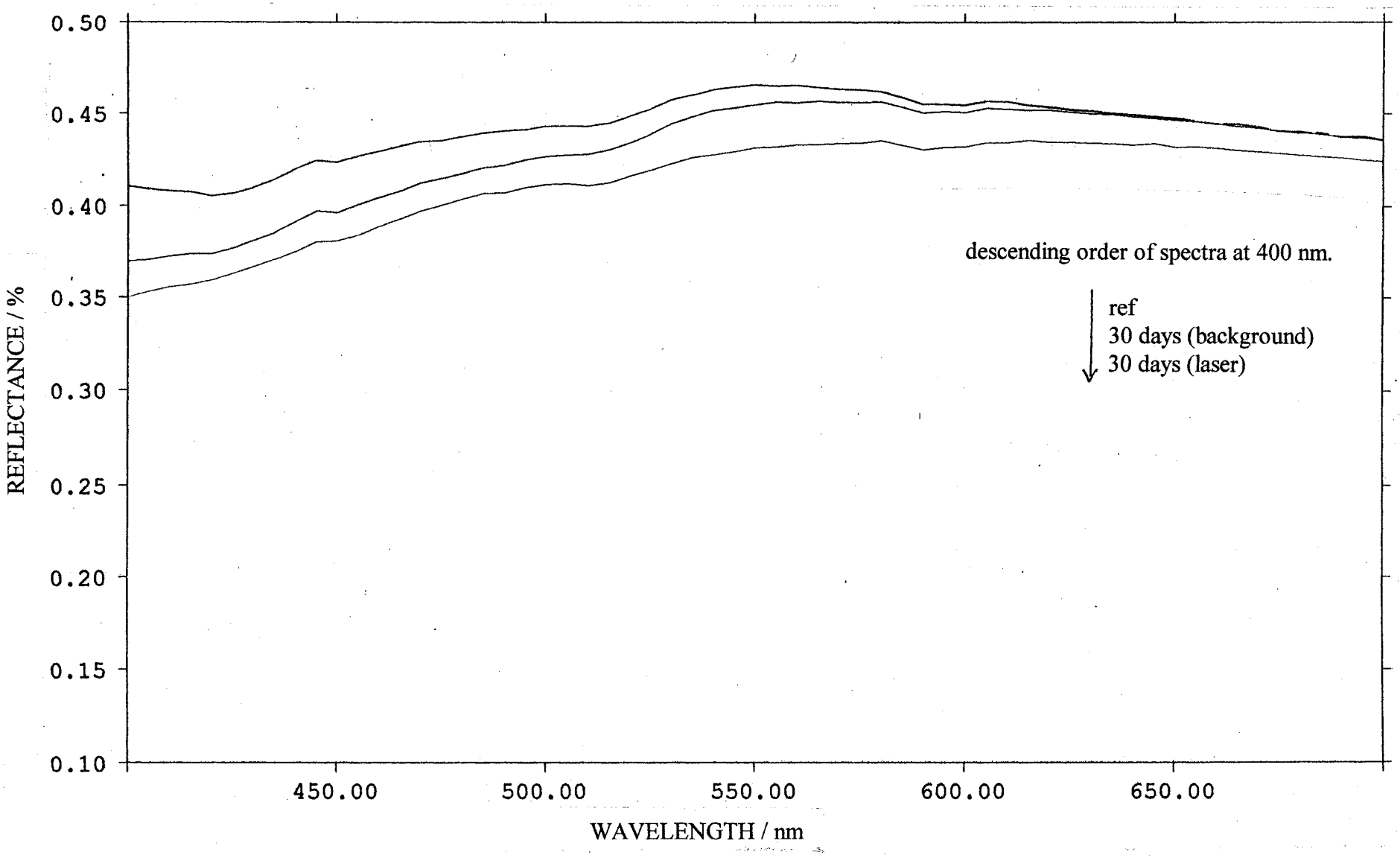

Fig. 69 Visible light reflectance spectra of humid aged standard sized 'Roma' cotton paper Nd:YAG laser treated using a nominal fluence of 24 ± 7 Jcm^{-2}. The beam was attenuated to maintain a pulse duration of 63 ns. Samples were aged in a humid oven at 90°C and 50% R.H., for one month. There is approximately 5 % less light reflected by the laser treated sample, at 400 nm.

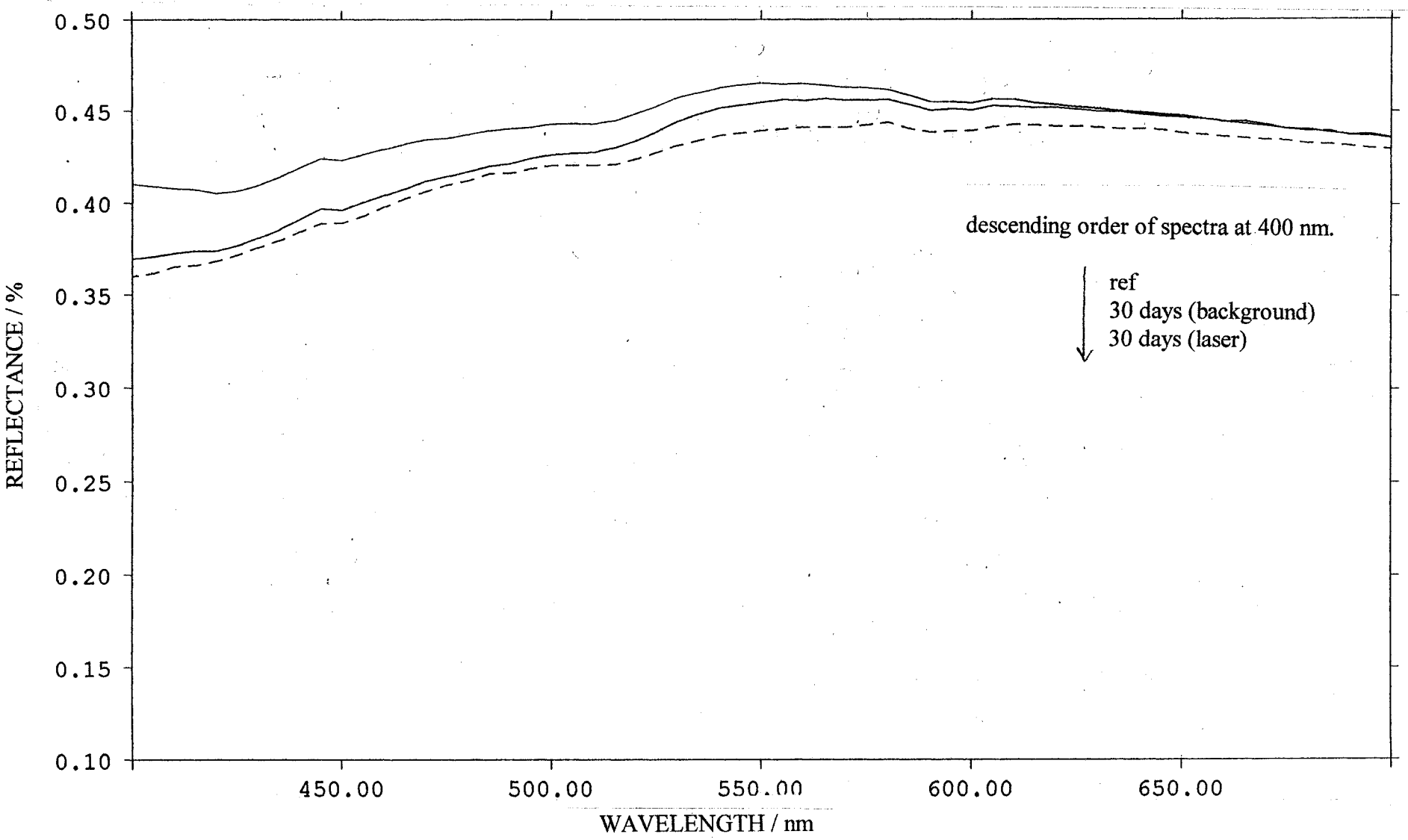

Fig. 70 Visible light reflectance spectra of humid aged standard sized 'Roma' cotton paper Nd:YAG laser treated using a nominal fluence of 20 ± 6 Jcm^{-2}. The beam was attenuated to maintain a pulse duration of 26 ns. Samples were aged in a humid oven at 90°C and 50% R.H., for one month. There is approximately 3 % less light reflected by the laser treated sample, at 400 nm.

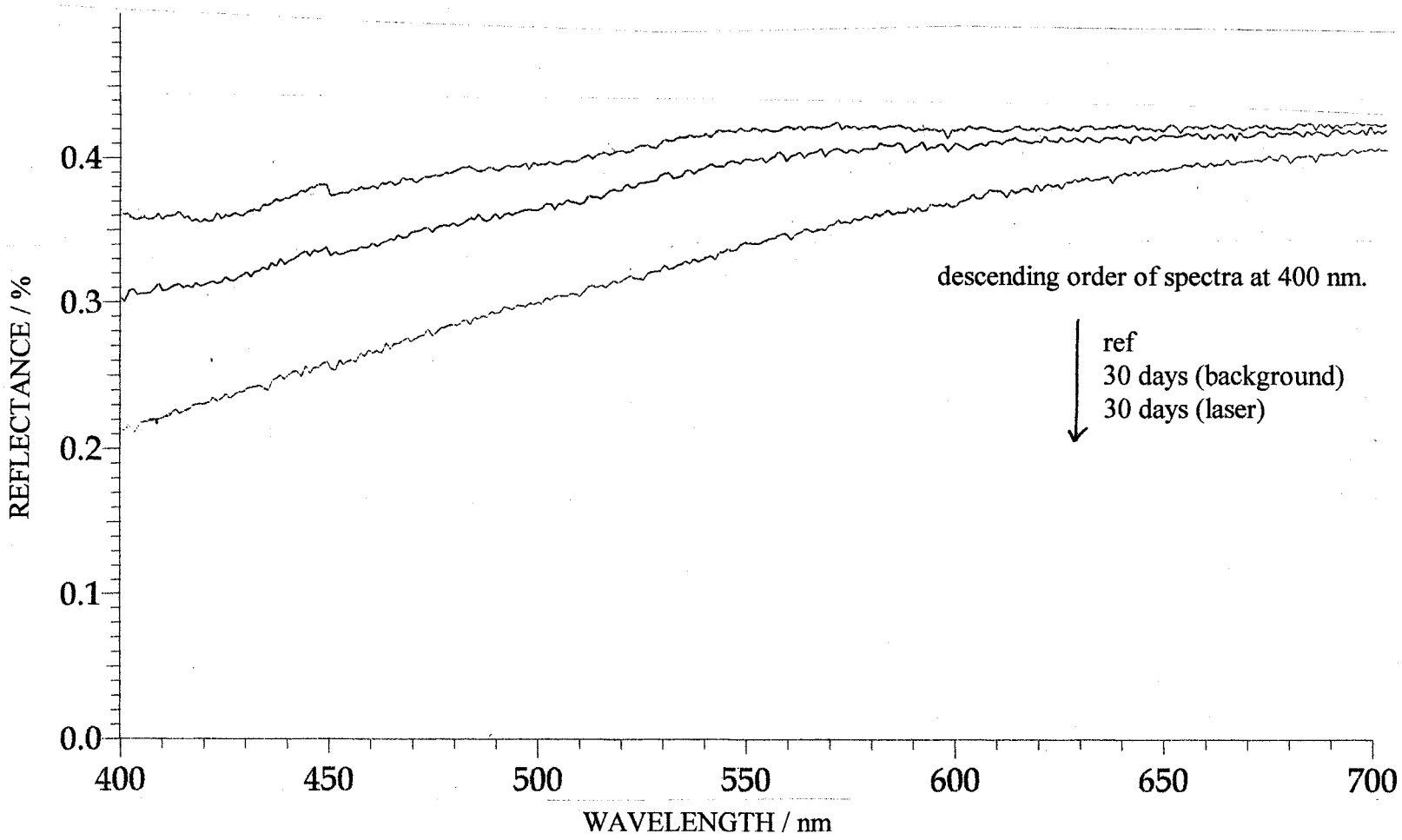

Fig. 71 Visible light reflectance spectra of humid aged standard sized 'Roma' cotton paper, Nd:YAG laser treated in an argon atmosphere, using a nominal fluence of 38 ± 11 Jcm^{-2}. Samples were aged in a humid oven at 90 °C and 50% R.H., for one month. There is approximately 30 % less light reflected by the laser treated sample, at 400 nm.

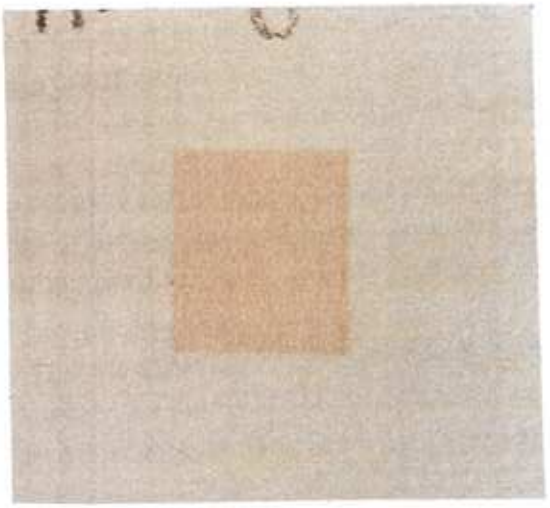

Fig 72 Photograph of standard sized 'Roma' cotton paper, Nd:YAG laser treated in an argon atmosphere, using a nominal fluence of 38 ± 11 Jcm^{-2}, and aged for one month in a humid oven, at 90 °C and 50% R.H. The laser treated region is clearly more discoloured than the untreated region.

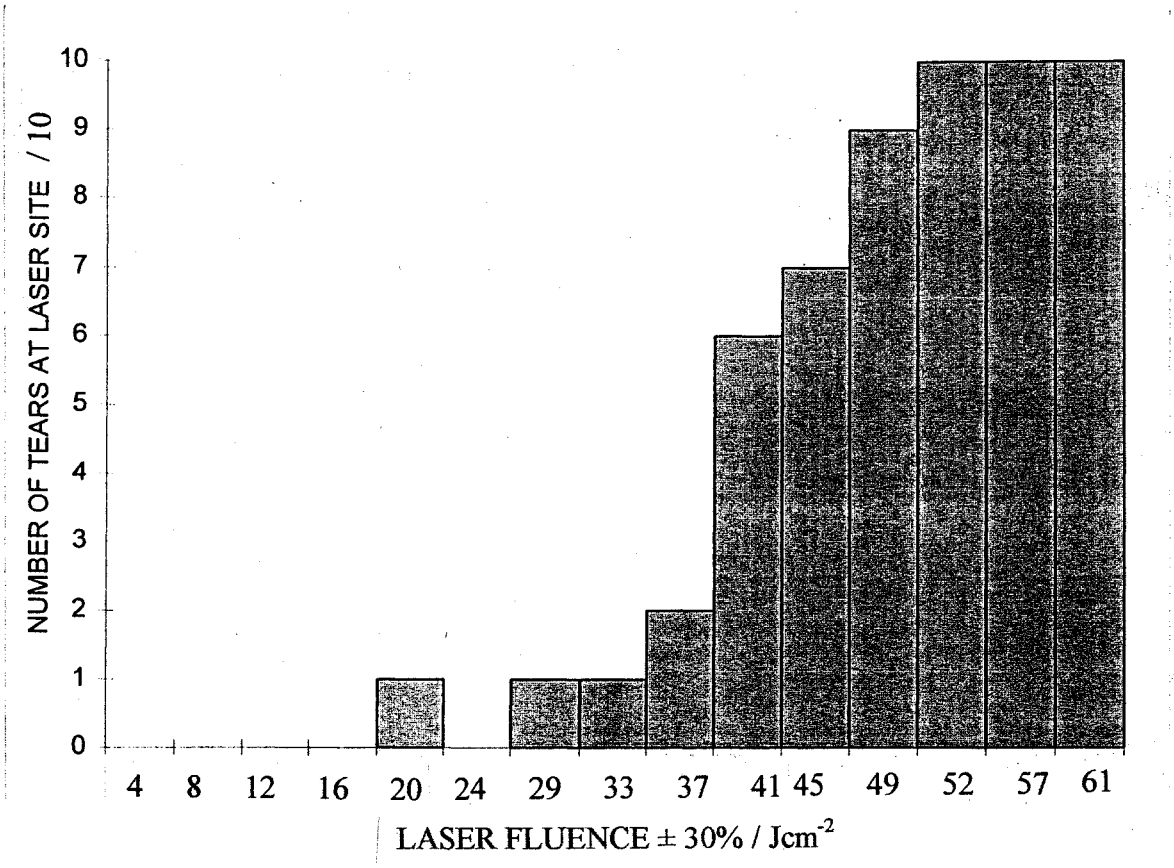

Fig. 73 Histogram showing the increasing tendency of 'Roma' cotton paper to tear at laser treatment sites, due to Nd:YAG laser treatment over a nominal fluence range of 0-61 Jcm^{-2}. Laser treatment carried out at right angles to the laid lines. For data see Table 39.

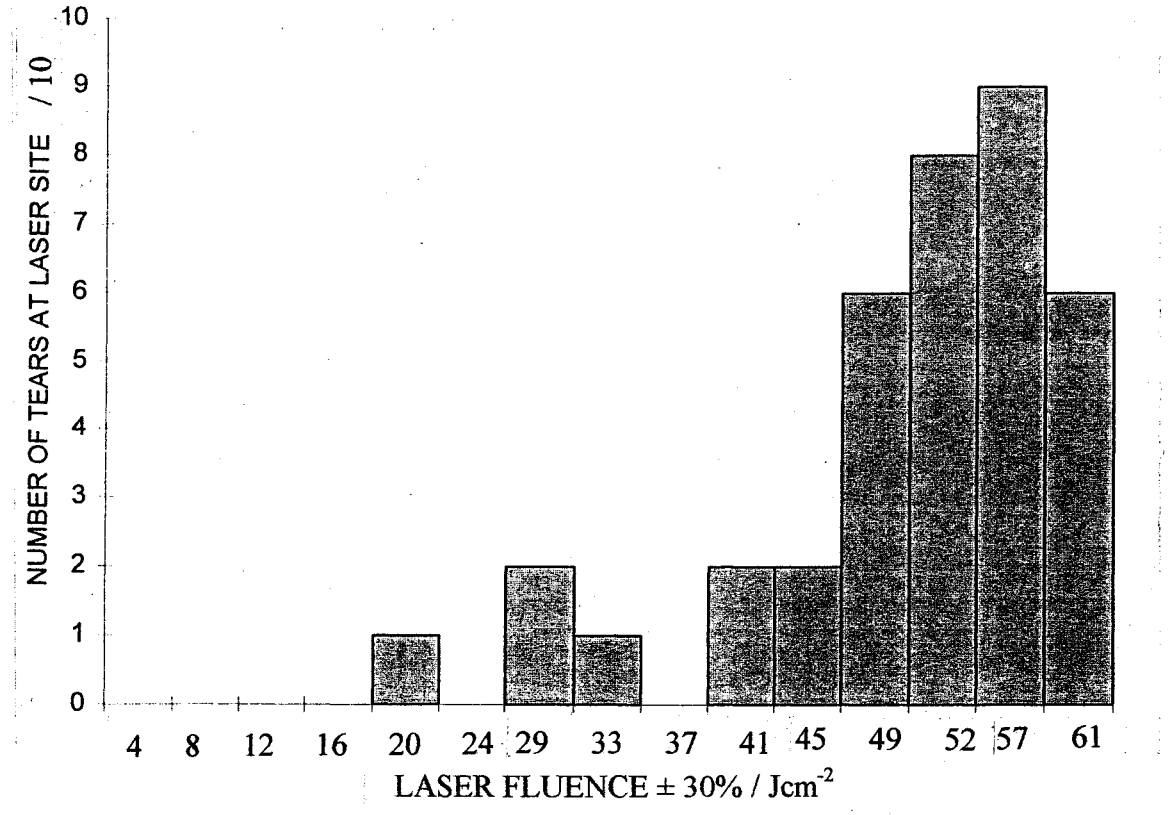

Fig. 74 Histogram showing the increasing tendency of 'Roma' cotton paper to tear at laser treatment sites, due to Nd:YAG laser treatment over a nominal fluence range of 0-61 Jcm^{-2}. Laser treatment carried out in the direction of laid lines. For data see Table 40.

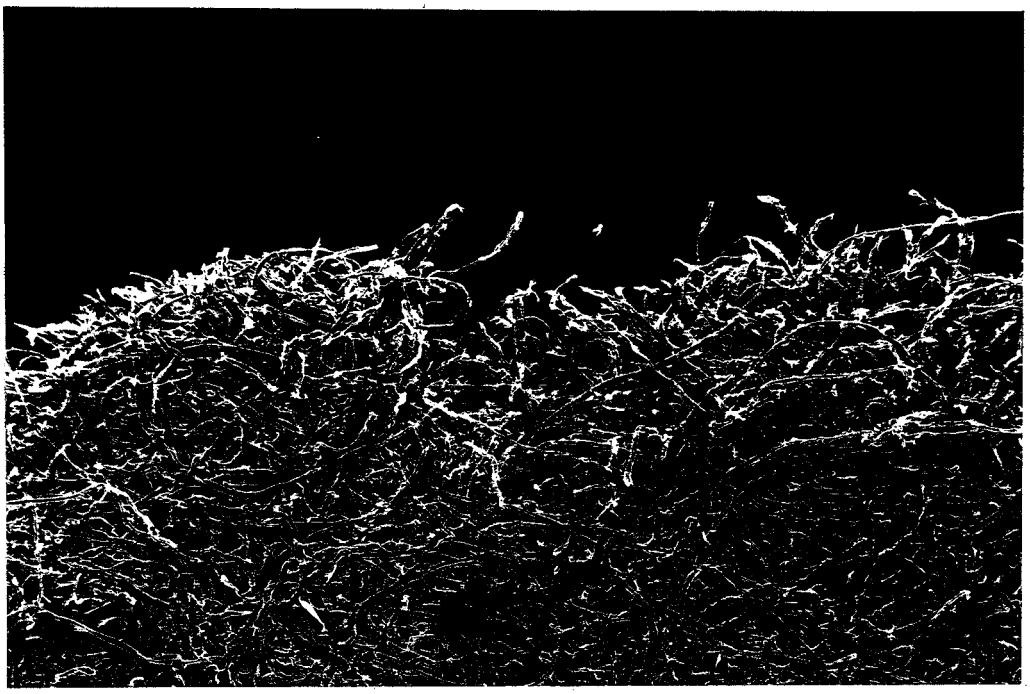

Fig. 75 SEM photograph (x20) of a tensile tear at right angles to the laid lines of a sheet of 'Roma' cotton paper. The tear does not follow a specific path, and is consequently uneven.

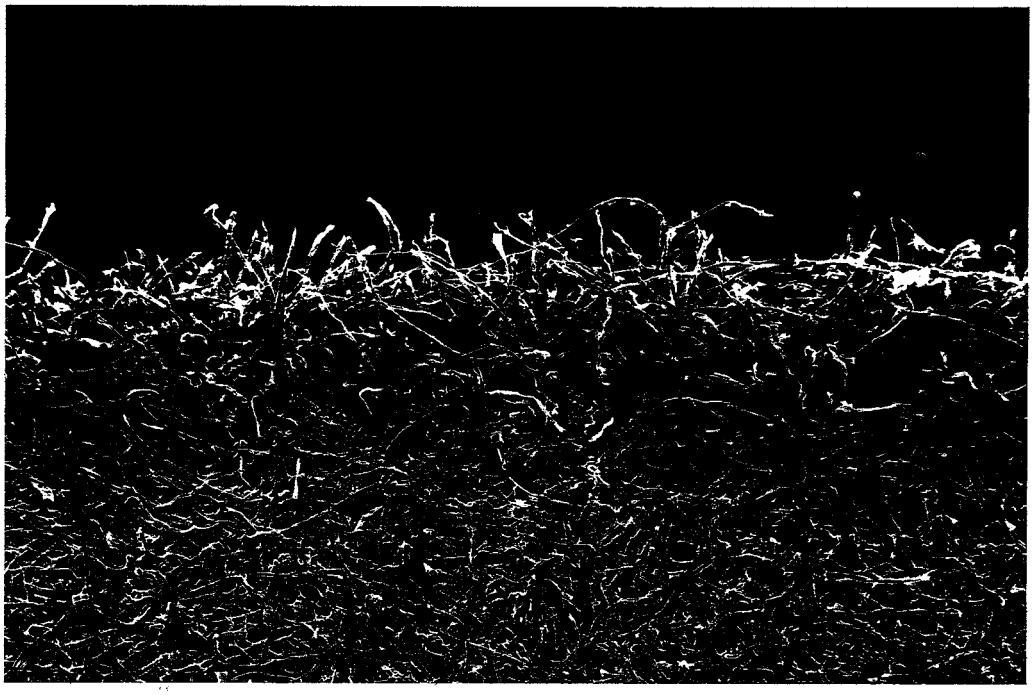

Fig. 76 SEM photograph (x20) of a tensile tear at right angles to the laid lines of a sheet of laser treated 'Roma' cotton paper. Treatment was carried out using a Q-switched Nd:YAG laser with a nominal fluence of 41 ± 12 Jcm^{-2}, pulse duration 87 ns. The tear follows the path of the laser line and is straight.

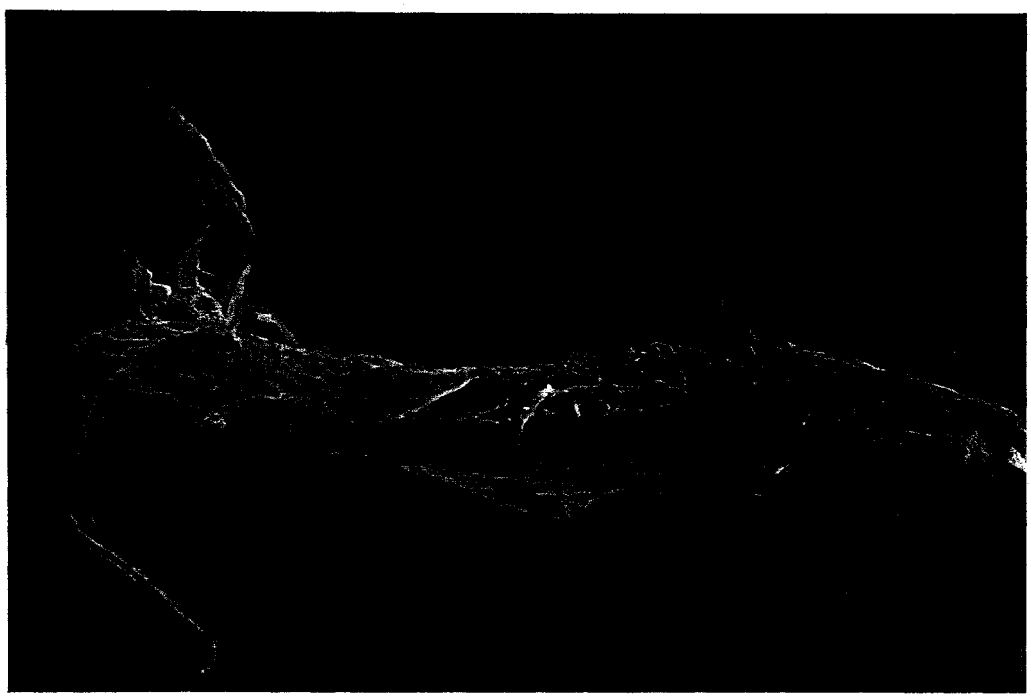

Fig. 77 SEM photograph (x1500) of the fracture tip of a single standard 'Roma' cotton fibre protruding from the tear (see Fig. 75). The long tapering break is characteristic of an undegraded fibre.

Fig. 78 SEM photograph (x1500) of the fracture tip of a single laser treated 'Roma' cotton fibre protruding from the tear (see Fig. 76). The short length and bluntness of the fracture infers that the fibre was significantly more brittle than the untreated standard sample.

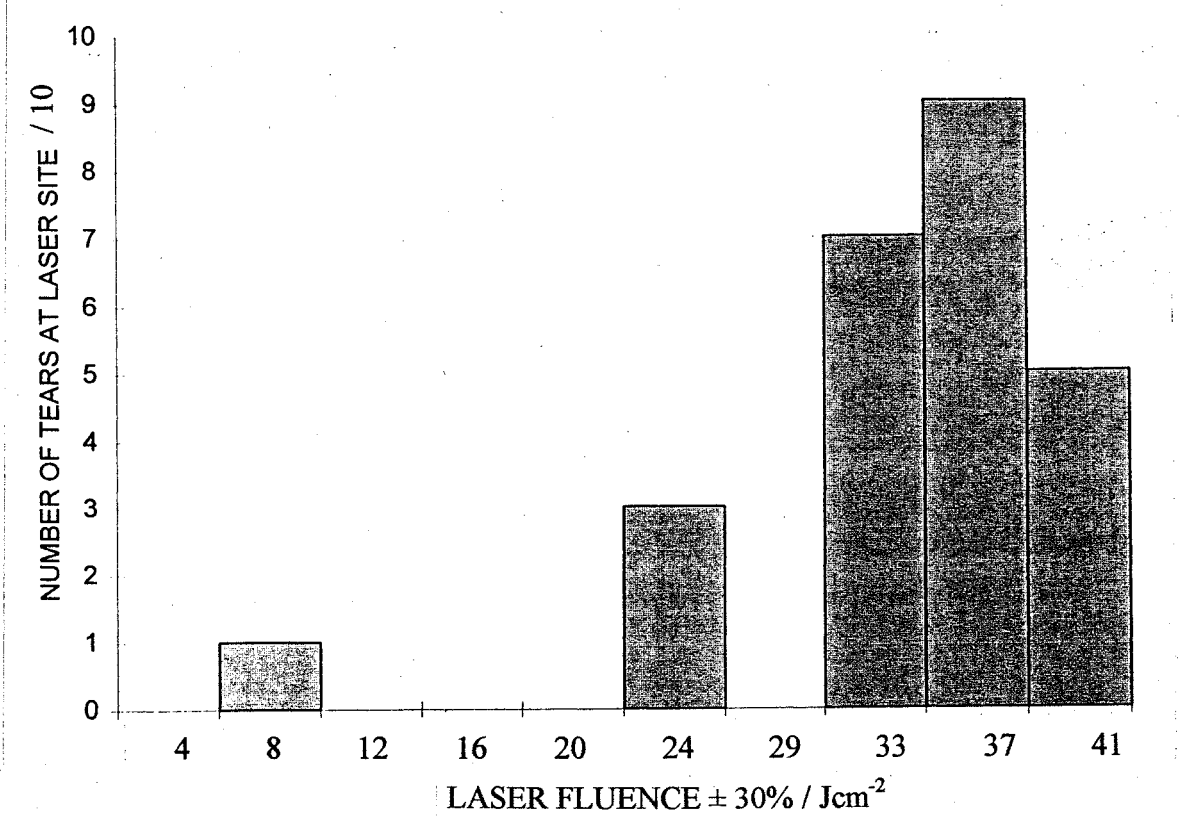

Fig. 79 Histogram showing the increasing tendency of 'Roma' cotton paper to tear at laser treatment sites, due to Nd:YAG laser treatment over a nominal fluence range of 0-41 Jcm^{-2}, followed by a month of humid ageing at 90 °C and 50% R.H. Laser treatment carried out at right angles to the laid lines. For data see Table 41.

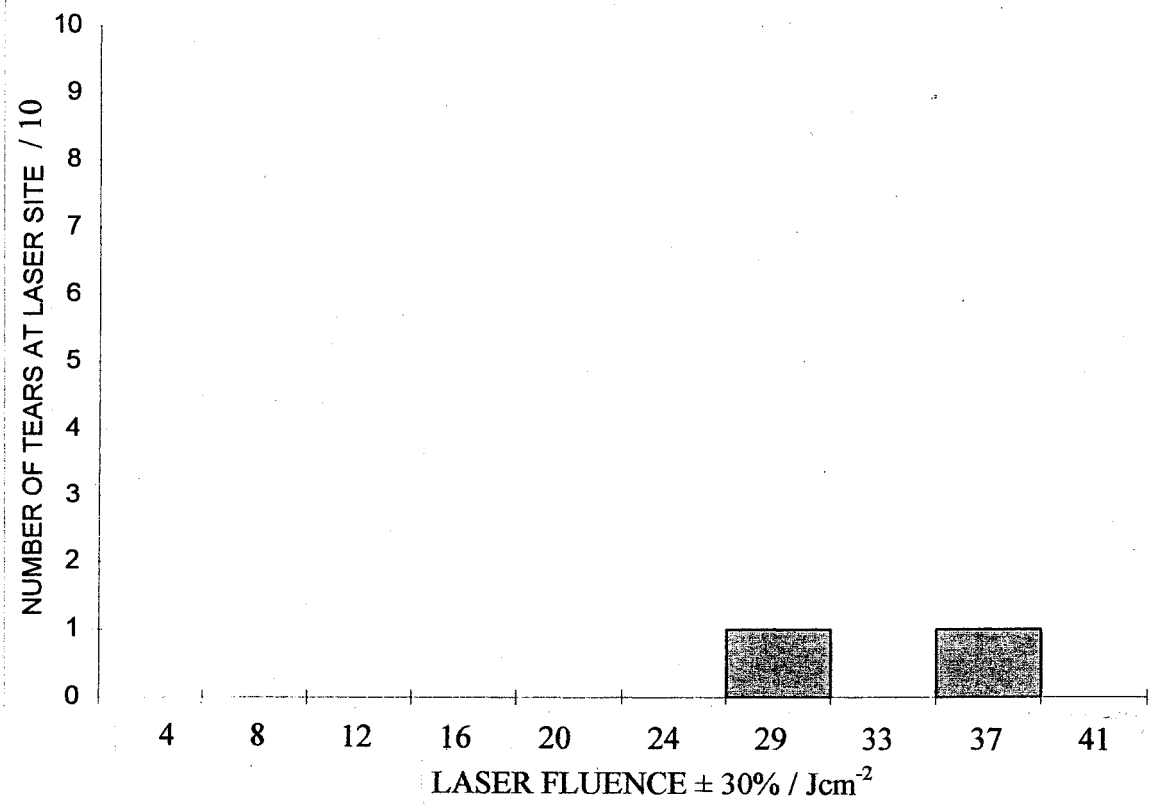

Fig. 80 Histogram showing the increasing tendency of 'Roma' cotton paper to tear at laser treatment sites, due to Nd:YAG laser treatment over a nominal fluence range of 0-41 Jcm^{-2}, followed by a month of humid ageing at 90 °C and 50% R.H. Laser treatment carried out in the direction of laid lines. For data see Table 42.

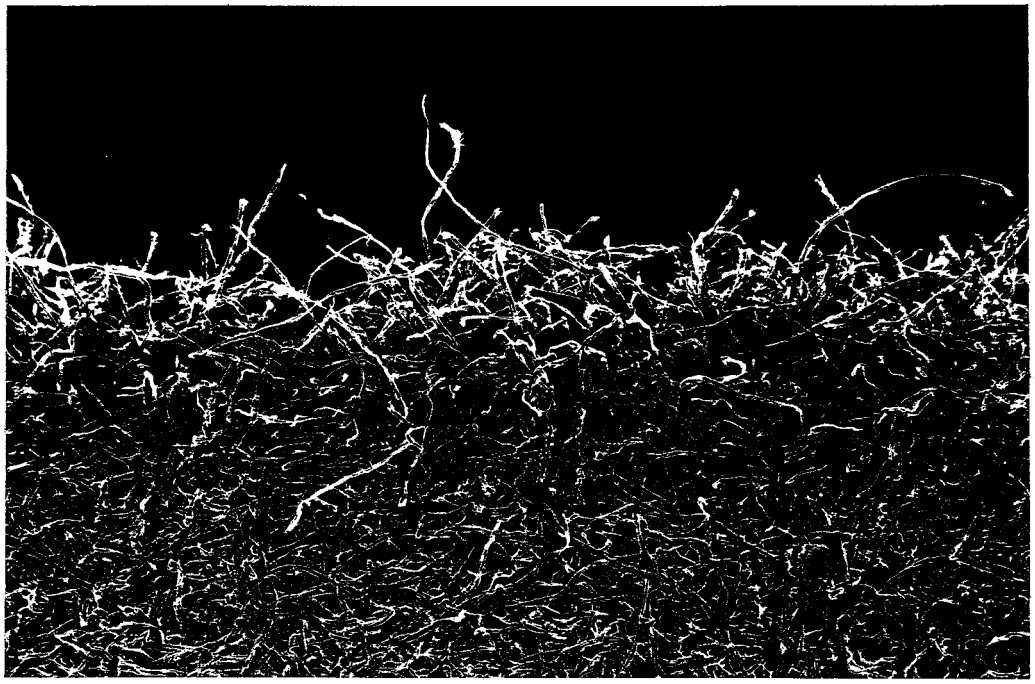

Fig. 81 SEM photograph (x20) of a tensile tear at right angles to the laid lines of a sheet of humid aged, laser treated 'Roma' cotton paper. Treatment was carried out using a Q-switched Nd:YAG laser with a nominal fluence of 41 ± 12 Jcm^{-2}, and the paper aged for one month at 90℃ and 50% R.H. The tear follows the path of the laser line and is straight.

Fig. 82 SEM photograph (x1500) of the fracture tip of a single humid aged, laser treated 'Roma' cotton fibre protruding from the tear (see Fig. 81). The short length and bluntness of the fracture infers that the fibre was significantly more brittle than the humid aged standard sample, and the laser treated unaged sample.

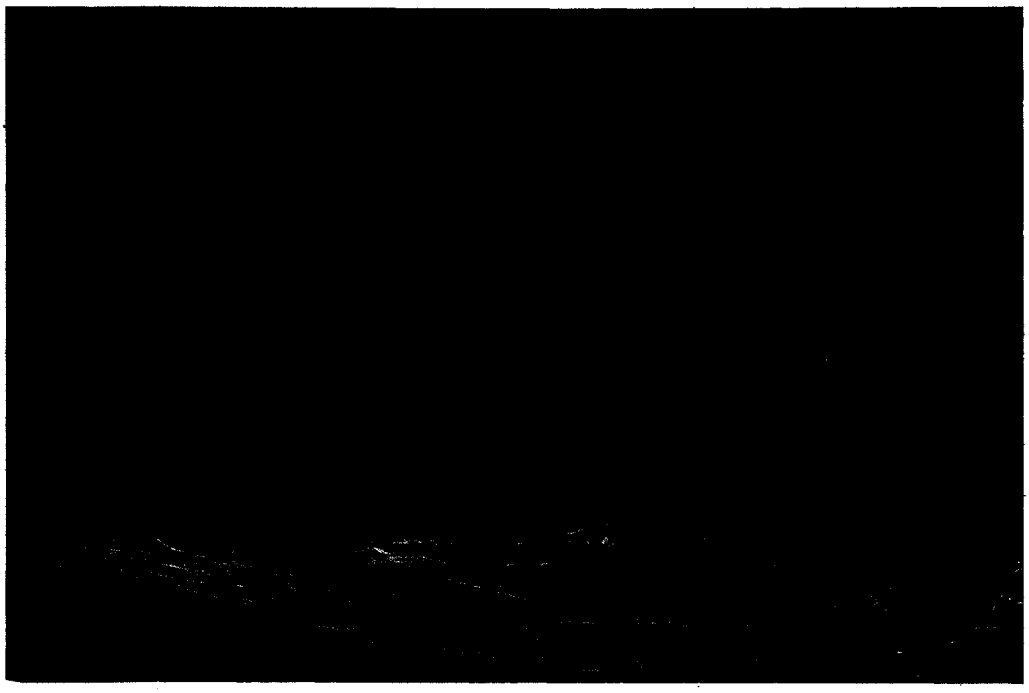

Fig. 83 SEM photograph (x1500) of the fracture tip of a single humid aged standard 'Roma' cotton fibre protruding from a tear. The long taper, slightly blunter than that of the un-aged fibre (Fig. 77) is characteristic of a fibre in good physical condition..

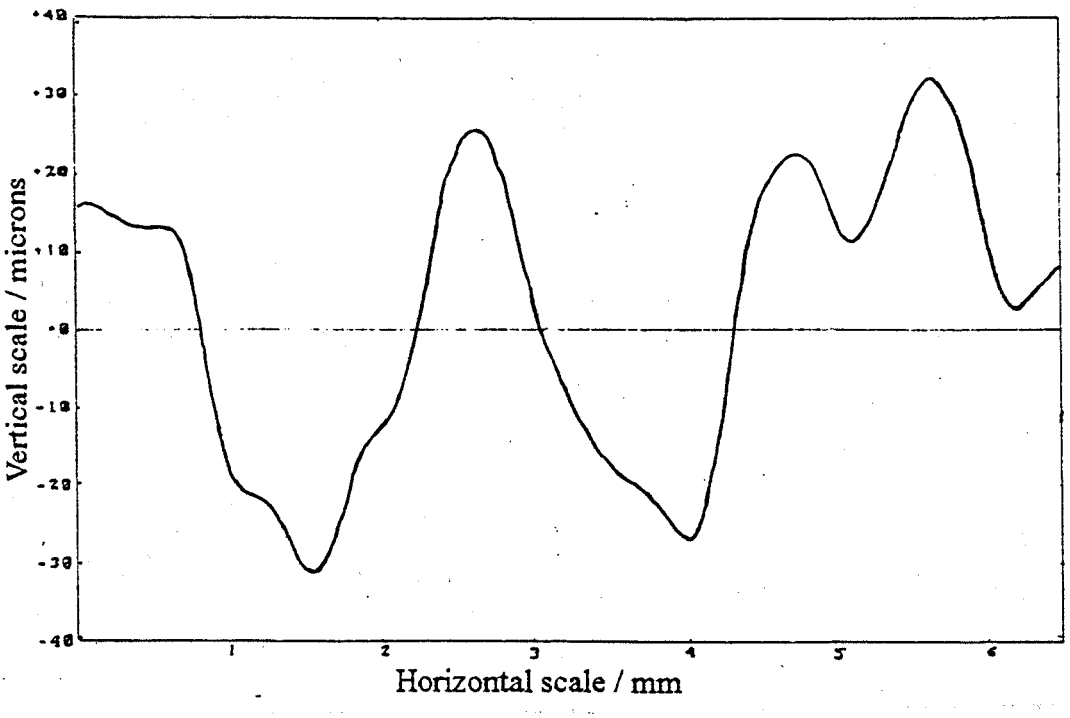

Fig. 84a) Talysurf reference profile of the standard 'Roma' paper, taken at right angles to the laid lines.

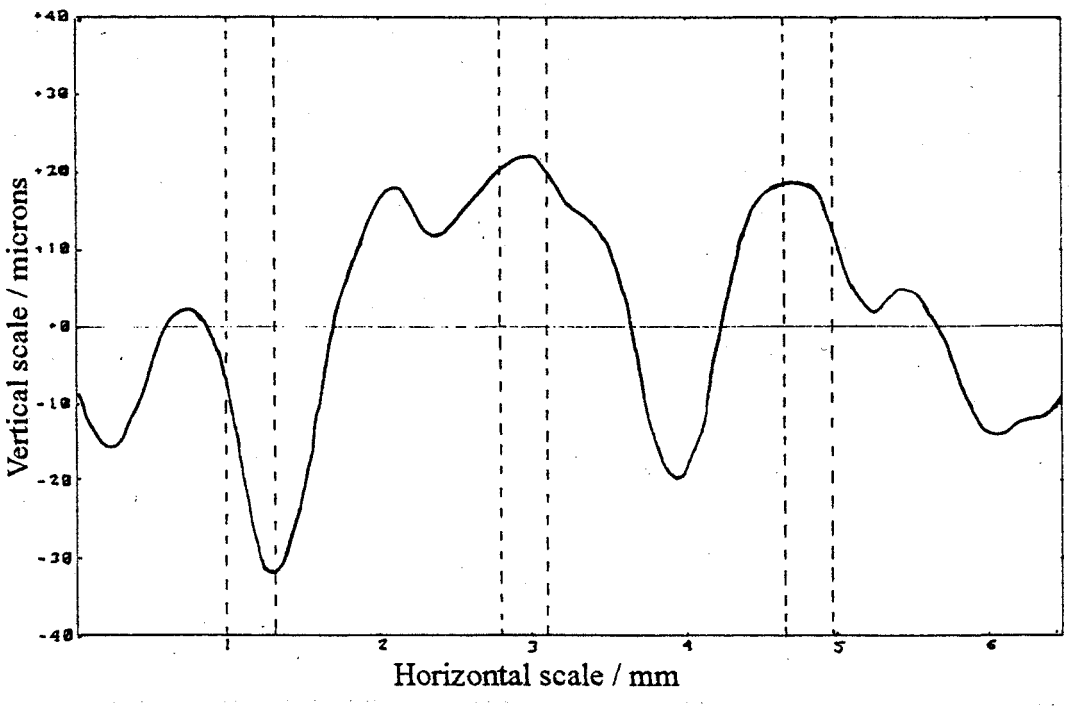

Fig. 84b) The effect on the reference profile of three Q-switched Nd:YAG laser lines produced in the direction of the laid lines. The nominal fluence was 41 ± 12 Jcm^{-2}, pulse duration 87 ns, and the dotted lines indicate the position of the laser treated areas.

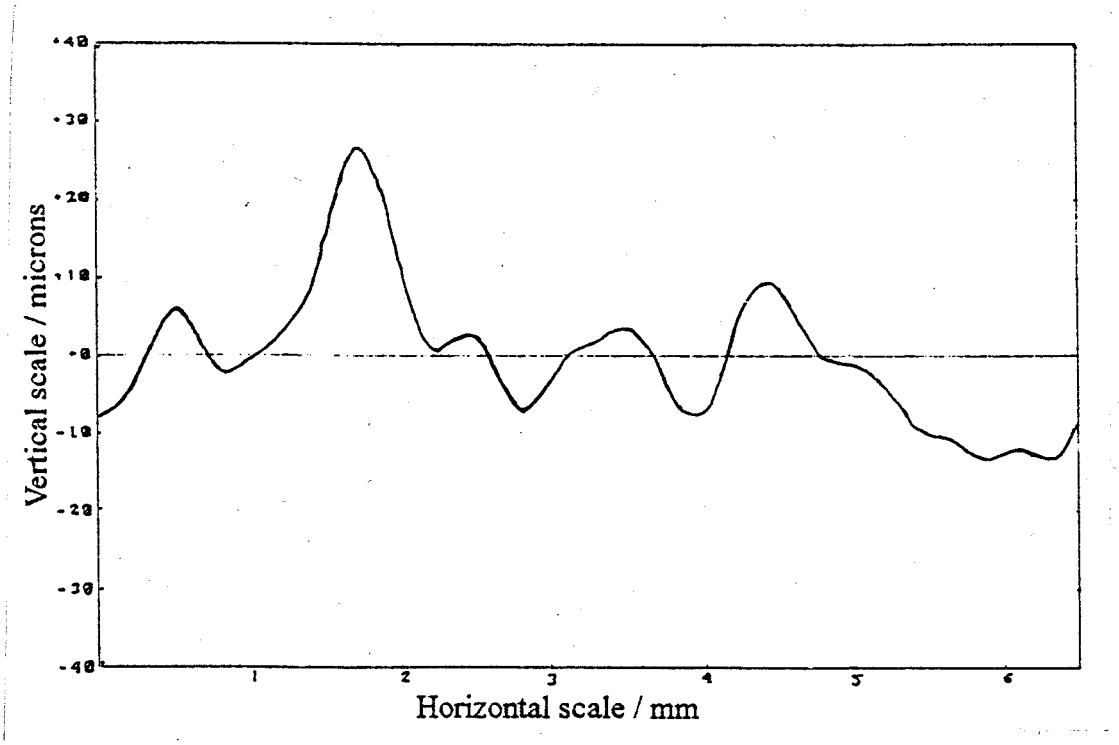

Fig. 85a) Talysurf reference profile of the standard 'Roma' paper, taken in the direction of the laid lines.

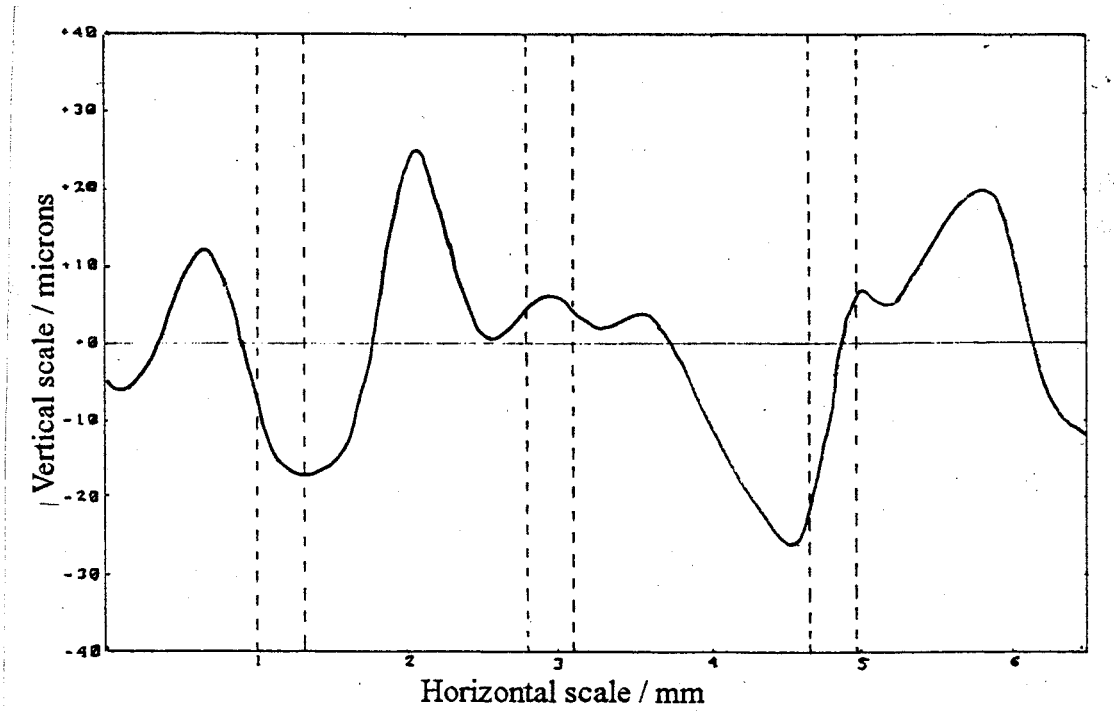

Fig. 85b) The effect on the reference profile of three Q-switched Nd:YAG laser lines produced at right angles to the laid lines. The nominal fluence was 41 ± 12 Jcm^{-2}, pulse duration 87 ns, and the dotted lines indicate the position of the laser treated areas.

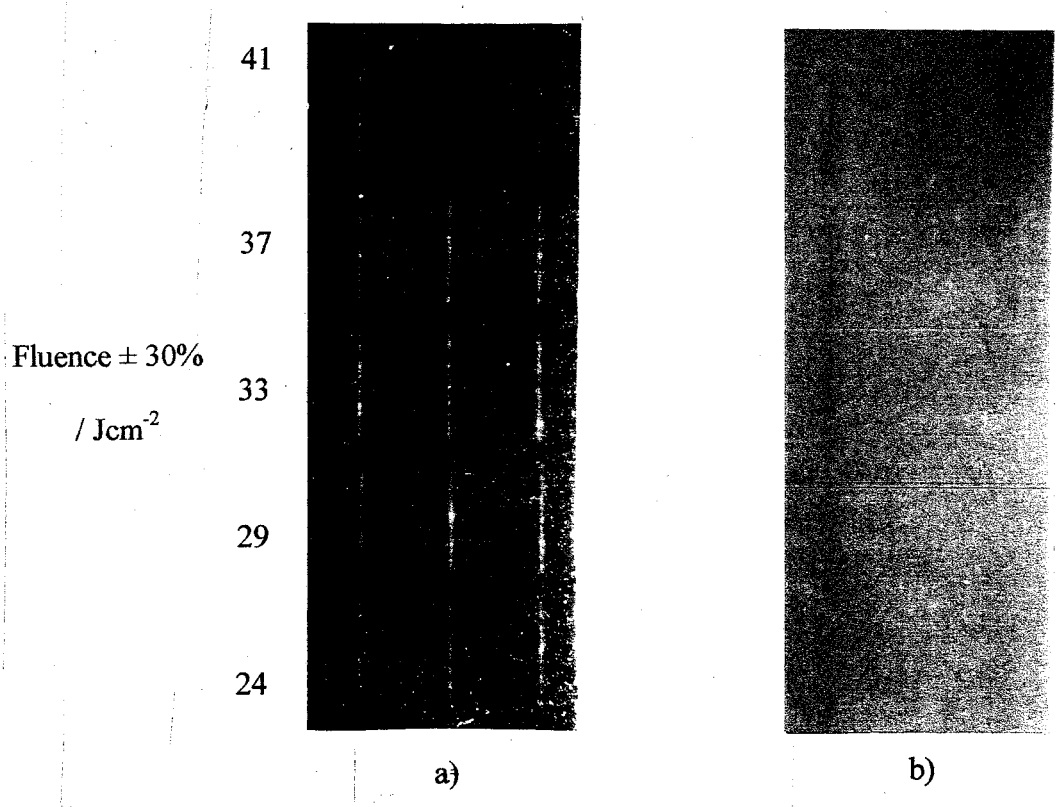

Fig. 86 The Russell effect image taken from standard sized 'Roma' cotton paper, a) immediately after and b) one week after Nd:YAG laser treatment, using a nominal fluence range of 24-41 Jcm^{-2} . For data see Table 43.

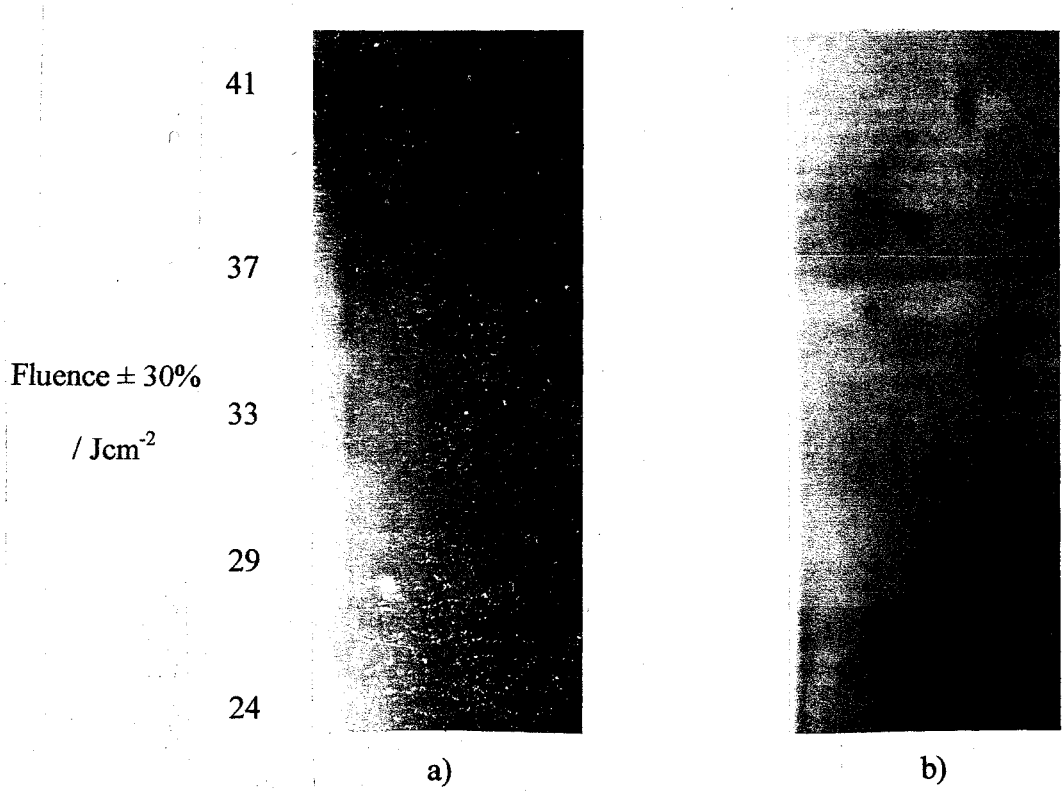

Fig. 87 The Russell effect image taken from size removed 'Roma' cotton paper, a) immediately after and b) one week after Nd:YAG laser treatment, using a nominal fluence range of 24-41 Jcm^{-2} . For data see Table 44.

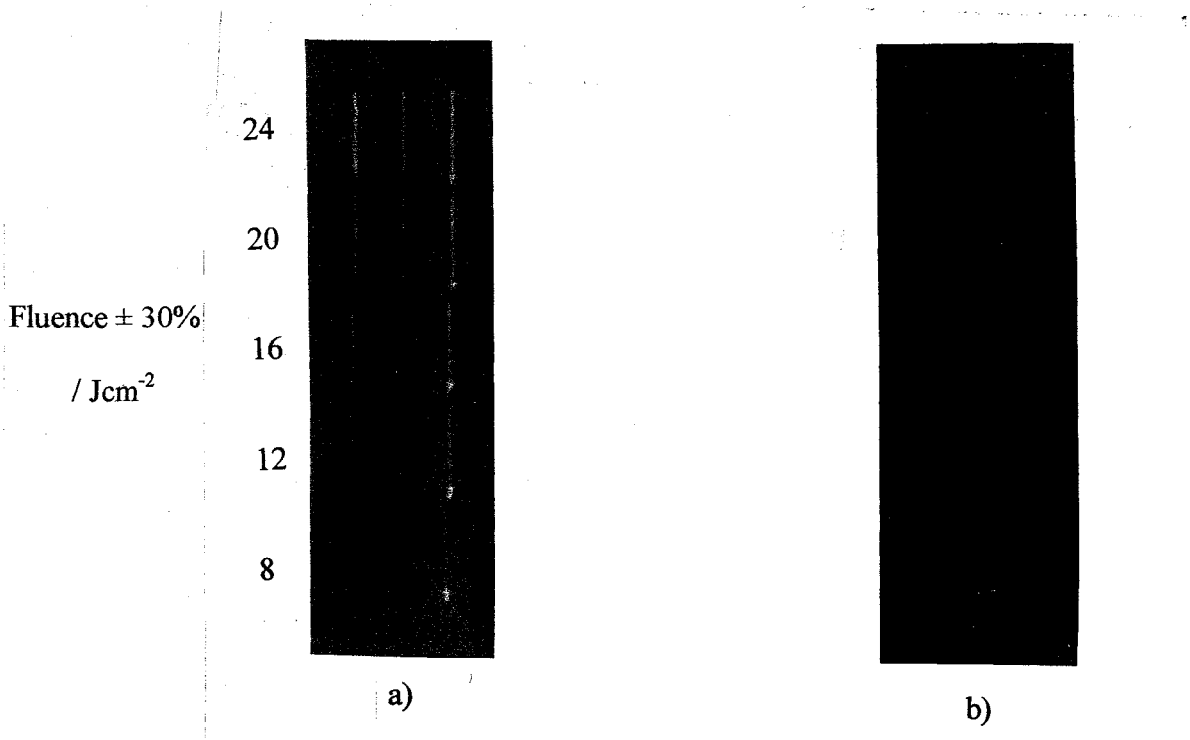

Fig. 88 The Russell effect image taken from standard sized 'Roma' cotton paper, a) immediately after, and b) two weeks after Nd:YAG laser treatment. Treatment was carried out using an attenuated beam with a flashlamp voltage of 600 V, a pulse duration of 63 ns, and a nominal fluence range of 24-41 Jcm^{-2}. For data see Table 46.

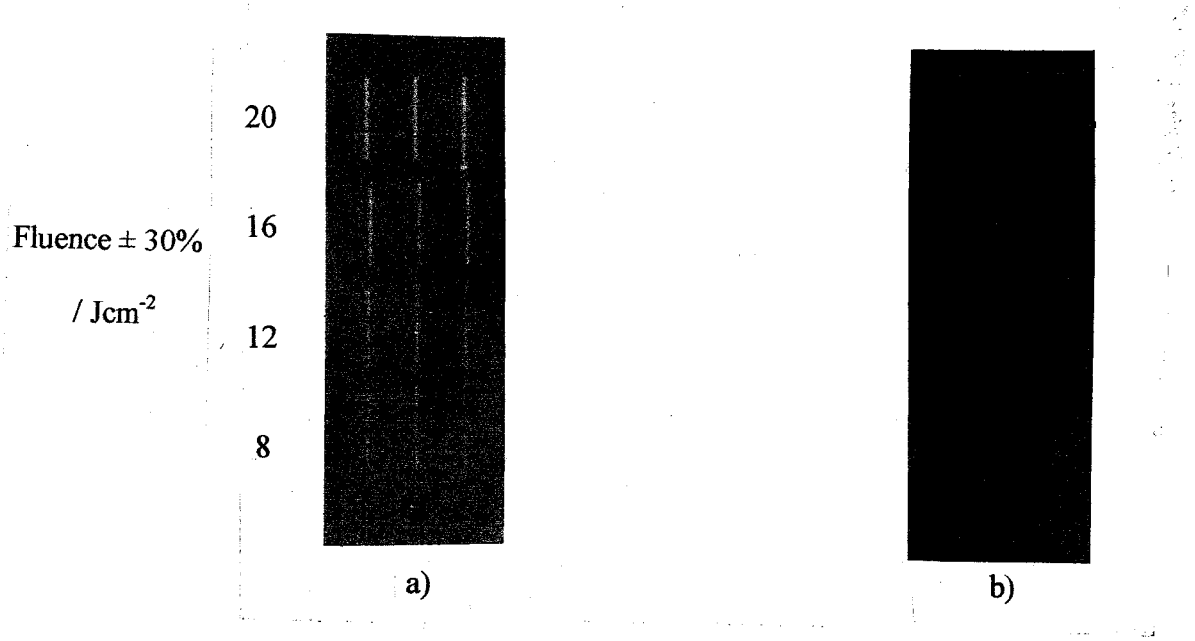

Fig. 89 The Russell effect image taken from standard sized 'Roma' cotton paper, a) immediately after and b) two weeks after Nd:YAG laser treatment. Treatment was carried out using an attenuated beam with a flashlamp voltage of 750 V, a pulse duration of 26 ns, and a nominal fluence range of 4-20 Jcm^{-2}. For data see Table 47.

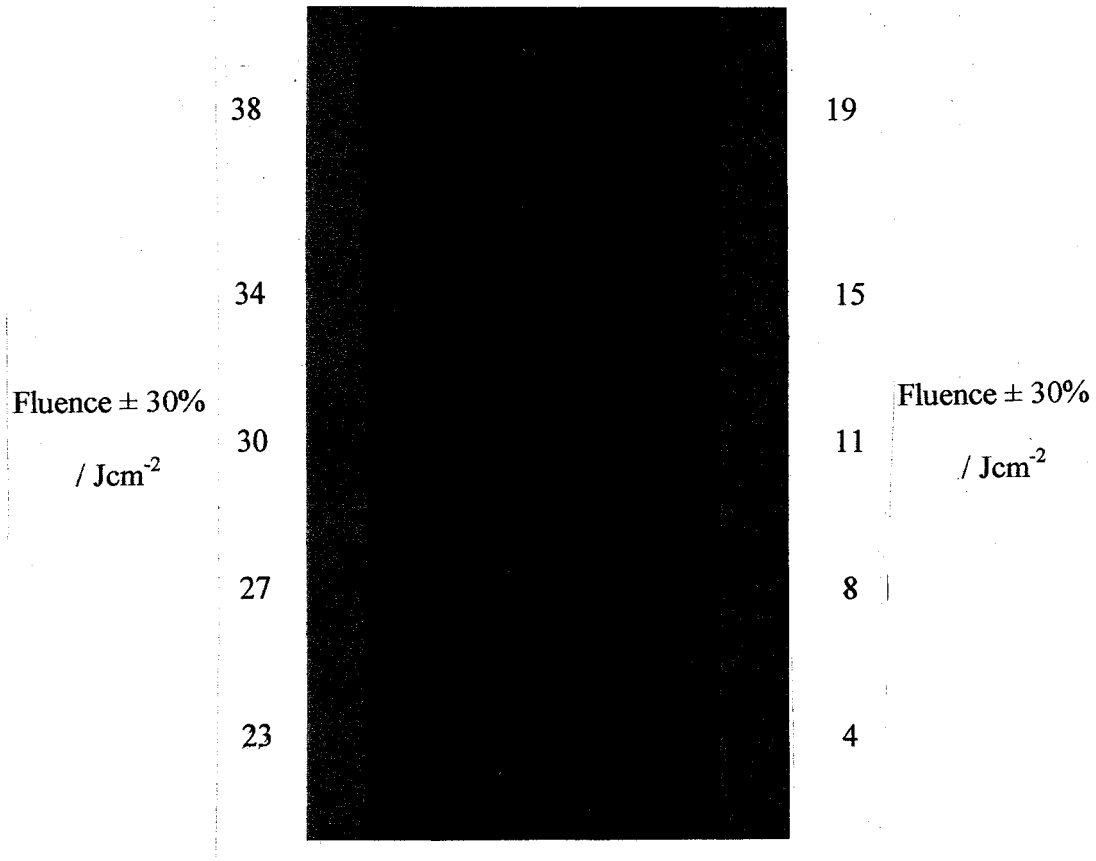

Fig. 90 The Russell effect image taken from standard sized 'Roma' cotton paper, immediately after Nd:YAG laser treatment in an argon atmosphere, using a nominal fluence range of 4-38 Jcm^{-2}. For data see Table 48.

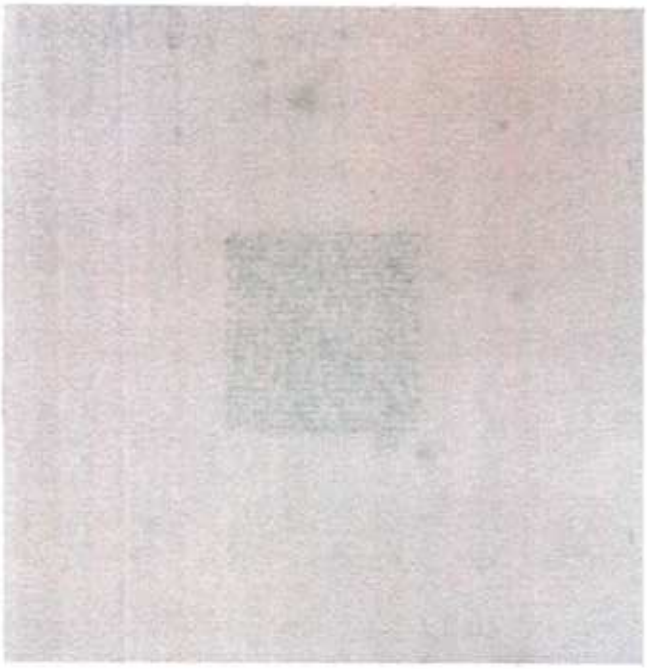

Fig. 91 Photograph of size removed 'Roma' cotton paper, Nd:YAG laser treated with a nominal fluence of 41± 12 Jcm^{-2} , and stained with methylene blue. The laser treated region has absorbed more methylene blue than the untreated region.

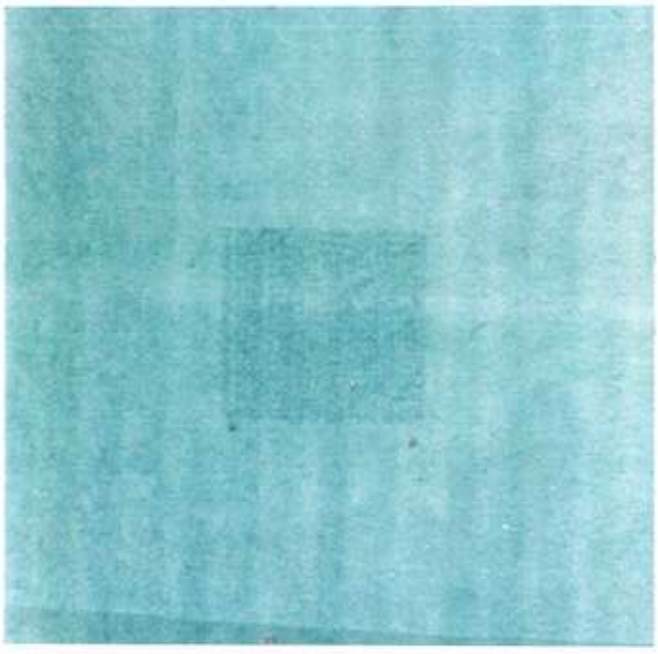

Fig. 92 Photograph of standard sized 'Roma' cotton paper, Nd:YAG laser treated with a nominal fluence of 41 ± 12 Jcm^{-2} , and stained with methylene blue. The laser treated region has absorbed more methylene blue than the untreated region.

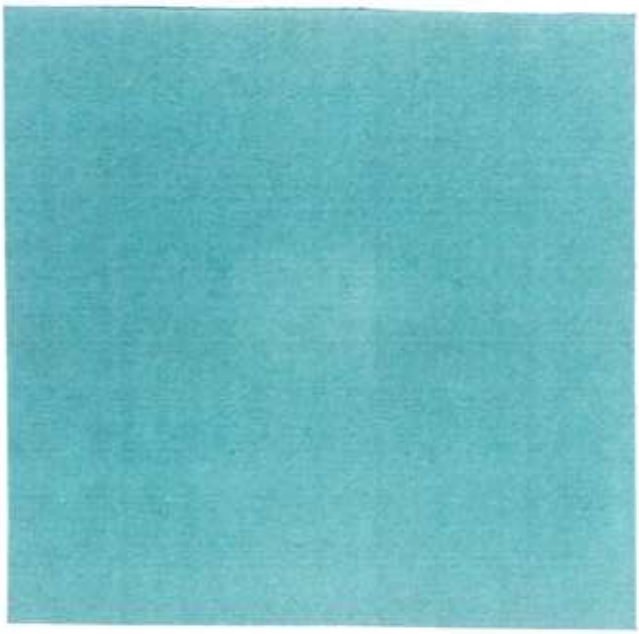

Fig. 93 Photograph of Nd:YAG laser treated, standard sized 'Roma' cotton paper, stained with methylene blue. The beam was attenuated to maintain pulse duration of 26 ns as the nominal fluence (20 ± 6 Jcm^{-2}), was achieved. The laser treated region has absorbed less methylene blue than the untreated region and appears as a white square.

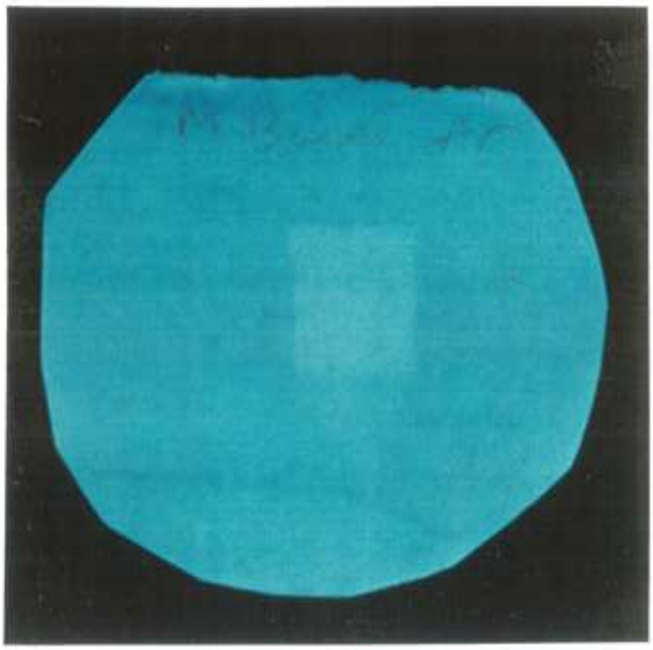

Fig. 94 Photograph of standard sized 'Roma' cotton paper, Nd:YAG laser treated in an argon atmosphere, using a nominal fluence of 38 ± 11 Jcm^{-2}, and stained with methylene blue. The laser treated region has absorbed less methylene blue than the untreated region and appears as a white square.

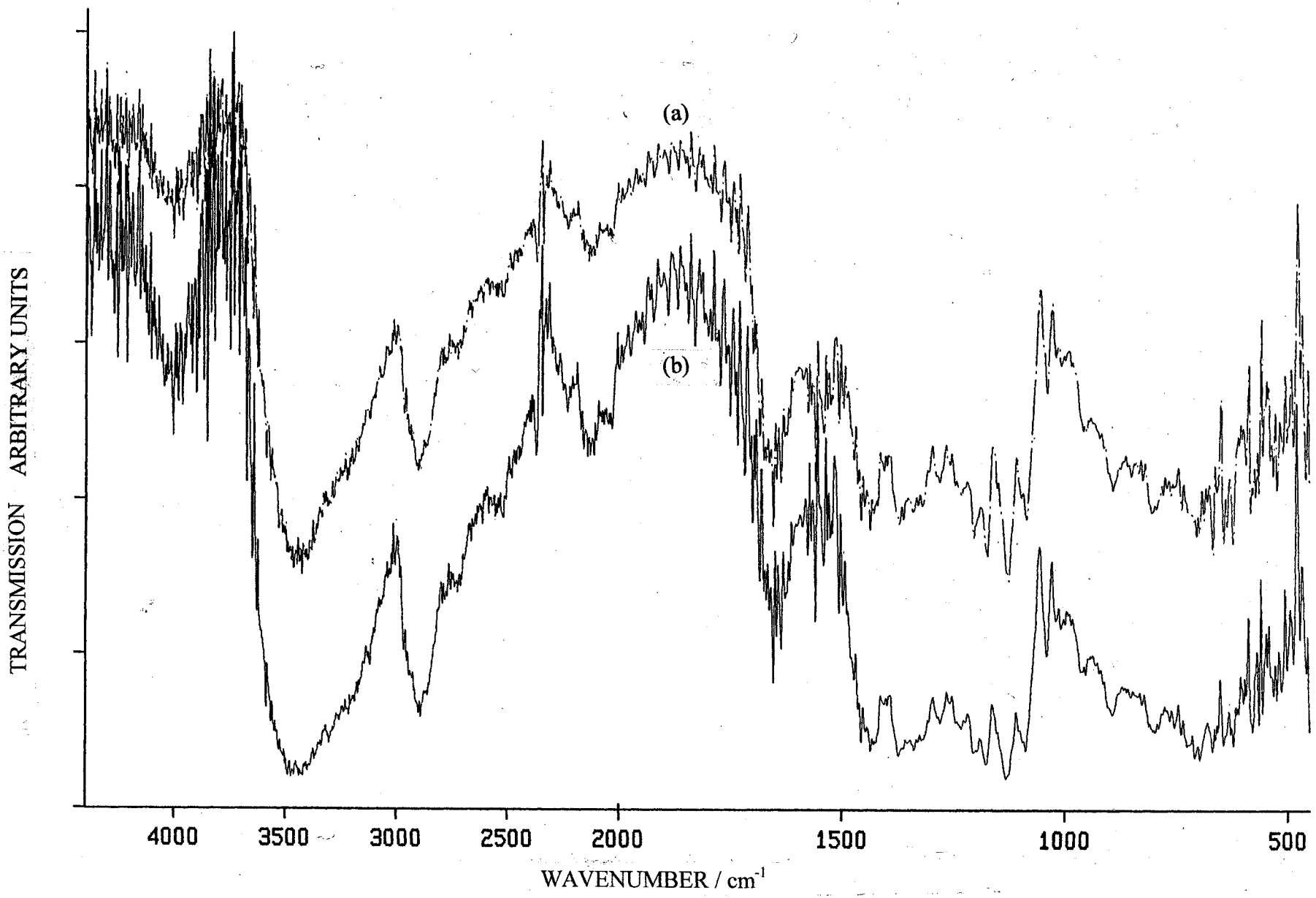

Fig. 95 DRIFT spectra of standard sized (a), and size removed (b) 'Roma' cotton paper.

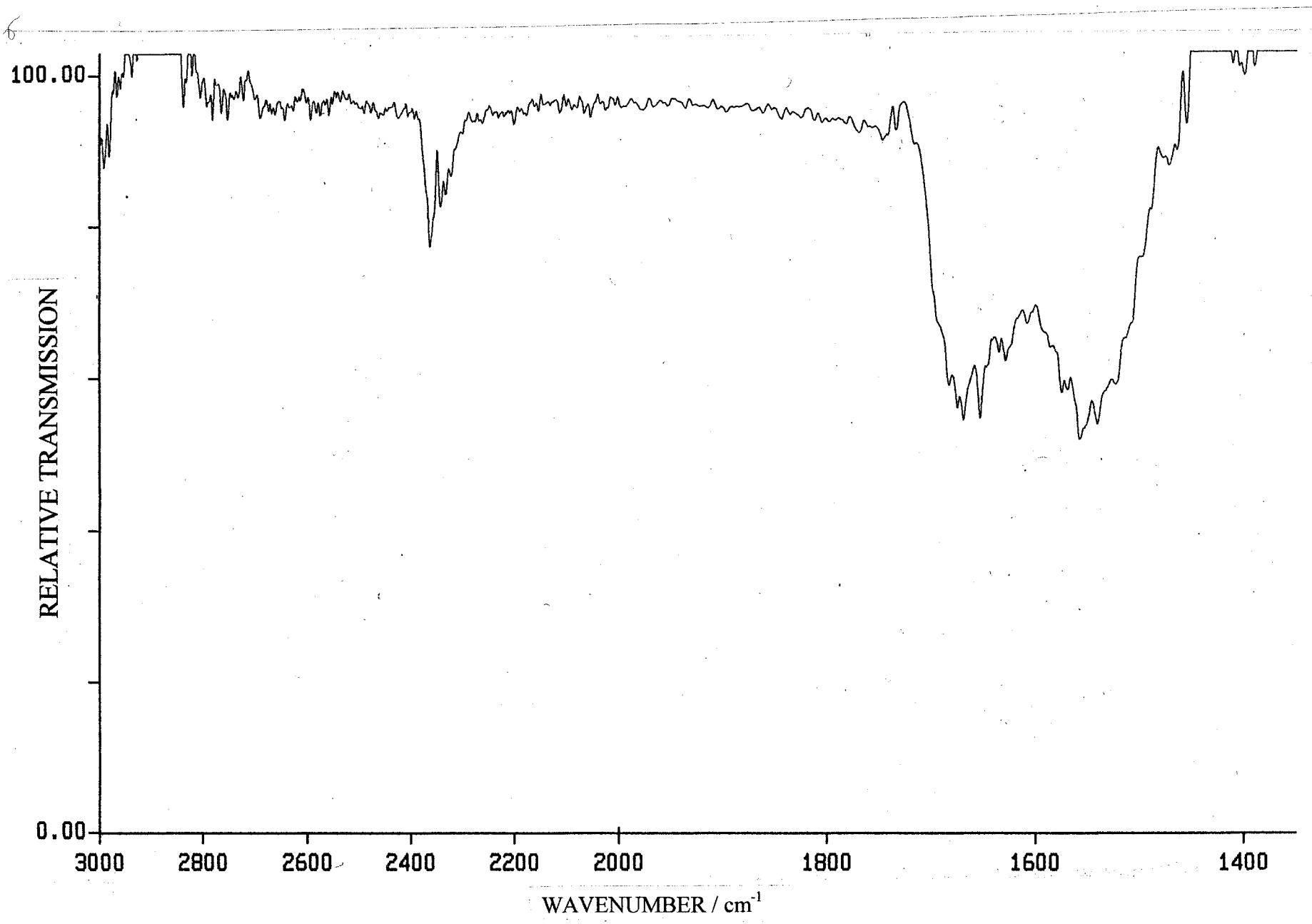

Fig. 96 Difference spectrum obtained when the spectrum of size removed 'Roma' paper (B), is subtracted from the standard sized equivalent (A).

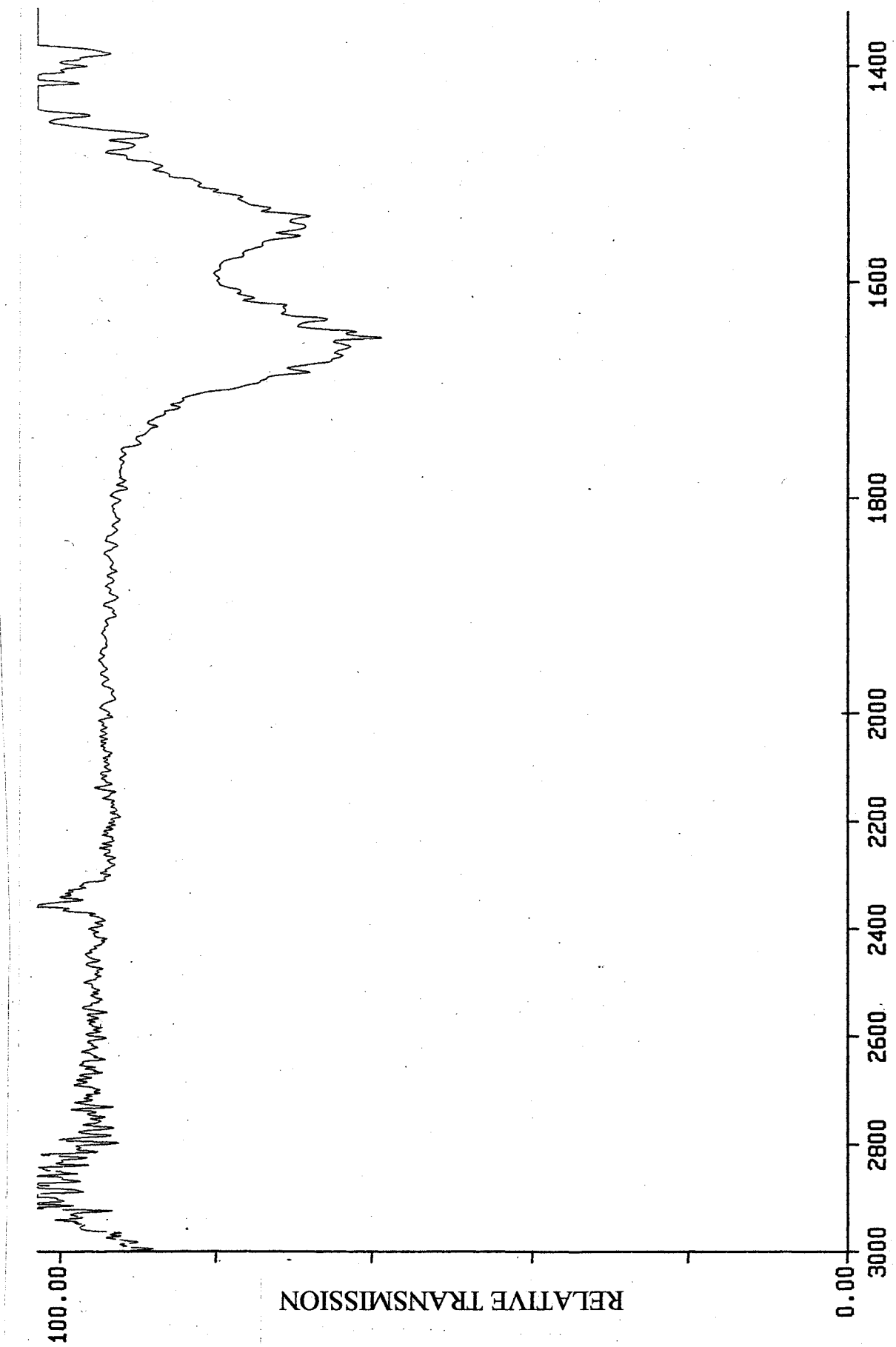

Fig. 97 Spectrum of gelatin, the sizing agent for 'Roma' paper.

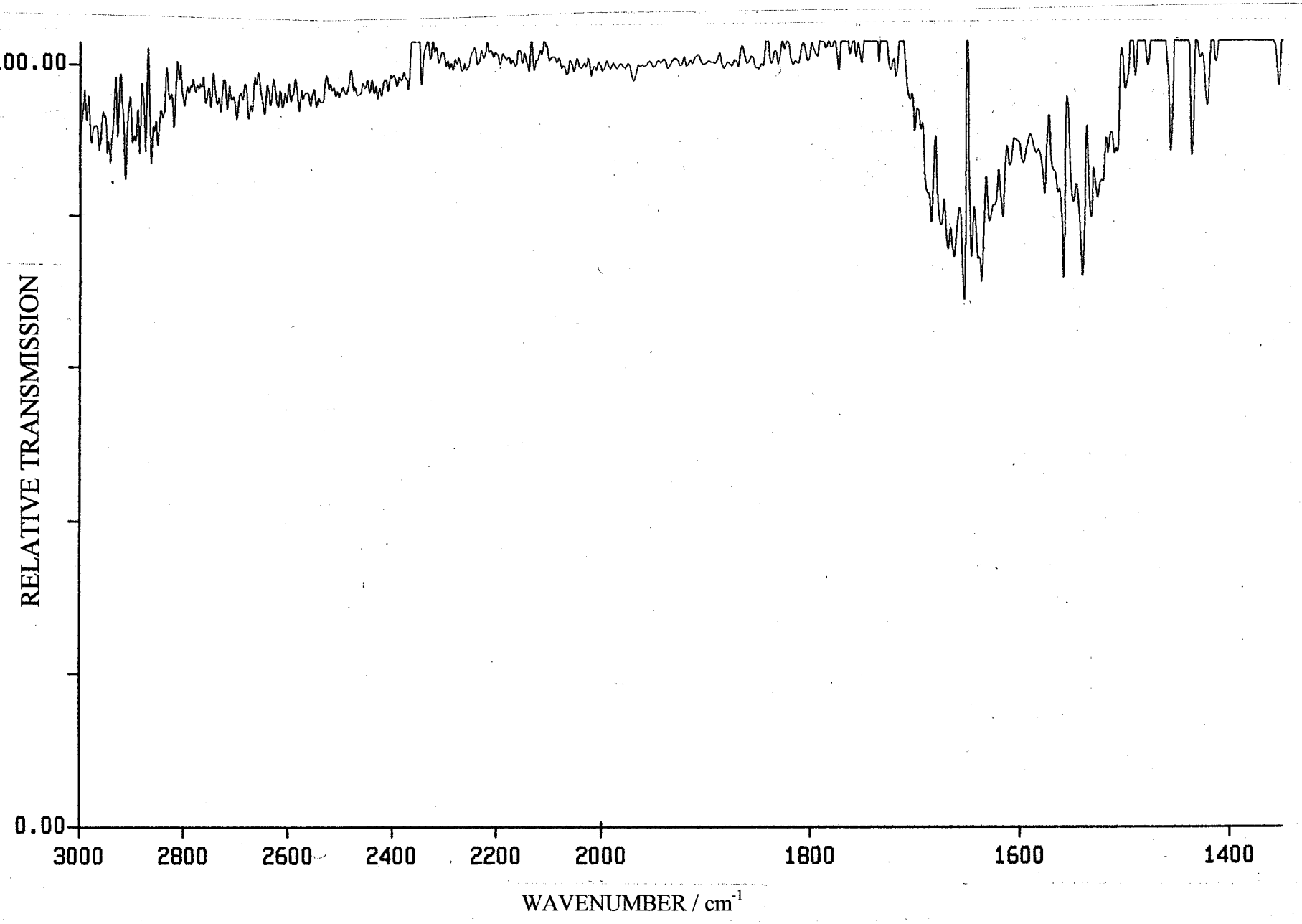

Fig. 98 Difference spectrum obtained when the spectrum of laser treated 'Roma' paper (C), is subtracted from standard sized 'Roma' paper (A). Laser treatment was carried out using a nominal fluence of 41 ± 12 Jcm^{-2}.

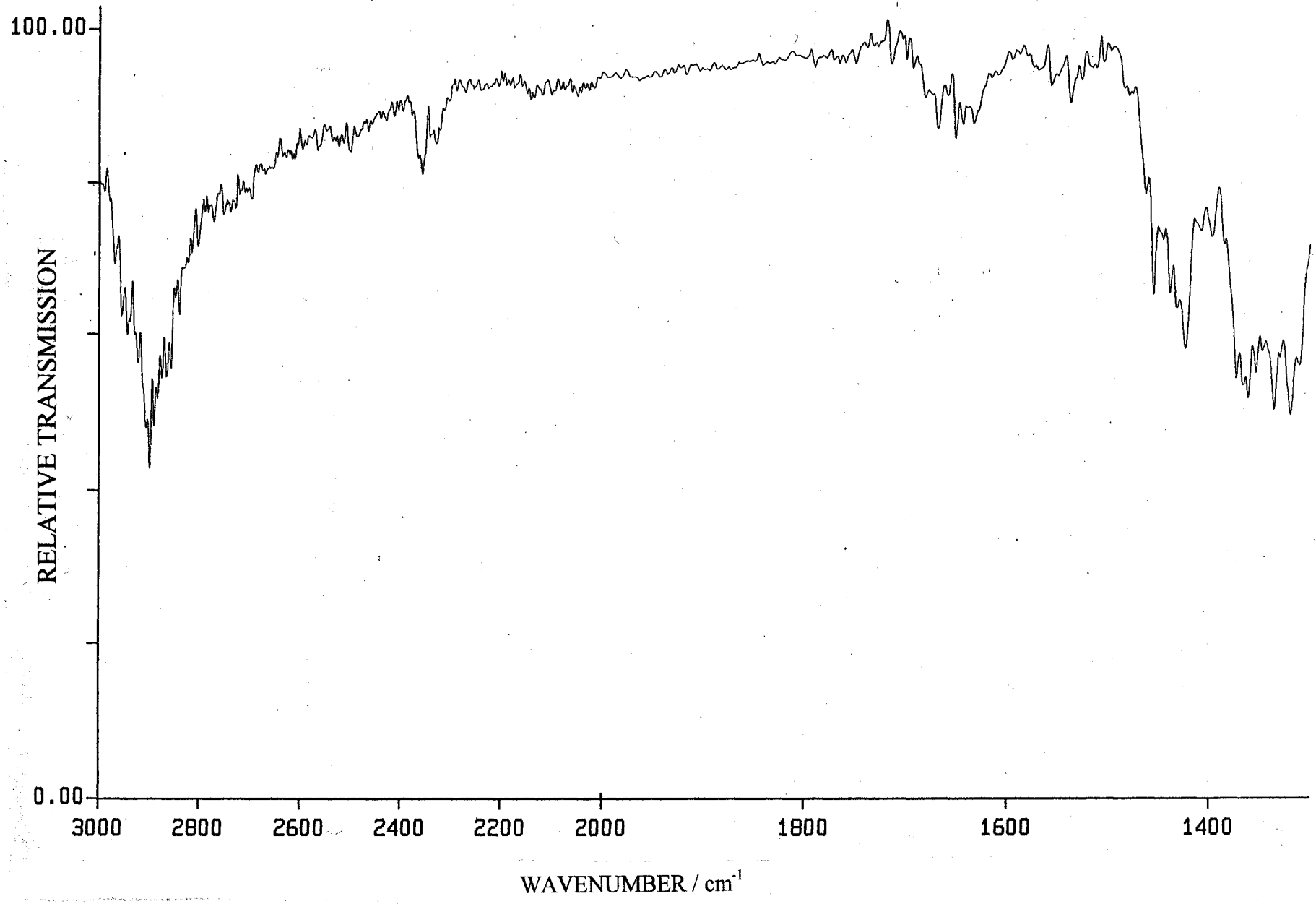

Fig. 99 Difference spectrum obtained when the spectrum of size removed 'Roma' paper (B), is subtracted from laser treated, size removed 'Roma' paper (D). Laser treatment was carried out using a nominal fluence of 41 ± 12 Jcm^{-2}.

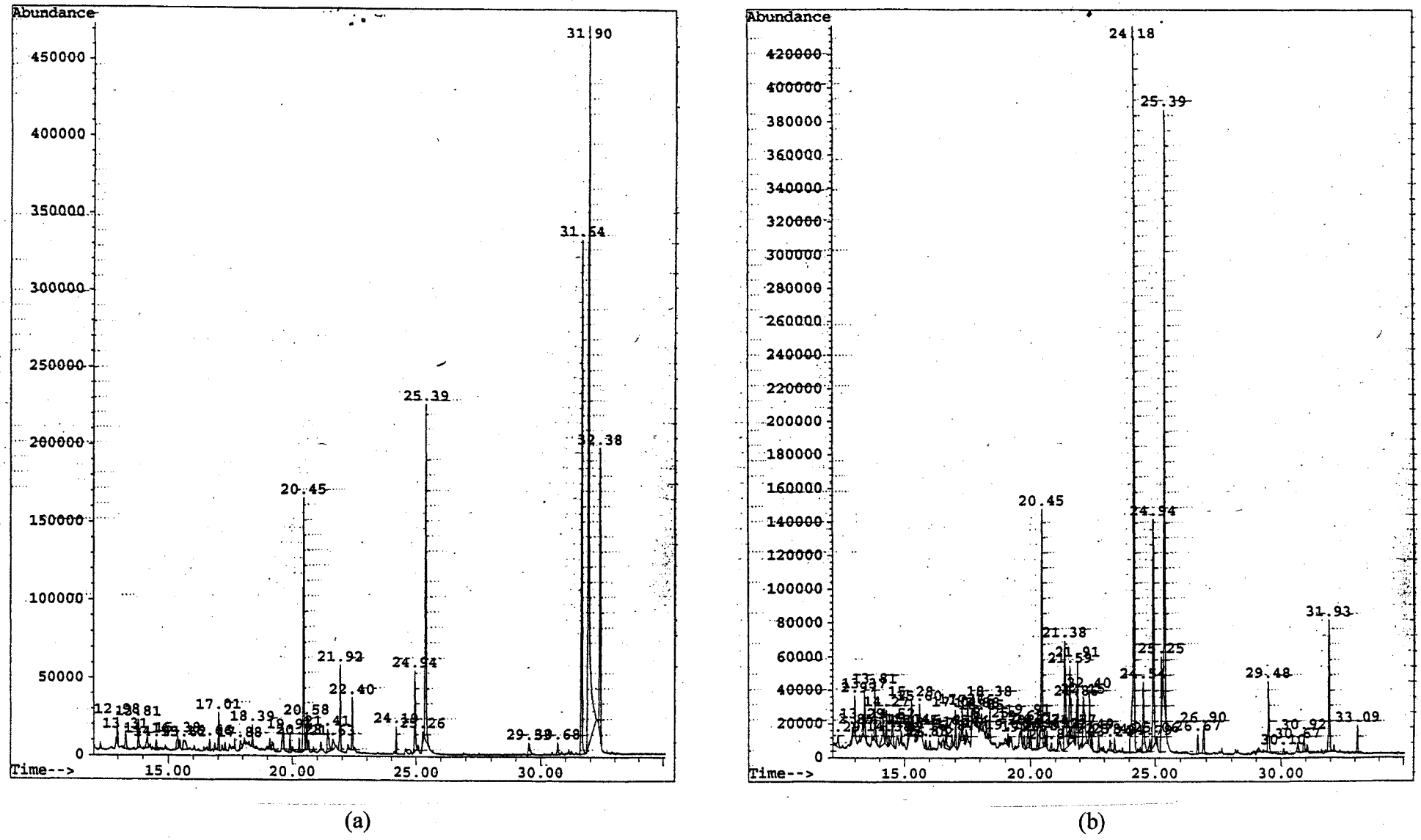

Fig. 100 Chromatograph obtained from GC/MS analysis of extract from a) untreated, and b) Nd:YAG laser treated, humid aged, standard sized 'Roma' paper.

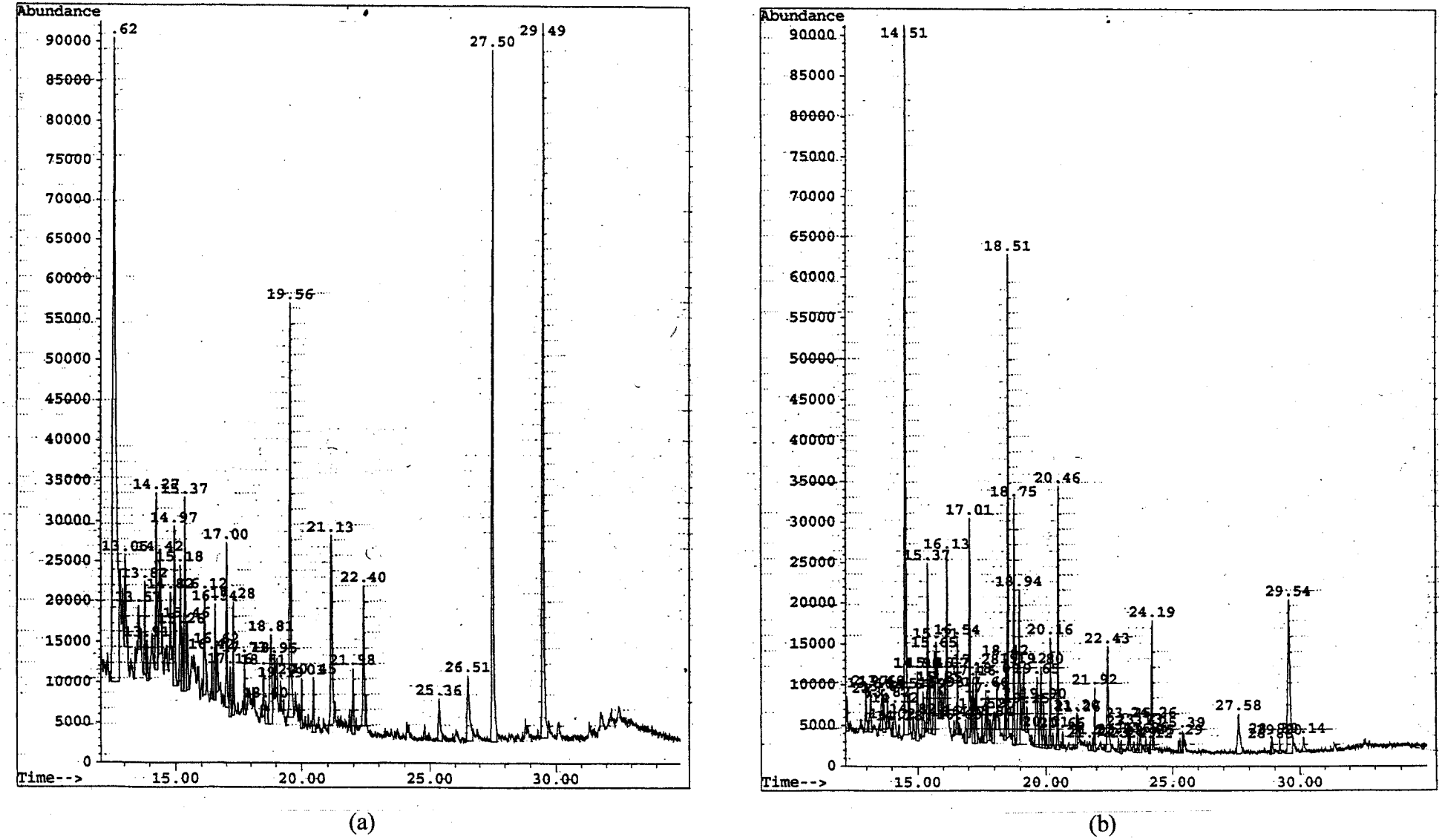

Fig. 101 Chromatograph obtained from GC/MS analysis of extract from a) untreated, and b) Nd:YAG laser treated, humid aged, size removed 'Roma' paper.

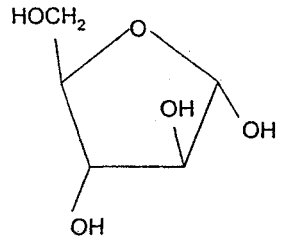

D – arabinofuranose

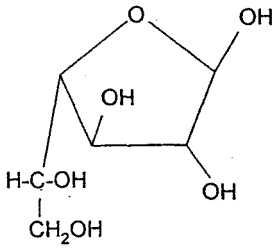

D – galactofuranose

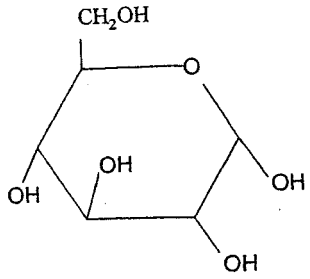

D – glucopyranose

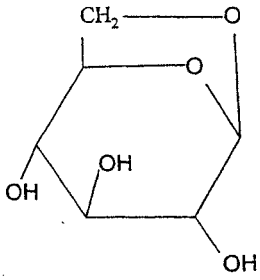

Levoglucosan

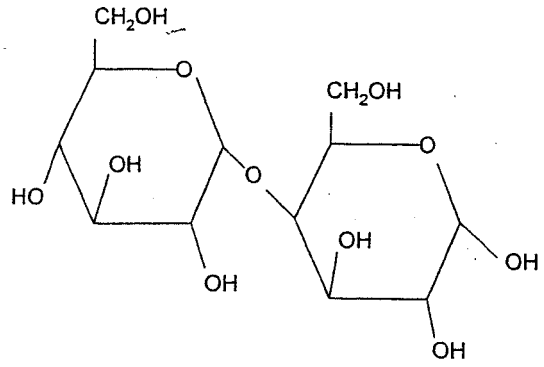

Maltose

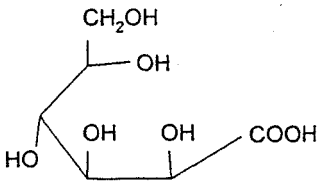

D – mannonic acid

Fig. 102 Structures of the compounds identified by GCMS from extracts of untreated, and Nd:YAG laser treated, standard sized and size removed 'Roma' cotton paper.

CHAPTER 4:

DISCUSSION

The aims of this research were to establish whether the Q-switched Nd:YAG laser could be successfully used as a tool for the controlled removal of ink from paper, and whether such laser treatment of paper would give rise to physical or chemical damage in the short or long term.

4.1 The effectiveness of ink removal from paper, using a Q-switched Nd:YAG laser (1064 nm).

4.1.1 Preliminary tests

The type of artefact the average paper conservator is required to restore is extremely varied, but the paper, on which most European works of art are executed, will generally comprise cotton or linen, mechanical woodpulp, or chemical woodpulp fibres. Four types of paper were chosen to assist in a preliminary investigation into the usefulness of the Nd:YAG laser to paper conservation. The paper samples comprised two 100% cotton papers (one thick and rough, and one smooth and thin); a medium weight mechanical woodpulp paper and a smooth surfaced chemical woodpulp cartridge paper.

Modern writing inks from ball-point pens, fibre tip pens and highlighter pens were chosen for the ink removal tests.

The un-focused Nd:YAG laser had no effect on the inked paper samples, however by focusing the beam onto the paper surface with a convex lens, ink was more readily removed (see section **3.1.1**). Working with a focused beam means the spot diameter is fairly small, 250 ± 36 μm (see section **2.2.2**), which was considered to be advantageous for the treatment of fine ink lines. Figure 20 shows that there is little difference in the spot size of the beam between 10.1 and 10.5 cm from the lens (f = 10.3 cm), which means that small variations in

the positioning of the laser for experiments will not have a significant effect on the average fluence received by the target.

One major disadvantage of working at the focus is that because the spot sizes are so small, relatively large average fluences are achieved using small pulse energies. This was not a problem for the initial part of the research where the efficiency of ink removal was under examination. Another possible criticism of the initial ink removal studies is that as the energy per pulse was increased (to achieve higher fluences), the pulse duration consequently decreased (see section **2.2.4**, Fig 27), and therefore the effect of each fluence increase cannot be accurately described in relation to the others. This was not considered significant at the time, the main concern being simply to establish whether the laser could remove ink from paper. The initial ink removal studies were also useful in establishing an initial ink removal, and paper damage threshold from which to consider improvements in operating efficiency. During the latter stages of the research, however, where the effect of pulse shortening was under observation, it was necessary to use an attenuating prism to reduce the pulse duration, whilst maintaining the same output range.

'Roma' 100% cotton paper

Tests on the 'Roma' 100% cotton paper were observed visually to establish quickly whether the ink removal treatment was successful (Table 27; section **3.1.1**). The results demonstrated that black (Fig. 38), blue and green ball-point pen inks were clearly removed from the paper in the nominal fluence range 16-45 Jcm^{-2} per pulse, although slight ink removal occurred at lower fluences. There did not appear to be any damage, however more rigorous investigation into damage was carried out later using microscopy. Red ball-point pen ink required a slightly greater fluence per pulse (37-45 Jcm^{-2}) to effect clearly visible removal. Damage was visible for all colours when nominal fluences greater than 45 ± 14 Jcm^{-2} were used.

Black, blue and green fibre tip pen ink was removed in the fluence range 29-61 Jcm^{-2} per pulse without damage visible to the eye, however damage was observed when removing red fibre tip pen ink above 37 ± 11 Jcm^{-2} per pulse, (Table 28; section **3.1.1**). Pink highlighter pen ink was partially removed but charring occurred before ink removal with yellow highlighter.

There was no visible sign of damage to the un-inked standard using nominal fluences below 16 ± 5 Jcm^{-2}, however above this figure the appearance of the paper surface changed. Initially the surface acquired a matt appearance, which became visible as fibre disruption at nominal fluences of 37 ± 11 Jcm^{-2} per pulse.

100% cotton endleaf archival paper

Black, blue and green ball-point pen ink on the 100% cotton endleaf paper was clearly removed in the nominal fluence range 12 -24 Jcm^{-2} per pulse without damage visible to the eye, (Table 29), although slight ink removal occurred at lower fluences. Red ball-point pen ink required considerably higher fluences per pulse (33 -45 Jcm^{-2}) to effect clearly visible removal.

Attempts to remove fibre tip pen ink of any colour from the paper sample resulted in visible damage and charring, (Table 30).

Damage was visible above a nominal fluence of 16 ± 5 Jcm^{-2} per pulse on the un-inked standard. Initially the surface lost its sheen, however above 29 ± 9 Jcm^{-2} per pulse fibre disruption was observed. As with the 'Roma', any damage appeared to be caused during the first few pulses with no further reaction thereafter.

Mechanical woodpulp paper

During tests on the mechanical woodpulp paper severe disruption of the paper surface accompanied the removal of ball-point pen ink and fibre tip pen over the nominal fluence range 4-24 Jcm^{-2} per pulse; (Tables 31 & 32). There was some charring at higher fluences. Excessive charring resulted from the attempted removal of highlighter pen ink (Fig. 39).

Damage and charring were also in evidence on the un-inked standard when using fluences above 4 ± 1 Jcm^{-2} (Fig. 40). These damages were immediate and not dependent on pulse repetition rate.

Chemical woodpulp paper

Excessive charring resulted during attempted ball-point pen ink removal from chemical woodpulp, (Table 33). Charring was also in evidence on the un-inked standard, and therefore no further tests were carried out regarding the removal of fibre tip pen ink from this paper.

The results from the preliminary ink removal tests, showed that the thresholds for the start of ink removal, clearly visible ink removal, and the onset of damage varied within the six repeated experiments for each paper sample. This is reflected in the fluence ranges recorded in the Tables 27-33 (see section **3.1.1**). The production of a range of results is not particularly surprising given the individuality of different areas of the same paper, and the 30 % uncertainty of the values of fluence used (see section **2.2.3**). The main factors that could influence the effect of the Nd:YAG laser on inked papers (apart from the laser parameters) are;

i) type of paper

ii) type of ink

iii) ink colour

Type of paper

The results from these preliminary tests suggest that 100% cotton papers are better able to withstand Nd:YAG laser treatment than woodpulp based papers. The 'Roma' paper and archival endleaf, showed only slight surface damage until nominal fluences of 37 ± 11, and 29 ± 9 Jcm^{-2} were reached at which point fibre disruption was visible. The fluences required to remove particular inks differed, but the general effects were very similar.

The two woodpulp papers were prone to significant fibre disruption and charring before complete removal of ink had been achieved. The tendency of woodpulp papers to char may be due to greater absorption of the laser energy, or to increased sensitivity of their components (hemicelluloses and lignin[36,61], size and fillers[60,62,63]) to the temperature increase.

Type of ink

Ball-point pen inks were successfully removed from the cotton papers without damage visible to the eye, however at higher fluences, surface disruption became noticeable. The Nd:YAG laser was not so successful in removing fibre tip pen and highlighter ink from the cotton papers, where physical disruption of the fibres, and in some cases charring, occurred.

Laser energy incident on a spot of black ball-point pen ink could readily be absorbed and vaporise the ink without greatly affecting the paper substrate. This is not the case with black fibre tip pen ink, which by having greater coverage will affect fibres to a greater depth (see section **3.1.1**). This may explain why ball-point pen ink seemed easier to remove, and why less damage was caused.

Ink colour

The results showed that red inks required greater fluences to remove, and the fluence range between safe ink removal and the onset of damage was much smaller than for other colours.

This is probably due to poorer absorption of the laser energy. Viscosity and colour may explain why some inks are easier to remove than others for a particular paper sample, but does not explain why a particular ink requires different amounts of fluence to be removed from the surface of a variety of papers. The difference may be due to the way in which the ink is distributed on the paper surface. 'Roma' and cotton endleaf are both 100% cotton papers, sized with gelatin (section **2.3.4**), however 'Roma' is a heavier weight, more heavily sized, longer fibred paper, and possesses a fairly rough surface. Ink lines drawn across the surface of 'Roma' tend to comprise thick clots, rather than the broad thin streaks witnessed on cotton endleaf.

4.1.2 Microscopic examination of surface damage.

It was clear from the preliminary ink removal tests that the Nd:YAG laser could be used for ink removal from cotton papers. The results suggested 'Roma' cotton paper and black ball-point pen ink would present the best combination to further investigate the cleaning properties of the Nd:YAG laser. The preliminary tests established roughly at what fluence, ink removal was visible, and at what point physical damage had occurred during treatment. However microscopic studies were necessary to determine threshold fluences for the removal of black ball-point pen ink from 'Roma', and the onset of physical damage as a result of laser treatment.

The microscopic studies were repeated six times for each set of laser parameters. As with the preliminary tests there was a certain degree of variation over the six samples, however accepting a 30 % uncertainty in the value of fluence, the nominal thresholds determined for ink removal and damage are typical of the observations made.

1. Threshold fluence for ink removal, and damage to paper, using a pulse length range 87 - >200 ns, normal atmosphere

The threshold for a continuous, even, removal of ink was 37 ± 11 Jcm^{-2}, however the paper appeared more thoroughly cleaned at a nominal fluence of 41 ± 12 Jcm^{-2} (Fig.42). Removal of ink at this fluence was accompanied by considerable sparking and cracking. The presence of sparks suggests the formation of a plasma as described by Cooper[7] ('Surface relaxation due to plasma effects' in section **1.3 Background on the mechanisms of lasers and laser cleaning**), in his study of the mechanisms of cleaning by short pulse radiation (5-30 ns). He also describes a mechanism ('acoustic shock-induced surface disruption'), which involves the production of an audible snapping sound, however an alternative explanation for the cracking, could be plasma breakdown in the air above the paper surface. It was not clear from the photomicrographs whether any damage had occurred.

Scanning electron microscopy (SEM) showed that the nominal threshold for damage to the inked paper was 24 ± 7 Jcm^{-2} , where the ink was thick at the centre of an 'X' shaped cross, although there was no sign of damage to the rest of the 'X', however the threshold for damage to un-inked paper was 37 ± 11 Jcm^{-2}, which was also the ink removal threshold (Fig. 44).

The process by which infra-red laser energy removes black encrustations from marble and stone objects has frequently been recorded[1-15]. Strong absorption of the laser energy by the dark material on the object surface results in explosive vaporisation of the material away from the object surface, leaving the object substrate unaffected. The interaction between the laser used for this research and inked paper appears to exhibit similarities. Black ball-point pen ink was removed from 'Roma' paper at a nominal fluence of 37 ± 11 Jcm^{-2}, with no further reaction by the paper after the initial clean. Because ball-point pen ink tends to cover the surface fibres of paper (see **Preliminary tests 3.1.1**) surface disruption is likely to

accompany ink removal which suggests that paper fibres in the presence of the ball-point pen ink are more at risk from damage than those in the un-inked regions.

At 41 ± 12 Jcm^{-2}, there was considerable disruption to the paper fibre lattice, which if viewed from the side is quite alarming (Figs. 45 & 46). It appears that the impact of the pulses has blown the fibres to a position where they are at right angles to the body of the paper. This phenomenon has been commented on by previous researchers[2,26,31,32,33,57], and is thought to be due to the rapid production and ejection of steam created from the effect of heating the water associated with the paper sheet (section **1.2 Choice of laser for the research programme**). Due to the hygroscopic nature of paper it would quickly re-absorb any moisture lost due to laser treatment, and therefore the removal of water from the paper could not be detected by the presence of water bands in the DRIFT difference spectra (see section **3.3.3**).

These results suggest that ink can only be removed safely from the paper by keeping a tight control on the fluence used. At fluences below 37 ± 11 Jcm^{-2}, incomplete ink removal is achieved, whereas above this fluence level visible damage to the paper occurs.

It was observed that at fluences between 16-33 Jcm^{-2} the width of the ink removal line was approximately 200-250microns, which is what was anticipated using a laser spot of 250 ± 36 microns in diameter (see Fig. 41). However the width of the ink removal line at 41 ± 12 Jcm^{-2} (Fig. 42) is between 400-450 microns. This means that the region affected by the laser pulse is considerably larger than the diameter of the spot. Cleaning at areas wider than $2W_z$ could be caused by plasma breakdown as described by Cooper[7], but this may not be the case within the beam profile.

It was noticeable that for un-inked regions of paper, sparking and cracking was still in evidence, at a nominal fluence of 37 ± 11 Jcm^{-2}, however if the mobile stage was stopped and the laser left running, the sparking stopped immediately. It was apparent that the laser was reacting with the paper for only the first few pulses, after which no further reaction occurred. Closer inspection of the regions of 'Roma' paper laser treated with a nominal fluence of 37 ± 11 Jcm^{-2} suggest that the laser is causing the removal of the size from the paper fibres (Figs. 47 & 48).

2. Threshold fluence for ink removal, and damage to paper, using an attenuated beam, normal atmosphere

By attenuating the beam to shorten the pulse length, the average fluence required for ink removal was reduced. Microscopy also established that using shorter pulse lengths resulted in considerably less visible damage.

For a pulse lasting 63 ns, the nominal threshold for a continuous, even, removal of ink was 20 ± 6 Jcm^{-2} (Fig. 49 Table 35; section **3.1.2**), however the paper appeared more thoroughly cleaned at a nominal fluence of 24 ± 7 Jcm^{-2}. SEM showed that the threshold for damage to the inked paper was 16 ± 5 Jcm^{-2} , but that threshold for damage to un-inked paper was 20 ± 6 Jcm^{-2}, which was also the threshold for ink removal. At 24 ± 7 Jcm^{-2}, there was considerable disruption to the paper fibre lattice, (Figs. 50 & 51), however not nearly as much as that witnessed when using the normal beam (Figs. 45 & 46).

By shortening the pulse to 26 ns, the nominal threshold for a continuous, even, removal of ink was reduced to 16 ± 5 Jcm^{-2} (Fig. 52), although the paper appeared more thoroughly cleaned at a nominal fluence of 20 ± 6 Jcm^{-2}. SEM showed that the threshold for damage to the inked paper was 12 ± 4 Jcm^{-2}. The damage threshold for un-inked paper was 16 ± 5 Jcm^{-2}, but even with a fluence of 20 ± 6 Jcm^{-2} the damage to the surface fibres (Figs. 53 & 54), was considerably less than that witnessed when using the normal beam (Figs. 45 & 46).

Therefore by shortening the pulse length to 63 ns and finally 26 ns, it was possible to remove the ink from 'Roma' using lower fluences, and suffering less physical disruption of the paper surface, than witnessed using the relatively long pulse length of 87 ns. Further experiments would be required to arrive at definite conclusions, as it is not known whether the same level of cleaning could have been achieved with less physical damage by using the attenuating prism to produce a lower nominal fluence than 41 ± 12 Jcm^{-2} with a pulse of 87 ns. However it can be seen by comparison of Figs. 49-54, that the same cleaning effect was achieved, with less physical damage, and at a lower fluence, by reducing the pulse length from 63 to 26 ns. Therefore it is reasonable to assume that the trend observed is, as suggested, the shorter the pulse, the less physically damaging and the lower the fluence required for cleaning.

One reason for the pulse length having such an effect on the observed damage is that where the pulse durations are very short, the energy is delivered to the target much faster, causing the target to vaporize rapidly. In such circumstances a considerable amount of the heat generated will be lost to radiation, rather than absorption, and hence the material around the pulse impact site is not exposed to the same heating effect.

The thresholds for ink removal from, and damage to, paper for a particular pulse depend on the peak power. Ordinarily shortening the pulse length at a particular energy would increase the peak power causing unwanted heating effects. The attenuating prism allowed for the peak power to remain roughly the same whilst shortening the pulse length. The consequence of this for fluence, was lower ink removal and damage thresholds at shorter pulse lengths.

Despite the reduction in the level of physical damage there appeared to be no change in the width of the region affected, which remained at 400-450 microns. Removal of ink with shorter pulses was again accompanied by considerable sparking and cracking, which suggests

that though the damage was reduced the mechanism was the same as when the longer pulses were used.

Microscopic examination of the fibres after treatment also suggested that though there had been a reaction with the size, some of the gelatin remained (Fig. 55).

3. Threshold fluence for ink removal, and damage to paper, using a pulse length range 87 - >200 ns, argon atmosphere

The ink removal experiments using long pulse lengths (87 –200 ns), were repeated in an argon atmosphere to see if ink removal and resultant damage was dependent on the presence of oxygen. The energy outputs used for the experiment were the same as those used in a normal atmosphere, however the energy received by the paper target was only 93% of this figure due to the loss of energy to the silica lid. The energy per pulse could have been increased to make up for the loss due to the silica lid, however this would have shortened the pulse duration (see Table 24, section **2.2.4)**, which it was assumed, would have produced a greater disparity.

The nominal threshold for a continuous, even, removal of ink was 34 ± 10 Jcm^{-2}, however the paper appeared more thoroughly cleaned at a nominal fluence of 38 ± 11 Jcm^{-2} (Table 38; Fig. 56, section **3.1.2**). As with laser treatment in a normal atmosphere, the removal of ink at this fluence was accompanied by considerable sparking and cracking. SEM showed that the threshold for damage to the inked paper was 30 ± 9 Jcm^{-2} , but that the threshold for damage to un-inked paper was 34 ± 10 Jcm^{-2}.

The region of paper affected by the laser treatment appeared to be the same as witnessed using a normal atmosphere (400-450 microns), although the disruption caused to the surface fibres (Figs. 57 &58), is significantly less than that witnessed in a normal atmosphere. This is

probably due to the lack of moisture in the paper. During Nd:YAG laser treatment of paper it is thought that water vapour associated with the cellulose rapidly vaporises and exits as steam causing considerable physical disruption of the fibres[31-33]. By passing argon over the sample for a few minutes prior to treatment most of the water vapour is flushed out. It was also apparent that laser treatment in an argon atmosphere did not result in complete removal of gelatin size (Fig. 59).

Taking into account the size of error attributable to the ink removal and damage thresholds, it appears that ink removal in an argon atmosphere, produces similar results to those achieved in a normal atmosphere. This is an important result as it shows that ink removal is not totally dependent on the presence of oxygen.

The earlier investigations into ink removal using a normal atmosphere suggested that the ink was removed via photothermal ablation, which may result in heating of the paper[7,57]. Shafizadeh[68,69] has shown that heating paper can result in (among other reactions) oxidation of the cellulose, which would be a disadvantageous result when considering lasers for treatment on paper artworks. It was therefore decided (re. Part Two of the research) to carry out an examination of the chemical effect on 'Roma' paper, after the use of the laser in an argon atmosphere as well as a normal atmosphere, to determine if there was a significant difference.

In summary, the results of Part One, an examination of the effectiveness of the Nd:YAG laser for ink removal from paper, suggest that the laser is very effective for viscous inks on well sized cotton paper, but that the effectiveness is reduced where free flowing inks and/or thinly sized paper is concerned. The laser was not, however, effective when treating paper derived from woodpulp as charring occurred. Where the laser was effective ('Roma' paper and ball-

point pen ink), efficiency could be increased by shortening the pulse length. This resulted in ink removal at lower fluences, and with less visible damage to the surface.

SEM showed that a certain amount of physical disruption accompanied ink removal, despite the use of short pulse lengths. The damage witnessed must however, be put into context. The traditional methods of mechanical ink removal employed by conservators involve the use of scalpels and erasers, which also cause damage to the paper. Comparisons with the physical damage caused by scalpel and eraser, show that overall less physical damage is created by the Nd:YAG laser (section **3.1.3**), and the damage occurs over a smaller area.

The comparison involved removal of an ink line from sample A, by laser at an average fluence of 37 Jcm^{-2}. The laser was operated in a normal atmosphere using a long pulse (Table 34, section **3.1.2**). A long pulse was deliberately chosen to give the most damaging effect with which to compare ink removal treatments. Ink removal caused some surface damage to the paper fibres, but this was restricted to the inked areas (Fig. 60). For sample B, which was cleaned using erasers the spread of damage was much more in evidence, 3 mm. compared to 400 μm. (Fig. 61). The scalpel on its own, sample C, created similar visible damage to that of the laser, however it did not successfully remove all the ink (Fig. 62). For complete removal of the ink line, it was necessary to use an eraser after the scalpel, sample D. This clearly produced the most destructive result (Fig. 63). Therefore even the most aggressive laser treatment parameters caused less disruption to the paper surface during ink removal. The ideal situation would obviously be total removal of ink without any surface disruption, however the level of damage caused by traditional methods is so high that any reduction could be tolerated as a viable conservation treatment provided there was no chemical alteration of the cellulose.

4.2 Investigation of physical damage to Nd:YAG treated paper

4.2.1 Accelerated ageing tests.

The apparent loss of size after laser treatment of 'Roma' (Figs. 47 & 48), did suggest that there was chemical change and not just physical disruption of the fibres. Small chemical changes to the structure of cellulose may cause significant changes to the physical properties of the paper sheet, however this may take a considerable time to become apparent. Artificial ageing has become a useful method of highlighting chemical changes in paper. The importance of artificial ageing has been discussed with reference to light ageing[121], humid ageing[122-128] and dry oven ageing[129-131] (section **1.5 Tests for the degradation of cellulose**).

Samples of the 'Roma' paper and Whatman filter paper were given laser treatment and then aged by exposure to light, humidity, and heat (section **2.3.4**). There was no visible change to the laser treated regions of the dry oven aged, and light aged samples. This result for light ageing suggests that the laser treatment does not alter the ultra-violet absorption properties of cellulose, i.e. does not create conjugated systems along the chains (see Fig. 10; section **1.4 The degradation of cellulose**).

Dry oven ageing at a temperature of 90° C was probably not high enough to increase the rate of degradation of the cellulose sufficiently to produce a visible change, however humid oven ageing at the same temperature caused considerable localised discoloration to the 'Roma' paper, particularly with the standard sized samples which developed a reddish/brown colour (Fig. 64; section **3.1.4**).

Humid ageing treatment accelerates the hydrolytic degradation of cellulose and is catalysed by acidic conditions (Fig.7; section **1.4 The degradation of cellulose**). The results of

accelerated ageing indicate that the effect of laser treatment on 'Roma', is to make either the cellulose or the gelatin in the paper more sensitive to hydrolysis. There are three possible explanations for this heightened sensitivity.

1. Hydrolysis of cellulose is catalysed by acidic conditions[64]. The Nd:YAG laser is known to give rise to a heating effect[1,2,6,7,9,25,26], which could create carboxylic acid groups on cellulose via thermal degradation[68,69]. These would act as catalysts for hydrolytic scission.

2. There have been persistent reports of the existence of a few bonds that are more susceptible to hydrolysis than the rest. Whitmore and Bogaard[71,72], and Ranby[73] suggest that weak links in cellulose are created due to the formation of carbonyl and/or carboxyl groups along the cellulose chains as opposed to those formed at chain ends. Nevell[64] also cites the presence of a few sugar units other than anhydroglucose as the possible cause of acid sensitivity. All these species could be products of thermal degradation.

3. The presence of gelatin may be significant. The standard sized paper sample exhibited considerable discoloration after ageing (Figs. 64 & 65), however the size removed sample discoloured very little. The use of the laser appears to remove gelatin from the paper (Figs. 48 & 49), however the pyrolysis products of gelatin (alkenes, benzene, toluene, styrene, acrolein, pyridine and pyrrole)[159], may be sensitive to hydrolytic degradation.

4.2.2 Reflectance measurements.

Figures 66-68 (see section **3.2.1**) show the change in the reflectance spectra of the laser treated regions of aged samples of, standard sized, and size removed 'Roma'. For the standard sized sample there is approximately 15% less visible light reflected at 400 nm (Fig. 67). The reduction is due to absorption of the light by chromophores in the modified cellulose (see section **1.4 The degradation of cellulose**), causing in a reddish/brown appearance (Fig. 64). This result would suggest that laser treatment, creates conjugated systems in cellulose, however for the size removed sample only 2% less light was reflected at 400 nm (Fig. 68). This indicates that the presence of gelatin in the sample is significant, however identical ageing to a standard sized 'Roma' sample, laser treated with short pulses (26 ns) resulted in only a 3% reduction in reflectance at 400 nm (Fig. 70). Clearly the pulse length has great significance in the level of chemical change witnessed.

Ageing of standard sized 'Roma', laser treated in an argon atmosphere produced more or less the same result as in a normal atmosphere, reddish-brown discoloration (Fig. 72), and a 30% reduction in reflectance at 400 nm (Fig. 71). This shows that the reaction between the laser and cellulose and/or gelatin is not dependent on the atmosphere used during treatment.

One possible criticism of the results from the reflectance measurements is that the tests were not all carried out at the same time, using the same sheet of paper. The tests were performed at different stages during a lengthy period of research, and consequently different sheets were used for each of the five experiments. This explains why the reference spectra, of un-aged, untreated paper, vary from one result to another. However, within each experiment the spectra are taken from the same sheet of paper. Important information can thus be determined from a comparison of the decrease in reflectance of each laser treated and aged sample relative to the untreated, aged sample. After one month of humid ageing the sized paper treated in both normal and argon environments, exhibited considerable reductions in

reflectance (15% and 30%, at 400 nm respectively), which suggests there is no dependence on the presence of oxygen for chemical damage. However the size removed sample and the samples prepared using short pulses all gave reflectance spectra approximately the same as their own aged backgrounds (2-5% difference at 400 nm) The results highlight the significance of pulse duration and the presence of a sizing agent as discussed above.

4.2.3 Tensile testing

The results of artificial ageing generally suggested that laser treatment of paper made the latter more prone to hydrolysis, which would result in lowering of DP. The lowering of DP can be identified by several methods (section **1.5 Tests for the degradation of cellulose**), however not all of these would be suitable for this research programme. Microscopic analysis during ink removal (see section **3.1.2**) suggested that only the surface of the paper is affected by the laser treatment, and therefore any change in DP would be extremely localised and subtle. This suggestion is endorsed by the cross section of aged, laser treated paper (Fig. 65, section **3.1.4**).

The extent of strength loss was investigated using tensile tests (see section **2.4.4**). The results (Tables 39 & 40; section **3.2.2**), show that the mean value of tensile index remained roughly the same for all samples. This would suggest that although use of the laser for ink removal causes surface damage to 'Roma' paper, the laser is not impacting deep enough into the paper to dramatically alter its physical strength. However there was an increasing tendency to tear at laser treatment sites, with increasing fluence, as illustrated by two histograms (Figs. 73 & 74). It can be seen that there was no tendency to tear at laser treatment sites below 37 ± 11 Jcm^{-2}, (the nominal threshold fluence for ink removal) however above 37 ± 11 Jcm^{-2} the tendency to tear at laser treatment sites was very strong, particularly when the laser treatment was at right angles to the laid lines (Fig. 73).

Further samples of 'Roma' were prepared and aged at 90° C and 50% RH, for one month and tensile tested (see section **2.4.4**). The results (Tables 41 & 42; section **3.2.2**), show that between 0-41 Jcm^{-2}, the mean value of tensile index remained roughly the same for all samples.

The tendency to tear at laser treatment sites, with increasing fluence, is illustrated by two histograms (Figs. 79 & 80). It can be seen that the tendency to tear at laser treatment sites for samples laser treated at right angles to the laid lines, was very strong for fluences above 33 ± 10 Jcm^{-2} (Fig. 79). However there was no tendency to tear at laser treatment sites for humid aged samples, laser treated in the direction of the laid lines.

This is not surprising as the laid lines are fairly deep rendering the paper quite thin in places (see Talysurf profile of 'Roma' Figure 84a). The paper would thus tend to tear wherever the paper was most thin. These results suggest that laser treatment may have significant effect on the tensile properties of laid paper as it ages, depending on the angle of the line of laser treatment to the laid lines.

Consequently the results from laser treatment at right angles to the laid lines yield more useful information.

SEM was used to observe the broken fibres created at the tear sites during tensile testing (section **3.2.2**). The tear in the standard sample follows no specific course (Fig. 75), but the tear in the laser treated sample barely wavers from the laser path (Fig. 76). Higher magnification revealed more differences. Previous SEM studies on the fractography of cotton fibres have shown that the length of the fracture surface, or degree of taper created by breakage under tension is an index of their brittleness[87,88]. Figure 77 illustrates a broken

standard 'Roma' cotton fibre, and is characteristic of the fracture pattern of an undegraded fibre. Figure 78 is typical of the 'Roma' cotton fibres protruding from the torn edge of the laser treated sample. The short length and bluntness of the fracture infers that the fibre was significantly more brittle than the untreated standard sample. Brittleness in cotton fibres tends to increase with crystallinity, which in turn is increased by both hydrolysis and heating[87,88].

SEM observation of broken fibres created at the tear sites of the humid aged samples produced similar results. The tear in the standard sample was haphazard (as with Fig. 75) but the tear in the laser treated sample did not deviate from the laser path (Fig. 81). At higher magnifications it was possible to see that for the humid aged laser treated sample (Fig. 82), the ends of the broken fibres were generally, more blunt than those of the humid aged standard (Fig. 83), and those of the un-aged laser treated sample (Fig. 78).

These results infer that the long pulse length (87 ns) laser treatment of 'Roma' is heating the paper, increasing the crystallinity and brittleness, and generally leaving the treated regions more prone to hydrolysis on ageing. The long term effect of the laser treatment is to render the paper more susceptible to tearing in laser treated regions. Tensile testing was not carried out using pulses shorter than 87 ns as other results had indicated there would be less physical damage, thus producing results too subtle to meaningfully record.

The surface profile of 'Roma' was recorded, and compared with the profile after laser treatment. The Talysurf reference profile of the standard 'Roma' paper (Fig. 84a), taken at right angles to the laid lines described a fairly regular, though undulating surface with peaks ca. 1.5 mm apart (average peak height between 25-35 μm; depth 20-30 μm). This general profile did not show any appreciable change when the Talysurf profiler was dragged across the three laser treated lines, running parallel to the laid lines (Fig. 84b). This was not particularly surprising as the peaks and troughs are far too great for the laser to make a strong impression.

The Talysurf reference profile of the standard 'Roma' paper (Fig. 85a), taken in the direction of the laid lines was much smoother and less ordered (average peak height 10-20 μm; depth 10-20 μm). This general profile did not show any appreciable change when the Talysurf profiler was dragged across the three laser lines, running at right angles to the to the laid lines (Fig. 85b).

These results suggest that Nd:YAG laser treatment of 'Roma' paper, at the fluence level required to remove ball-point pen ink, does not cause significant alteration to the surface profile of the paper, but does illustrate the large variation in thickness across the sheet.

4.3 Investigation of chemical damage to Nd:YAG treated paper

The investigations into physical damage caused by laser treatment (see sections **2.4.3**, **2.4.4**, and **2.4.5**) suggested a heating effect to the paper. Shafizadeh[68,69], describes the effect of heat on cellulose as being primarily oxidation below 300°C, and primarily depolymerisation above 340°C (see section **1.4 The degradation of cellulose**). The laser treatment produced no visible evidence of charring or discoloration, which is caused by thermal degradation. This would infer that any chemical damage would primarily be caused by oxidation. However, the results from treatment in an argon atmosphere were very similar to those in a normal atmosphere, and could not have been produced due to oxidation. It was decided to investigate further and look for evidence of both oxidation and depolymerisation, in order to develop a more thorough understanding of the reactions taking place at the paper surface.

Shafizadeh[68,69], lists the appearance of free radicals and hydroperoxides, and the formation of carbonyl and carboxyl groups among the oxidation reactions of cellulose (see **1.4 The degradation of cellulose**). Daniels [90-92], has worked extensively with the Russell effect (see **1.5 Tests for the degradation of cellulose**), to detect signs of peroxide activity in oxidising materials, therefore it was decided to use his methods to detect possible peroxide activity on the laser treated paper. It was also decided to follow Eusman[98] and Dupont[103], who have both used methylene blue to act as a marker for regions of paper with increased levels of carboxyl groups. It was hoped that DRIFT spectroscopy could be employed to detect increases in the levels of both carbonyl and carboxyl groups[115,116].

The depolymerisation of cellulose and subsequent isomerisation of the glucose produced would result in its decomposition to form various sugars amongst other degradation products[68,69]. Oxidation of the cellulose would produce various uronic acids on subsequent depolymerisation and isomerisation. Dupont[139] has used GC/MS to investigate the

compounds present in the discoloration created at the wet/dry interface of water stained paper. Among the degradation compounds were sugars, as a sign of thermal depolymerisation, and uronic acids as a sign of oxidation, in laser treated paper.

4.3.1 Russell effect tests

The production of peroxides as a result of oxidation (Shafizadeh[68,69]) was tested for by means of the Russell effect (see section **2.5.1**) as described by Daniels[90-92], (see section **1.5 Tests for the degradation of cellulose**).

1. Russell effect after laser treatment using a pulse length range of 87 - >200 ns, normal atmosphere

Russell effect images were developed for laser treated, standard sized and size removed 'Roma' paper (Tables 43 & 44; **3.3.1**). The Russell effect test results were completely different for the two paper samples. The Russell image from the standard sized 'Roma' paper sample, created immediately after laser treatment, clearly showed a series of white lines where the laser had passed, for all fluences above 16 ± 5 Jcm^{-2} (Fig. 86a). One week later the Russell image showed black lines for fluences above 29 ± 9 Jcm^{-2}, (Fig. 86b). After two weeks the black lines were still in evidence albeit slightly paler, and it was not until four weeks had elapsed that all signs of the laser treatment disappeared.

The Russell image from the size removed 'Roma' paper sample, created immediately after laser treatment, clearly showed a series of black lines where the laser had passed, for all fluences above 24 ± 7 Jcm^{-2}, (Fig. 87a). Repeat tests one week later showed only faint black lines for fluences above 33 ± 10 Jcm^{-2}, (Fig. 87b). After two weeks there were no discernible laser treatment lines for the size removed sample.

The dark lines on the developed Russell images indicate an increased presence of peroxides in the laser treated regions of the paper samples (this has been shown by Eusman[98], section **1.5 Tests for the degradation of cellulose**). Laser treatment of both the standard sized and size removed 'Roma' resulted in increased levels of peroxides, although those in standard sized 'Roma' remained significantly longer. The white lines registered initially on the Russell image of standard sized 'Roma', are due to the removal of gelatin size (Figs. 47 & 48). The size is responsible for considerable production of peroxides. This is shown by the dark background coloration of the standard sized Russell images. On removal of the size the abundance of peroxides registered is temporarily decreased (Fig. 103).

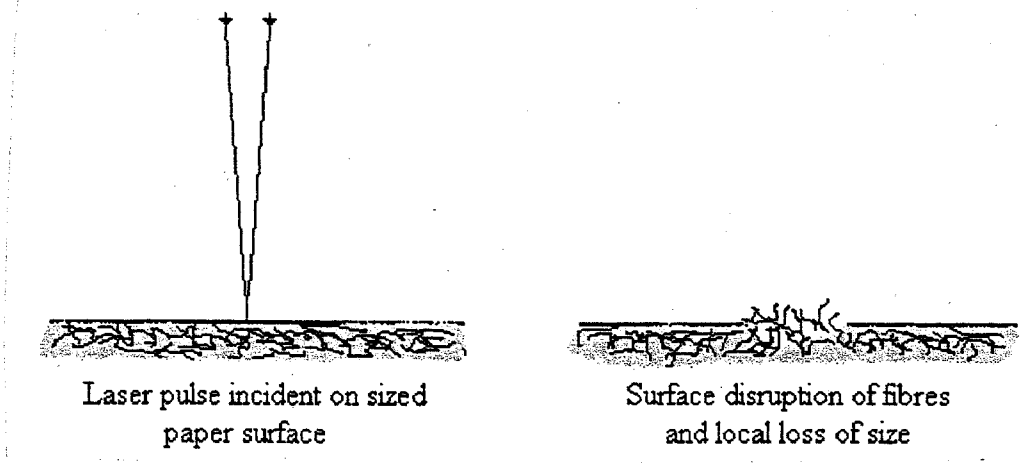

Figure 103. Diagram to illustrate the initial reduction in peroxide activity of laser treated standard sized 'Roma', as registered by the Russell effect test.

The Russell effect tests were repeated using paper samples scratched with a scalpel, (Table 45; section **3.3.1**). The results are very similar to those achieved using the laser (Tables 43 & 44), the creation of dark lines which gradually disappeared after a few weeks. This suggests that by disrupting the paper surface (using a scalpel or laser), un-oxidised material is exposed and auto-oxidation is accelerated. This suggestion is backed up by the results for microscopic comparison of ink removal techniques (section **3.1.3**), which showed that the laser caused less physical damage than mechanical ink removal methods.

There were no visible Russell images created on the Whatman filter paper sample by either laser treatment or scratching, which suggests that there is no significant thermal oxidation due to the laser, and no appreciable increase in the normal rate of auto-oxidation. These results suggest that the increased activity cannot be due to the cellulose alone. It is most likely that the increased activity is due to the exposure of un-oxidised gelatin. If this is the case it must be assumed that there was a residue of size left in the size removed paper. This could also explain why there was no discernible colour change to humid aged, laser treated Whatman filter paper, but a slight colour change to the aged size removed 'Roma'.

2. Russell effect after laser treatment using attenuated pulse lengths of 63, and 26 ns

Laser treatment of standard sized 'Roma' using an attenuated beam to produce shorter pulses produced a far weaker result. Initially white lines were seen on the Russell images (Figs 88a & 89a, Tables 46 & 47; section **3.3.1**). These white lines were still visible one week later albeit far weaker. It took two weeks before any dark lines were recorded (one faint line for each sample Figs. 88b & 89b), and these had disappeared by the third week. The creation of white lines suggests that the laser does react with some of the gelatin at the surface, thus reducing the amount of background peroxide activity. As no strong black lines developed within three weeks, the results suggest that there was a negligible increase in the local abundance of peroxides. This is probably due to the reduced surface damage recorded previously (**3.1.2**), resulting in less un-oxidised material being exposed for auto-oxidation.

3. Russell effect after laser treatment using a pulse length range 87 - >200 ns, argon atmosphere

Laser treatment of standard sized 'Roma' in an argon atmosphere, produced almost the same Russell effect as that witnessed in a normal atmosphere, (Fig. 90, Table 48; section **3.3.1**). Initially there were white lines, followed by dark lines, which remained for three weeks

before disappearing, which suggests there is little significance in the atmosphere used during laser treatment of paper.

4.3.2 Methylene blue tests

Methylene blue was used in this research to help qualitative detection of carboxyl groups on laser treated 'Roma' paper samples (section **2.5.2**). The dye was absorbed by both standard sized, and size removed 'Roma' reference samples, and coloured the paper blue. This is due to the presence of carboxylic acid groups (this has been shown by Eusman[98] and Dupot[103], section **1.5 Tests for the degradation of cellulose**), however the laser appears to have had a significant effect on the paper samples (Figs. 91 & 92), which clearly absorbed more methylene blue in the treated region. However, it was discovered that scratching the surface of paper samples prior to methylene blue immersion, also yielded a slight darkening.

The Whatman filter paper samples absorbed very little methylene blue, which indicates a limited presence of carboxylic acid groups. There was a very slight increase in the absorption of dye as a result of both laser treatment and scratching. This is an unexpected result because it suggests that by causing surface disruption either mechanically or by laser accelerates auto-oxidation and promotes the production of carboxyl groups, but the result from the Russell effect test inferred that surface damage of Whatman paper did not increase auto-oxidation. Therefore it may be that simply roughening the surface of paper promotes the absorption of methylene blue.

Laser treatment of standard sized 'Roma' using an attenuated beam to produce shorter pulses caused no visible change in the amount of methylene blue absorption for the sample prepared using 63 ns laser pulses, but the sample prepared using 26 ns laser pulses, absorbed less methylene blue in the laser treated region creating a light coloured square (Fig. 93).

The lightening is due to the partial removal of gelatin through interaction with the laser (see Fig. 55). If the surface layer of gelatin is partially removed, the absorption of dye will not be as strong in that region, and this coupled with the reduced level of surface damage (compared to long pulse treatments) results in a paler appearance. The white square is not witnessed by long laser pulse treatment of 'Roma' (which completely removes gelatin, Fig. 48), due to the increased roughening of the surface, which seems to promote absorption of the dye.

Samples prepared in an argon environment, also absorbed less methylene blue in the laser treated region creating a light coloured square (Fig. 94). As with the short pulse treatments, the samples prepared in an argon atmosphere only partially remove the gelatin size (see Fig. 59), and cause less surface damage than treatment in a normal atmosphere.

4.3.3 DRIFT Spectroscopy

Neither the Russell effect tests, nor the methylene blue tests had been able to provide compelling evidence to suggest strong oxidation of the cellulose during laser treatment of 'Roma' paper. It was hoped that Diffuse Reflectance Infrared Fourier Transform (DRIFT) spectroscopy could be used to positively identify the presence of any carbonyl and/or carboxyl groups produced by thermal oxidation (see section **3.3.3**).

There was very little variation between the DRIFT spectrum of standard sized 'Roma', the spectrum of size removed 'Roma', and their laser treated equivalents (Fig. 95). The difference between the various spectra could only be assessed by subtraction of one spectra from another (see section **2.5.3**).

By subtracting the spectrum of size removed 'Roma' (B), from standard sized 'Roma' (A), the subtle difference between the two was observed (Fig. 96, Table 49; section **3.3.3**).

Individual peaks were not resolvable however, this spectrum has essentially the same absorption peaks as Figure 97, the spectrum of gelatin (Table 50). This result serves as an illustration of how subtle local differences in functional groups on the surface of a material can be detected by subtraction of one spectrum from another.

The rationale for this method of studying the spectra, was that by subtracting the reference spectrum from the laser treated equivalent, for a particular paper sample, the difference between the spectra would be attributable to chemical change brought about by laser treatment.

Unfortunately the 'difference' spectra did not produce particularly useful results. When the laser treated, standard sized spectrum (C) was subtracted from its untreated reference (A) the result was a spectrum (Fig. 98) resembling that of gelatin (Fig. 97). It seemed that the only change detected by DRIFT spectroscopy was that the laser treatment had removed the gelatin. Hence no further tests were carried out on short pulses, or differing atmospheres since the same result would have been achieved.

Subtraction of the size removed reference spectrum (B), and the Whatman filter paper (E), from their laser treated equivalents (D & F), did not produce any resolvable peaks.

FTIR analysis of the three paper sample types (standard sized and size removed 'Roma', and Whatman No 1 filter paper) was repeated using paper freshly reduced by immersion in sodium borohydride solution (section **2.5.4**), however no identifiable peaks were recorded from the difference spectra.

The results from the investigation into oxidation of laser treated paper show,

1) Whatman filter paper appeared to be unaffected as a result of laser treatment. The Russell effect test did not indicate any oxidation had occurred, and there was no significant impact on the ageing properties of the paper. The positive result from the methylene blue is probably due to the disruption of the paper surface.

2) size removed 'Roma' cotton paper appeared to suffer some oxidation of the cellulose due to laser treatment. The Russell effect test indicated increased peroxide activity, and the humid ageing studies showed a slight increase in the local discoloration of the laser treated regions the (section **3.2.1**). The size removed 'Roma' ought to produce the same result as laser treatment to Whatman filter paper given that they are both size, and acid free, pure cellulose. It was assumed therefore that there may have been a residual amount of size left in the size removed 'Roma', which was responsible for the results obtained. The positive result from the methylene blue is probably mostly due to the disruption of the paper surface.

3) standard sized 'Roma' cotton paper appeared to suffer considerably more oxidation due to laser treatment, than the size removed equivalent. The Russell effect test indicated increased peroxide activity, and considerable discoloration was noticeable after accelerated ageing. FTIR ought to have shown any significant increase in oxidation of cellulose, however the loss of peaks attributable to gelatin tended to overshadow the creation of others due to oxidation reactions. The positive result from the methylene blue is probably due to the disruption of the paper surface.

4) the signs of oxidation of standard sized 'Roma' paper were significantly reduced by shortening the laser pulses from 87 ns to 26 ns. The Russell effect test did indicate increased peroxide activity, however the level of activity more closely resembled that witnessed using the size removed paper. The humid ageing studies showed only a slight local discoloration to laser treated regions, reminiscent of the aged size removed samples.

5) the level of oxidation suffered by paper during or after laser treatment is independent of the atmosphere used during treatment.

The results indicate that the level of oxidation depends on the pulse duration, and presence (and quantity) of size within the paper. This inference is supported by the work of Kolar[43], who has found that use of a Nd:YAG laser (1064 nm, 1.5 Jcm^{-2}) with a pulse duration of 6 ns, does not create discernible changes to the spectra of Whatman filter or gelatin sized papers in the 730 – 550 cm^{-1} region. She also found that humid ageing the laser treated samples (90° C, 50% RH for 28 days), caused only 0.7% reduction in reflectance (457 nm) for the gelatin sized sample and an increase in brightness for the Whatman paper.

It became clear from the results obtained during this research programme, that pure cellulose is not oxidised by laser treatment, and even the standard sized 'Roma' paper is not oxidised sufficiently to discolour to the extent witnessed after humid ageing. Therefore the thermal degradation responsible for the colour change must be produced via an alternative mechanism.

4.3.4 GC/MS analysis

Daniels[66] has discussed the tendency of certain food products to turn brown with age, due to a reaction between gelatin and sugars (products of natural ageing), and suggests this as a reason for the discoloration of many gelatin sized papers. Shafizadeh[68,69], has shown that between 300-340°C cellulose depolymerises to form a variety of sugar related products (Fig.12; section **1.4 The degradation of cellulose**). Therefore sugars produced in paper via Nd:YAG laser treatment could accelerate the discoloration by reaction with the gelatin size.

Samples of humid aged, laser treated, sized and size removed 'Roma' paper were extracted and analysed using GC/MS to help identify the products of laser treatment (see section **2.5.5**). The chromatograms for the standard sized sample (Fig. 102, Table 53; section **3.3.5**), show;

1) the disappearance of disaccharide peaks (maltose) after laser treatment. This suggests thermal decomposition of the cellulose molecule as described by Shafizadeh[68,69].
2) a significant increase in the abundance of mannonic acid after laser treatment. This suggests oxidation of mannose to produce the carboxylic acid (Fig. 8).

The chromatograms for the size removed sample (Fig. 103, Table 54; section **3.3.5**), show;

1) significant increases in the abundance of galactofuranose and glucopyranose after laser treatment. This suggests thermal decomposition of the cellulose molecule as described by Shafizadeh[68,69].
2) a slight increase in the abundance of mannonic acid after laser treatment. This suggests oxidation of mannose to produce the carboxylic acid (Fig. 8).

The results from GC analysis of both the sized, and size removed samples suggest that laser treatment of 'Roma' paper causes thermal degradation resulting in depolymeristion of

cellulose followed by oxidation. These reactions are more prevalent where gelatin size is present.

The GC analysis suggested that the degradation of paper, is primarily due to depolymerisation. This is supported by the results of the chemical tests in an argon atmosphere. Humid ageing the 'Roma' paper, laser treated in an argon atmosphere, produced a similar result to that achieved in a normal atmosphere, a brown discoloration to the treated region. This infers that the reaction is not atmosphere dependent and is therefore not oxidation.

The Russell effect test on samples prepared in an argon atmosphere produced more or less the same result as those witnessed in a normal environment, which leads to the conclusion that the peroxide activity recorded is due to an increased rate of auto-oxidation brought about by the exposure of un-oxidised gelatin.

Methylene blue tests on samples prepared in an argon environment produced a curious result in which less dye was absorbed, which illustrates that oxidation had not occurred in this instance. The interesting point about this result is that it is very similar to that achieved using samples produced in a normal atmosphere, but with short pulse lengths (26 ns). This of course does not prove that there was no oxidation to these latter samples, but the similarity of result does provide a strong suggestion that the level of oxidation is not significant.

CHAPTER 5:

SUMMARY OF RESEARCH AND RECOMMENDATIONS FOR FUTURE STUDIES

5.1 Summary of research

The aims of the research programme were:-

i) to investigate the ability of the Nd:YAG (1064 nm) laser for the removal of modern ink from paper and establish damage thresholds.

ii) to investigate possible physical and chemical damage to paper as a result of Nd:YAG laser treatment.

iii) to explore methods of improving the efficiency of ink removal, and the reduction of damage during treatment.

The work carried out in this study has established that the Nd:YAG (1064 nm) laser will satisfactorily remove ink from some papers with fairly long pulse lengths (87 ns), although this does cause both physical and chemical change to gelatin sized paper. Size free paper such as Whatman filter paper suffers some physical damage, but remains unaffected chemically. The physical damage, which visibly takes the form of fibre disruption, is most severe for heavily sized papers, however size free papers also suffer from fibre disruption. This damage could possibly be due to the ejection of steam due to the vaporisation of water as suggested by several researchers [2,26,31,32,33,57], however this theory is speculative. The presence of gelatin appears to increase energy absorption, producing a more violent reaction. Ink removal thresholds were significantly reduced by shortening the pulse length, but were relatively unaffected by changing the atmosphere to argon. However the surface damage appeared to be reduced by the use of shorter pulse lengths (26 ns), and treatment in a dry atmosphere such as argon. It has not been established whether further improvement could be made by use of short pulse lengths in a dry atmosphere.

The preliminary tests (using 87 ns pulses) suggested that ink removal from cotton papers was more successful than from wood-pulp papers, and that the removal of viscous ink such as ball-point pen ink was more successful than the removal of inks which flowed more freely

such as fibre tipped pen inks or highlighters. The investigation did establish that the fluence required for ink removal depended on the paper type, the ink type and the colour of ink. It also established that damage to un-inked regions of paper occurred at ink removal threshold fluences. In this respect the process cannot be considered self-limiting, and clearly each cleaning treatment would have to be carefully controlled. For each new treatment it is recommended that the laser be operated using short pulse lengths, and the fluence increased slowly until ink removal is observed. Because the threshold for damage to un-inked paper seems to be the same as the ink removal threshold, it is considered prudent to create a shield, or mask, around the ink to be removed, to prevent unnecessary damage to the surrounding paper fibres.

Physical testing of laser treated blank 'Roma' paper (41 ± 12 Jcm^{-2}, 87 ns, spot diameter 250 ± 36 μm) showed no discernible loss of tensile strength although the paper tended to tear at laser treatment sites at, or above the ink removal threshold. After accelerated ageing the tendency to tear at laser treatment sites was even more prevalent, which infers a decrease in the degree of polymerisation (DP). SEM studies of the broken fibres from the fracture sites show the fibres from the laser treated regions to be considerably more blunt than those from untreated regions. The bluntness suggests an increase in crystallinity (and decrease in DP), which is generally caused by thermal degradation[87,88].

Tensile testing was not carried out using pulses shorter than 87 ns as it was considered that the results would prove too subtle to meaningfully record. It was anticipated that the use of short laser pulses ought to lessen any reduction in DP. Indeed the research of Kolar[43], who used much shorter laser pulse lengths on cellulose, actually showed an increase in the DP when using 6 ns pulses. The ideal result as far as treatment of artwork is concerned, would be a choice of pulse length that caused no change to the DP.

Chemical testing (using the Russell effect, and methylene blue) of laser treated blank 'Roma' paper (41 ± 12 Jcm^{-2}, 87 ns, spot diameter 250 ± 36 μm), suggested that the treatment did not create many carbonyl and/or carboxyl groups via direct oxidation, however the disruption to the paper surface did cause an acceleration to the rate of auto-oxidation of the cellulose. By operating in an argon atmosphere, or by shortening the pulse length (26 ns) the recorded increase in the rate of auto-oxidation was significantly reduced due to reduced levels of surface damage to the paper.

Humid ageing laser treated Whatman filter paper did not cause any discernible colour change to the laser treated areas, however similar treatment of 'Roma' which has a gelatin size caused significant local discoloration to the treated regions. This is considered to be due to reaction between gelatin, and sugars created by thermal depolymerisation of cellulose during laser treatment. An increased presence of sugars in laser treated 'Roma' was confirmed by GC/MS. Therefore the extent to which a paper will discolour after laser treatment, appears to depend on the level of size within the paper, and the amount of sugars created during the treatment. For treatment of artworks it is not practical to remove or reduce the size, however by using short laser pulses, the depolymerisation of cellulose (and hence production of sugars) should be reduced. This has yet to be confirmed using GC/MS, however the results from humid ageing (where considerably less discoloration was observed) suggest that less thermal degradation is caused using short (26 ns) pulses.

The general conclusion from this research programme is that the Q-switched Nd:YAG laser (1064 nm) does offer a practical alternative to the current methods of ink removal from artworks on paper (scalpel and eraser), as the level of damage is reduced and less spread. However the cost of such a laser would be a considerable disincentive unless further conservation uses could be found. It must also be stressed that considerable care be exercised in determining the least fluence required for ink removal to prevent unnecessary damage. The

main concerns with laser treatment of paper are the physical disruption of the surface, and general weakening through thermal degradation.

It has been shown that the majority of chemical damage occurs via depolymerisation of the cellulose to produce sugars, but that the level of chemical damage can be controlled, by shortening the pulse length (increasing peak power), thus reducing the average fluence required to perform treatments. However as discussed previously Kolar[43], found an increase in the DP of cellulose, due to cross-linking during very short pulse length (6 ns) laser treatment on paper. Optimistically, there may be an optimum pulse length (not yet determined) from which to safely operate on paper, that causes minimal de-polymerisation and minimal cross-linking.

It may be possible to reduce the risk of thermal degradation by slowing the pulse repetition rate. The pulse rate used for this research was 10 Hz, but unfortunately the only slower option available was single shot mode, which would not have been practical at the start of the programme. However observation of the interaction between the laser and ink/paper shows that ink removal, size removal and damage sustained all occur within the first two or three pulses. It was found that after the initial reaction had occurred, no further reaction took place or damage sustained with the laser pulsing continuously in the same spot. It may therefore be possible to remove ink with one pulse and avoid the reaction with size and water.

On the basis of the results obtained the optimum operating parameters for this laser would include a dry atmosphere and as short a pulse length as possible, although it must be pointed out that these results were achieved using blank paper and the effect of the interaction between the laser and the ink, has not been established. A black ball-point pen ink might be expected to absorb more infra-red radiation than a pale paper surface, and have an affect over a wide area. The photographs taken during the microscopic analysis of surface damage Figs.

38 -58, certainly suggest that the surface of paper affected by the laser treatment (400-450 microns) is considerably in excess of the measured laser spot diameter (250 ± 36 microns). However Figs 42, 49, 52 &56 all suggest that the width of surface damage remains constant whether ink is present or not. This infers that the size of plasma plume is the same for an inked surface as for an un-inked surface. Although we must assume the presence of gelatin size is largely responsible for the creation of the plasma plume on the un-inked samples. The possibility of reaction between the ink and paper during cleaning has yet to be investigated. However there did not appear to be any immediate discoloration or charring after the removal of ink from the cotton papers tested (see section **3.1.1**). Analysis of such reactions would require more sensitive tests than the ones used in this research to detect oxidation, however, GC/MS may prove far more versatile in identifying reaction products.

The discoloration of the treated samples after ageing is a major concern, however if the cause of the discoloration lies primarily with soluble degradation products derived from sugars then this problem could be alleviated by washing in water, which would remove a large proportion of the monosaccharides. Washing in water is a standard course of treatment for paper conservation and would not constitute a problem.

This research programme has been concerned with the removal of ink lines from paper and as such it has been convenient to operate with a focused laser where considerable control could be maintained, however using an un-focused spot size (typically 5-8 mm in diameter) could pose serious problems with the unintentional removal of ink or pigment. Use of the un-focused laser may well be a situation, which could benefit from single pulse mode operation.

5.2 Recommendations for future studies

Further research involving the GC analysis of extracts from recently laser treated 'Roma', is recommended in order to gain more understanding of the oxidising and depolymerising effect the laser has on cellulose. The study of size removed 'Roma', and Whatman No 1 filter paper should give a clearer picture of the reactions taking place on cellulose, however it is important not to forget that most art papers contain significant amounts of sizing agent. This research programme has shown that the chemical reactivity of 'Roma' paper with the Nd:YAG laser, is considerably greater when the paper contains gelatin size.

The use of short laser pulse lengths certainly reduced the physical disruption of the fibres and appeared to cause significantly less chemical damage. Comparison of FTIR spectra of long, and short pulse, laser damage to 'Roma' paper may help to clarify questions over the level of oxidation caused by laser treatment. It is recommended that only un-sized samples be analysed as the absorption peaks of the size tend to mask any subtle changes in the spectrum. There was no significant change in colour to samples that were prepared using short pulse lengths before humid ageing. This suggests that the depolymerisation of cellulose, witnessed using long length pulses, does not occur with the shorter pulse.

One form of analysis not available to this research programme was the study of gaseous emissions during laser treatment. GC/MS analysis of the emissions produced by laser induced pyrolysis of wood[141], and proteins[158] have proved extremely useful in understanding the breakdown reactions. This form of analysis may well prove most useful for the study of degradation products due to short pulse treatments. With short pulses the energy is delivered to the target much faster, possibly causing the target to vaporize rapidly, and consequently many of the degradation products are lost as gas.

'Roma' is a good quality cotton paper, manufactured fairly recently and showing little sign of degradation, however most of the works of art requiring conservation would be at least 50 years old and show evidence of considerable oxidation and hydrolysis. To gain a truer understanding of the likely effect of the YAG laser on real artworks it would be necessary to repeat some of the tests carried out in this programme on some naturally aged paper samples.

This research has concentrated solely on the use of infra-red radiation, however it may be that visible light or ultra-violet light offer a less degrading alternative. Visible and ultra-violet radiation sources were avoided for this research due to the known damaging effect of ultra-violet radiation on a wide range of paper[36-40], and the susceptibility of certain papers to photo-oxidation on exposure to visible light[41]. However the initial results achieved by Kautek[31-33] on parchment, and Freiberg[34-36] on paper, suggest that excimer lasers achieve the cleaning of paper with less physical damage than the infra-red equivalent. The usefulness of excimer lasers to paper conservation would largely depend on the results from chemical analysis of treated papers. If the laser could be operated to specifically remove ink, mould or dirt without interacting with the paper substrate then there could be real future for excimer laser treatments.

Visible light laser radiation has received less attention than infra-red and ultra-violet for use in paper cleaning treatments, but in theory should tend to produce less thermal degradation than infra-red sources, and less photo-oxidation than ultra-violet. This theory however has yet to be tested practically.

REFERENCES

1. Watkins, K.G. A review of materials interaction during laser cleaning in art restoration. International Conference on Lasers in the Conservation of Artworks, 1996. Restauratorenblatter, Sonderband. Lacona I, Kautek, W. and Konig, E. (eds.), Mayer & Comp., Wien, 1997, p. 7-16.

2. Larson, J. Current developments in the application of laser technology to the treatment and recording of artworks. Conservation News, 53, 1994, p. 13-14.

3. Asmus, J.F. et al. Holography in the conservation of statuary. Studies in Conservation, 18, 1973, p. 49-63.

4. Asmus, J.F. et al. Surface morphology of laser-cleaned stone. Lithoclastia, 1, 1976, p. 23-46.

5. Asmus, J.F. Properties of laser-cleaned Carrara marble surfaces. Geological Society of America, 1978, p. 81-88.

6. Asmus, J.F. More light to art conservation. Circuits and Devices Magazine, 2, 1986, p. 6-14.

7. Cooper, M. Laser Cleaning in Conservation, Butterworth Heinmann, 1998.

8. Cooper, M. and Larson, J. The use of laser cleaning to preserve patina on marble sculpture. The Conservator, 20, 1996, p. 28-36.

9. Teppo, E. and Calcagno, G. Restoration with lasers halts decay of ancient artefacts. Laser Focus World, June, 1995, p. 55-59.

10. Salimbeni, S. et al. Control of the mechanical effects induced by laser cleaning of stones: Dependence on the laser pulse duration. 2nd. International Conference on Lasers in the Conservation of Artworks, 1997. Restauratorenblatter, Sonderband. Lacona II, Kautek, W. and Konig, E. (eds.), in press.

11. Maravelaki, P.V. et al. Diagnostic techniques for laser cleaning of marble. International Conference on Lasers in the Conservation of Artworks, 1996. Restauratorenblatter, Sonderband. Lacona I, Kautek, W. and Konig, E. (eds.), Mayer & Comp., Wien, 1997, p. 31-36.

12. Wiedemann, G. Experiences in the removal of thin layers and in the cleaning of artworks by means of Nd:YAG pulse laser. International Conference on Lasers in the Conservation of Artworks, 1996. Restauratorenblatter, Sonderband. Lacona I, Kautek, W. and Konig, E. (eds.), Mayer & Comp., Wien, 1997, p. 45-50.

13. Weeks, C. Laser cleaning at Amiens Cathedral. Conservation News, 58, 1995, p. 67-69.

14. Verges-Belmin, V. Comparison of three cleaning methods - microsandblasting, chemical pads and Q-switched YAG laser - on the portal of the cathedral Notre-Dame in Paris, France. International Conference on Lasers in the Conservation of Artworks, 1996. Restauratorenblatter, Sonderband. Lacona I, Kautek, W. and Konig, E. (eds.), Mayer & Comp., Wien, 1997, p. 17-24.

15. Calcagno, G. et al. Laser based cleaning on stonework at St. Stephan's cathedral, Vienna. International Conference on Lasers in the Conservation of Artworks, 1996. Restauratorenblatter, Sonderband. Lacona I, Kautek, W. and Konig, E. (eds.), Mayer & Comp., Wien, 1997, p. 39-44.

16. Shekede, L. Lasers; a preliminary study of their potential for the cleaning and uncovering of wallpaintings. International Conference on Lasers in the Conservation of Artworks, 1996. Restauratorenblatter, Sonderband. Lacona I, Kautek, W. and Konig, E. (eds.), Mayer & Comp., Wien, 1997, p. 51-56.

17. Krarup, T. and Nimmrichter, J. Laserstrahlen auf polychromen steinoberflachen. Versuche zur restaurierung des 'Riesentors'. Restauro, 6, 1998, p. 404-409.

18. Sportun, S. The cleaning of parchment with the Nd:YAG laser. 2nd. International Conference on Lasers in the Conservation of Artworks, 1997. Restauratorenblatter, Sonderband. Lacona II, Kautek, W. and Konig, E. (eds.), in press.

19. Heinrich, P. Ein eiserner byzantinischer ringkettenpanzer. Lasereinsatz bei archaeologischem kulturgut. Restauro, 6, 1998, p. 383-387.

20. Hartmann, B. and Wiedemann, G. Aufsatzsekretar mit muscheldekor aus dem stadtmuseum Koln. Die reinigung von mollusken mittels impulslaser. Restauro, 6, 1998, p. 388-393.

21. Reichert, U. Reinigungsversuche an textilien mittels lasertechnik. Restauro, 6, 1998, p. 416-420.

22. Conrad, W. et al. Freilegungvon Grunpatina mit dem laserstrahl. Die bronzebuste des Johannes Bugenhagen in Lutherstadt- Wittenberg. Restauro, 6, 1998, p. 422-428.

23. Szczepanowska, H.M. and Moomaw, W.R. Laser stain removal of fungus-induced stains from paper. Journal of the American Institute for Conservation, 33, 1994, p. 25-32.

24. Kearns, A. et al. The effect of wavelength in Nd:YAG laser cleaning. 2nd. International Conference on Lasers in the Conservation of Artworks, 1997. Restauratorenblatter, Sonderband. Lacona II, Kautek, W. and Konig, E. (eds.), in press.

25. Fotakis, C. Lasers for art's sake! Optics and Photonics News, 6, 1995, p. 30-35.

26. Fotakis, C. et al. Laser applications in painting conservation. International Conference on Lasers in the Conservation of Artworks, 1996. Restauratorenblatter, Sonderband. Lacona I, Kautek, W. and Konig, E. (eds.), Mayer & Comp., Wien, 1997, p. 57-60.

27. Fotakis, C. et al. Laser technology in art conservation. OSA Trends in Optics and Photonics Series, Optical Society of America, Washington, D.C. 9, 1997, p. 99-104.

28. Fotakis, C. et al. Lasers in art conservation in Bradley, S. (ed.) Interface between Science and Art Conservation, British Museum. Occasional paper No. 116, 1998, p. 83-87.

29. Hontzopoulos, E. et al. Excimer laser in art restoration in Fotakis C. (ed.) SPIE, The International Society of Optical Engineering, 1810, Bellingham, Washington, 1992, p. 749.

30. Heilein, K. Uberzuge auf empfindlichen malschichten. Untersuchungen zum abtragen mit unterschiedlichen lasergraten. Restauro, 6, 1998, p. 410-415.

31. Kautek, W. et al. Laser cleaning of ancient parchments. International Conference on Lasers in the Conservation of Artworks, 1996. Restauratorenblatter, Sonderband. Lacona I, Kautek, W. and Konig, E. (eds.), Mayer & Comp., Wien, 1997, p. 69-78.

32. Kautek, W. et al. Progress in cleaning of 15th. century parchments. 2nd. International Conference on Lasers in the Conservation of Artworks, 1997. Restauratorenblatter, Sonderband. Lacona II, Kautek, W. and Konig, E. (eds.), in press.

33. Kautek, W. et al. Laserreinigung von pergament und papier. Experimente an modellsystemen und historischen originalen. Restauro, 6, 1998, p. 396-402.

34. Friberg, T.R. et al. Removal of fungi and stains from paper substrates using laser cleaning stategies. International Conference on Lasers in the Conservation of Artworks, 1996. Restauratorenblatter, Sonderband. Lacona I, Kautek, W. and Konig, E. (eds.), Mayer & Comp., Wien, 1997, p. 79-83.

35. Friberg, T.R. et al. Excimer removal of mould from paper: Sterilisation and environmental considerations. 2nd. International Conference on Lasers in the Conservation of Artworks, 1997. Restauratorenblatter, Sonderband. Lacona II, Kautek, W. and Konig, E. (eds.), in press.

36. Hon, D.N-S. Yellowing of modern papers. Preservation of Paper and Textiles of Historic and Artistic Value II, Advances in Chemistry Series 193, American Chemical Society,Washington D.C. 1981, p. 119-41.

37. Hon, D.N-S. Discoloration and deterioration of modern papers. Technology in the Science of Conservation. Proceedings of the IIC Congress, 1982, p. 89-92.

38. Mills, J.S. and White, R. The Organic chemistry of Museum Objects, Butterworth Heinemann, 1987.

39. Phillips, G.O. and Jett, A. Photochemistry and radiation chemistry of cellulose in Nevell, T.P.and Zeronian, S.H. (eds.) Cellulose Chemistry and its applications, Ellis Horwood Ltd. 1985, p. 290-311.

40. Brill, T.B. Light: its interaction with art and antiquities, Plenum Press, N.Y. 1980.

41. Lee, S.B. et al. Damaging effects of visible and near- ultraviolet radiation on paper. 19th. Meeting of the American Chemical Society L.A. September, 1988, Historic Textile and Paper Materials II: Conservation and Characterisation, 1989, p. 54-62.

42. Private communication with A. Loton, Product Manager, Laser Division, Hodge Clemco Ltd. Sheffield.Feb 1995.

43. Kolar, J. et al. The effect of Nd:YAG laser radiation at 1064 nm on paper. Restaurator, 2000, p.9-18.

44. Hecht, J. The Laser Guidebook. McGraw Hill, 1986.

45. Crafter, R.C. An introduction to lasers in Crafter, R.C. and Oakley, P.J. (eds.), Laser Processing in Manufacturing, Chapman and Hall, 1993, p. 1-18.

46. Luxon, J.T. and Parker, D.E. Industrial Lasers and their Applications, Prentice Hall Inc. 1992.

47. Hecht, J. The Laser Guidebook. McGraw Hill, 1986.

48. Crafter, R.C. and Oakley, P. J. Background to laser processing in Crafter, R.C. and Oakley, P.J. (eds.), Laser Processing in Manufacturing, Chapman and Hall, 1993, p. 19-44.

49. Weedon, M.W. Pulsed Nd:YAG lasers in manufacturing applications in Crafter, R.C. and Oakley, P.J. (eds.), Laser Processing in Manufacturing, Chapman and Hall, 1993, p. 67-90.

50. May, A.B. Continuous wave and pulsed Q-switched Nd:YAG lasers in Crafter, R.C. and Oakley, P.J. (eds.), Laser Processing in Manufacturing, Chapman and Hall, 1993, p. 91-114.

51. Williams, C. CO_2 industrial laser systems and applications in Crafter, R.C. and Oakley, P.J. (eds.), Laser Processing in Manufacturing, Chapman and Hall, 1993, p. 141-162.

52. Gower, M.C. Excimer lasers: principles of operation and equipment in Crafter, R.C. and Oakley, P.J. (eds.), Laser Processing in Manufacturing, Chapman and Hall, 1993, p. 163-188.

53. Gower, M.C. Excimer lasers: current and future applications in industry and medicine in Crafter, R.C. and Oakley, P.J. (eds.), Laser Processing in Manufacturing, Chapman and Hall, 1993, p. 163-188.

54. Ready, J.F. Effects of High-Power Laser Radiation, New York: Academic Press, 1971, p. 67-124.

55. Kogelnik, H. and Li, T. Laser beams and resonators, Applied Optics, 5, 1966, p. 1550-67.

56. Wilson, J. and Hawkes, J.F.B. Laser Principles and Applications, Prentice Hall International, 1987.

57. Tam, A.C. et al. Laser-cleaning techniques for removal of surface particulates. Journal of Applied Physics, 71, 7, 1992, p. 3515-3523.

58. Hill, J.M. and Dewynne, J.N. Heat Conduction, Blackwell Scientific Publications, 1987.

59. Dodd, J.W. and Tonge, K.H. Thermal Methods. Analytical Chemistry by Open Learning, J. Wiley & Sons. 1987.

60. Hunter, D. Papermaking. Dover, 1978.

61. Nevell T.P.and Zeronian, S.H. Cellulose chemistry fundamentals in Nevell T.P.and Zeronian, S.H. (eds.) Cellulose Chemistry and its applications, Ellis Horwood Ltd. 1985, p. 1-29.

62. Gettens, R.J. and Stout, G.L. Painting Materials. Dover, 1966, p. 114.

63. Mark, H.F. et al (eds.) Encyclopaedia of Polymer Science and Technology, (9), Interscience Publishers N.Y. London Sydney 1965, p. 740-741.

64. Nevell, T.P. Degradation of cellulose by acids, alkalis, and mechanical means in Nevell, T.P.and Zeronian, S.H. (eds.) Cellulose Chemistry and its applications, Ellis Horwood Ltd. 1985, p. 223-242.

65. Nevell, T.P. Oxidation of cellulose in Nevell, T.P.and Zeronian, S.H. (eds.) Cellulose Chemistry and its applications, Ellis Horwood Ltd. 1985, p. 243-265.

66. Daniels, V. The discolouration of paper on ageing. The Institute of Paper Conservation,Conference Papers, Oxford 1986, Leigh: IPC, 1988, p. 93-100.

67. Lewin, M. The yellowing of cotton cellulose pt. II & III. Textile Restoration Journal, 1965, p. 935-42 and 979-86.

68. Shafizadeh, F. Thermal degradation of cellulose in Nevell, T.P.and Zeronian, S.H. (eds.) Cellulose Chemistry and its applications, Ellis Horwood Ltd. 1985, p. 266-289.

69. Shafizadeh, F. Pyrolysis and combustion of cellulosic materials in Wolfrom, M.L. and Tipson, R.S. (eds.) Advances in Carbohydrate Chemistry, 23, Academic Press N.Y. and London 1968, p. 419-465.

70. Nevell, T.P.and Zeronian, S.H. Cellulose chemistry fundamentals in Nevell, T.P.and Zeronian, S.H. (eds.) Cellulose Chemistry and its applications, Ellis Horwood Ltd. 1985, p. 25.

71. Whitmore, P.M. and Bogaard, J. Determination of the cellulose scission route in the hydrolytic and oxidative degradation of paper. Restaurator, 15, 1994, p. 26-45.

72. Whitmore, P.M. and Bogaard, J. The effect of oxidation on the subsequent oven aging of filter paper. Restaurator, 16, 1995, p. 10-30.

73. Ranby, B.G. 'Weak links' in polysaccharide chains as related to modified groups. Journal of Polymer Science, 53, 1961, p. 131-40.

74. Whistler, R.L. (ed.) Methods in Carbohydrate Chemistry, (3), Academic Press N.Y. and London 1963.

75. Mark, H.F. et al (eds.) Encyclopaedia of Polymer Science and Technology, (3), Interscience Publishers N.Y. London Sydney 1965, p. 226-229.

76. Martin, A.F. Tests for cellulose and its derivatives in Ott, E. et al (eds.) Cellulose and Cellulose Derivatives, Interscience Publishers N.Y. London 1955, p. 1357-1396.

77. Clark, J. Properties and treatment of pulp for paper in Ott, E. et al (eds.) Cellulose and Cellulose Derivatives, Interscience Publishers N.Y. London 1955, p. 621-672.

78. Test for intrinsic viscosity of cellulose, ASTM, D 1795-60T, American Society for Testing Materials, Philadelphia 1960.

79. Test for cellulose chain length uniformity, ASTM, D 1716-60T, American Society for Testing Materials, Philadelphia 1960.

80. Evans, R. et al. Molecular weight distribution of cellulose as its tricarbanilate by High Performance Size Exclusion Chromatography. Journal of Applied Polymer Science, 37, 1989, p. 3291-3303.

81. Lloyd, L.L et al. Cellulose molecular weights by GPC/LiCl-DMAC solvent system. Chromatography and Analysis, April, 1991, p. 11-13.

82. Burgess, H. Gel Permeation Chromatography in investigating the degradation of cellulose during conservation bleaching. IIC Washington Congress, September, 1982,(Pre-prints), International Institute for Conservation.

83. Tensile breaking strength of paper and paperboard, Tappi, T404 m-50.

84. Bursting strength of paper, Tappi, T403 m-52.

85 Folding endurance of paper, Tappi, T423.

86. Tensile breaking properties of paper and paperboard (using constant rate of elongation apparatus), Tappi, T494om-88.

87. Berry, S.P. et al. Reinforcing degraded textiles in Williams, J.C. (ed.) Preservation of Paper and Textiles of Historic and Artistic Value, American Chemical Society Advances in Chemistry Series 164,Washington, D.C., 1977, p. 228-248.

88. Hearle, J.W.S. and Sparrow, J.T. The fractography of cotton fibers. Textile Research Journal, 41, 1971, p. 736-749.

89. Kolar, J. Mechanism of autoxidative degradation of cellulose. Restaurator, 18, 1997, p. 163- 217.

90. Daniels, V. The Russell Effect. Studies in Conservation, 29, 1984, p. 57-62.

91. Daniels, V. A photographic method for detecting the oxidation of materials. ICOM 7th. Triennial Meeting ,Copenhagen, 1984, Preprints p. 84.1.51-53.

92. Daniels, V. Monitoring the auto-oxidation of paper using photographic materials in Needles, H.L. and Zeronian, S.H. (eds.) Historic Textile and Paper Materials, Advances in Chemistry Series 212, American Chemical Society ,Washington, D.C. 1986. p. 318-327.

93. Russell, W.J. On the action exerted by certain metals and other sudstances on a photographic plate. Proceedings of the Royal Society, 61, 1897, p. 424-433.

94. Russell, W.J. On the action of wood on a photographic plate in the dark. Proceedings of the Royal Society, 74, 1904, p. 131-134.

95. Russell, W.J. The action of plants on a photographic plate in the dark. Proceedings of the Royal Society B, 78, 1906, p. 386-390.

96. Russell, W.J. On hydrogen peroxide as the active agent in producing pictures on a photographic plate in the dark. Proceedings of the Royal Society, 64, 1899, p. 409-419.

97. Clifford, R.D. Detection of certain chemical species using a photographic technique. Chemistry and Industry, 1975, p. 925.

98. Eusman, E. Tideline formation in paper objects: cellulose degradation at the wet-dry boundary. Conservation Research 1995. Studies in the History of Art, 51, National Gallery of Art, Washington, 1995, p. 11-27.

99. Lomax. S.Q. Analysis of peroxides. Scientific Research Department, National Gallery of Art, Washington, May 1993.

100. Lomax. S.Q. Analysis of tidelines. Scientific Research Department, National Gallery of Art, Washington, September 1993.

101. Davidson, G.F. The acidic properties of cotton cellulose and derived oxycelluloses. Part II The absorption of methylene blue. Journal of the Textile Institute, 39, (T65), 1948, p. 65-86.

102. ASTM Standard Test D1926-63: Standard test methods for carboxyl content of cellulose.

103. Dupont, A.L. Degradation of cellulose at the wet/dry interface. I. The effects of some conservation treatments on brown lines. Restaurator, 17, 1996, p 1-21.

104. Burgess, H.D. The bleaching efficiency and colour reversion of three borohydride derivatives. 10th. Annual Meeting of the American Institute for Conservation, Milwaukee, Wisconsin, 1982, p. 40-48.

105. Tang, L.C. Stabilization of paper through sodium borohydride treatment. Historic Textile and Paper Materials: Conservation and Characterization, American Chemical Society Advances in Chemistry Series 212, Washington, 1986, p. 427-441.

106. Hon, D.N-S. Fourier Transform IR spectroscopy and electron spectroscopy for chemical analysis. American Chemical Society, 1986, p. 349-361.

107. Cardamone, J.M. Application of nondestructive FTIR spectroscopy for identification of textile materials. Scottish Society for Conservation and Restoration, Glasgow, September, 1991, p. 49-58.

108. Reffner, J.A. and Martoglio, P.A. Uniting microscopy and spectroscopy in Humecki, H.J. (ed.) Practical Guide to Infrared Microspectroscopy, Marcel Decker, Inc. 1995, p. 41-84.

109. Derrick, M.R. Analysis of cultural artifacts in Humecki, H.J. (ed.) Practical Guide to Infrared Microspectroscopy, Marcel Decker, Inc. 1995, p. 287-322.

110. Grosso, V. Fourier Transform infrared and Raman spectroscopy of ancient paper. Canadian Conservation Institute, Ottawa, October 1988, 1994, p. 245-250.

111. Langkilde, F.W. and Svantesson, A. Identification of celluloses with Fourier-Transform (FT) mid-infrared, FT- Raman and near infrared spectrometry. Journal of Pharmaceutical and Biomedical Analysis, 13, (4/5), 1995, p. 409-414.

112. Pande, A. and Singh, M.M. Studies of molecular structure of cellulose and chemically modified cellulose by infra-red spectroscopy. Laboratory Practice, 15, (5), 1966, p. 544-550.

113. Blackwell, J. and Marchessault, R.M. Investigation of the structure of cellulose and its derivatives. High Polymer, 5, (4), 1971, p. 1-39.

114. Sistach, C.M. et al. Fourier transform infrared spectroscopy applied to the analysis of ancient manuscripts. Restaurator, 19, 1998, p. 171-186.

115. Choisy, A. et al. Non invasive techniques for the investigation of foxing stains on graphic art material. Restaurator, 18, 1997, p. 131-152.

116.Berben S.A. et al. Estimation of lignin in wood pulp by diffuse reflectance Fourier-transform infrared spectrometry. Tappi Journal, November, 1987, p. 129-133.

117. Conley, R.J. Infrared Spectroscopy, Allyn and Bacon, Boston, 1972.

118. Dyer, J.R. Applications of Absorption Spectroscopy of Organic Compounds, Prentice-Hall Inc., 1965.

119. Zhbankov, R.G. Infrared Spectra of Cellulose and its Derivatives, NY Consultant Bureau, 1966.

120. Higgins, H.G. et al. Infrared spectra of cellulose and related polysaccharides. Journal of Polymer Science (A Polymer Chemistry), 51, 1961, p. 59-84.

121. Feller, R.L. Accelerated aging: photochemical and thermal aspects. Getty Conservation Institute, 1994.

122. Erhardt, D. et al. The comparison of accelerated aging conditions through the analysis of extracts of artificially aged paper. Preprints: AIC 1987 Annual Meeting, Washington, DC: American Institute for Conservation, 1995, p. 43-55.

123. Zou, X. Accelerated aging of papers of pure cellulose: mechanism of cellulose degradation and paper embrittlement. Polymer Degradation and Stability, 43, 1994, p. 393-402.

124. Bansa, H. Accelerated ageing tests in Conservation Research: Some ideas for a future method. Restaurator, 13, 1992, p. 114-137.

125. Stroefer-Hua, E. Experimental measurement: Interpreting, extrapolation and prediction by accelerated ageing. Restaurator, 11, 1990, p. 254-266.

126. Richter, G.A. and Wells, F.L. Influence of moisture in accelerated aging of cellulose. Tappi, 39, (8), 1956, p. 603-608.

127. Wilson, W.K. et al. Accelerated aging of record papers compared with normal aging. Tappi, 38, (9), 1955, p. 543-548.

128. Cuddihy, E.F. The aging correlation (RH + t): relative humidity (%) + temperature (°C). Corrosion Science, 27, (5), 1986, p. 463-474.

129. Lee, S.B. et al. Accelerated thermal degradation of pulp sheets: Effect of beating and importance of humidity in Schuerch, C. (ed.) Cellulose and Wood-Chemistry and Technology, Proceedings 10th Cellulose Conference, Syracuse, N.Y. 1988, p. 863-84.

130. Arney, J.S. and Jacobs, A.J. Accelerated aging of paper - the relative importance of atmosperic oxygen. Tappi, 62, (7), 1979, p. 89-91.

131. Arney, J.S. and Jacobs, A.J. Newsprint deterioration - the influence of temperature on the relative contribution of oxygen-independent and oxygen-dependent processes in the total rate. Tappi, 63, (1), 1980, p. 75-77.

132. Marraccini, L.M. and Kleinert, T.N. Aging and color reversion of bleached pulps: Pt. 1 Peroxide formation during aging. Svensk Papperstidning, 65, 1962, p. 126-131.

133. Kleinert, T.N. and Marraccini, L.M. Aging and color reversion of bleached pulps: Pt.2 Influence of air and moisture. Svensk Papperstidning, 66, 1963, p. 189-195.

134. Feller, R.L. et al. The kinetics of cellulose deterioration. American Chemical Society, 1986, p. 329-347.

135. Du Plooy, A.B.J. The influence of moisture content and temperature on the aging rate of paper. Australian Pulp and Paper Industry Technical Association, 34, (4), 1981, p. 287-292.

136. Brown, D.J. The questionable use of the Arrhenius equation to describe cellulose and wood pyrolysis. Thermochimica Acta, 54, 1982, p. 377-379.

137. Agrawal, R.K. On the use of the Arrhenius equation to describe cellulose and wood pyrolysis. Thermochimica Acta, 91, 1985, p. 343-349.

138. Bayer, F.L. and Morgan, S.L. The analysis of biopolymers by Analytical Pyrolysis Gas Chromatography in Liebman, S.A. and Levy, E.J. (eds.) Pyrolysis and GC in Polymer Analysis, Marcel Dekker Inc. New York, Chapter 6, 1985.

139. Dupont, A.L. Degradation of cellulose at the wet/dry interface. II. An approach to the identification of the oxidation compounds. Restaurator, 17, 1996, p 145-164.

140. Vallance, S.L.et al. The development and initial application of a gas chromatographic method for the characterization of gum media. Journal of the American Institute for Conservation, 37, 1998, p. 294-311.

141. Engel, K. et al. Review of scientific research in the Federal Republic of Germany concerning emissions in laser material processing. International Laser Safety Conference Proceedings, 1990, section 5, p. 29-52.

142. Sasnett, M.W. Propagation of multimode laser beams - The M^2 factor in Hall, D.R. and Jackson, P.E. (eds.) The Physics and Technology of Laser Resonators, Adam Hilger N.Y. 1989, p. 132-42.

143. Johnston Jr, T.F. M^2 concept characterizes beam quality, Laser Focus World, May, 1990, p. 173-83.

144. Arnaud, J.A. et al. Technique for fast measurement of Gaussian beam parameters, Applied Optics, 10, 1971, p. 2275-6.

145. Mauck, M. Knife-edge profiling of Q-switched Nd:YAG laser beam and waist, Applied Optics, 18, 1979, p. 599-600.

146. Kimura, S. and Munakata, C. Method for measuring the spot size of a laser beam using a boundary-diffraction wave, Optics Letters, 12, 1987, p. 552.

147. Karim, M.A. et al. Gaussian laser-beam-diameter measurement using sinusoidal and triangular rulings, Optics Letters, 12, 1987, p. 93.

148. Fleisher, J.M. and Hitz, C.B. Gaussian beam profiling:how and why, Laser Optronics, 6, 1987, p. 61.

149. Wazen, P. Influence of laser beam intensity distibution on laser cleaning. 2nd. International Conference on Lasers in the Conservation of Artworks, 1997. Restaurratorenblatter, Sonderband. Lacona II, Kautek, W. and Konig, E. (eds.), in press.

150. Young, M. Optics and Lasers, Springer-Verlag, Berlin Heidelberg New York and Tokyo, 1986, p. 180-185.

151. Pedrotti, F.L. and Pedrotti, L.S. Introduction to Optics, Prentice-Hall International, 1996, p. 310-312.

152. Shafizadeh, F. and Bradbury, A.G.W. Thermal degradation of cellulose in air and nitrogen at low temperatures. Journal of Applied Polymer Science, 23, 1979, p. 1431-1442.

153. Major, W.D. The degradation of cellulose in oxygen and nitrogen at high temperatures. Tappi, 41, (9), 1958, p. 530-537.

154. Philipp, B. et al. Influence of the supramolecular structure on structural and chemical changes in the thermal degradation of cellulose fibers. Tappi, 52, (4), 1969, p. 693-698.

155. Pfingstag, G. Colorants in inks for writing, drawing and marking. International Paper History, 4, (2), 1994, p. 25-29.

156. Sakayanagi, M. et al. Analysis of ballpoint pens by field desorption mass spectrometry. Journal of Forensic Science, 44, (6), 1999, p. 1204-1214.

157. Segal, J. and Cooper, D. The use of enzymes to release adhesives. The Paper Conservator, 2, 1977, p. 47-50.

158. Townsend, J. Surface studies on varnishes for paintings. Conservation Science in the U.K., Conference at the University of Strathclyde, 1995.

159. Kokosa, J.M. and Eugene, J. Chemical composition of laser-tissue interaction smoke plume. Journal of Laser Applications, July, 1989, p. 59-63.

APPENDECES

APPENDIX 1

Calculation of errors

During this research programme, the final result of certain experiments has required a calculation involving several measured quantities, each with an error. The error associated with the final result has been determined by use of the following equations;-

1. When $X = A - B$, the error ΔX is given by $\Delta X^2 = \Delta A^2 + \Delta B^2$

2. When $X = A^n$, the error ΔX is given by $(\Delta X/X)^2 = n^2(\Delta A/A)^2$

3. When $X = A/B$, the error ΔX is given by $(\Delta X/X)^2 = (\Delta A/A)^2 + (\Delta B/B)^2$

The calculation of the error on nominal fluence requires the use of all three equations.

The spot size W_z was calculated from the knife edge experiment (see Table 21, section **2.2.2**) as $(A - B)/2$ where A was the position the knife edge first attenuated the laser beam, and B was the position the knife edge completely attenuated the beam. The error in the spot diameter is therefore given by,

$$\Delta X^2 = \Delta A^2 + \Delta B^2$$

$$\Delta X^2 = (6.25 \times 10^{-6}) + (6.25 \times 10^{-6})$$

$$\Delta X^2 = 1.25 \times 10^{-5}$$

$$\Delta X = 3.54 \times 10^{-3}$$

and the radius error $\Delta W_z = 1.77 \times 10^{-3}$ cm ≈ 18 μm.

The error in the spot area was determined using equation 2,

$$(\Delta Area/Area)^2 = 4(\Delta radius/radius)^2$$

$$(\Delta Area/Area)^2 = 4(18/125)^2$$

$$(\Delta Area/Area)^2 = 0.0829$$

$$(\Delta Area/Area) = 0.288$$

$$\Delta Area = 0.288 \times 4.909 \times 10^{-4}$$

$$\Delta Area = 1.41 \times 10^{-4}\ cm^2$$

The error in the values of fluence used can be determined from equation 3,

$$(\Delta Fluence/Fluence)^2 = (\Delta Energy/Energy)^2 + (\Delta Area/Area)^2$$

however the error in area is much larger than the error in energy, which results in a 30% error in fluence for example the fluence 41 Jcm^{-2} (Table 26, section **2.3.2**).

$$(\Delta Fluence/Fluence)^2 = (\Delta 0.5/20)^2 + 0.0829$$

$$(\Delta Fluence/Fluence)^2 = 0.0006 + 0.0829$$

$$(\Delta Fluence/Fluence)^2 = 0.0835$$

$$(\Delta Fluence/Fluence) = 0.289$$

$$\Delta Fluence = 41 \times 0.289$$

$$\Delta Fluence = 12\ Jcm^{-2}$$

APPENDIX 2

Glossary of terms

Ablation Ejection of material from a surface due to irradiation by a laser beam.

Absorptivity The amount of incident energy absorbed by a surface.

Attenuate Reduce in force or value.

Cellulose Polymeric carbohydrate composed of long linear chains of ß- linked anhydroglucopyranose.

Chromophore Component of an organic molecule that absorbs visible light.

Collimated Parallel.

Conjugation System of alternating double bonds and single bonds in an organic molecule.

Consolidation Stabilisation of degraded material on the surface of a work of art.

Dissociation Splitting of molecules into atoms or smaller molecules.

Filler White, inert, transparent material, low in refractive index, used in paste form to fill imperfections in a paper surface.

Fluence Pulse energy incident on a surface per unit area (Jcm^{-2}).

Gain medium The medium in a laser which provides the energy levels necessary for stimulated emission.

Grammage Mass per unit area of material (gm^{-2}).

Hemicellulose Amorphous polymeric carbohydrate.

Lignin Three dimensional, highly cross-linked, amorphous polymer.

Normal mode A laser operated in normal mode emits energy in pulses of relatively long duration (microseconds or milliseconds).

Optical cavity The part of a laser which comprises the gain medium and the mirrors.

Overpaint Layers of paint added to paintings during previous restorations.

Patina Layer formed on the surface of an object as a result of environmental ageing.

Photochemical effects Chemical effects on a material due to the absorption of light.

Photon The quantum of electromagnetic radiation.

Photosensitized reactions Reactions which are initiated by the absorption of radiation by one of the reactants.

Photothermal effects Thermal effects on a material due to the absorption of light.

Plasma Highly ionised gas.

Population inversion A condition necessary for laser operation in which there are more atoms in a high energy level than in a low one.

Pulse energy The amount of energy (J) in a single laser pulse.

Pulse length The duration of a single laser pulse.

Pumping source The source of power that enables the gain medium to achieve popuklation inversion.

Q-switching A shutter in the optical cavity of a laser is kept closed until the population inversion has reached a maximum when it is opened.

Radical An extremely reactive chemical species with unpaired electrons.

Reflectivity The amount of incident energy reflected by a surface.

Relative humidity (RH) The mass of water in a given volume of air divided by the mass of water required to saturate the same volume of air at the air temperature.

Repetition rate The number of pulses per second (Hz).

Rise time Time taken to reach peak power for a single laser pulse.

Self limiting Cleaning is self limiting where removal of material from a surface stops as soon as the dirt has been removed.

Size Material used to fill or prepare a porous surface.

Specific heat capacity the amount of heat required to raise the temperature of unit mass of a substance by one degree ($Jkg^{-1}K^{-1}$).

Stimulated emission The process in which a photon triggers a transition from a high energy level E_2 to a lower energy level E_1, with the emission of a photon of energy E, where $E = E_2 - E_1$.

Tensile index Tensile strength of a material divided by the grammage (Nmg^{-1}).

Tensile strength The force per unit width required to snap a piece of paper (Nm^{-1}).

Tidelines The creation of brown lines when degraded paper is wet with drops of water.

Thermal conductivity A measure of how well a material conducts heat ($Wm^{-1}K^{-1}$).

Thermal diffusivity A measure of how rapidly a material will absorb and conduct heat (m^2s^{-1}).

Transmissivity The amount of incident energy transmitted through a material.